Université de Montréal

# LOX and LOX-Like Proteins as Potential Therapeutic Target for Atrial Fibrillation

par

**Doa'a Ghazi Al-u'datt**

Département de Pharmacologie et Physiologie, Université de Montréal
Faculté de Médecine

Thèse présentée à la Faculté des études supérieures
en vue de l'obtention du grade de PhD
en Physiologie

Janvier, 2019

Université de Montréal
Faculté de Médecine

Cette thèse intitulée:

# LOX and LOX-Like Proteins as Potential Therapeutic Target for Atrial Fibrillation

Présentée par:

**Doa'a Ghazi Al-u'datt**

A été évaluée par un jury composé des personnes suivantes:

| | |
|---|---|
| Dr. Yahye Merhi | Président-rapporteur |
| Dr. Stanley Nattel | Directeur de recherche |
| Dr. Bruce Allen | Co-directeur de recherche |
| Dr. Guy Rousseau | Membre du jury |
| Dr. Zamaneh Kassiri | Examinateur externe |
| Dr. René Cardinal | Représentant du doyen |

# Résumé

Les lysyl-oxydases (LOX) et LOX-like (LOXL-1, 2, 3 et 4) influencent le remodelage de la matrice extracellulaire (MEC) lors d'anomalies cardiaques comme l'insuffisance cardiaque (IC) ou la fibrose. L'objectif principal était d'étudier les fonctions matrice-dépendantes et -indépendantes des LOX et LOXL dans la transduction des signaux favorisant la fibrose et la fibrillation atriales (FA). Dans l'oreillette gauche (OG) de chiens IC, nous avons observé une augmentation de la régulation de : LOX et LOXL-1 dans le tissue atrial, LOX et LOXL-2 dans les fibroblastes ainsi que LOX, LOXL-1, LOXL-3 et LOXL-4 dans les myocytes. Nous avons évalué le rôle des isoformes des LOX dans la signalisation de la fibrose et de la FA dans l'OG de rats avec infarctus du myocarde (IM). Chez le chien et les cellules cardiaques de rats néonataux, nous avons exploré le rôle des LOX et LOXL sur la fonction matrice-dépendante et -indépendante des fibroblastes et myocytes cardiaques, en utilisant un traitement à l'angiotensine-II (Ang II) et un knockdown par si-ARN des isoformes de LOX.

L'augmentation de l'expression des ARNm de LOX et LOXL était associée à une augmentation de l'expression des ARNm de COL 1A1, FN 1, TGF-β1, CTGF, periostin, α-SMA et MMP-2 dans la zone infarcie du ventricule gauche (VG). L'expression des ARNm de LOXL-1, LOXL-3, COL 1A1, TGF-β1 et periostin était significativement augmentée dans l'OG. L'administration de β-aminopropionitrile (BAPN) post-IM a diminué significativement l'expression des ARNm de LOXL-1,2,3. Le BAPN a aussi diminué l'expression d'ARNm de marqueurs pro-fibrotiques dans l'OG. Ces changements n'étaient pas significatifs dans le VG. Le BAPN a diminué la fibrose dans l'OG ainsi que le ratio de cross-linking du collagène, mais pas significativement dans le VG. Le BAPN a réduit les remodelages structuraux et fonctionnels

de l'OG sans influencer significativement ceux-ci dans le VG. L'IM était associé à une augmentation de la durée de l'onde P ainsi que la durée et l'inductibilité des FA que le BAPN a significativement réduit. Chez des rats néonataux, des fibroblastes et des myocytes de ventricule ont été mis en culture et traités à l'Ang II.

Les LOX et LOXL-2 sécrétées et le ratio de cross-linking du collagène ont été augmentés; et contribueraient au remodelage de la MEC. Chez le chien, la contractilité des myocytes de l'OG a été augmentée suivant le knockdown de LOX et LOXL-1 associé à des changements de concentrations calciques. Dans les fibroblastes, le knockdown de LOXL-3 a réduit l'expression des ARNm de LOXL-2,3,4, associé à une réduction de la prolifération cellulaire et de l'expression des ARNm de COL 1A1, COL 3A1 et CCNE 2. Ces résultats suggèrent que LOXL-2,3,4 influenceraient la prolifération des fibroblastes et la synthèse du collagène. Le knockdown de LOXL-4 a augmenté ratio de l'expression en ARNm de BAX/BLC-2, ainsi LOXL-4 pourrait avoir un effet protecteur contre l'apoptose.

En conclusion, les LOX et LOXL sont des médiateurs potentiels de la fibrose et la FA dans l'OG chez le rat infarci. Les LOX et LOXL seraient alors impliqués dans la régulation des fonctions des fibroblastes et myocytes cardiaques.

**Mot-clefs:** Insuffisance cardiaque, Fibrillation atriale, fibrose, Lysyl-oxydase (LOX), LOX-like (LOXL), cross-linking du collagène, Fibroblaste, Myocyte.

# Abstract

Lysyl oxidase (LOX) and LOX-like (LOXL-1, 2, 3 and 4) proteins have a crucial role in extracellular matrix (ECM) remodeling in several types of heart disease, such as heart failure (HF) and fibrosis. The main objective of this thesis was to address the matrix-dependent and matrix-independent functions of LOX and LOXL proteins in signal transduction, leading to atrial fibrosis and atrial fibrillation (AF). We noted upregulation of LOX and LOXL-1 in tissues, LOX and LOXL-2 in fibroblasts and LOX, LOXL-1, LOXL-3 and LOXL-4 in myocytes of the canine left atrium (LA) in congestive heart failure (CHF). Based on these findings, we studied the roles of LOX isoforms as upstream targets in the signaling pathways of LA fibrosis and AF in a rat model following myocardial infarction (MI). Additionally, we explored the physiological roles of LOX and LOXL proteins in matrix-dependent and matrix-independent functions of cardiac fibroblasts and myocytes through angiotensin II (Ang II) treatment and siRNA-mediated knockdown of LOX isoforms in canine and neonatal rat cells.

Upregulation of the mRNA expression of LOX and LOXL was accompanied by an increase in mRNA expression of COL 1A1, FN 1, TGF-β1, CTGF, periostin, α-SMA and MMP-2 in the infarcted area of the left ventricle (LV). mRNA expression of LOXL-1, LOXL-3, COL 1A1, TGF-β1 and periostin were significantly increased in the LA post-MI. Administration of β-aminopropionitrile (BAPN) post-MI significantly reduced the mRNA expression of LOXL-1, LOXL-2 and LOXL-3 along with a decrease in the mRNA expression of several profibrotic markers in the LA without significant changes to those in the LV. Moreover, the administration of BAPN post-MI reduced LA fibrosis and the collagen cross-linking ratio without significantly changing those in the LV. BAPN administration post-MI reduced the adverse structural and

functional remodeling of LA without significantly changing those in the LV. Furthermore, MI caused an increase in the P-wave duration, AF duration and AF inducibility, while the values of those parameters were significantly reduced upon BAPN administration post-MI.

The protein expression of secreted LOX and LOXL-2 were increased in cultured neonatal rat ventricular fibroblasts and myocytes along with an increase in the collagen cross-linking ratio in fibroblasts upon treatment with Ang II. The secretion of LOX and LOXL-2 from cardiac fibroblasts and myocytes may contribute to ECM remodeling. Moreover, the contractility of canine LA myocytes was enhanced upon knockdown of LOX or LOXL-1 along with slight changes in $Ca^{2+}$ transients. Upon knockdown of LOXL-3 in fibroblasts, LOXL-2, LOXL-3 and LOXL-4 mRNA expression levels were reduced along with reduced proliferation and mRNA expression of COL 1A1, COL 3A1 and CCNE 2. The results showed that LOXL-2, LOXL-3 and LOXL-4 may promote fibroblast proliferation and collagen synthesis. LOXL-4 knockdown increased the mRNA expression of the BAX/BCL-2 ratio, suggesting that LOXL-4 may protect against apoptosis in cardiac fibroblasts and myocytes.

In conclusion, LOX and LOXL proteins are prominent mediators of LA fibrosis and AF post-MI. Additionally, these findings suggested that LOX and LOXL proteins are implicated in the regulation of various aspects of cardiac fibroblast and myocyte functions.

**Keywords:** Heart failure, Atrial fibrillation, Fibrosis, Lysyl oxidase (LOX), LOX-like (LOXL) proteins, Collagen cross-linking, Fibroblast, Myocyte.

# Table of contents

# List of tables

## Chapter 1

## Part II



## Chapter 2



## Chapter 3

# List of figures

## Chapter 1

## Part I



## Part II

## Chapter 2

## Chapter 3

# List of abbreviations

| | |
|---|---|
| **$2^{-\Delta\Delta Ct}$:** | Comparative threshold cycle. |
| **αβ:** | Integrin receptor α and β subunits. |
| **α-SMA:** | α-smooth muscle actin. |
| **e':** | Mitral annulus moving velocity during early filling. |
| **A:** | Atrial transmitral filling velocity. |
| **ACE:** | Angiotensin-converting enzyme. |
| **Ac-SDKP:** | N-acetyl-seryl-aspartyl-lysyl-proline. |
| **Aden-LOX:** | Adenovirus encoding lysyl oxidase. |
| **Aden-GFP:** | Adenovirus encoding green fluorescent protein. |
| **AF:** | Atrial fibrillation. |
| **AGEs:** | Advanced glycation end products. |
| **ALK:** | Activin receptor-like kinase. |
| **Ang I:** | Angiotensin I. |
| **Ang II:** | Angiotensin II. |
| **Anget:** | Angiotensinogen. |
| **ANOVA:** | Analysis of variance. |
| **AP-1:** | Activator protein 1. |
| **APD:** | Action potential duration. |
| **ARBs:** | Angiotensin receptor blockers. |
| **AS:** | Aortic stenosis. |
| **ATP:** | Adenosine triphosphate. |
| **AT1R:** | Ang II type I receptor. |
| **AT2R:** | Ang II type II receptor. |
| **AV node:** | Atrioventricular node. |
| **B2m:** | β2 microglobulin. |
| **BAPN:** | β-aminopropionitrile. |
| **BAX:** | BCL-2-associated X protein. |
| **BCL-2:** | B-cell lymphoma 2. |
| **BMP-1:** | Bone morphogenetic protein 1. |
| **BW:** | Body weight. |
| **CaMKII:** | $Ca^{2+}$/calmodulin-dependent protein kinase II. |

**CCND 1:** Cyclin D1.

**CCNE 2:** Cyclin E2.

**CHF:** Congestive heart failure.

**CM:** Cardiomyocyte.

**COL 1:** Collagen 1.

**COL 1A1:** Collagen 1A1.

**COL 3A1:** Collagen 3A1.

**CRL:** Cytokine receptor-like.

**CT-1:** Cardiotrophin-1.

**CTGF:** Connective tissue growth factor.

**CVD:** Cardiovascular disease.

**Cx:** Connexins.

**DADs:** Delayed afterdepolarization.

**DCM:** Dilated cardiomyopathy.

**DDR:** Discoidin domain receptor.

**E:** Early diastolic transmitral filling velocity.

**EADs:** Early afterdepolarizations.

**ECG:** Electrocardiogram.

**ECM:** Extracellular matrix.

**EDA:** Extra domain A.

**EDB:** Extra domain B.

**EF:** Ejection fraction.

**EGF:** Epidermal growth factor.

**EMT:** Epithelial-mesenchymal transition.

**EndMT:** Endothelial-mesenchymal transition.

**ER:** Endoplasmic reticulum.

**ERK:** Extracellular signal-regulated kinases.

**ERP:** Effective refractory period.

**ET:** Endothelin.

**$FAC_{LA}$:** Fractional area changing of LA.

**$FAC_{RA}$:** Fractional area changing of RA.

**Fbs:** Fibroblasts.

**FBS:** Fetal bovine serum.

**FGF:** Fibroblast growth factor.

**FN:** Fibronectin.

**FS:** Fractional shortening.

**FSP1:** Fibroblast-specific protein 1.

**G6PD:** Glucose 6-phosphate dehydrogenase.

**GAGs:** Glycosaminoglycans.

**GAPDH:** Glyceraldehyde 3-phosphate dehydrogenase.

**GJA1 Cx 43:** Gap junction protein connexin43.

**Grb2:** Growth-factor receptor-binding protein 2.

**HF:** Heart failure.

**HFD:** High-fat diet.

**HIF-1α:** Hypoxia-inducible factor 1-α.

**HRP:** Horseradish peroxidase.

**HW/BW:** Heart weight/body weight.

**$I_{CaL}$:** L-type $Ca^{2+}$ current.

**IFN:** Interferon.

**IGF-1:** Insulin-like growth factor-1.

**$I_{K1}$:** Background $K^+$ current.

**$I_{KACh}$:** Constitutive acetylcholine-regulated $K^+$ current.

**IL:** Interleukin.

**$I_{Na}$:** $Na^+$ current.

**Inf:** Infarct.

**IP3R:** Inositol trisphosphate receptor.

**$I_{to}$:** Transient outward $K^+$ current.

**JAK:** Janus kinase.

**JNK:** c-jun N-terminal kinases.

**Kir:** Inwardly rectifying $K^+$ channels.

**Kv4.3:** Voltage-dependent $K^+$ channel 4.3.

**LA:** Left atrium.

**$LAA_d$:** LA area at end diastole.

**$LAA_s$:** LA area at end systole.

**$LAD_d$:** LA diameter at end diastole.

**$LAD_s$:** LA diameter at end systole.

**LIF:** Leukemia inhibitory factor.

**LOX:** Lysyl oxidase.

**LOXL:** Lysyl oxidase like proteins.

**LTQ:** Lysine tyrosylquinone.

**LV:** Left ventricle.

**$LVAW_d$:** LV anterior wall thickness at end diastole.

**$LVD_d$:** LV diameter at end diastole.

**$LVD_s$:** LV diameter at end systole.

**$LVPW_d$:** LV posterior wall thickness at end diastole.

**$LVV_d$:** LV volume at end diastole.

**$LVV_s$:** LV volume at end systole.

**MAPK:** Mitogen-activated protein kinase.

**MI:** Myocardial infarction.

**miRNAs:** MicroRNAs.

**MMPs:** Matrix metalloproteinases.

**mTORC:** Mammalian target of rapamycin complex 1.

**MPI:** Myocardial performance index.

**MRTF:** Myocardin-related transcription factor.

**MVco:** Mitral valve closing to opening.

**NADPH:** Nicotinamide adenine dinucleotide phosphate.

**NCX:** $Na^+$-$Ca^{2+}$ exchanger.

**NF-κB:** Nuclear factor-kappa β.

**NFAT:** Nuclear factor of activated T-cells.

**NFDM:** Non-fat dry milk.

**OPN:** Osteopontin.

**P:** Phosphorus group.

**PCPase:** Procollagen C-proteinase.

**PDGF:** Platelet derived growth factor.

**PGs:** Proteoglycans.

**PI3K:** Phosphoinositide 3-kinase.

**PKC:** Protein kinase C.

**PLC:** Phospholipase C.

**PMSF:** Phenylmethanesulfonyl fluoride.

**PNPase:** Procollagen N-proteinase.

**P/S:** Penicillin/streptomycin.

**PUFAs:** Polyunsaturated fatty acids.

**PVDF:** Polyvinylidene difluoride.

**PW:** Pulsed wave.

**qPCR:** Quantitative real-time polymerase chain reaction.

**R:** Receptor.

**$R^2$:** Correlation coefficient.

**RA:** Right atrium.

**$RAA_d$:** RA area at end diastole.

**$RAA_s$:** RA area at end systole.

**RAAS:** Renin-angiotensin-aldosterone system.

**Rac 1 GTPase:** Rac family small GTPase 1.

**$RAD_s$:** RA diameter at end systole.

**RacET:** Transgenic mice with Rac1 overexpression.

**Rem:** Remote.

**ROS:** Reactive oxygen species.

**RT:** Reverse transcription.

**RV:** Right ventricle.

**RyRs:** Ryanodine receptors.

**S6K1:** Ribosomal protein S6 kinase β-1.

**SA node:** Sinoatrial node.

**ScRNA:** Scrambled control.

**SDS-PAGE:** Sodium dodecyl sulfate polyacrylamide gel electrophoresis.

**SEM:** Standard error mean.

**SERCA:** SR $Ca^{2+}$ ATPase.

**Shc:** Src homologous and collagen protein.

**siRNA:** Small interfering RNA.

**$S_L$:** Lateral wall systolic contractility.

**SM22α:** Smooth muscle protein 22α.

**SMAD:** Mothers against decapentaplegic homolog transcription factor.

**SOS:** Son of sevenless protein.

**SPARC:** Secreted protein acidic and rich in cysteine

**SR:** Sarcoplasmic reticulum.

**Src:** Sarcoma proto-oncogene tyrosine kinase.

**SRCR:** Scavenger receptor cysteine rich.

**SRF:** Serum-response transcription factor.

**$S_s$:** Septum systolic contractility.

**STAT:** Signal transducers and activators of transcription.

**TAC:** Transverse aortic constriction.

**TBS:** Tris-buffered saline.

**TCF:** Transcription factor.

**TGF-β:** Transforming growth factor β.

**TgLOX:** Transgenic mice with overexpression of LOX.

**Thy:** Thymus cell antigen.

**TIMPs:** Tissue inhibitors of metalloproteinases.

**TKs:** Tyrosine kinases.

**TMF:** Transmitral flow.

**TNF-α:** Tumor necrosis factor α.

**TSPs:** Thrombospondins.

**VEGF:** Vascular endothelial growth factor.

**VO:** Volume overload.

**VSMCs:** Vascular smooth muscles cells.

**VTP:** Ventricular tachypacing.

**WMSI:** Wall motion score index.

# Dedication

*To my husband.*

*To my mother and father.*

*To my two kids.*

# Acknowledgements

**In the Name of God, the Most Gracious and the Most Merciful**

First and foremost, I would like to express my deepest and sincere appreciation to my supervisor and mentor, Dr. Stanley Nattel, for his flexible attitude, enthusiasm, patience, guidance, encouragement and tremendous support during my PhD study. You always encouraged and taught me to explore an innovative research idea through critical thinking and rigorous questioning. Dr. Nattel offered me a great chance to be one of his research team and I feel lucky to be one of Dr. Nattel's research team. I would also like to gratefully thank my co-supervisor and mentor, Dr. Bruce Allen, for his support, constructive suggestions, patience, guidance and encouragement throughout this project. I greatly appreciate his support when I was going through some difficulties in biochemistry part and making his laboratory facilities available for me.

I am very grateful to acknowledge my deep thanks for the members of the jury for evaluating this thesis; Dr. Yahye Merhi, Dr. Guy Rousseau, Dr. René Cardinal and Dr. Zamaneh Kassiri. I am also thankful to Dr. Eric Thorin for valuable suggestions during the accomplishment of my project. I would like to thank Dr. Martin Sirois and Cynthia Torok for their support and supervision the histology part. I greatly appreciate the assistance of Dr. Yanfen Shi and Dr. Jean-Claude Tardif in the echocardiographic analysis.

I would gratefully like to express my deep thanks to Dr. Roddy Hiram, an exceptional postdoc in Dr. Nattel's lab, for his help, time, suggestion, generosity, and great advises. I am also extremely grateful to Dr. Patrice Naud for his patience and help in technically challenging

experiments, I extremely appreciate your feedbacks and advises in writing protocols, manuscripts and presentations as well as your time towards my project. I sincerely thank Dr. Jiening Xiao and Dr. Xiaoyan Qi for their friendship, help, time, patience and support. I am also thankful to Jennifer Anne Bacchi, Dr. Nattel's administrative assistance, for her support in processing and organizing my documents. My special deep thanks to Chantal St-Cyr, the most honest, organized and helpful person I met in my life. I greatly appreciate the assistance from Nathalie LHeureux in organizing the *in vivo* studies, lab meeting and animal protocols. I would also like to thank my colleagues in Dr. Nattel's lab; Dr. Abhijit Takawale, Dr. Donghai Liu, Dr. Hua, Dr. Anna Garcia, Dr. Sirirat Surinkaew, Dr. Martin Aguilar, Dr. Yu Chen, Mozhdeh, Faeze, Xixiao, Dr. Feng Xiong, Dr. Tao Liu, Dr. Jonathan Melka, Eric Duong, Dr. Patrick Vigneault, Dr. Jean-Baptiste Guichard and Dr. Wang Zq as well as from Dr. Allen's lab, Dr. Sherin Nawaito, Dr. Fatiha Sahmi and Dr. Pramod Sahadevan. I would also like to extend my thanks to Natacha Daquette for performing the MI surgery.

I merely do not have appropriate words to express my deep thanks and appreciation to my grateful husband (Muhammad) and my little kids (Sarah and Amro) whose numerous sacrifices to make my education possible. My truthful and warm appreciation goes to my father (Ghazi), my mother (Abeer), my father-in-law (Hussein), my mother-in-law (Seteh), my late grandmother (Sheika), my aunt (Samieha), my brothers (Bilal, Mohammad and Ahmad), my sisters (Walaa, Razan and Leena), my brothers-in-law (Hashem, Waleed, Ahmad, Rezeq, Anas and Mutasem) and my sisters-in-law (Suha and Fatima) for their understanding, support and encouragement. Financial support, in the form of a scholarship from Jordan University of Science and Technology, is gratefully acknowledged. Finally, I gift this work to all residing in my heart, to whom concerned with my matter, to who's tried to help even with a smile.

# Chapter 1: Introduction

# Part I– Cardiac pathophysiology and management

## 1. Overview

Chronic fibrosis, a common pathological disorder, is characterized by deposition of extracellular matrix (ECM) proteins, which affects many organ systems, such as the skin, lungs, kidneys, heart and liver [1]. Furthermore, fibrosis leads to severe stiffness and impaired organ function [2]. Worldwide, 45 % of the total deaths per year are caused by fibrotic diseases [3]. The biological key point of fibrosis is the deposition of cross-linked collagen and elastin within the ECM, which is initiated by enzymatic (lysyl oxidase (LOX) and LOX-like (LOXL) proteins) and non-enzymatic (advanced glycation end-products; AGEs) pathways [4-6]. Cardiac fibrosis causes a substantial proportion of deaths among other types of fibrosis [3]. Cardiac fibrosis has been involved in various forms of cardiovascular disease (CVD). CVD is the main cause of death in the world, representing 31 % of total deaths annually [7]. Cardiac fibrosis is initially an adaptive and protective mechanism. Nevertheless, prolonged fibrosis leads to adverse remodeling and distinct impairment of organ function [1, 8]. The incidence of and death from cardiac fibrosis have increased in aged individuals [8]. In the heart, increased ECM protein deposition is caused by several pathological conditions, such as pressure overload, myocardial infarction (MI), diabetes and cardiomyopathy [9]. Chen and Frangogiannis [10] reported that activated inflammatory and fibrogenic signaling pathways induce heart failure (HF). HF is associated with significant structural remodeling (fibrosis) of the atria that can lead to an increase in atrial fibrillation (AF) susceptibility [11]. Recently, the AF incidence has reached 13 % among the world population [12]. AF is the most common type of sustained cardiac arrhythmia and is associated with high mortality and morbidity rates [13]. AF is common among HF and MI patients [14-16].

To date, the role of LOX and LOXL proteins in cardiac fibrosis underlying the development of AF are not well understood. The main objective of this thesis was to address the roles of LOX and LOXL proteins in the signal transduction, leading to atrial fibrosis, AF and atrial remodeling. The literature review in this thesis is divided into two parts: part I provides information and discusses topics related to the pathophysiology of AF, cardiac fibrosis and MI. Following this part is a review paper that covers a substantial number of studies related to the role of the LOX family in cardiac function and diseases, which was accepted in Cardiovascular Research Journal (Chapter 1- Part II).

## 2. Cardiac anatomy and physiology

### 2.1 Cardiac structure and function

The heart, a muscular pump, directs oxygenated blood throughout the body through the circulatory system [17-19]. The normal human heart beats 100,000 times/day and pumps more than 16,000 liters of blood to all organs [17, 19]. The heart consists of four chambers, including two inferior chambers (right and left ventricles; RV and LV, respectively) and two superior chambers (right and left atria; RA and LA, respectively) [17, 18]. The RV and LV are separated by the interventricular septum, whereas the RA and LA are separated by the interatrial septum [17-19]. The heart is encircled by coronary arteries that carry all of the blood supply to the heart [17, 18]. The main coronary arteries are the left anterior descending, left coronary, right coronary and circumflex coronary [17, 18]. Furthermore, the heart is enclosed by a fibroelastic sac called the pericardium, which is important for cardiac protection from surrounding infection and prevention of heart overfilling [17, 18]. The LV and LA are responsible for maintaining the systemic circulation, while the RV and RA are essential for sustaining the pulmonary circulation [17, 19]. The systemic circulation passes the oxygenated

blood to all body parts and returns the deoxygenated blood to the lungs [19-21]. The ventricles have thicker and stronger muscular walls compared with those of the atria, enabling the ventricles to pump the blood to distant areas of the body. Usually, the atria and ventricles exist in either relaxation (diastole) or contraction (systole) status [20, 22]. Cardiac output is the volume of ejected blood by the heart in one minute, with a value of 5-5.5 liters/min during rest [17, 18, 22]. Figure 1 illustrates the anatomy of the heart.

The sinoatrial node (SA node) is considered as the pacemaker of the heart and is located in the superior wall of the RA [18]. Normally, the SA node spontaneously fires to start stimulating the atria, followed by the atrioventricular node (AV node) [18]. Following AV node stimulation, signals slowly move to the ventricles to initiate filling of the ventricles [18]. Finally, the stimulation proceeds to the His Purkinje system, leading to a more robust and coordinated contraction of the ventricles [18]. Normal cardiac rhythm, sinus rhythm, mediates the accurate stimulation of the whole heart in the proper sequence [18]. However, an arrhythmia is defined as any deviation from sinus rhythm [23]. An electrocardiogram (ECG) records the electrical activity of the heart and serves as an important indicator of several heart diseases [23, 24]. A normal ECG shows a single synchronized electrical wave during beating of the heart [24]. In an ECG, a P-wave is produced by atrial depolarization, a QRS wave is generated by ventricular depolarization and a T wave is produced by ventricular repolarization [24]. Differences in the shape of the waves and the distance between the ECG peaks are indicators of cardiac diseases, such as congenital heart conditions, arrhythmias and MI [22].

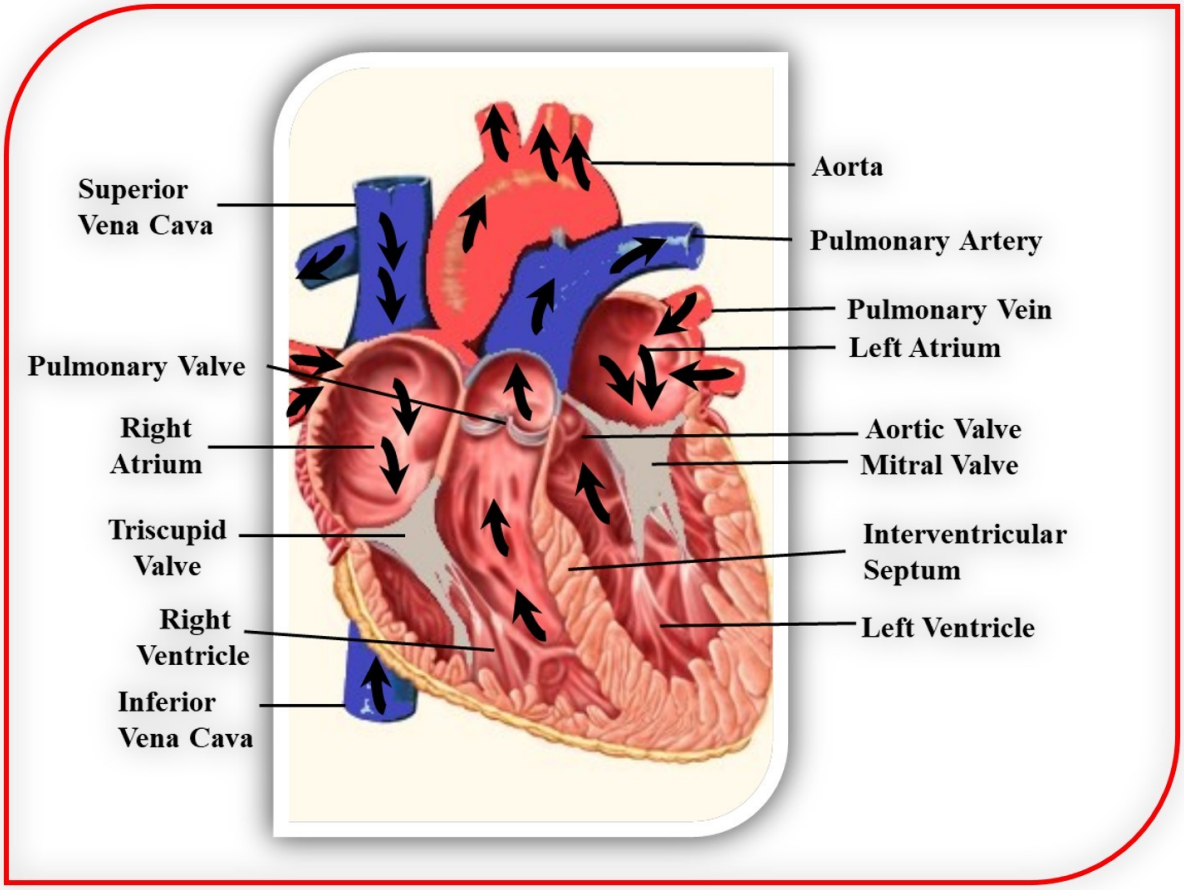


**Figure 1. Anterior view of the human heart.** This figure shows the cardiac chambers, valves and major vessels. The black arrows indicate the normal blood flow direction due to the contraction of the heart chambers.

### 2.2 Cellular components

The cardiac wall is composed of three layers, including the endocardium, myocardium and epicardium [25, 26]. The heart interstitium consists of different cell types, such as cardiomyocytes, fibroblasts, endothelial cells, smooth muscle cells, macrophages, pericytes and mast cells [27, 28]. Cardiac fibroblasts and myocytes account for 27 % and 56 % of the total cell number in the adult murine heart, respectively [29]. Cardiac cells communicate with each other in several ways, including through direct cell-cell interactions as well as through the paracrine and autocrine effects of released factors [25].

#### 2.2.1 Cardiomyocytes

Cardiomyocytes, the most important cardiac cells, constitute approximately 75 % of the heart tissue volume and are essential for maintaining the automaticity and contractility of the heart [30]. During the fetal life, cardiomyocytes proliferate at a rapid rate and become unable to proliferate immediately after birth [31]. Thus, upon neurohormonal stimulation or mechanical stress, cardiomyocytes are elongated and hypertrophied to maintain the stroke volume [31]. Cardiomyocytes are firmly bound and linked by gap junctions to pass the ions [32]. Derived action potentials from the pacemaker cells stimulate the cardiomyocytes and then proceed to neighboring cardiomyocytes to produce an organized contraction of the ventricles and atria [32]. Several factors are implicated in the hypertrophy of cardiomyocytes during cardiac remodeling, such as transforming growth factor β (TGF-β), angiotensin II (Ang II) and tumor necrosis factor α (TNF-α) [33, 34].

### 2.2.2 Fibroblasts

Fibroblasts are flat spindle-shaped cells in perivascular and interstitial matrices that originate from circulating fibrocytes, cardiac resident fibroblasts, perivascular cells, epithelial cells via epithelial-mesenchymal transition (EMT), bone marrow-derived progenitor cells or endothelial cells via endothelial-mesenchymal transition (EndMT) [35-39]. Fibroblasts are well known as the most predominant cells in the adult heart [29]. Recently, endothelial cells and cardiomyocytes have been recognized as the most predominant cells among all cardiac cell types [40]. Fibroblasts are found between cardiomyocytes as sheets and strands and have a crucial role in preserving cardiac structure and function [40]. During the heart development, fibroblasts activate the proliferation of cardiomyocytes through the secretion of fibroblast growth factor (FGF) and periostin [1, 28, 41, 42]. Fibroblasts are characterized by a high membrane resistance that makes them an excellent passive follower for electrical signals [1, 39, 43]. Cardiomyocyte generates action potential that drives fibroblast membrane polarization due their limited capacity and high resistance [39, 43]. Fibroblasts don't generate an action potential in response to electrical stimuli, but they respond to mechanical stimuli with changes in their membrane potential [44-46]. Upon exposure of fibroblasts to mechanical stretch, $Ca^{2+}$, $K^{+}$ and $Na^{+}$ channels are stimulated and depolarize the fibroblast membrane [1, 44-46].

Fibroblasts play numerous roles in the heart, including tissue repair, synthesis and degradation of ECM proteins, inflammation, proliferation, angiogenesis, scar formation and fibrosis [39, 47, 48]. Fibroblasts produce ECM components, such as structural proteins (elastin and collagen), adhesive (fibronectin (FN) and laminin) proteins, glycosaminoglycans (GAGs) and proteoglycans (PGs) [47]. Furthermore, fibroblasts regulate ECM degradation through the production of matrix metalloproteinases (MMPs) and tissue inhibitors of metalloproteinases (TIMPs) [47]. Fibroblasts secrete many growth factors and cytokines that affect surrounding cells through

paracrine and autocrine signaling pathways [1, 49, 50]. Moreover, fibroblasts activate the synthesis of vascular endothelial growth factor (VEGF), FGF, connective tissue growth factor (CTGF) and platelet-derived growth factor (PDGF), which have important roles in maintaining proper vascularization of the heart [1, 51]. Different stimuli can alter fibroblast functions, such as mechanical, electrical and biochemical stimuli [52, 53]. There are several stimulators of fibroblast proliferation, differentiation and collagen secretion, such as TGF-β1, vasopressin, PDGF, cardiotrophin-1 (CT-1), FGF 2, endothelin (ET), mast cell-specific proteases (chymase and tryptase), MMPs, TIMPs and Ang II [48, 54-56].

### 2.2.3 Other cardiac cell types

The coronary artery consists of endothelial cells that participate in tissue healing via stimulation of myofibroblasts and new blood vessel formation [35, 57]. Communication of endothelial cells with fibroblasts modulates the formation of new blood vessels via released VEGF and FGF from fibroblasts during wound healing [39, 58]. Travers *et al.* [59] reported that fibroblasts derived from circulating progenitor and endothelial cells have a vital role in the fibrotic response. During an injury, macrophages spread and secrete MMPs and cytokines within the myocardium to induce cardiac remodeling [60]. Pericytes are located in the perivascular area and are important for preserving cardiac vessel integrity [61]. Additionally, pericytes release several cytokines that can modify fibroblast status [62].

## 2.3 Cardiomyocyte–fibroblast communication

Cardiac fibroblasts are imbedded in the matrix and distributed around the myocytes [39]. Cardiac fibroblasts communicate with neighboring myocytes, and thus contribute to ventricular

contraction and transduction of mechanical and electrical signals [63]. Cardiac myocytes and fibroblasts communicate either directly through gap junctions or indirectly through paracrine factors [63]. Moreover, Ongstad and Kohl [43] reported that cardiac fibroblasts have direct communication with cardiomyocytes via gap junctional proteins called connexins, such as Cx 45, Cx 40 and Cx 43. Cardiac fibroblasts cannot be excited, but they have the ability to transfer currents between myocytes via connexins [64]. Cardiac myocytes release several factors that can alter the functions of fibroblasts and other heart cell types, leading to cardiac fibrosis and hypertrophy [65]. Furthermore, cardiac fibroblasts stimulate myocyte proliferation via the ECM, heparin-binding epidermal growth factor (EGF), FGF and the FN-integrin β1 pathway [28, 42]. Ang II stimulates cardiomyocyte hypertrophy through the secretion of ET and TGF-β1 from fibroblasts [66]. However, cardiomyocytes secrete several molecules, such as TGF-β, Ang II and ET that activate fibroblast differentiation, proliferation and secretion of ECM proteins [66, 67]. Cardiomyocyte-specific Ang II type I receptor (AT1R) knockout leads to decreased fibroblast proliferation around myocytes [67].

### 2.4 Cardiac ECM components

The ECM is a highly organized acellular network that surrounds fibroblasts, myocytes, and vascular and immune cells [68]. It is primarily composed of matricellular proteins, PGs, structural fibrous proteins, GAGs and adhesive glycoproteins [68]. The ECM has various functions in the heart, such as cell proliferation and motility, structural framework formation, mechanical signal distribution and blood flow modulation [1, 68-70]. Additionally, the ECM contains cytokines, MMPs, TIMPs and growth factors that affect ECM homeostasis by regulating the synthesis and degradation of ECM components [68]. In response to cardiac injury, MMPs, TGF-β, VEGF and FGF

are activated and released into the ECM to participate in cardiac remodeling [71]. Disruption of ECM homeostasis following a cardiac injury is the main cause of cardiac fibrosis and dysfunction [72].

### 2.4.1 Collagen

Collagens, major fibrous ECM proteins, are classified into four groups, namely membrane-associated collagens with interrupted triple helices, fibril-associated collagens with interrupted triple helices, multiple triple-helix domains and fibrillar collagens (such as types I, II, III, V, and XI) [73]. Collagen types I and III are the most predominant structural fibrous ECM proteins and are synthesized by fibroblasts and myofibroblasts [68]. Collagen type I represents approximately 85 % of the total collagen and is characterized by thick fibers with high tensile strength, while collagen type III constitutes approximately 11 % of the total collagen and is described as thin fibers with elastic properties [74, 75]. Collagen type I, a triple helix, is composed of three polypeptide α chains, including the two α1 chains and one α2 chain [76]. The triple helix of collagen type III consists of three identical α1 chains, and each α chain contains three repeating amino acids (glycine, proline and hydroxyproline) [76].

Collagens are produced by fibroblasts and myofibroblasts as large inactive molecules called preprocollagens and then secreted into the ECM for processing, assembly and cross-linking [77]. Preprocollagens are subjected to cleavage of their signal peptides in the endoplasmic reticulum to form procollagens, followed by packing of these procollagens into vesicles to be released in the extracellular area for further modifications, including the elimination of C- and N- terminal propeptides by procollagen C-proteinase ($PCP_{ase}$) and procollagen N-proteinase ($PNP_{ase}$), respectively [78]. The resulting mature collagen self-assembles to form collagen microfibrils and is then cross-linked by enzymatic (LOX) and non-enzymatic (AGEs) pathways [79]. The cross-linking

step during collagen processing is essential for increasing the tensile strength and stability of collagen fibers [40, 80-83]. The mature collagen fibers are very stable, with a half-life of 80 to 120 days [84]. Excessive deposition of collagen in the interstitial space leads to an increase in ventricular stiffness and impairs diastolic function [84]. Kong *et al.* [85] reported that the changes in ECM composition stimulate fibroblast migration and proliferation. In the healthy heart, there is a tight balance between the formation of new collagen and degradation of old collagen [84, 86, 87], while the disruption of this balance leads to great changes in cardiac structure and function [84].

### 2.4.2 Other ECM proteins

The cardiac ECM also contains less abundant proteins, such as laminin, fibrillin, elastin, other collagen types (IV, V, and VI) and FN [88]. Laminin, a glycoprotein, consists of different binding domains for ECM components, such as cell membrane receptors and collagens [89]. Laminin is primarily produced by cardiomyocytes, endothelial cells and vascular smooth muscle cells (VSMCs) [89, 90]. Elastin proteins are important as they provide tissues with elastic properties, allowing them to be stretched without breakage [47]. FN, a glycoprotein, is found as cellular (insoluble) and plasma (soluble) forms in tissues and controls cell migration and adhesion [91]. FN is composed of homologous domains that are spliced into a longer protein with two extra domains: A and B (EDA and EDB, respectively) [91]. Various cardiac cells, such as endothelial cells, fibroblasts and macrophages, secrete FN [92, 93], which is involved in different cardiac functions, including ECM stability, mechanotransduction, cell adhesion, collagen deposition and cell migration [94, 95]. Moreover, FN plays a crucial role in fibrillin-1 assembly into structural networks [96]. Arslan *et al.* [97] demonstrated that EDA domain deletion attenuates the adverse cardiac remodeling following MI in mice.

Matricellular proteins, non-structural ECM proteins, have an essential role in tissue healing and repair [98]. The matricellular protein family consists of tenascin-C, secreted protein acidic and rich in cysteine (SPARC), osteopontin (OPN), CCN family members, thrombospondins (TSPs) and periostin [99]. Matricellular proteins act as bridges between cells and matrix proteins to regulate the activity of various growth factors and cytokines [99]. The most important cellular targets of matricellular proteins are vascular cells, fibroblasts and macrophages [99]. Tenascin-C is not found in healthy rat hearts and is highly expressed in fibroblasts following MI [100]. The TSP family is composed of five secreted glycoproteins that participate in the cardiac remodeling process [98]. Kong *et al.* [85] reported that the abundance of periostin in the ECM and myofibroblasts is increased during cardiac fibrosis. The CCN family consists of six proteins that have matricellular and non-matricellular roles such as CCN2/CTGF [99].

## 3. Cardiac remodeling

Cardiac remodeling is defined as the modification of cardiac structure (such as shape, size, dimension and mass) and function in response to cardiac injury and/or hemodynamic load [101]. Cardiac remodeling can be categorized into adaptive (physiological) or maladaptive (pathological) remodeling [102]. Physiological remodeling represents the compensatory dimensional and functional changes that occur when the heart is exposed to physiological stimuli, such as pregnancy and intensive exercise. The heart responds to these stimuli by increasing the stroke volume or heart rate to preserve the cardiac output and LV function [103]. Physiological remodeling, a reversible adaptation, is associated with normal or increased heart function, while pathological remodeling, an irreversible process, is associated with declined cardiac function, excessive deposition of collagen and higher mortality rates [103]. There are several causes of pathological remodeling,

including volume overload, cardiac injury and pressure overload [104-106]. At the cellular level, cardiac remodeling involves proliferation and differentiation of fibroblasts as well as hypertrophy and apoptosis of myocytes [104-106]. These changes deteriorate cardiac functions and increase the risk of arrhythmia development [101]. The adverse remodeling impairs heart function and leads to HF [101]. During pathological conditions, ventricular remodeling is classified into three main patterns, namely eccentric, concentric and post-infarction remodeling [107]. Eccentric remodeling is characterized by increasing the length of myocytes to compensate for the increase in volume load [107], while concentric remodeling is characterized by deposition of ECM proteins and thickening of myocytes due to pressure overload [107]. Post-infarction remodeling involves a series of adverse events, such as dilatation of infarcted tissues as well as combined pressure and volume loads in the non-infarcted areas [107]. Figure 2 illustrates the roles of fibroblast-cardiomyocyte communications in cardiac remodeling.

## 4. Atrial fibrillation (AF)

AF, a common clinical dysrhythmia, is often initiated by fast firing from the pulmonary veins, with the atria beating in a chaotic manner (350–600 bpm) [14, 108] (Figure 3). Rapid and disorganized atrial impulses move to the ventricles and mediate irregular and rapid contraction of the ventricles [14, 108]. Sinus rhythm can be spontaneously re-established in the early stage of AF that develops to a permanent or persistent pattern over time [108]. On surface ECG, AF is characterized by unequal R-R intervals, missing P waves and a rapid heart rhythm for at least 30 sec [16] (Figure 3).

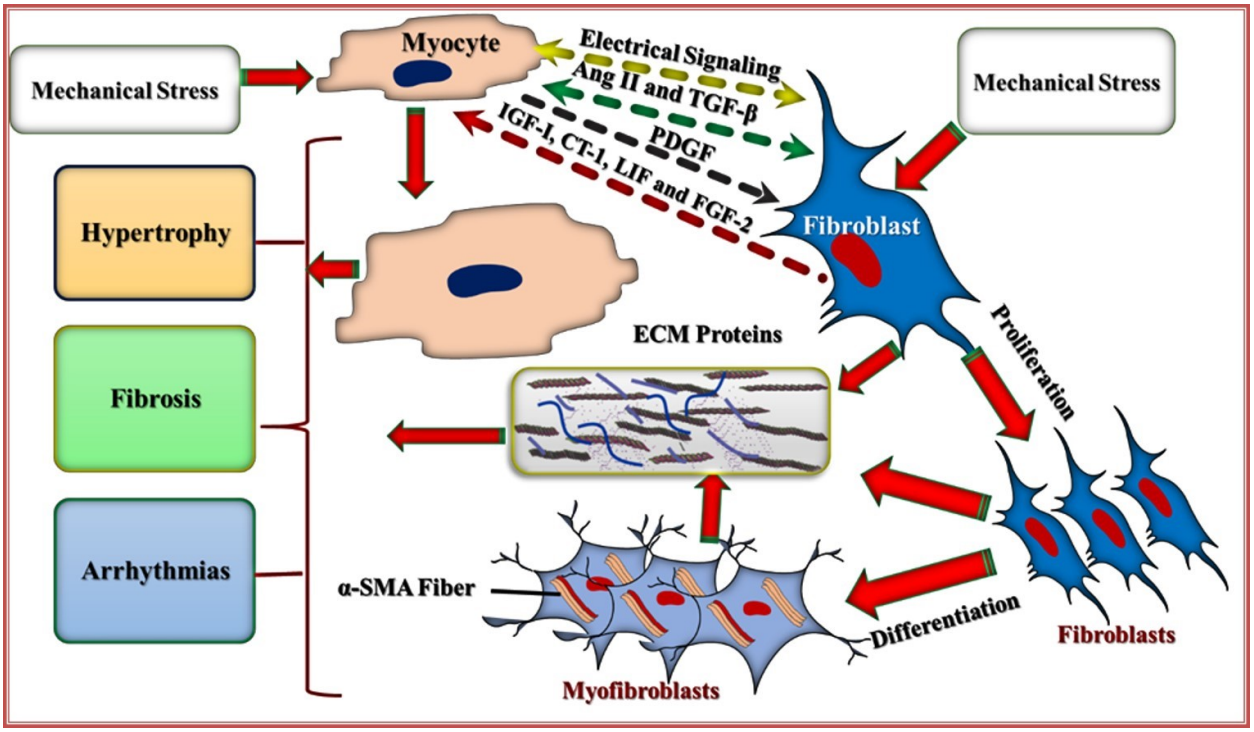


**Figure 2. Fibroblast-cardiomyocyte interactions.** Fibroblasts and cardiomyocytes respond to mechanical stress and communicate via electrical and chemical coupling. Several cytokines and growth factors act in the paracrine and/or autocrine manner and induce fibrosis, arrhythmias and cardiomyocyte hypertrophy. Ang II: angiotensin II, CT-1: Cardiotrophin-1; ECM: Extracellular matrix; TGF-β: Transforming growth factor-β; FGF2: Fibroblast growth factor 2; IGF-1: Insulin-like growth factor-1; LIF: Leukemia inhibitory factor; PDGF: Platelet-derived growth factor; α-SMA: α-smooth muscle actin.

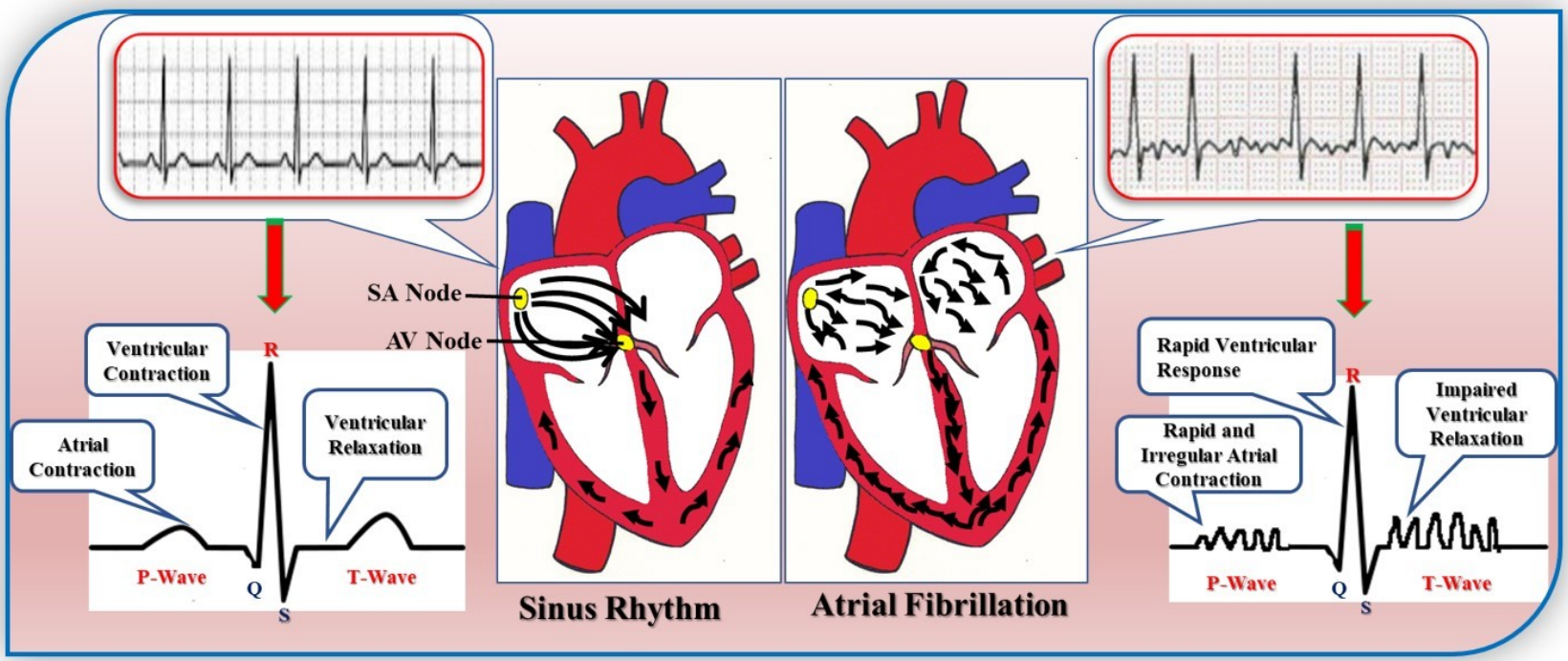


**Figure 3. Illustration of heart with normal sinus rhythm and atrial fibrillation (AF).** Cardiac rhythm is initiated by the sinoatrial (SA) node causing atrial contraction, followed by atrioventricular conduction through the atrioventricular (AV) node and His-Purkinje system, leading to ventricular contraction. AF causes highly irregular and rapid atrial contraction. The black arrows show the spread of the electrical impulses through the atria and ventricles. Electrocardiogram (ECG) recordings for normal sinus rhythm and AF.

The prevalence of AF is approximately 1 to 2 % of the population, with a predicted increase in the future [109]. AF frequently occurs among older patients with other cardiac diseases and is accompanied by various pathological changes [12, 110]. Rates of AF incidence increase to 0.5, 5-15 and 20 % among people of 40-50, 80 and 85 years old, respectively [56, 109, 111]. Aged myocardium is characterized by fibroblast overproliferation, myofiber alignment modification, collagen accumulation and cardiomyocyte hypertrophy [56, 112].

### 4.1 Risk factors

AF is prevalent among patients with diastolic and systolic HF, diabetes mellitus, valvular and coronary artery diseases, hypertension and MI [15, 16]. High-risk AF patients are characterized by LV diastolic and systolic dysfunction, LV hypertrophy and LA dilatation [16]. Lone AF occurs in the absence of systemic or cardiac diseases. However, it is strongly associated with structural heart diseases [16]. AF is considered as a cause and result of HF with complicated interactions that result in systolic and diastolic dysfunction [113]. HF, a common health problem, occurs in more than 23 million people worldwide [97, 114]. HF is associated with increased mortality rates (40 to 60 %) within five years after diagnosis [114]. The AF incidence is 10-50 % in chronic HF patients and is associated with poor prognosis [115, 116]. MI is associated with LV remodeling that may predispose patients to AF development [117]. AF can occur as a result of non-cardiac conditions, including systemic inflammation, metabolic syndrome, thyrotoxicosis and obstructive sleep apnea [118]. Patients with inflammatory conditions, such as inflammatory bowel disease, pericarditis, myocarditis and pneumonia, have a high risk for AF [119]. Atrial fibrosis has been accompanied by inflammatory infiltrates and upregulation of inflammatory chemokines and cytokines, such as monocyte chemoattractant protein 1, TNF-α and interleukins (IL-1 and IL-6) in AF patients [120-122]. Several

changes occur during inflammation, such as infiltration of macrophages and release of reactive oxygen species (ROS) within the myocardium [56]. The inflammation is additionally aggravated by stimulation of the renin-angiotensin-aldosterone system (RAAS) and nicotinamide adenine dinucleotide phosphate (NADPH) oxidase, which lead to TGF-β1-induced electrical and structural remodeling [122]. Oxidative stress induces inflammatory signaling pathways and cell death that ultimately cause fibrosis and AF [123]. Obesity is associated with atrial dilatation, LV diastolic dysfunction, myocardial lipidosis, atrial inflammatory cell infiltration, interstitial fibrosis and abnormal atrial conduction, which all lead to AF [124]. Many signaling pathways are involved in obesity-induced AF, such as oxidative stress, TGF-β1, ET and PDGF [125]. Furthermore, deposition of fat in the pericardial envelope impairs cardiac relaxation [125]. Obstructive sleep apnea causes AF through delaying atrial conduction, a decreased atrial refractory period, fibrosis and myocyte apoptosis [126]. Figure 4 demonstrates the pathophysiology of AF, including clinical risk factors, mechanisms and complications.

### 4.2 Mechanisms

Ectopic firing (triggered activity) and re-entry are the main AF determinants [127]. Ectopic firing can result from delayed afterdepolarizations (DADs), early afterdepolarizations (EADs) or increased atrial automaticity [13]. Ectopic firing initiates AF by providing triggers to induce re-entry [13]. Re-entry needs an initiating trigger and susceptible substrate [127]. Re-entry development depends on the tissue properties, including conduction and refractoriness [127]. The probability of the re-entry formation increases in tissues with abnormal conduction and short refractoriness [127]. In the literature, four main mechanisms are shown to create re-entrant circuits or triggers for AF, including $Ca^{2+}$ handling abnormalities, electrical remodeling, autonomic nervous system changes

and structural remodeling [13, 128]. The predominant hypothesis regarding AF development is the initiation of a fast trigger that mediates the spread of re-entrant waves in susceptible atrial substrates [117, 129]. Atrial remodeling modulates re-entry and ectopic firing mechanisms of arrhythmia, thus leading to AF maintenance [13, 130] (Figure 4).

### 4.2.1 $Ca^{2+}$ handling abnormalities

$Ca^{2+}$ handling abnormalities are important candidates for AF initiation and perturbation (Figure 4) [13, 128]. During systole, $Ca^{2+}$ mainly enters cells via L-type $Ca^{2+}$ channels, and this entry stimulates the $Ca^{2+}$ release from sarcoplasmic reticulum (SR) via ryanodine receptors (RyRs) [13]. During diastole, $Ca^{2+}$ is removed from the cytoplasm by two main pathways, including extrusion of $Ca^{2+}$ across the cell membrane via a $Na^{+}$-$Ca^{2+}$ exchanger (NCX) or active entry of $Ca^{2+}$ into SR via SR $Ca^{2+}$ ATPase (SERCA) [13]. Normally, atrial myocytes inhibit the $Ca^{2+}$ overload by decreasing the entry of $Ca^{2+}$ by L-type $Ca^{2+}$ channels [128]. SERCA is controlled by phospholamban, which decreases the inhibitory function of SERCA and increases the uptake of SR $Ca^{2+}$ upon its phosphorylation [13]. In AF, there are changes in the phosphorylation status of several $Ca^{2+}$ handling proteins, such as hyperphosphorylation of phospholamban and RyR by $Ca^{2+}$/calmodulin-dependent protein kinase II (CaMKII) and protein kinase A [131]. Hyperphosphorylation of phospholamban causes $Ca^{2+}$ overload and DAD activity in congestive heart failure (CHF) [132]. RyR binds to an accessory protein (FKBP12.6) that stabilizes and inhibits the opening of RyR during diastole [13]. Furthermore, adrenergic stimulation increases the SR $Ca^{2+}$ load, L-type $Ca^{2+}$ current ($I_{caL}$) and RyR2 opening probability [128]. During diastole, $Ca^{2+}$ leak occurs in several conditions, such as malfunction of RyRs, increased diastolic $Ca^{2+}$, calsequestrin deficiency and increased NCX activity, which leads to DAD-related arrhythmias [13]. Narayan *et al.* [133] reported that $Ca^{2+}$

mishandling in HF patients causes $Ca^{2+}$ overload and arrhythmia development. Additionally, increased intracellular $Ca^{2+}$ levels activate small conductance $Ca^{2+}$-activated $K^+$ channels that promote AF [128].

### 4.2.2 Electrical remodeling

Electrical remodeling, ion channel remodeling, includes changes in the atrial expression of ion channels or in the current density [129] (Figure 4). Electrical remodeling results from the following changes: abnormal expression of the gap junctional proteins, an increase in inward-rectifier $K^+$ currents (e.g., constitutive acetylcholine-regulated $K^+$ currents ($I_{KACh}$) and background $K^+$ currents ($I_{K1}$)) or a decrease in $Na^+$ currents ($I_{Na}$), $I_{CaL}$ and transient outward $K^+$ currents ($I_{to}$) [134-139]. The ionic changes are associated with $Ca^{2+}$ overload, along with prolongation of the atrial action potential duration (APD), eventually increases the risk for DADs [117]. Furthermore, $I_{CaL}$ reduction causes a decrease in the influx of $Ca^{2+}$ into the cell, resulting in APD shortening and AF maintenance [128]. Tyrosine kinases, oxidative stress and zinc homeostasis can alter $I_{CaL}$ currents [140-142]. van der Velden *et al.* [143] reported that their AF model demonstrated several changes in the expression and distribution of Cx 40. $I_{K1}$ is formed by inwardly rectifying $K^+$ channel (Kir2) family subunits and determines the cardiomyocyte resting action potential [13, 144]. mRNA and protein expression of Kir2.1 have been upregulated along with APD shortening in AF [137, 145]. $I_{KACh}$ is activated by acetylcholine release from the vagal nerve after parasympathetic stimulation [13]. The continuous activation of $I_{KACh}$ causes hyperpolarization of the cell membrane and APD shortening, thus favoring atrial re-entry and AF maintenance [13]. In AF, upregulation of $I_{KACh}$ results from the increase in protein kinase C-induced phosphorylation [138, 146]. Furthermore, decreased $I_{to}$ may promote wave propagation via an indirect increase of action potential amplitude rather than a

decrease in APD [128]. Yue *et al.* [147] noted that voltage-dependent $K^+$ channel 4.3 (Kv4.3), a pore-forming subunit of $I_{to}$, is decreased in the AF dog model.

### 4.2.3 Autonomic nerve remodeling

The autonomic nervous system, particularly the cardiac nerve supply, consists of sympathetic and parasympathetic components that are implicated in arrhythmia development [148]. Stimulation of the autonomic nervous system strongly affects the electrophysiology of the atria and AF development [149] (Figure 4). Atrial sympathetic activation has been heterogeneously increased in AF or MI models [150]. Both parasympathetic and sympathetic nervous systems have crucial roles in the initiation process of AF [151, 152]. Stimulation of the sympathetic nervous system by β-adrenoceptors modifies RyR2 opening probability, $I_{CaL}$ and phospholamban phosphorylation, thus augmenting spontaneous $Ca^{2+}$ release and inducing arrhythmogenesis [153]. Parasympathetic activation increases $I_{KACh}$ and shortens APD through cholinergic stimulation [149].

### 4.2.4 Structural remodeling

The principal characteristics of atrial structural remodeling are dilatation and fibrosis of the atria, which contribute to AF development [154] (Figure 4). Atrial fibrosis strongly contributes to AF through disturbing the electrical coupling, thus acting as a substrate for re-entry and AF maintenance [16, 155]. Severe atrial fibrosis is accompanied by recurrent AF that is resistant to antiarrhythmic drugs [156]. AF patients are characterized by greater atrial volume, size and fibrosis than sinus rhythm patients [157].

### 4.3 Complications

AF is associated with high morbidity and mortality due to several complications, including LV dysfunction, HF, stroke, thromboembolism, hospitalization and poor quality of life [12, 13] (Figure 4). Systemic embolism and stroke are the most common AF complications and result from impaired atrial contraction, atrial blood stagnation and clot formation [158].

## 5. Cardiac fibrosis

### 5.1 Pathogenesis

Cardiac fibrosis is one of the main myocardial remodeling components [56] that occurs due to the imbalance between ECM production and degradation [159]. Cardiac fibrosis is an essential constituent of several cardiac diseases and is characterized by an increase in collagen type I and type III deposition in the cardiac interstitium [74, 85, 160]. Collagen is an important ECM protein that preserves the structural integrity of tissues without compensating cellular functions. The heart adapts to chemical, mechanical and electrical stimuli through the formation and rearrangement of connective tissue fibers [56]. This adaptation occurs in both cellular and extracellular components [56].

Fibroblasts and myofibroblasts are the main cells that are implicated in cardiac fibrosis [161]. The cardiac fibroblast number is increased in pathological conditions through differentiation from several cell lines, such as pericytes, endothelial cells and monocytes [64]. Collagen is subjected to qualitative and quantitative changes during the progression of many cardiac diseases, such as MI and dilated cardiomyopathy [162]. The augmentation of cardiac fibrosis results in the impairment of diastolic and systolic functions, cardiac structure alteration, HF and arrhythmia [161, 162]. Borer *et al.* [163] reported that volume overload caused by valvular dysfunction leads to cardiac fibrosis.

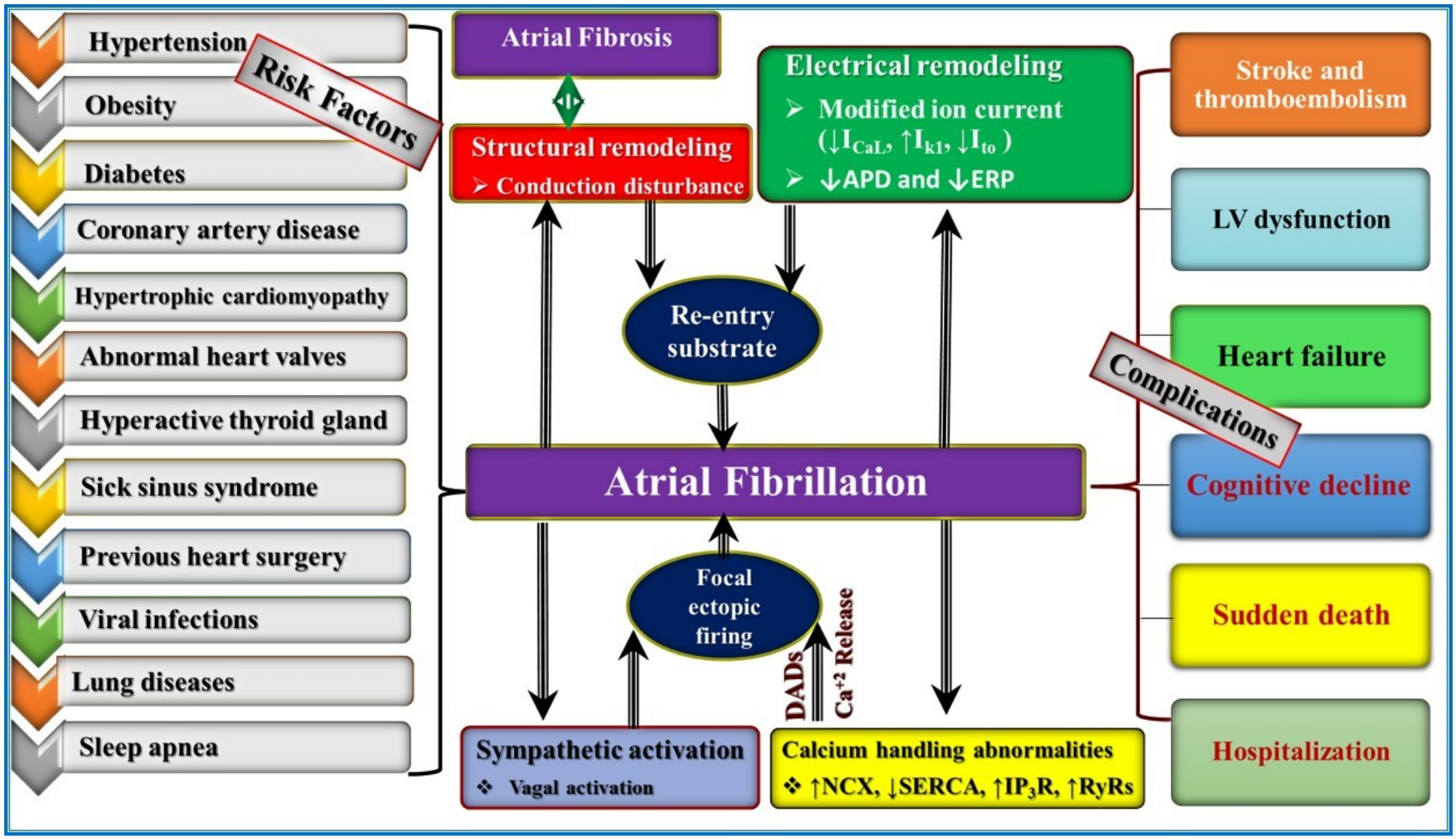


**Figure 4. Schematic diagram for the pathophysiology of atrial fibrillation, including clinical risk factors, mechanisms ($Ca^{2+}$ handling abnormalities, structural, autonomic nerve (sympathetic activation) and electrical remodeling) and complications.** Focal ectopic firing usually results from DADs that produce a spontaneous action potential. The susceptible re-entry substrate needs shortening of refractoriness and disturbances in conduction. ERP: Effective refractory period, $I_{CaL}$: L-type $Ca^{2+}$ current, $I_{K1}$: Background $K^+$ current; $I_{to}$: Transient outward $K^+$ current, NCX: $Na^+$-$Ca^{2+}$ exchanger, SR: Sarcoplasmic reticulum, SERCA: SR $Ca^{2+}$ ATPase, APD: Action potential duration, DADs: Delayed afterdepolarizations, IP3R: Inositol trisphosphate receptor, RyRs: Ryanodine receptors.

Furthermore, pressure overload that is induced by aortic stenosis (AS) or high blood pressure mediates cardiac fibrosis, diastolic dysfunction and HF [164]. Additionally, metabolic disorders (e.g., obesity and diabetes) and toxic compounds are accompanied by severe cardiac fibrosis [165].

### 5.2 Differentiation of fibroblasts into myofibroblasts

Cardiac fibroblasts have a critical function in ECM formation and remodeling after injury [39]. Under stressful conditions, fibroblasts differentiate into myofibroblasts, migrate to an area of cell loss (infarcted area) and then spread to areas without cell loss (non-infarcted areas) to produce collagen [161]. Protomyofibroblasts, immature forms of myofibroblasts, express mature focal adhesive and stress fibers but not α-smooth muscle actin (α-SMA) [40]. Myofibroblasts manufacture higher amounts of collagen than fibroblasts [56]. Collagens are mainly synthesized by myofibroblasts during the progression of cardiac fibrosis [77]. Myofibroblasts are not found in the healthy heart, but they share similar features to those of both smooth muscle cells and fibroblasts [40]. Myofibroblasts have several features, including production of a large ECM, resistance to apoptosis and a contractile phenotype [47, 166]. In response to profibrotic and proinflammatory stimuli, myofibroblasts secrete several chemokines and cytokines [166].

Differentiation of cardiac fibroblasts into myofibroblasts is a complicated process that is induced by several molecular mechanisms [167]. TGF-β, the main fibrotic regulator, stimulates fibroblasts to express α-SMA through nuclear shuttling of myocardin-related transcription factor (MRTF) and mothers against decapentaplegic homolog transcription factor 3 (SMAD3) signaling pathways [168, 169]. MRTF stimulates serum-response transcription factor (SRF), which triggers the transcription of α-SMA [168, 169]. Additionally, TGF-β induces SRF expression through p38 mitogen-activated protein kinase (MAPK), which activates the differentiation of fibroblasts into

myofibroblasts [170, 171]. Collagen type IV stimulates fibroblast differentiation, whereas collagen type I and type III enhance the proliferation of fibroblasts [172].

There are several selective and non-specific biomarkers for fibroblasts and myofibroblasts, including α-SMA, collagen 1A1 (COL 1A1), discoidin domain receptor 2 (DDR2), periostin, transcription factor 21 (TCF21), thymus cell antigen 1 (Thy-1)/CD90, fibroblast-specific protein 1 (FSP1), vimentin, PDGF and PDGF receptor-α [173]. α-SMA is a non-specific biomarker for myofibroblasts because it is found in pericytes and smooth muscle cells [174]. COL 1A1 has been expressed in the adventitia of large blood vessels, cardiac fibroblasts and epicardium [175]. DDR2, tyrosine kinase receptor for collagen, has been recognized in fibroblasts, smooth muscle cells, epicardium, myocytes and endothelium [176, 177]. Periostin is highly expressed in cardiac fibroblasts and myofibroblasts following pressure overload and MI [61, 178, 179], and it is also expressed in VSMCs and epicardium [180]. TCF21 is found in embryonic cardiac epicardium and controls the development of cardiac fibroblasts [181]. Furthermore, TCF21 is often used for fibroblast identification because it is not expressed in immune cells. Thy-1/CD90, a membrane glycoprotein, plays a role in cell adhesion [182] and is detected in pericytes, immune cells and endothelial cells [183]. Therefore, it is not a useful fibroblast marker [183]. FSP1, S100 $Ca^{2+}$ binding protein A4, exists in fibroblasts as well as immune, smooth muscle and endothelial cells [173]. Binding of FSP1 depends on the $Ca^{2+}$ level to mediate cell mobilization [173]. Vimentin, a filamentous protein, has been detected in fibroblasts and endothelial cells [184]. The PDGF receptor is composed of two forms, including PDGFR-α and PDGFR-β [179]. Cardiac fibroblasts show greater PDGFR-α expression than smooth muscle cells [179], while PDGFR-β is found in several cell types, such as neurons, pericytes and smooth muscle cells [179]. These markers are not specific for fibroblasts and myofibroblasts; therefore, most studies use a combination of these biomarkers [174].

### 5.3 Molecular pathways

Cardiac fibrosis is controlled through matricellular proteins and direct communication between cardiac fibroblasts and the ECM via integrins [185]. Various factors promote myocardial fibrosis, including TGF-β, Ang II, ET-1, PDGF, microRNAs (miRNAs), ROS, CTGF and FGF [13, 186]. Figure 5 demonstrates schematic signaling pathways for cardiac fibrosis.

#### 5.3.1 TGF-β

TGF-β is described as a multifunctional growth factor and cytokine, which activates the immune response, differentiation of fibroblasts into myofibroblasts and secretion of ECM proteins [187-189]. The TGF-β family is composed of three isoforms, namely TGF-β 1, 2 and 3, which are encoded by three different genes [190]. TGF-β isoforms have different expression patterns, but they bind to similar receptors on the cell surface [190]. TGF-β1 is the most predominant isoform in the heart [190]. In a healthy heart, TGF-β1 exists as a latent form that cannot bind to its receptors [190]. Upon cardiac injury, latent TGF-β1 is converted to active TGF-β1 to mediate cellular effects [191]. TGF-β binds with two heterodimeric receptors in the plasma membrane, namely TGF-β type I and TGF-β type II receptors, to initiate canonical (SMAD2/3-dependent) and non-canonical (SMAD2/3-independent) signaling pathways [192]. The canonical signaling pathway involves phosphorylation of transcription factors (SMAD2 and SMAD3), which later interact with SMAD4 in the cytoplasm and translocate to the nucleus to increase gene transcription of α-SMA, FN, CTGF, periostin, collagen type III alpha 1 chain (COL 3A1) and COL 1A1 [192-196]. However, the non-canonical pathway involves MAPK activation and ultimately results in extracellular signal-regulated kinases 1 and 2 (ERK1/2), c-Jun NH-terminal kinases (JNK1/2) and p38 signaling [194, 197]. TGF-β is the most common mediator of the differentiation of fibroblasts, pericytes, endothelial

cells and epithelial cells into myofibroblasts. TGF-β can be stimulated by several factors, such as MMP-2, MMP-9, TSP-1, ROS and plasmin, that maintain ECM stability [191, 198, 199].

### 5.3.2 Ang II

Ang II regulates various cardiac fibroblast functions (e.g., migration, proliferation, differentiation and secretion of collagen, growth factors and cytokines) and stimulates cardiomyocyte hypertrophy via activation of both canonical and non-canonical signaling pathways [161, 200-203]. Ang II exerts its effect through binding to distinct receptors; AT1R and Ang II type II receptor (AT2R) [156]. AT1R induces fibrotic effects via activation of cardiomyocyte apoptosis and hypertrophy as well as fibroblast proliferation [156]. Moreover, AT1R stimulates several molecular pathways, such as signal transducers and activators of transcription (STAT), MAPKs, protein kinase C (PKC), tyrosine kinases, phospholipase D and phospholipase Cβ, in cardiac fibroblasts [54]. Additionally, AT1R activates the small GTPase Ras protein, which triggers phosphorylation of MAPK-induced remodeling [156]. Activation of AT1R leads to upregulation of TGF-β expression, thus induction of cardiac fibrosis and hypertrophy [161], while AT2R has antiproliferative effects through inhibition of MAPK [204]. Both cardiomyocytes and fibroblasts secrete TGF-β1, which is a downstream mediator of Ang II actions [205]. Ang II induces cardiac fibrosis in several cardiac diseases, such as MI, CHF, cardiomyopathy and hypertension [13]. The atria of AF patients are characterized by elevated AT1R and angiotensin-converting enzyme (ACE) expression along with fibrosis [206]. AT1R plays a significant role in the electrical and structural remodeling of atria [206]. Furthermore, Ang II along with aldosterone induces inflammation and oxidative stress via stimulation of NADPH oxidase [207].

### 5.3.3 ET-1

The ET family is composed of three isoforms, namely ET-1, ET-2 and ET-3 [208]. ET-1, the most important isoform in humans, is mainly synthesized from endothelial cells and plays a crucial role in the pathogenesis of several cardiac diseases, such as HF and fibrosis [188]. ET-1, a strong fibrotic mediator, acts downstream of the Ang II and TGF-β signaling pathways in numerous cell types [209]. Moreover, ET-1 promotes fibroblast proliferation and differentiation as well as ECM protein production [85, 210, 211]. Various animal models of hypertension and cardiac fibrosis show an increase in ET-1 [212]. Cardiac-specific overexpression of ET-1 augments cardiac fibrosis along with systolic and diastolic dysfunction, while the ET-1 antagonist attenuates cardiac fibrosis in hypertensive and MI models [210, 211].

### 5.3.4 PDGF

PDGF, a VEGF family member, is composed of four chains (A, B, C and D) that are synthesized and assembled inside cells [159]. PDGF mediates migration, proliferation and differentiation through the binding of two different class III receptor tyrosine kinases, namely PDGFR-α and PDGFR-β [213]. Binding of PDGF with its receptor causes dimerization of the receptor and activation of tyrosine kinase Janus kinases (JAKs), which initiates the phospholipase C (PLC)/PKC, JAK/STAT, phosphoinositide 3-kinase (PI3K)/AKT and RAAS/ERK1 signaling pathways [13, 214]. Furthermore, PDGF increases the transcription of mitogenic genes (Fos and c-Myc) [13, 214]. PDGF-A, PDGF-B, and PDGF-C have an affinity to bind to PDGFR-α, while PDGF-B and PDGF–D have an affinity to bind to PDGFR-β [215]. Transgenic mice with cardiac-specific PDGF-A, PDGF-C or PDGF-D overexpression are more prone to cardiac fibrosis and HF [216, 217]. PDGF has an important function in the proliferation and maturation stages post-MI [186].

### 5.3.5 miRNAs

miRNAs, short single-stranded non-coding RNAs, degrade and prevent translation of their target mRNAs, and thus control gene expression [218]. miRNAs induce fibrosis (e.g., miRNA-208, miRNA-21, miRNA-199b and miRNA-34) or protect against fibrosis (e.g., miRNA-26a, miRNA-133/miRNA-30, miRNA-1, miRNA-29, miRNA-214 and miRNA-133a) [219]. miRNA-133 inhibits CTGF expression and decreases cardiac fibrosis [218]. miRNA-133 and miRNA-1 reduce LV fibrosis in pressure overload animal models [220-222]. Knockout mice of miRNA-133 have severe cardiac fibrosis and HF [223], while overexpression of miRNA-133 causes a reduction in apoptosis and cardiac fibrosis [221]. miRNA-29 upregulates collagen (type I and type III), and miRNA-21 regulates antiapoptotic genes, MMP-2 and the ERK pathway [224-226].

### 5.3.6 CTGF

Cardiac fibroblasts produce CTGF, which plays a significant role in ECM synthesis, cell adhesion, proliferation and migration through binding to heparin and integrins [227]. CTGF, a cysteine-rich protein, is concurrently expressed with TGF-β1 because the promoter of CTGF contains TGF-β1 responsive elements [228, 229]. Expression of CTGF is regulated by many factors, including VEGF, TGF-β1, ROS, TNF-α and Ang II, as well as cell stretch and shear stress [149, 230]. CTGF stimulates TGF-β, which enhances ECM synthesis [98]. Additionally, CTGF can bind to FN and act as a bridge, which helps in intracellular and extracellular signaling interactions [149, 230]. Overexpression of CTGF in pressure overload mice causes substantial cardiac fibrosis [231], while administration of an antibody against CTGF in pressure overload mice has a protective effect on ventricular function [231].

### 5.3.7 MMPs and TIMPs

MMPs, an endopeptidase family, consist of twenty-six members of zinc-dependent enzymes that are responsible for degradation of ECM proteins [83, 232, 233]. The activity of MMPs is suppressed by TIMPs via binding with the catalytic domain of MMPs [232, 234-236]. The TIMP family is composed of four members, including TIMP-1, TIMP-2, TIMP-3 and TIMP-4 [237]. MMPs and TIMPs are produced and secreted from different cardiac cells (e.g., neutrophils, fibroblasts, macrophages, cardiomyocytes and endothelial cells) to maintain ECM homeostasis [232, 234, 236, 238, 239]. The expression of MMPs and TIMPs is modulated by ROS, Ang II, inflammatory cytokines, neurohormonal peptides and growth factors [240-242]. MMPs induce connective tissue synthesis through acting as ligands for leukocyte integrins and stimulating fibroblast differentiation [243]. The activity of MMPs is increased during cardiac fibrosis progression [243]. After 10 min of coronary ligation, MMPs are stimulated to degrade ECM proteins [244]. Overexpression of MMPs is associated with hypertrophy and elevated collagen levels in the heart [243].

### 5.3.8 Oxidative stress

Several inflammatory mediators, IL-6, IL-1β and TNF-α, can modify fibroblast behavior by stimulating transcription factors (activator protein 1 (AP-1) and nuclear factor-kappa β (NF-κB)) through ROS, ERKs, p38 or JNK pathways [245, 246]. ROS are produced from activation of NADPH oxidase [245, 247]. ROS have numerous roles in cardiac fibrosis, including preservation of the balance between MMP and TIMP, augmentation of fibroblast proliferation and deposition of collagen [245, 247].

### 5.4 Types of cardiac fibrosis

Cardiac fibrosis is classified into two types as follows: (1) reactive or interstitial fibrosis, in which collagen fibers expand without loss of cardiomyocytes; and (2) replacement or reparative fibrosis, in which collagen deposition replaces dead cardiomyocytes [156, 248].

#### 5.4.1 Replacement fibrosis

Replacement fibrosis, or reparative fibrosis, is characterized by replacement of dead myocytes by a collagenous scar [160]. The cardiomyocytes are more sensitive to ischemia during MI than fibroblasts, endothelial cells or mast cells [249]. The death of cardiomyocytes is caused by the diminished oxygen supply during MI, and thus triggers a series of events to prevent ventricular wall rupture [250, 251]. Replacement fibrosis is crucial for maintaining LV structural integrity via collagen deposition in the infarcted area [159, 252, 253]. Ischemic injury results in secretion of MMPs from fibroblasts to initiate the migration of cells to injured areas [254]. Cleavage of collagen type I by MMPs is crucial for fibroblast migration and tissue repair post-MI [255]. Moreover, ischemic injury stimulates secretion of many chemokines that recruit inflammatory cells to eliminate dead cells from infarcted areas [254]. A few days post-MI, several proinflammatory cytokines are significantly increased, such as IL-6, TNF-α and IL-1β [254]. In the infarcted areas of myocardium, TGF-β is also produced and released by leukocytes, fibroblasts and platelets [189].

#### 5.4.2 Ventricular interstitial fibrosis

Interstitial fibrosis, or reactive fibrosis, develops in the absence of cardiomyocyte death [160]. The released profibrotic factors from myofibroblasts in the infarcted area may cross into the non-infarcted area and augment collagen accumulation in the adventitia of coronary blood vessels and interstitial areas, eventually leading to perivascular and interstitial fibrosis, respectively [201].

Perivascular fibrosis causes narrowing in the lumen of blood vessels and decreases blood flow causing cardiomyocyte hypoxia [159, 256]. Interstitial fibrosis increases myocardial stiffness and impairs systolic and diastolic function due to collagen deposition between muscular spaces and around coronary arterioles and arteries [159, 252, 256]. Furthermore, interstitial fibrosis acts as an insulator between cardiomyocytes, and thus disturbs cardiac electrical conduction [159, 257] (Figure 6). During MI, remodeling of the non-infarcted area involves cardiomyocyte hypertrophy to reduce overload and LV wall tension [258]. The remodeling in the non-infarcted area of myocardium significantly contributes to HF development [258]. In the non-infarcted area of the LV, stress stimulates latent TGF-β [201]. Moreover, upregulation of TGF-β and Ang II expression in the non-infarcted area of myocardium indicates their important roles in reactive fibrosis [259, 260].

### 5.4.3 Atrial interstitial fibrosis

Atrial fibrosis occurs in several pathological conditions, such as HF [261], mitral valve diseases [262], dilated cardiomyopathy [263], hypertension [261], AF [120] and age [264]. There are quantitative and qualitative variations between atrial and ventricular remodeling in HF models [265]. In HF, greater structural remodeling is found in the atria compared with the ventricles because the atria are smaller, thinner and contain more fibroblasts, ECM proteins and fibrosis than the ventricles [11, 154, 266]. Cardiac fibroblasts have a role in the electrical remodeling via shortening the action potential during AF [56]. Atrial fibrosis adversely affects normal conduction without significantly changing the effective refractory period (ERP) in animal HF models [154, 267]. Atrial remodeling occurs as a result of LV diastolic dysfunction [268]. HF is associated with significant structural remodeling of atria that ultimately increases AF susceptibility [11]. Several studies have reported that AF is strongly correlated with atrial fibrosis in the HF model induced by ventricular tachypacing (VTP) [269].

The exact mechanisms of atrial dilatation and fibrosis in AF are complicated and not well understood [156]. Atrial dilatation and fibrosis are usually accompanied by an increase in the atrial ERP and AF cycle length, which subsequently decrease AF frequency [11]. Atrial fibrosis is substantially more prevalent than ventricular fibrosis in AF patients [270]. In AF, ventricular and atrial fibrosis have common signaling pathways but differ in the extent of these pathways [271]. Furthermore, atrial fibroblasts are more sensitive to profibrotic stimuli (e.g., ET, Ang II and PDGF) than ventricular fibroblasts [156]. Profibrotic gene expression levels of the atria are distinctly higher than those of ventricles in mice with TGF-β1 overexpression [271]. In volume and pressure overload models, structural remodeling of the atria is markedly greater than that in ventricles due to the limited capacity of the atria to sustain rapid stimulation [135]. Numerous mechanisms control the severity of atrial fibrosis, such as mechanical stretch, hemodynamic changes and variations in proinflammatory cytokines, hormones and growth factors [56]. Rapid atrial pacing elevates collagen levels in the atria due to upregulation of TGF-β1 and Ang II [272]. Cardiac overexpression of active TGF-β1 is associated with atrial fibrosis and AF development [273]. PDGF promotes atrial fibrosis and contributes to electrical remodeling via decreasing $I_{CaL}$ and shortening APD in cardiomyocytes [156, 274, 275]. Activation of the RAAS and neurohormonal imbalance induce LA fibrosis and AF maintenance [276]. Transgenic mice with cardiac ACE overexpression are more susceptible to atrial fibrosis and AF along with atrial dilatation [277]. Expression of Ang II and TGF-β1 is increased in the atria in VTP-induced CHF [269, 278]. The atrial CTGF expression is upregulated along with an increase in LA fibrosis in a variety of AF models [279-282]. Moreover, atrial tissues of AF patients show a decrease in TIMP-1, TIMP-2, and TIMP-4 expression, as well as an increase in MMP-9 and MMP-2 expression [155, 266, 283-285]. Figure 6 illustrates the complication of interstitial fibrosis, leading to AF.

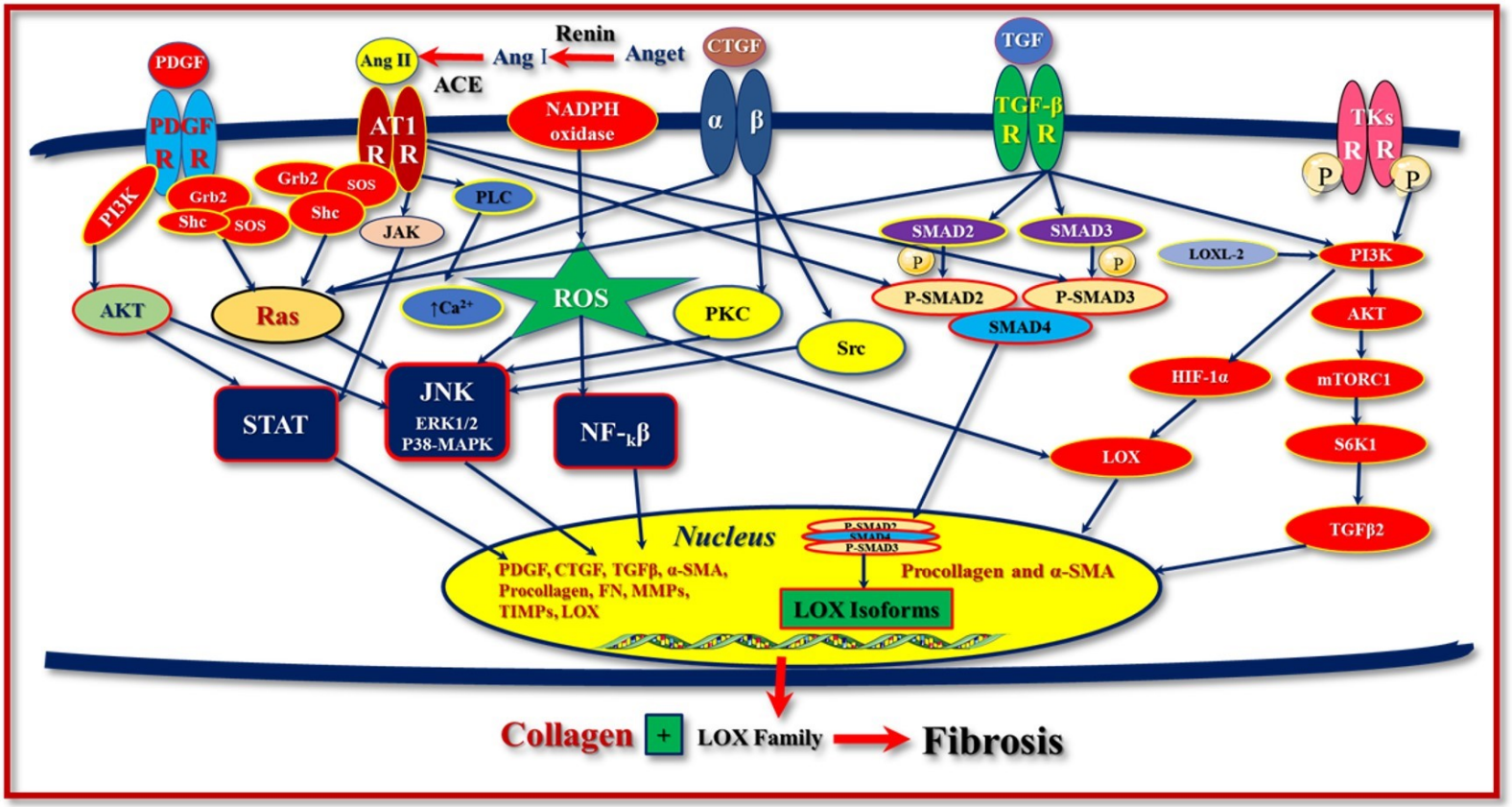


**Figure 5. Schematic showing the proposed signaling pathways of cardiac fibrosis.** R: Receptor; TKs: Tyrosine kinases; αβ: Integrin receptor α and β subunits; AT1: Angiotensin type I; Ang I: Angiotensin I; Ang II: Angiotensin II; Anget: Angiotensinogen; ACE: Angiotensin-converting enzyme; CTGF: Connective tissue growth factor; PDGF: Platelet-derived growth factor; NADPH oxidase: Nicotinamide adenine dinucleotide phosphate oxidase; TGF-β: Transforming growth factor β; SMAD: Mothers against decapentaplegic homolog transcription factor; HIF-1α: Hypoxia-inducible factor 1-α; S6K1: Ribosomal protein S6 kinase β-1; LOX: Lysyl oxidase; PKC: Protein kinase C; P: Phosphorus group; COL 1: Collagen 1; α-SMA: α-smooth muscle actin; FN: Fibronectin; MMPs: Matrix metalloproteinases; TIMPs: Tissue inhibitors of metalloproteinases; LOXL-2: Lysyl oxidase like protein 2; JNK: c-Jun N-terminal kinase; ERK1/2: Extracellular signal-related kinase ½; NF-$_{\kappa}$β: Nuclear factor-kappa β; STAT: Signal transducers and activators of transcription; PI3K: Phosphoinositide 3-kinase; Grb2: Growth-factor receptor-binding protein 2; Shc: Src homologous and collagen protein; ROS: Reactive oxygen species; PLC: Phospholipase C; JAK: Janus kinase; MAPK: Mitogen-activated protein kinase; SOS: Son of sevenless protein; Src: Sarcoma proto-oncogene tyrosine kinase; mTORC: Mammalian target of rapamycin complex 1.

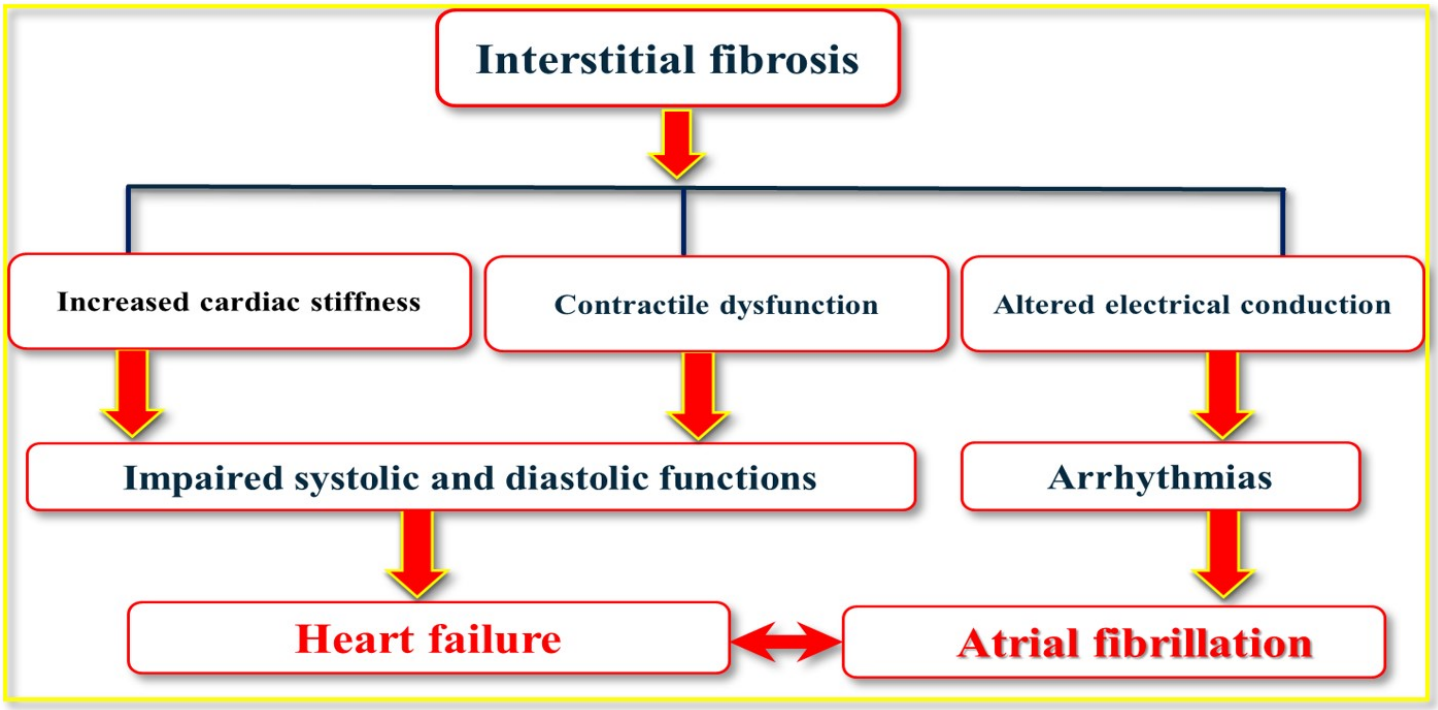


**Figure 6. Overview of cardiac interstitial fibrosis complications contributing to heart failure and atrial fibrillation.**

## 6. Myocardial infarction (MI)

The incidence of MI increases with age, and men are more susceptible than women [286]. MI causes more than one-third of CVD-associated deaths [8]. Numerous risk factors contribute to CVD, such as diabetes, hypertension, hyperlipidemia, obesity, smoking and physical inactivity [286]. MI is induced by several conditions, such as coronary artery atherosclerosis, arteritis, congenital coronary artery anomalies, coronary embolism and elevated myocardial oxygen demand [50, 287]. MI occurs due to incomplete or complete occlusion of the coronary artery that leads to cardiomyocyte death in the myocardial area [49, 288]. Coronary artery occlusion decreases oxygen tension and induces cardiomyocyte ischemia [288]. Cardiomyocyte ischemia suppresses oxidative phosphorylation and adenosine triphosphate (ATP) generation, which is essential for $Na^+/K^+$-ATPase function [288]. $Na^+/K^+$-ATPase dysfunction leads to increased intracellular $Na^+$ levels, decreased intracellular $K^+$ levels, water accumulation and cardiomyocyte swelling [288], resulting in cardiomyocyte repolarization failure and excitation loss [50, 289]. Upregulation of the cytosolic $Ca^{2+}$ level during ischemia may increase the risk for arrhythmia development [50].

During the first minute following ischemia, the cardiac contractility progressively decreases [288]. Irreversible cellular changes may occur after 20 to 30 min of ischemia without reperfusion [50, 288]. Fibroblasts are the main cells that mediate cardiac repair following MI [40]. MI, pressure and volume overload models have been associated with an increase in the number of myofibroblasts in the interstitial matrix [85, 290]. Following MI, a significant loss of cardiomyocytes induces an inflammatory response that stimulates fibroblasts to produce a collagen scar [160, 288]. CT-1, an IL-6 family member, controls fibroblast proliferation and ECM synthesis by activating the AKT, JAK and p42/44 MAPK pathways following MI in rats [291, 292].

### 6.1 Stages of post-MI healing

Following injury, fibroblasts are stimulated and undergo several changes in their phenotypes to repair the damaged tissue by secretion of ECM proteins [249]. Macrophages, endothelial cells and myofibroblasts play a crucial role in the repair and healing of the injured area post-MI [293]. Cardiac fibroblasts have an essential function in all stages of the cardiac repair process [294]. Cardiac healing following MI comprises three stages, which partially overlap, including early inflammatory, mid-proliferative and late maturation stages [40].

#### 6.1.1 Early inflammatory stage

During the early stage (0 to 2 days post-MI), the acute innate reaction is initiated and causes significant cardiomyocyte death in rodents [48, 98]. The death of myocytes triggers neutrophil migration from blood circulation to the injured area to eliminate the cellular debris [98]. Following debris clearance, inflammation is resolved, and neutrophils are engulfed by macrophages [98]. The macrophages secrete several cytokines and growth factors, such as TGF-β, TNF, PDGF and IL-10, to terminate the inflammatory reaction and initiate healing [98, 295]. Appropriate termination of the inflammatory phase is important for the repair process to be effective. However, inappropriate termination of inflammation may mediate LV dilatation [296]. The major changes that occur during the early stage of MI are replacement of the dead cells with a collagen scar, thinning of the infarcted area and lengthening of the cardiomyocytes [8].

#### 6.1.2 Mid-proliferative stage

In the proliferative stage (2 to 5 days post-MI), fibroblasts migrate to the injured area and differentiate into myofibroblasts in rodents [48, 98]. Myofibroblasts synthesize a large amount of

ECM proteins, mainly collagen type I and type III [249]. Deposition of collagen is important to enhance the tensile strength and inhibit rupture of the ventricular wall [249]. When the inflammatory phase is terminated, fibrosis starts to develop at 3 to 5 days post-MI due to upregulation of IL-10, TGF-β and anti-inflammatory cytokines, as well as programmed death of inflammatory cells [161]. Myofibroblasts release matricellular proteins and FN, which further encourage myofibroblast migration to continue tissue healing [98].

### 6.1.3 Late maturation stage

The maturation stage starts one-week post-MI and involves a series of events that create a mature scar, including inhibition of cell migration and proliferation, cross-linking of collagen and apoptosis of the remaining cells in rodents and rabbits [48, 297, 298]. Moreover, collagen type III is replaced with collagen type I, which is cross-linked by LOX [249]. Collagen cross-linking enhances the tensile strength of the scar and alters the ventricular chamber geometry [252]. Numerous studies reported that osteopontin and syndecan 4 stimulate FGF2, which later initiates the collagen cross-linking process via LOX activation [299, 300]. However, the deletion of FGF2 decreases fibroblast proliferation, ECM synthesis and infarct expansion [55]. Several changes occur during the maturation stage, including enlargement of the ventricular chamber, increase of the ventricular wall mass and hypertrophy of cardiomyocytes in the non-infarcted areas [301]. Several autocrine, hormonal and paracrine factors contribute to fibrosis post-MI [85, 189]. After collagenous scar formation in the infarcted area, myofibroblasts are cleared from the scarred area by apoptosis [249].

### 6.2 MI-associated complications

MI is associated with several complications, such as pericardial diseases, cardiogenic shock, LV free wall rupture, ventricular aneurysm, infarct expansion and ventricular arrhythmias [50, 302-304]. Pericardial effusion and pericarditis represent approximately 43 % and 7-41 % of deaths following MI, respectively [50, 305, 306]. Cardiogenic shock occurs due to pump failure and is accompanied by a high mortality rate post-MI [50]. LV rupture is a fatal MI complication that occurs because of the decline in the strength of infarcted myocardium [307]. Multiple factors contribute to cardiac rupture, such as prolonged reparative wound healing, an excessive inflammatory response, a large transmural scar and increased MMP activity [50, 302, 308, 309]. Ventricular arrhythmia is the main cause of death during the early and late stages following MI [50]. Electrical and structural remodeling mediate ventricular arrhythmia post-MI [50]. Ventricular remodeling post-MI involves ventricular dilatation, myocyte hypertrophy, arrhythmia, HF and death [310]. Dysregulation of the healing process leads to excessive collagen deposition and LV diastolic dysfunction [293]. The degree of ventricular remodeling is largely affected by the infarct size and excessive ECM accumulation [294]. There are currently no drugs that can reverse the pathological remodeling post-MI [114]. However, inhibition of TGF-β can convert activated myofibroblasts to non-activated fibroblasts during scar formation [311].

## 7. Pharmacological therapies targeting cardiac fibrosis and AF

AF therapy aims to prevent AF occurrence and adverse consequences [203, 312]. AF management involves the prevention of thromboembolic events using direct thrombin inhibitors and vitamin K antagonists [313]. Two strategies are used for AF management, including rhythm

and rate control [314]. The rhythm control strategy restores normal sinus rhythm, while the rate control strategy targets the ventricular rate and reduces AF symptoms [314]. The rhythm controllers, which are anti-arrhythmic drugs, are $Na^+$ and $K^+$ channel blockers that prevent AF via prolongation of atrial refractoriness [315]. The rate controllers include $Ca^{2+}$ channel blockers, β-blockers and digoxin. There are several limitations to pharmacological AF therapy, such as substantial adverse effects and incomplete efficacy [13].

Clinically, AF treatment depends on the AF duration, other medical conditions and symptom severity [315]. When AF is present for a long time, the treatment becomes less efficient in terminating AF [129]. Non-pharmacological AF therapies, which are only effective in particular cases that are resistant to pharmacological options, include implantation of pacemakers, AV node ablation and LA ablation [128]. There is a need for the development of new safe and efficient drugs for AF management.

Upstream therapy of AF targets atrial structural changes, such as oxidative stress, fibrosis, inflammation and hypertrophy, which directly or indirectly modulate the atrial electrophysiology [203, 312]. Several therapies are used to delay atrial structural remodeling in AF, such as 3-hydroxy-3-methyl-glutaryl-CoA reductase inhibitors, PDGF inhibitors, TGF-β1 inhibitors, mineralocorticoid/aldosterone receptor antagonists and RAAS inhibitors [16, 316, 317]. Atrial structural remodeling and AF occurrence can be decreased upon treatment with antioxidant and anti-inflammatory agents [318-320]. RAAS inhibitors consist of angiotensin receptor blockers (ARBs) and ACE inhibitors. Trandolapril, an ACE inhibitor, decreases AF incidence in acute MI patients [321]. Valsartan, an ARB, reduces AF risk in HF patients [322]. However, the effect of RAAS inhibition is not completely proven in preventing AF associated

with coronary artery diseases, diabetes mellitus and hypertension [317]. ARBs and ACE inhibitors may be more effective in preventing AF occurrence rather than decreasing AF recurrences [312]. Shimada *et al.* [323] stated that blockers of AT1R prevent the production of collagen. Moreover, ACE inhibitors decrease cardiac fibrosis in HF models [323]. Statins, which are 3-hydroxy-3-methyl-glutaryl-CoA reductase inhibitors, can decrease AF incidence by improving lipid metabolism or reducing inflammatory mediators and MMP expression [317]. In the guidelines of the European Society of Cardiology, statins are recommended to be used for the treatment of AF with CHF or postoperative AF [324]. Polyunsaturated fatty acids (PUFAs) have anti-fibrillatory effects through modulating MAPK activity, membrane fluidity and several ion channels [317]. Administration of omega-3 PUFAs decreases atrial structural remodeling and AF incidence [325-327]. Corticosteroids, which are anti-inflammatory agents, are less efficient in preventing postoperative AF [328, 329]. However, a high dose of corticosteroids may induce AF [330]. There is no strong evidence for the use of corticosteroids or PUFAs in AF management [312]. As a TGF-β1 inhibitor, pirfenidone attenuates atrial remodeling and AF susceptibility [269, 331]. Activin receptor-like kinase 5 (ALK5), a blocker of TGF-β type I receptors, decreases cardiac fibrosis in MI and pressure overload models [332]. Moreover, blocking PDGF receptors post-MI attenuates fibrosis progression in the non-infarcted area of the myocardium in rats [333]. PDGFR-α-specific antibodies suppress atrial fibrosis and AF development in a pressure overload model [275].

# Part II– Role of the lysyl oxidase enzyme family in cardiac function and disease

## Article 1

## Article Title: Role of the lysyl oxidase enzyme family in cardiac function and disease

This article was submitted to Cardiovascular Research on 19th February 2019 and it was accepted on 9th May 2019.

## Contributions of authors

**Doa'a Ghazi Al-u'datt** designed the covered topic, wrote the draft of manuscript, generated tables and figures, and revised the manuscript.

**Bruce Allen** edited and approved the final draft of the manuscript.

**Stanley Nattel** conceived the original idea, supervised the project, provided intellectual ideas for the topics, proposed generated tables and figures, revised the manuscript and approved the final draft.

# Role of the lysyl oxidase enzyme family in cardiac function and disease

**Doa'a Al-u'datt[1,2], Bruce G. Allen[1,2,3,4], and Stanley Nattel[1,2,3,5]**

[1]Department of Pharmacology and Physiology, Université de Montréal, Montreal, Quebec, Canada.

[2]Montreal Heart Institute and Université de Montréal, Montreal, Quebec, Canada.

[3]Department of Medicine, Montreal Heart Institute, Montreal, Quebec, Canada.

[4]Department of Biochemistry and Molecular Medicine, Université de Montréal, Montreal, Quebec, Canada.

[5]Department of Pharmacology and Therapeutics, McGill University, Montreal, Quebec, Canada.

**Running head:** LOX and LOX-like enzymes in heart

*Address correspondence to: Stanley Nattel, Montreal Heart Institute, 5000 Belanger Street East, Montreal, Quebec, H1T 1C8, Canada. Tel.: 514-376-3330; Fax: 514-376-1355. E-mail: stanley.nattel@icm-mhi.org.

## Abstract

Heart diseases are a major cause of morbidity and mortality world-wide. Lysyl oxidase (LOX) and related LOX-like (LOXL) isoforms play a vital role in remodeling the extracellular matrix (ECM). The LOX family controls ECM formation by cross-linking collagen and elastin chains. LOX/LOXL proteins are copper-dependent amine oxidases that catalyze the oxidation of lysine, causing cross-linking between the lysine moieties of lysine-rich proteins. Dynamic changes in LOX and LOXL protein-expression occur in a variety of cardiac pathologies; these changes are believed to be central to the associated tissue-fibrosis. An awareness of the potential pathophysiological importance of LOX has led to the evaluation of interventions that target LOX/LOXL proteins for heart-disease therapy. The purposes of this review article are: 1) To summarize the basic biochemistry and enzyme function of LOX and LOXL proteins; 2) To consider their tissue and species distribution; and 3) To review the results of experimental studies of the roles of LOX and LOXL proteins in heart disease, addressing involvement in the mechanisms, pathophysiology and therapeutic responses based on observations in patient samples and relevant animal models. Therapeutic targeting of LOX family enzymes has shown promising results in animal models, but small-molecule approaches have been limited by non-specificity and off-target effects. Biological approaches show potential promise but are in their infancy. While there is strong evidence for LOX-family protein participation in heart failure, myocardial infarction, cardiac hypertrophy, dilated cardiomyopathy, atrial fibrillation and hypertension, as well as potential interest as therapeutic targets, the precise involvement of LOX-family proteins in heart disease requires further investigation.

**Keywords** LOX • LOX-like (LOXL) proteins • Myocardial infarction • Heart failure • Hypertrophy • Dilated cardiomyopathy • Atrial fibrillation • Fibrosis • Hypertension.

## Abbreviations

α-SMA: α-smooth muscle actin; Ac-SDKP: N-acetyl-seryl-aspartyl-lysyl-proline; AF: Atrial fibrillation; AGEs: Advanced glycation end products; Ang II: Angiotensin II; AS: Aortic stenosis; BAPN: β-aminopropionitrile; BMP-1: Bone morphogenetic protein 1; CRL: Cytokine receptor-like; CTGF: Connective tissue growth factor; DCM: Dilated cardiomyopathy; ECM: Extracellular matrix; FGF2, Fibroblast growth factor-2; ER: Endoplasmic reticulum; HF: Heart failure; HFD: High-fat diet; HW: Heart weight; IFN: Interferon; IL-6: Interleukin 6; LA: Left atrium; LOX: Lysyl oxidase; LOXL: Lysyl oxidase like; LTQ: Lysine tyrosylquinone; LV: Left ventricle; MI: Myocardial infarction; miRNA: MicroRNA; MMPs: Matrix metalloproteinases; NF-κB: Nuclear factor-kappa β; NFAT: Nuclear factor of activated T-cells; p38 MAPK: p38 mitogen-activated protein kinase; PCPase: Procollagen C-proteinase; PNPase: Procollagen N-proteinase; RA: Right atrium; Rac 1 GTPase: Rac family small GTPase 1; RacET: Transgenic mice with Rac1 overexpression; ROS: Reactive oxygen species; siRNA: Small interfering RNA; SM22α: Smooth muscle protein 22α; SRCR: Scavenger receptor cysteine rich; TAC: Transverse aortic constriction; TGF-β: Transforming growth factor β; TgLOX: Transgenic mice with LOX overexpression; TIMPs: Tissue inhibitors of MMPs; TNF-α*:* Tumor necrosis factor-α; VSMCs: Vascular smooth muscle cells; VO: Volume overload.

# 1. Introduction

The extracellular matrix (ECM) plays a key role in cardiac function. It establishes a skeleton into which the cellular components of the heart, notably cardiomyocytes and the vascular elements that form blood vessels, are structurally integrated to ensure proper function. Fibrotic expansion of the ECM is a characteristic part of the cardiac response to many stressors and pathologies, including pressure overload, myocardial infarction (MI) and cardiomyopathy [1, 2]. Fibrosis is a complex process, characterized by excessive secretion by fibroblasts of ECM-related proteins, including procollagen and fibronectin, insoluble collagen and enzymes that modify structural ECM proteins (like matrix metalloproteinases (MMPs) and tissue inhibitors of MMPs (TIMPs)) [3]. While fibrosis is crucial for wound healing as occurs in MI [4]. maladaptive fibrosis leads to stiffening of the ventricles and progression of heart failure (HF) [4-6]. Under normal conditions, there is a balance between synthesis and degradation of fibrillar collagen; [7] when the heart is injured, or exposed to a range of pathological stressors, collagen accumulation exceeds degradation, producing fibrosis [1, 8].

Fibrosis impairs myocardial relaxation and causes diastolic dysfunction, [9] increasing the probability of HF development [10]. HF is associated with substantial morbidity and mortality [11]. Cardiac fibrosis also impedes propagation of the cardiac impulse, leading to arrhythmias such as atrial fibrillation (AF) [12]. AF is the most common sustained arrhythmia and is associated with adverse outcomes like stroke, HF and death [13].

Collagen, the most abundant protein of the ECM, is composed of three polypeptide α-chains, [3, 14] which form a triple helix of tropocollagen molecules wrapped around each other in a rope-like manner [3, 14, 15]. As shown in Figure 1, collagens are synthesized as large precursor

procollagen molecules [3, 14-17]. Procollagen is post-translationally modified within the endoplasmic reticulum (ER) through glycosylation of the triple helices and hydroxylation of proline and lysine residues to enhance helix stability, [14, 16, 17] and then translocated from the ER to the Golgi apparatus to be exported from the cell via exocytosis [14, 17]. In the extracellular space, procollagen is subjected to enzymatic cleavage of the amino and carboxy termini by procollagen N-proteinase (PNPase) and procollagen C-proteinase (PCPase), respectively, following which collagen assembles into fibrils [18]. Collagen fibrils are converted to mature collagens through intermolecular and intramolecular cross-linking, which increases fiber strength and stability [19]. Collagen cross-linking occurs via two mechanisms: an enzymatic (catalyzed via members of the transglutaminase or lysyl oxidase (LOX) family) and a non-enzymatic (promoted by advanced glycation end-products; AGEs) process [20-23].

AGEs are products of the condensation of carbohydrates (like glucose or fructose) or lipids with proteins through spontaneous non-enzymatic reactions [24]. AGEs modify the mechanical properties of collagen through cross-linking processes that increase myocardial stiffness [24]. AGEs can also upregulate LOX mRNA in some pathological conditions [25]. In one study, alagebrium (ALT-711), which blocks AGE-mediated cross-linking, improved cardiac function through reduction of collagen cross-linking in hypertensive rats [26]. Transglutaminases, a group of multifunctional enzymes, cross-link lysine and glutamine residues to produce proteolysis resistant products (ε-(γ-glutamyl)-lysine isopeptide bonds, resulting in stability and rigidity of ECM [22, 23]. LOX is a copper-dependent amine oxidase that oxidizes lysine to form cross-links in elastin and collagen [27]. While elastin cross-links are irreversible, collagen cross-linking may be reversible [15]. Recent studies suggest that LOX-family inhibition can improve cardiac function in various experimental models, suggesting that LOX might provide a novel

therapeutic target. The purpose of this paper is to address the roles of LOX isoforms in heart disease, specifically focusing on: 1) The biochemical properties of LOX-family proteins; 2) Evidence for their role in a variety of cardiac conditions including HF, MI, hypertrophy, cardiomyopathies, hypertension and AF; and 3) The opportunities and challenges associated with targeting the LOX-family as a therapeutic intervention.

## 2. Historical overview

LOX was first identified by Pinnell and Martin [28] as the enzyme involved in elastin and collagen cross-linking in connective tissue derived from bone [29]. Subsequent studies characterized its chemical properties and classified LOX and related enzymes as amine oxidases known collectively as the LOX family [27]. Two subfamilies of LOX have been identified during metazoan evolution, including specifically: (1) LOX, LOX-like protein 1 (LOXL-1) and LOXL-5, (2) LOXL-2, LOXL-3 and LOXL-4, based on overall domain structure and the similarity of sequence in the catalytic domain [30]. LOXL-5 is exclusively found in fish [30]. Tsuda *et al.* [31] reported that LOX is markedly upregulated in the mouse heart during early embryonic heart development (days 11 and 13), pointing to a role in tissue differentiation. The highest expression of LOX-family isoforms is found in vertebrates, [30] with five recognized in mammals: LOX, LOXL-1, LOXL-2, LOXL-3, LOXL-4 [32]. LOX acts on lysine within peptides; free lysine is not a substrate [28]. Each of the LOX subfamilies has distinct molecular and functional features, as detailed below.

## 3. LOX-family structure and biochemical function

### 3.1 Chemical structure of LOX-family

LOX proteins (Figure 2) comprise three domains: The N-terminal domain, the N-terminal signal peptide sequence and the C-terminal domain required for catalytic activity [33]. LOX and LOXL proteins (Figure 2) share amine oxidase function mediated by a common catalytic domain, including a copper-binding motif, cytokine receptor-like (CRL) domain, lysine tyrosylquinone (LTQ) cofactor-moiety and twelve cysteine residues [34-36]. Ten of the cysteine residues are located in the catalytic site, while two are within the propeptide domain [37]. The C-terminal motifs are highly conserved across species, including *Drosophila*, mouse, rat, chicken, fish and human [37, 38]. LOX/LOXL proteins contain four unique histidine residues within the copper binding domain [39]. LTQ, a unique carbonyl cofactor essential for the catalytic function of LOX/LOXL, is formed by autocatalytic hydroxylation and oxidation of Tyr349 with the assistance of a copper ion cofactor at the active site [40]. The CRL domain is located within the C-terminus, similar to the N-terminal domain of the cytokine receptor and growth-factor family [34, 35]. LOX and LOXL-1 have distinctive propeptide areas. LOXL-2, LOXL-3 and LOXL-4 contain four conserved scavenger receptor cysteine-rich (SRCR) domains in their N-terminal [41]. Martinez *et al.* [42] noted that SRCR domains may mediate protein-protein interactions in the ECM.

LOX is encoded in humans by a gene containing seven exons located at chromosome 5q23.3-31.2 [27, 43]. The 417 amino-acid LOX protein is the most abundant isoform in skeletal muscle, heart, kidneys and lungs. The LOXL-1 gene located on chromosome 15 encodes a 574-

amino acid protein predominant in the pancreas, skeletal muscle, spleen, heart and lungs. LOXL-2, encoded on chromosome 8, includes 774 amino acids and is principally expressed in testis, ovary, thymus, skin and lung cells. LOXL-3 and LOXL-4 are composed of 753 and 756 amino acids, respectively (encoded on chromosomes 2 and 10, respectively), and are predominant in ovary, uterus, testis, heart, pancreas and skeletal muscle [20, 44]. The catalytic domains of LOX and LOXL-1 show the greatest similarity, with 88% homology; LOXL-2, LOXL-3 and LOXL-4 show approximately 67% catalytic-domain homology with LOX and about 88% homology with each other [34]. LOXL-4 contains an 13 amino acid insert that is not found within LOXL-2 or LOXL-3 [44]. Copper is critical to LOX enzyme activity: [39, 45, 46] The first step in LOX-induced catalysis, involving aldehyde formation, requires the presence of copper ions [46]. Additionally, copper is needed to stabilize enzyme-structure [46]. Copper-deficiency in rodents is associated with decreased collagen cross-linking as a result of decreased LOX activity, [47] producing a syndrome with multiple arterial aneurysms similar to the consequences of genetic LOX-dysfunction [48]. Tinker *et al.* [49] reported that a copper-deficient diet decreases collagen cross-linking and increases elastin degradation in chick aorta, whereas copper supplements restore cross-linking. LOX activity and collagen cross-linking in cardiac tissues were affected by gender and dietary carbohydrate types in copper-deficient rats [50].

### 3.2 LOX-dependent enzymatic reactions in heart

Collagen is subjected to a range of post-translational modifications, including hydroxylation of lysine and proline, glycosylation of hydroxylysine and oxidative deamination of lysine residues [51]. LOX/LOXL enzymes are secreted into the extracellular space, where they act on the ECM [20, 52]. The LOX family may also have intracellular functions, such as regulating

the motility and migration of fibroblasts, monocytes and smooth muscle cells and altering gene-transcription [53].

Figure 3 shows the reaction sequence for collagen-processing by LOX-family enzymes, including conversion of the ε-amino group in peptidyl lysine to peptidyl aldehyde in the presence of oxygen and water with the formation of hydrogen peroxide. LOX-family catalysis is highly specific for lysine and hydroxylysine residues [54]. The primary step in elastin and collagen cross-linking is the formation of an α-aminoadipic-δ-semialdehyde from peptidyl lysine or hydroxylysine, [55] producing hydroxyallysyl or allysyl residues [27, 36, 52]. These semialdehydes can spontaneously react and condense with neighboring amino groups or peptidyl aldehydes to form dehydrolysinonorleucine and aldol condensation byproducts, respectively [27, 36, 52]. The dehydrolysinonorleucine and aldol condensation byproducts are rearranged through non-enzymatic reactions to form the final products deoxypyridoline and pyridoline, which are responsible for collagen cross-linking [27, 56]. The reduced enzyme is then re-oxidized in the presence of oxygen and the LTQ group is hydrolyzed, releasing ammonia and hydrogen peroxide [28]. The resulting intramolecular cross-links connect chains within tropocollagen molecules, while intermolecular cross-links occur between tropocollagens [15].

### 3.3 Biosynthesis, secretion and activation of LOX

Figure 4 illustrates the biosynthesis, secretion and activation of LOX in heart tissues. LOX is regulated at three stages: first, through its precursor synthesis by fibroblasts; second, at the transformation of precursor to an active form; and third, by stimulation of enzyme activity [57]. Post-translational processing of the immature LOX proenzyme involves removal of the signal peptide by cleavage at Cys21-Ala22 and N-terminal glycosylation in the ER and Golgi apparatus

[20, 33]. The 50-kDa LOX proenzyme is secreted from the Golgi apparatus into the extracellular space, where it is cleaved between Gly168 and Asp169 by PCPase, and to a lesser extent by aminopeptidase-B or mammalian Tolloid-like-1 protein, to yield the active 30-kDa LOX and 18-kDa LOX-derived peptide [20, 40, 58-61]. PCPase, a member of the astacin family of metalloproteinases, is strongly expressed in the myocardium [62, 63]. In addition, fibronectin facilitates cleavage of the LOX proenzyme by PCPase, possibly by serving as a scaffold for the proteinase-substrate complex [64]. Mitochondrial-derived reactive oxygen species (ROS) initiate collagen cross-linking through activation of LOX enzymes in cultured fibroblasts [65]. The specific biochemical features of the LOX family provide insights into function, along with potential therapeutic targets for intervention.

## 4. Overview of LOX expression and function in different systems

Members of the LOX family can oxidize a variety of basic proteins [66]. In addition to collagen and elastin cross-linking, LOX has been implicated in other cellular functions, including control of epithelial-mesenchymal transition; cell migration, adhesion, growth and transformation; monocyte chemotaxis; gene regulation; Ras oncogene inhibition; and collagen promotor activation [36, 67-71]. The LOX family plays a significant role in the genesis and repair of respiratory, skeletal and cardiovascular systems [20, 27, 36, 72]. The upregulation of LOX isoforms is associated with the imbalance between ECM degradation and synthesis involved in fibrotic disorders including liver fibrosis, glaucoma, cardiac fibrosis, diabetic nephropathy, atherosclerosis and pulmonary fibrosis [35, 40, 73-76]. Changes in ECM composition and associated fibrosis contribute to functional and structural alterations in the cardiovascular system caused by obesity and metabolic syndrome [77, 78]. Thus, in addition to a well-known role in the ECM,

LOX-family members might participate in other functions in the heart and elsewhere. These might mediate therapeutic effects but also adverse actions, and need to be better understood.

## 5. Role of LOX-family enzymes in heart disease

Limited information is available concerning the role of LOX-family proteins in normal cardiac function. Fibrotic ECM remodeling is a major contributor to cardiac dysfunction in a wide range of cardiac pathologies [79-84]. Figure 5 illustrates the principal role of the LOX-family in heart disease.

### 5.1 Role of LOX-family enzymes in ventricular dysfunction

Hypertension, pressure overload, ischemia and metabolic alterations upregulate hypoxia inducible factor-1α (HIF-1α), AGEs, transforming growth factor β (TGF-β), PCPase and ROS, leading to increased expression and activity of LOX/LOXL proteins [85]. Cardiac hypertrophy initially occurs as an adaptive process, but can progress to maladaptive pathological hypertrophy via multiple signaling pathways that ultimately lead to reduced contractility and diastolic dysfunction [86, 87]. The shift from cardiac hypertrophy to HF is correlated with cardiomyocyte death and alterations in the ECM [88]. Hypertrophied rat and human hearts show increases in total collagen, collagen-I and collagen-III [89]. LOX-family isoform expression correlates with fibrosis [90, 91]. LOX mRNA is upregulated in a wide variety of animal heart-disease models (hypertrophied hearts of spontaneously hypertensive rats, diet-induced metabolic syndrome) and patient (DCM and HF) models [20, 57, 92]. Collagen tensile strength is closely related to cross-linking, [41] which is a critical step that determines myocardial stiffness in HF [93-95]. Excessive myocardial collagen cross-linking is associated with higher risk for hospitalization in

hypertensive patients with HF [96]. In chronic volume-overloaded rats, an increase in LOX expression and activity, total collagen and collagen cross-linking are associated with the development of HF; these are attenuated by LOX inhibition [97-99]. LOXL-2 expression is increased in the cardiac interstitium and correlates with collagen cross-linking and cardiac dysfunction in failing human hearts [84]. LOXL-2 is also increased in the serum of HF-patients, correlating with biomarkers of HF, collagen cross-linking and cardiac dysfunction [84].

During MI, there is substantial remodeling of ECM to form a scar, and cardiac dysfunction associated with MI leads to interstitial fibrosis in the non-infarcted tissue [95]. Upregulation of LOX isoforms contributes to cardiac ECM remodeling and myocardial dysfunction after MI [95, 100]. Left and right ventricular fibrosis were associated with an upregulation of LOX expression in the infarcted rats with HF [101]. Rhesus monkeys with MI induced by ligation of the left anterior descending artery show increased LOX activity/expression in the scar region [102]. Table 1 summarizes the results of selected studies of LOX-family isoforms in HF pathophysiology.

Table 2 summarizes selected studies of LOX-family involvement in cardiac remodeling associated with hypertension, metabolic syndrome, and pressure overload and other conditions producing cardiac hypertrophy. Hypertensive patients show increases in LV-stiffness, collagen content, collagen cross-linking and LOX expression [57, 103]. The progression from hypertensive heart disease to HF involves prominent fibrosis associated with LOX-induced collagen cross-linking [57, 104, 105]. The induction of collagen cross-linking by LOX is strongly correlated with fibrosis and LV-rigidity, but does not correlate directly with blood pressure [106]. LOX expression, collagen cross-linking and LV-rigidity are correlated with active PCPase in the myocardium of HF and hypertensive patients [107].

LOXL-1 mRNA is upregulated in response to a range of hypertrophic stimuli, and cardiomyocyte-specific transgenic overexpression of LOXL-1 induces cardiac hypertrophy and interstitial fibrosis in mice [108]. Transgenic LOX overexpression enhanced LOX-levels in cardiomyocytes and cardiac fibroblasts, producing mild left ventricular (LV) hypertrophy and diastolic dysfunction even in the absence of stressors [109]. In the presence of a cardiac stressor (angiotensin-II (Ang II) infusion), LOX overexpression increased cardiac fibrosis and hypertrophy and reduced LV-function [109]. Yang *et al.* [84] reported that a monoclonal antibody to LOXL-2 is capable of preventing diastolic dysfunction, tissue fibrosis and chamber dilation in mice subjected to transverse aortic constriction (TAC).

### 5.2 LOX-family enzymes in atrial disorders

Atrial fibrosis disturbs conduction properties and promotes re-entrant AF [12]. Left atrial (LA) fibrosis in AF-patients is accompanied with increases in microRNA-21, Ang II, Rho-GTPase Rac1, connective tissue growth factor (CTGF) and LOX [20, 57, 91, 110-112]. Adam *et al.* [91] demonstrated that AF-patients showed higher levels of total collagen, cross-linked collagen, fibronectin, CTGF, Rac1 activity and LOX compared to sinus-rhythm patients. Furthermore, mineralocorticoid receptor signaling stimulates atrial fibrosis and is associated with activation of fibrotic mediators like miRNA-21, LOX, CTGF, collagen and RhoA activity [113]. Transgenic mice with cardiac Rac1 (RacET) overexpression are susceptible to AF and show increased levels of LOX, fibronectin and CTGF, as well as collagen cross-linking [91]. Zhong *et al.* [114] showed that LOXL-2 is significantly upregulated in the right atria (RA) of patients with long-standing AF, but not with paroxysmal AF. LOXL-2 upregulation is accompanied by increases in collagen (type I and type III), fibronectin, TGF-β2 and CTGF [114]. LOXL-2 plasma concentrations are

increased in AF patients and correlate with LA fibrosis [115]. Table 3 summarizes the principal published reports regarding the role of LOX/LOXL proteins in AF. There is thus extensive evidence for a role of LOX-family members in a variety of forms of heart disease, raising the interesting possibility of therapeutic targeting.

## 6. Therapeutic modulation of LOX-family protein function in cardiac diseases

A number of studies have begun to address the potential value of inhibiting LOX-family proteins and thereby decreasing the amount of insoluble cross-linked collagen as a therapeutic approach for heart disease. The majority of presently-available small-molecule LOX inhibitors are reactive, toxic and non-specific [116-118]. LOX inhibitors are classified into two groups: primary amines (benzylamines, taurine, allylamines and β-aminopropionitrile (BAPN)), and hydrazines (thiosemicarbazide, semicarbazide and isoniazide derivatives) [119-124]. Homocysteine thiolactone, a metabolic byproduct of *S*-adenosylhomocysteine, inhibits LOX activity through conjugation with the LTQ cofactor [123]. Hydroxamate derivatives of diaminoacid-containing compounds, including glutamic, diamino and succinic acids, have been shown to inhibit extracellular LOX activity by binding to zinc in the active site of PCPase [125-127]. Vicinal diamines such as aminoalkylaziridines, hydralazines and halogenated allyl amines also inhibit LOX [122, 124, 128]. Furthermore, *in vitro* and *in vivo* studies have reported that heparin, niacine, 2-mercaptopyridine-*N*-oxide, taurine, thiram and disulfiram inhibit LOX-activity [69, 129-131]. Hajdu *et al.* [131] used a 2-dimensional ligand-based chemoinformatic method and identified ten synthesized ligands (TGX-L series) with significant inhibitory activity for LOX isoforms.

BAPN, the most commonly used LOX inhibitor, was first employed to block LOX action in the early 1970s [132]. BAPN inhibits LOX directly by forming an irreversible covalent bond in the catalytic site of LOX, possibly involving the primary amine of BAPN and carbonyl group in the LOX catalytic site, blocking the conversion of lysyl to allysyl residues in substrate proteins [15, 133]. BAPN, which has no effect on other amine oxidases, [134] decreases collagen cross-linking and LV-stiffness in adult pigs [135] and cardiac fibrosis in aging mouse and hypertrophic rat hearts [136, 137]. The toxic vascular manifestations of lathyrism/odoratism, classically caused by overconsumption of *Lathyrus odoratus* (sweet pea) seeds, result from effects of the nitrile and unsubstituted amino groups in the β-aminopropionitrile structure [138, 139]. BAPN or LOX knockdown reduces the ability of leptin to enhance collagen-I synthesis, ROS production and the expression of profibrotic mediators in vascular and cardiac cells [77]. BAPN also attenuates cardiac hypertrophy induced by Ang II infusion *in vivo* [108]. BAPN prevents the increase in MMPs, collagen-I/III and collagen cross-linking, while improving cardiac function, in volume-overloaded rats [98, 99]. AB0023, a LOXL-2-inhibitory monoclonal antibody, prevents fibroblast activation, reduces tumor formation, prevents pathological fibrosis across several disease models, and reverses bleomycin-induced lung fibrosis [140]. AB0023 was more effective than BAPN in reducing MDA-MB-435 cell tumor volume [140]. Both AB0023 administration and the conditional, global knockout of LOXL-2 reduce TAC-induced cardiac fibrosis and chamber dilatation, while improving systolic and diastolic function, in mice [84].

TGF-β upregulates LOX mRNA and protein expression in fibroblasts [141, 142]. P144, a TGF-β inhibitor peptide, reduces LOX expression and decreases cross-linked collagen deposits without toxic effects in spontaneously-hypertensive rats [103]. Similarly, TGF-β blockade by an

orally-available ALK5-inhibitor improves cardiac function in aortic-banded rats through reduction of collagen cross-linking and deposition [143].

The beneficial actions of a variety of drugs may be mediated, at least in part, by reduced LOX/LOXL-action. LOX is overexpressed in human HF, and torasemide-treated patients show lower LOX-expression and greater normalization of LV-stiffness than patients treated with furosemide [57]. Torasemide inhibits aldosterone synthase in human lung fibroblasts, while reducing CTGF and LOX expression in cardiac fibroblasts and preventing atrial fibrosis and AF in a transgenic mouse model [144]. Gonzalez *et al.* [145] reported that the N-acetyl-seryl-aspartyl-lysyl-proline (Ac-SDKP), a tetrapeptide produced from thymosin-β4, prevents Ang II-induced increases in total and cross-linked collagen, LOX mRNA expression, LOXL-1 protein expression, nuclear translocation of nuclear factor-kappa β (NF-κB), CD4+/CD8+ lymphocyte infiltration and CD68+ macrophage infiltration. A losartan metabolite, EXP3179, decreases LV stiffness, cardiac fibrosis, collagen cross-linking, CTGF and LOX expression in hypertensive patients [146].

Slow but steady progress is being made in the development of more specific LOX-family inhibitors, including agents that target selected isoforms [116]. In addition, biological therapies such as antibodies and RNA-interfering agents may allow for more specific and clinically-applicable LOX targeting in the future [77, 84, 95]. These and other forms of more specific LOX targeting will be essential for LOX-based therapeutics to move forward into the clinically useful arena.

## 7. Conclusions

Emerging evidence points to an important role of LOX and LOXL proteins in a variety of cardiac disease conditions, mediated principally by cross-linking structural ECM-proteins. Other potentially-important effects may exist but are under-studied. Recently-emerging data point to a potentially promising therapeutic role for LOX-family targets in treating heart disease, but lack of specificity and potential adverse consequences of LOX/LOXL-inhibition remain significant limitations of the available agents. More specific small molecule inhibitors and biological therapies hold promise for the future.

## Acknowledgements

The authors thank Lucie Lefebvre for expert secretarial assistance with the manuscript.

**Conflict of interest**

None.

## Funding

This study was supported by the Canadian Institutes of Health Research (Foundation Grant 148401) and the Heart and Stroke Foundation of Canada (18-0022032).

## References

1. Eckhouse SR, Spinale FG. Changes in the myocardial interstitium and contribution to the progression of heart failure. *Heart Fail Clin* 2012;**8**:7-20.

2. Cieslik KA, Trial J, Crawford JR, Taffet GE, Entman ML. Adverse fibrosis in the aging heart depends on signaling between myeloid and mesenchymal cells; role of inflammatory fibroblasts. *J Mol Cell Cardiol* 2014;**70**:56-63.

3. Nattel S. Molecular and cellular mechanisms of atrial fibrosis in atrial fibrillation. *JACC Clini Electrophysiol* 2017;**3**:425-435.

4. Kania G, Blyszczuk P, Eriksson U. Mechanisms of cardiac fibrosis in inflammatory heart disease. *Trends Cardiovasc Med* 2009;**19**:247-252.

5. Krenning G, Zeisberg EM, Kalluri R. The origin of fibroblasts and mechanism of cardiac fibrosis. *J Cell Physiol* 2010;**225**:631-637.

6. Murtha LA, Schuliga MJ, Mabotuwana NS, Hardy SA, Waters DW, Burgess JK, Knight DA, Boyle AJ. The processes and mechanisms of cardiac and pulmonary fibrosis. *Front Physiol* 2017;**8**:777.

7. Barasch E, Gottdiener JS, Aurigemma G, Kitzman DW, Han J, Kop WJ, Tracy RP. Association between elevated fibrosis markers and heart failure in the elderly: The cardiovascular health study. *Circ Heart Fail* 2009;**2**:303-310.

8. Pauschinger M, Knopf D, Petschauer S, Doerner A, Poller W, Schwimmbeck PL, Kuhl U, Schultheiss HP. Dilated cardiomyopathy is associated with significant changes in collagen type I/III ratio. *Circulation* 1999;**99**:2750-2756.

9. Burlew BS, Weber KT. Cardiac fibrosis as a cause of diastolic dysfunction. *Herz* 2002;**27**:92-98.

10. Brower GL, Gardner JD, Forman MF, Murray DB, Voloshenyuk T, Levick SP, Janicki JS. The relationship between myocardial extracellular matrix remodeling and ventricular function. *Eur J Cardiothorac Surg* 2006;**30**:604-610.

11. Metra M, Teerlink JR. Heart failure. *Lancet* 2017;**390**:1981-1995.

12. Burstein B, Nattel S. Atrial fibrosis: Mechanisms and clinical relevance in atrial fibrillation. *J Am Coll Cardiol* 2008;**51**:802-809.

13. Andrade J, Khairy P, Dobrev D, Nattel S. The clinical profile and pathophysiology of atrial fibrillation: Relationships among clinical features, epidemiology, and mechanisms. *Circ Res* 2014;**114**:1453-1468.

14. Mouw JK, Ou G, Weaver VM. Extracellular matrix assembly: A multiscale deconstruction. *Nat Rev Mol Cell Biol* 2014;**15**:771-785.

15. Martin GR, Pinnell SR, Smgal RC, Goldstein ER. Lysyl oxidase: The enzymatic step in collagen and elastin cross-linking. In: Chemistry and molecular biology of the inter-cellular matrix. (E A Balazs, Ed), Vol I, *London and New York: Academic Press* 1970:405-410.

16. Myllyharju J. Intracellular post-translational modifications of collagens. In: Brinckmann J, Notbohm H, Müller PK, eds. Collagen: Primer in structure, processing and assembly. *Berlin, Heidelberg: Springer Berlin Heidelberg,* 2005:115-147.

17. Takawale A, Sakamuri SS, Kassiri Z. Extracellular matrix communication and turnover in cardiac physiology and pathology. *Compr Physiol.* 2015;**5**:687-719.

18. Hulmes DJ. Building collagen molecules, fibrils, and suprafibrillar structures. *J Struc Biol* 2002;**137**:2-10.

19. Eyre DR, Weis MA, Wu JJ. Advances in collagen cross-link analysis. *Methods* 2008;**45**:65-74.

20. Lopez B, Gonzalez A, Hermida N, Valencia F, de Teresa E, Diez J. Role of lysyl oxidase in myocardial fibrosis: From basic science to clinical aspects. *Am J Physiol Heart Circ Physiol* 2010;**299**:H1-9.

21. Heymans S, González A, Pizard A, Papageorgiou AP, López-Andrés N, Jaisser F, Thum T, Zannad F, Díez J. Searching for new mechanisms of myocardial fibrosis with diagnostic and/or therapeutic potential. *Eur J Heart Fail* 2015;**17**:764-771.

22. Lorand L, Graham RM. Transglutaminases: Crosslinking enzymes with pleiotropic functions. *Nat Rev Mol Cell Biol* 2003;**4**:140-156.

23. Eckert RL, Kaartinen MT, Nurminskaya M, Belkin AM, Colak G, Johnson GV, Mehta K. Transglutaminase regulation of cell function. *Physiol Rev* 2014;**94**:383-417.

24. Avendano GF, Agarwal RK, Bashey RI, Lyons MM, Soni BJ, Jyothirmayi GN, Regan TJ. Effects of glucose intolerance on myocardial function and collagen-linked glycation. *Diabetes* 1999;**48**:1443-1447.

25. Papachroni KK, Piperi C, Levidou G, Korkolopoulou P, Pawelczyk L, Diamanti-Kandarakis E, Papavassiliou AG. Lysyl oxidase interacts with AGE signalling to modulate collagen synthesis in polycystic ovarian tissue. *J Cell Mol Med* 2010;**14**:2460-2469.

26. Susic D, Varagic J, Ahn J, Frohlich ED. Cardiovascular and renal effects of a collagen cross-link breaker (ALT 711) in adult and aged spontaneously hypertensive rats. *Am J Hypertens* 2004;**17**:328-333.

27. Smith-Mungo LI, Kagan HM. Lysyl oxidase: Properties, regulation and multiple functions in biology. *Matrix Biol* 1998;**16**:387-398.

28. Pinnell SR, Martin GR. The cross-linking of collagen and elastin: Enzymatic conversion of lysine in peptide linkage to alpha-aminoadipic-delta-semialdehyde (allysine) by an extract from bone. *Proc Natl Acad Sci U S A* 1968;**61**:708-716.

29. Siegel RC, Pinnell SR, Martin GR. Cross-linking of collagen and elastin. Properties of lysyl oxidase. *Biochemistry* 1970;**9**:4486-4492.

30. Grau-Bove X, Ruiz-Trillo I, Rodriguez-Pascual F. Origin and evolution of lysyl oxidases. *Sci Rep* 2015;**5**:10568.

31. Tsuda T, Pan TC, Evangelisti L, Chu ML. Prominent expression of lysyl oxidase during mouse embryonic cardiovascular development. *Anat Rec A Discov Mol Cell Evol Biol* 2003;**270**:93-96.

32. Miana M, Galan M, Martinez-Martinez E, Varona S, Jurado-Lopez R, Bausa-Miranda B, Antequera A, Luaces M, Martinez-Gonzalez J, Rodriguez C, Cachofeiro V. The lysyl oxidase inhibitor beta-aminopropionitrile reduces body weight gain and improves the metabolic profile in diet-induced obesity in rats. *Dis Models Mech* 2015;**8**:543-551.

33. Sethi A, Wordinger RJ, Clark AF. Focus on molecules: Lysyl oxidase. *Exp Eye Res* 2012;**104**:97-98.

34. Finney J, Moon H-J, Ronnebaum T, Lantz M, Mure M. Human copper-dependent amine oxidases. *Arch Biochem Biophys* 2014;**546**:19-32.

35. Csiszar K. Lysyl oxidases: A novel multifunctional amine oxidase family. *Prog Nucleic Acid Res Mol Biol* 2001;**70**:1-32.

36. Lucero HA, Kagan HM. Lysyl oxidase: An oxidative enzyme and effector of cell function. *Cell Mol Life Sci* 2006;**63**:2304-2316.

37. Kagan HM, Reddy VB, Narasimhan N, Csiszar K. Catalytic properties and structural components of lysyl oxidase. *Ciba Found Symp* 1995;**192**:100-115.

38. Langenau DM, Goetz FW, Roberts SB. The upregulation of messenger ribonucleic acids during 17alpha, 20beta-dihydroxy-4-pregnen-3-one-induced ovulation in the perch ovary. *J Mol Endocrinol* 1999;**23**:137-152.

39. Kosonen T, Uriu-Hare JY, Clegg MS, Keen CL, Rucker RB. Incorporation of copper into lysyl oxidase. *Biochem J* 1997;**327 (Pt 1)**:283-289.

40. Kagan HM, Li W. Lysyl oxidase: Properties, specificity, and biological roles inside and outside of the cell. *J Cell Biochem* 2003;**88**:660-672.

41. Trackman PC. Diverse biological functions of extracellular collagen processing enzymes. *J Cell Biochem* 2005;**96**:927-937.

42. Martinez VG, Moestrup SK, Holmskov U, Mollenhauer J, Lozano F. The conserved scavenger receptor cysteine-rich superfamily in therapy and diagnosis. *Pharmacol Rev* 2011;**63**:967-1000.

43. Hamalainen ER, Jones TA, Sheer D, Taskinen K, Pihlajaniemi T, Kivirikko KI. Molecular cloning of human lysyl oxidase and assignment of the gene to chromosome 5q23.3-31.2. *Genomics* 1991;**11**:508-516.

44. Asuncion L, Fogelgren B, Fong KS, Fong SF, Kim Y, Csiszar K. A novel human lysyl oxidase-like gene (LOXL4) on chromosome 10q24 has an altered scavenger receptor cysteine rich domain. *Matrix Biol* 2001;**20**:487-491.

45. Iguchi H, Sano S. Cadmium- or zinc-binding to bone lysyl oxidase and copper replacement. *Connect Tissue Res* 1985;**14**:129-139.

46. Gacheru SN, Trackman PC, Shah MA, O'Gara CY, Spacciapoli P, Greenaway FT, Kagan HM. Structural and catalytic properties of copper in lysyl oxidase. *J Biol Chem* 1990;**265**:19022-19027.

47. Farquharson C, Duncan A, Robins SP. The effects of copper deficiency on the pyridinium crosslinks of mature collagen in the rat skeleton and cardiovascular system. *Proc Soc Exp Biol Med* 1989;**192**:166-171.

48. Rowe DW, McGoodwin EB, Martin GR, Sussman MD, Grahn D, Faris B, Franzblau C. A sex-linked defect in the cross-linking of collagen and elastin associated with the mottled locus in mice. *J Exp Med* 1974;**139**:180-192.

49. Tinker D, Romero-Chapman N, Reiser K, Hyde D, Rucker R. Elastin metabolism during recovery from impaired crosslink formation. *Arch Biochem Biophys* 1990;**278**:326-332.

50. Werman MJ, Barat E, Bhathena SJ. Gender, dietary copper and carbohydrate source influence cardiac collagen and lysyl oxidase in weanling rats. *J Nutr* 1995;**125**:857-863.

51. Kagan HM, Trackman PC. Properties and function of lysyl oxidase. *Am J Respir Cell Mol Biol* 1991;**5**:206-210.

52. Rodriguez C, Martinez-Gonzalez J, Raposo B, Alcudia JF, Guadall A, Badimon L. Regulation of lysyl oxidase in vascular cells: Lysyl oxidase as a new player in cardiovascular diseases. *Cardiovasc Res* 2008;**79**:7-13.

53. Payne SL, Hendrix MJ, Kirschmann DA. Paradoxical roles for lysyl oxidases in cancer--a prospect. *J Cell Biochem* 2007;**101**:1338-1354.

54. Rojkind M, Hhamabata A, Gonzm E, Rendon G. Intermolecular cross-links in rat skin and rat tail collagen. In: Chemistry and molecular biology of the intercellular matrix, Balazs, E. A., Ed. *London and New York: Academic Press* 1970;**I**:293-303.

55. Bornstein P, Kang AH, Piez KA. The nature and location of intramolecular cross-links in collagen. *Proc Natl Acad Sci U S A* 1966;**55**:417-424.

56. Robins SP. Biochemistry and functional significance of collagen cross-linking. *Biochem Soc Trans* 2007;**35**:849-852.

57. Lopez B, Querejeta R, Gonzalez A, Beaumont J, Larman M, Diez J. Impact of treatment on myocardial lysyl oxidase expression and collagen cross-linking in patients with heart failure. *Hypertension* 2009;**53**:236-242.

58. Pischon N, Babakhanlou-Chase H, Darbois L, Ho WB, Brenner MC, Kessler E, Palamakumbura AH, Trackman PC. A procollagen C-proteinase inhibitor diminishes collagen and lysyl oxidase processing but not collagen cross-linking in osteoblastic cultures. *J Cell Physiol* 2005;**203**:111-117.

59. Uzel MI, Shih SD, Gross H, Kessler E, Gerstenfeld LC, Trackman PC. Molecular events that contribute to lysyl oxidase enzyme activity and insoluble collagen accumulation in osteosarcoma cell clones. *J Bone Miner Res* 2000;**15**:1189-1197.

60. Uzel MI, Scott IC, Babakhanlou-Chase H, Palamakumbura AH, Pappano WN, Hong HH, Greenspan DS, Trackman PC. Multiple bone morphogenetic protein 1-related mammalian metalloproteinases process pro-lysyl oxidase at the correct physiological site and control lysyl oxidase activation in mouse embryo fibroblast cultures. *J Biol Chem* 2001;**276**:22537-22543.

61. Lijnen PJ, Petrov VV, Turner M, Fagard RH. Collagen production in cardiac fibroblasts during inhibition of aminopeptidase B. *J Renin Angiotensin-Aldosterone Syst* 2005;**6**:69-77.

62. Kessler E, Takahara K, Biniaminov L, Brusel M, Greenspan DS. Bone morphogenetic protein-1: The type I procollagen C-proteinase. *Science* 1996;**271**:360-362.

63. Hopkins DR, Keles S, Greenspan DS. The bone morphogenetic protein 1/Tolloid-like metalloproteinases. *Matrix Biol* 2007;**26**:508-523.

64. Fogelgren B, Polgar N, Szauter KM, Ujfaludi Z, Laczko R, Fong KS, Csiszar K. Cellular fibronectin binds to lysyl oxidase with high affinity and is critical for its proteolytic activation. *J Biol Chem* 2005;**280**:24690-24697.

65. Majora M, Wittkampf T, Schuermann B, Schneider M, Franke S, Grether-Beck S, Wilichowski E, Bernerd F, Schroeder P, Krutmann J. Functional consequences of mitochondrial DNA deletions in human skin fibroblasts: Increased contractile strength in collagen lattices is due to oxidative stress-induced lysyl oxidase activity. *Am J Pathol* 2009;**175**:1019-1029.

66. Kagan HM, Williams MA, Williamson PR, Anderson JM. Influence of sequence and charge on the specificity of lysyl oxidase toward protein and synthetic peptide substrates. *J Biol Chem* 1984;**259**:11203-11207.

67. Higgins DF, Kimura K, Bernhardt WM, Shrimanker N, Akai Y, Hohenstein B, Saito Y, Johnson RS, Kretzler M, Cohen CD, Eckardt KU, Iwano M, Haase VH. Hypoxia promotes fibrogenesis *in vivo* via HIF-1 stimulation of epithelial-to-mesenchymal transition. *J Clin Invest* 2007;**117**:3810-3820.

68. Lazarus HM, Cruikshank WW, Narasimhan N, Kagan HM, Center DM. Induction of human monocyte motility by lysyl oxidase. *Matrix Biol* 1995;**14**:727-731.

69. Giampuzzi M, Botti G, Di Duca M, Arata L, Ghiggeri G, Gusmano R, Ravazzolo R, Di Donato A. Lysyl oxidase activates the transcription activity of human collagene III promoter. Possible involvement of Ku antigen. *J Biol Chem* 2000;**275**:36341-36349.

70. Nellaiappan K, Risitano A, Liu G, Nicklas G, Kagan HM. Fully processed lysyl oxidase catalyst translocates from the extracellular space into nuclei of aortic smooth-muscle cells. *J Cell Biochem* 2000;**79**:576-582.

71. Kobayashi H, Ishii M, Chanoki M, Yashiro N, Fushida H, Fukai K, Kono T, Hamada T, Wakasaki H, Ooshima A. Immunohistochemical localization of lysyl oxidase in normal human skin. *Br J Dermatol* 1994;**131**:325-330.

72. Li, Liu G, Chou IN, Kagan HM. Hydrogen peroxide-mediated, lysyl oxidase-dependent chemotaxis of vascular smooth muscle cells. *J Cell Biochem* 2000;**78**:550-557.

73. Wordinger RJ, Clark AF. Lysyl oxidases in the trabecular meshwork. *J Glaucoma* 2014;**23**:S55-58.

74. Genovese F, Manresa AA, Leeming DJ, Karsdal MA, Boor P. The extracellular matrix in the kidney: A source of novel non-invasive biomarkers of kidney fibrosis? *Fibrogenesis Tissue Repair* 2014;**7**:4.

75. Schuppan D. Liver fibrosis: Common mechanisms and antifibrotic therapies. *Clin Res Hepatol Gastroenterol* 2015;**39 Suppl 1**:S51-59.

76. Ho YY, Lagares D, Tager AM, Kapoor M. Fibrosis--a lethal component of systemic sclerosis. *Nat Rev Rheumatol* 2014;**10**:390-402.

77. Martinez-Martinez E, Rodriguez C, Galan M, Miana M, Jurado-Lopez R, Bartolome MV, Luaces M, Islas F, Martinez-Gonzalez J, Lopez-Andres N, Cachofeiro V. The lysyl oxidase inhibitor (beta-aminopropionitrile) reduces leptin profibrotic effects and ameliorates cardiovascular remodeling in diet-induced obesity in rats. *J Mol Cell Cardiol* 2016;**92**:96-104.

78. Zibadi S, Vazquez R, Moore D, Larson DF, Watson RR. Myocardial lysyl oxidase regulation of cardiac remodeling in a murine model of diet-induced metabolic syndrome. *Am J Physiol Heart Circ Physiol* 2009;**297**:H976-982.

79. Schelbert EB, Fonarow GC, Bonow RO, Butler J, Gheorghiade M. Therapeutic targets in heart failure: Refocusing on the myocardial interstitium. *J Am Coll Cardiol* 2014;**63**:2188-2198.

80. Butler J, Fonarow GC, Zile MR, Lam CS, Roessig L, Schelbert EB, Shah SJ, Ahmed A, Bonow RO, Cleland JG, Cody RJ, Chioncel O, Collins SP, Dunnmon P, Filippatos G, Lefkowitz MP, Marti CN, McMurray JJ, Misselwitz F, Nodari S, O'Connor C, Pfeffer MA, Pieske B, Pitt B, Rosano G, Sabbah HN, Senni M, Solomon SD, Stockbridge N, Teerlink JR, Georgiopoulou VV, Gheorghiade M. Developing therapies for heart failure with preserved ejection fraction: Current state and future directions. *JACC Heart Fail* 2014;**2**:97-112.

81. Davis J, Molkentin JD. Myofibroblasts: Trust your heart and let fate decide. *J Mol Cell Cardiol* 2014;**70**:9-18.

82. Kong P, Christia P, Frangogiannis NG. The pathogenesis of cardiac fibrosis. *Cell Mol Life Sci* 2014;**71**:549-574.

83. Schelbert EB, Piehler KM, Zareba KM, Moon JC, Ugander M, Messroghli DR, Valeti US, Chang CC, Shroff SG, Diez J, Miller CA, Schmitt M, Kellman P, Butler J, Gheorghiade M, Wong TC. Myocardial fibrosis quantified by extracellular volume is associated with subsequent hospitalization for heart failure, death, or both across the spectrum of ejection fraction and heart failure stage. *J Am Heart Assoc* 2015;**4**:e002613.

84. Yang, Savvatis K, Kang JS, Fan P, Zhong H, Schwartz K, Barry V, Mikels-Vigdal A, Karpinski S, Kornyeyev D, Adamkewicz J, Feng X, Zhou Q, Shang C, Kumar P, Phan D, Kasner M, Lopez B, Diez J, Wright KC, Kovacs RL, Chen PS, Quertermous T, Smith V, Yao L, Tschope C, Chang CP. Targeting LOXL2 for cardiac interstitial fibrosis and heart failure treatment. *Nat Commun* 2016;**7**:13710.

85. Maki JM. Lysyl oxidases in mammalian development and certain pathological conditions. *Histol Histopathol* 2009;**24**:651-660.

86. Manabe I, Shindo T, Nagai R. Gene expression in fibroblasts and fibrosis: Involvement in cardiac hypertrophy. *Circ Res* 2002;**91**:1103-1113.

87. Frey N, Olson EN. Cardiac hypertrophy: The good, the bad, and the ugly. *Ann Rev Physiol* 2003;**65**:45-79.

88. Colucci WS. Molecular and cellular mechanisms of myocardial failure. *Am J Cardiol* 1997;**80**:15l-25l.

89. Yang CM, Kandaswamy V, Young D, Sen S. Changes in collagen phenotypes during progression and regression of cardiac hypertrophy. *Cardiovasc Res* 1997;**36**:236-245.

90. Yu Q, Vazquez R, Zabadi S, Watson RR, Larson DF. T-lymphocytes mediate left ventricular fibrillar collagen cross-linking and diastolic dysfunction in mice. *Matrix Biol* 2010;**29**:511-518.

91. Adam O, Theobald K, Lavall D, Grube M, Kroemer HK, Ameling S, Schafers HJ, Bohm M, Laufs U. Increased lysyl oxidase expression and collagen cross-linking during atrial fibrillation. *J Mol Cell Cardiol* 2011;**50**:678-685.

92. Sivakumar P, Gupta S, Sarkar S, Sen S. Upregulation of lysyl oxidase and MMPs during cardiac remodeling in human dilated cardiomyopathy. *Mol Cell Biochem* 2008;**307**:159-167.

93. Norton GR, Tsotetsi J, Trifunovic B, Hartford C, Candy GP, Woodiwiss AJ. Myocardial stiffness is attributed to alterations in cross-linked collagen rather than total collagen or phenotypes in spontaneously hypertensive rats. *Circulation* 1997;**96**:1991-1998.

94. Badenhorst D, Maseko M, Tsotetsi OJ, Naidoo A, Brooksbank R, Norton GR, Woodiwiss AJ. Cross-linking influences the impact of quantitative changes in myocardial collagen on cardiac stiffness and remodelling in hypertension in rats. *Cardiovasc Res* 2003;**57**:632-641.

95. Gonzalez-Santamaria J, Villalba M, Busnadiego O, Lopez-Olaneta MM, Sandoval P, Snabel J, Lopez-Cabrera M, Erler JT, Hanemaaijer R, Lara-Pezzi E, Rodriguez-Pascual F. Matrix cross-linking lysyl oxidases are induced in response to myocardial infarction and promote cardiac dysfunction. *Cardiovasc Res* 2016;**109**:67-78.

96. Lopez B, Ravassa S, Gonzalez A, Zubillaga E, Bonavila C, Berges M, Echegaray K, Beaumont J, Moreno MU, San Jose G, Larman M, Querejeta R, Diez J. Myocardial collagen cross-linking is associated with heart failure hospitalization in patients with hypertensive heart failure. *J Am Coll Cardiol* 2016;**67**:251-260.

97. El Hajj EC, El Hajj MC, Ninh VK, Gardner JD. Cardioprotective effects of lysyl oxidase inhibition against volume overload-induced extracellular matrix remodeling. *Exp Biol Med* 2016;**241**:539-549.

98. El Hajj EC, El Hajj MC, Ninh VK, Bradley JM, Claudino MA, Gardner JD. Detrimental role of lysyl oxidase in cardiac remodeling. *J Mol Cell Cardiol* 2017;**109**:17-26.

99. El Hajj EC, El Hajj MC, Ninh VK, Gardner JD. Inhibitor of lysyl oxidase improves cardiac function and the collagen/MMP profile in response to volume overload. *Am J Physiol Heart Circ Physiol* 2018;**315**:H463-h473.

100. Ovet H, Oztay F. The copper chelator tetrathiomolybdate regressed bleomycin-induced pulmonary fibrosis in mice, by reducing lysyl oxidase expressions. *Biol Trace Elem Res* 2014;**162**:189-199.

101. Stefanon I, Valero-Munoz M, Fernandes AA, Ribeiro RF, Jr., Rodriguez C, Miana M, Martinez-Gonzalez J, Spalenza JS, Lahera V, Vassallo PF, Cachofeiro V. Left and right ventricle late remodeling following myocardial infarction in rats. *PloS One* 2013;**8**:e64986.

102. Xie Y, Chen J, Han P, Yang P, Hou J, Kang YJ. Immunohistochemical detection of differentially localized up-regulation of lysyl oxidase and down-regulation of matrix metalloproteinase-1 in rhesus monkey model of chronic myocardial infarction. *Exp Biol Med* 2012;**237**:853-859.

103. Hermida N, Lopez B, Gonzalez A, Dotor J, Lasarte JJ, Sarobe P, Borras-Cuesta F, Diez J. A synthetic peptide from transforming growth factor-beta1 type III receptor prevents myocardial fibrosis in spontaneously hypertensive rats. *Cardiovasc Res* 2009;**81**:601-609.

104. Weber KT. Fibrosis and hypertensive heart disease. *Curr Opin Cardiol* 2000;**15**:264-272.

105. Levy D, Larson MG, Vasan RS, Kannel WB, Ho KK. The progression from hypertension to congestive heart failure. *Jama* 1996;**275**:1557-1562.

106. Yu Q, Horak K, Larson DF. Role of T lymphocytes in hypertension-induced cardiac extracellular matrix remodeling. *Hypertension* 2006;**48**:98-104.

107. Lopez B, Gonzalez A, Beaumont J, Querejeta R, Larman M, Diez J. Identification of a potential cardiac antifibrotic mechanism of torasemide in patients with chronic heart failure. *J Am Coll Cardiol* 2007;**50**:859-867.

108. Ohmura H, Yasukawa H, Minami T, Sugi Y, Oba T, Nagata T, Kyogoku S, Ohshima H, Aoki H, Imaizumi T. Cardiomyocyte-specific transgenic expression of lysyl oxidase-like protein-1 induces cardiac hypertrophy in mice. *Hypertens Res* 2012;**35**:1063-1068.

109. Galan M, Varona S, Guadall A, Orriols M, Navas M, Aguilo S, de Diego A, Navarro MA, Garcia-Dorado D, Rodriguez-Sinovas A, Martinez-Gonzalez J, Rodriguez C. Lysyl oxidase overexpression accelerates cardiac remodeling and aggravates angiotensin II-induced hypertrophy. *FASEB J* 2017;**31**:3787-3799.

110. Adam O, Frost G, Custodis F, Sussman MA, Schafers HJ, Bohm M, Laufs U. Role of Rac1 GTPase activation in atrial fibrillation. *J Am Coll Cardiol* 2007;**50**:359-367.

111. Adam O, Lavall D, Theobald K, Hohl M, Grube M, Ameling S, Sussman MA, Rosenkranz S, Kroemer HK, Schafers HJ, Bohm M, Laufs U. Rac1-induced connective tissue growth factor regulates connexin 43 and N-cadherin expression in atrial fibrillation. *J Am Coll Cardiol* 2010;**55**:469-480.

112. Adam O, Lohfelm B, Thum T, Gupta SK, Puhl SL, Schafers HJ, Bohm M, Laufs U. Role of miR-21 in the pathogenesis of atrial fibrosis. *Basic Res Cardiol* 2012;**107**:278.

113. Lavall D, Selzer C, Schuster P, Lenski M, Adam O, Schafers HJ, Bohm M, Laufs U. The mineralocorticoid receptor promotes fibrotic remodeling in atrial fibrillation. *J Biol Chem* 2014;**289**:6656-6668.

114. Zhong H, Liang X-H, Neef S, Popov A, Maier LS, Yao L, Belardinelli L. Expression of lysyl oxidase-like 2 (LOXL2) correlates with left atrial size and fibrotic gene expression in human atrial fibrillation. *J Am Coll Cardiol* 2014;**63**:A285.

115. Zhao Y, Tang K, Tianbao X, Wang J, Yang J, Li D. Increased serum lysyl oxidase-like 2 levels correlate with the degree of left atrial fibrosis in patients with atrial fibrillation. *Biosci Rep* 2017;**37**. pii: BSR20171332. doi: 10.1042/BSR20171332.

116. Trackman PC. Lysyl oxidase isoforms and potential therapeutic opportunities for fibrosis and cancer. *Expert Opin Ther Targets* 2016;**20**:935-945.

117. Wunberg T, Hendrix M, Hillisch A, Lobell M, Meier H, Schmeck C, Wild H, Hinzen B. Improving the hit-to-lead process: Data-driven assessment of drug-like and lead-like screening hits. *Drug Discov Today* 2006;**11**:175-180.

118. Brenk R, Schipani A, James D, Krasowski A, Gilbert IH, Frearson J, Wyatt PG. Lessons learnt from assembling screening libraries for drug discovery for neglected diseases. *ChemMedChem* 2008;**3**:435-444.

119. Tang SS, Simpson DE, Kagan HM. Beta-substituted ethylamine derivatives as suicide inhibitors of lysyl oxidase. *J Biol Chem* 1984;**259**:975-979.

120. Williamson PR, Kagan HM. Electronegativity of aromatic amines as a basis for the development of ground state inhibitors of lysyl oxidase. *J Biol Chem* 1987;**262**:14520-14524.

121. Levene CI, Sharman DF, Callingham BA. Inhibition of chick embryo lysyl oxidase by various lathyrogens and the antagonistic effect of pyridoxal. *Int J Exp Pathol* 1992;**73**:613-624.

122. Gacheru SN, Trackman PC, Calaman SD, Greenaway FT, Kagan HM. Vicinal diamines as pyrroloquinoline quinone-directed irreversible inhibitors of lysyl oxidase. *J Biol Chem* 1989;**264**:12963-12969.

123. Liu G, Nellaiappan K, Kagan HM. Irreversible inhibition of lysyl oxidase by homocysteine thiolactone and its selenium and oxygen analogues. Implications for homocystinuria. *J Biol Chem* 1997;**272**:32370-32377.

124. Nagan N, Callery PS, Kagan HM. Aminoalkylaziridines as substrates and inhibitors of lysyl oxidase: Specific inactivation of the enzyme by N-(5-aminopentyl)aziridine. *Front Biosci* 1998;**3**:A23-26.

125. Robinson, Wilson DM, Delaet NG, Bradley EK, Dankwardt SM, Campbell JA, Martin RL, Van Wart HE, Walker KA, Sullivan RW. Novel inhibitors of procollagen C-proteinase. Part 2: Glutamic acid hydroxamates. *Bioorg Med Chem Lett* 2003;**13**:2381-2384.

126. Delaet NG, Robinson LA, Wilson DM, Sullivan RW, Bradley EK, Dankwardt SM, Martin RL, Van Wart HE, Walker KA. Novel inhibitors of procollagen C-terminal proteinase. Part 1: Diamino Acid hydroxamates. *Bioorg Med Chem Lett* 2003;**13**:2101-2104.

127. Bailey S, Fish PV, Billotte S, Bordner J, Greiling D, James K, McElroy A, Mills JE, Reed C, Webster R. Succinyl hydroxamates as potent and selective non-peptidic inhibitors of procollagen C-proteinase: Design, synthesis, and evaluation as topically applied, dermal anti-scarring agents. *Bioorg Med Chem Lett* 2008;**18**:6562-6567.

128. Mure M. Tyrosine-derived quinone cofactors. *Acc Chem Res* 2004;**37**:131-139.

129. Blaisdell RJ, Giri SN. Mechanism of antifibrotic effect of taurine and niacin in the multidose bleomycin-hamster model of lung fibrosis: Inhibition of lysyl oxidase and collagenase. *J Biochem Toxicol* 1995;**10**:203-210.

130. Anderson C, Bartlett SJ, Gansner JM, Wilson D, He L, Gitlin JD, Kelsh RN, Dowden J. Chemical genetics suggests a critical role for lysyl oxidase in zebrafish notochord morphogenesis. *Mol BioSyst* 2007;**3**:51-59.

131. Hajdu I, Kardos J, Major B, Fabo G, Lorincz Z, Cseh S, Dorman G. Inhibition of the LOX enzyme family members with old and new ligands. Selectivity analysis revisited. *Bioorg Med Chem Lett* 2018;**28**:3113-3118.

132. Narayanan AS, Siegel RC, Martin GR. On the inhibition of lysyl oxidase by β-aminopropionitrile. *Biochem Biophys Res Commun* 1972;**46**:745-751.

133. Tang SS, Trackman PC, Kagan HM. Reaction of aortic lysyl oxidase with beta-aminopropionitrile. *J Biol Chem* 1983;**258**:4331-4338.

134. Page RC, Benditt EP. Interaction of the lathyrogen beta-aminopropionitrile (BAPN) with a copper-containing amine oxidase. *Proc Soc Exp Biol Med* 1967;**124**:454-459.

135. Kato S, Spinale FG, Tanaka R, Johnson W, Cooper Gt, Zile MR. Inhibition of collagen cross-linking: Effects on fibrillar collagen and ventricular diastolic function. *Am J Physiol* 1995;**269**:H863-868.

136. Bing OH, Fanburg BL, Brooks WW, Matsushita S. The effect of lathyrogen beta-amino proprionitrile (BAPN) on the mechanical properties of experimentally hypertrophied rat cardiac muscle. *Circ Res* 1978;**43**:632-637.

137. Rosin NL, Sopel MJ, Falkenham A, Lee TD, Legare JF. Disruption of collagen homeostasis can reverse established age-related myocardial fibrosis. *Am J Pathol* 2015;**185**:631-642.

138. Bachhuber TE, Lalich JJ, Angevine DM, Schilling ED, Strong FM. Lathyrus factor activity of beta-aminopropionitrile and related compounds. *Proc Soc Exp Biol Med* 1955;**89**:294-297.

139. Granchi C, Funaioli T, Erler JT, Giaccia AJ, Macchia M, Minutolo F. Bioreductively activated lysyl oxidase inhibitors against hypoxic tumours. *ChemMedChem* 2009;**4**:1590-1594.

140. Barry-Hamilton V, Spangler R, Marshall D, McCauley S, Rodriguez HM, Oyasu M, Mikels A, Vaysberg M, Ghermazien H, Wai C, Garcia CA, Velayo AC, Jorgensen B, Biermann D, Tsai D, Green J, Zaffryar-Eilot S, Holzer A, Ogg S, Thai D, Neufeld G, Van Vlasselaer P, Smith V. Allosteric inhibition of lysyl oxidase-like-2 impedes the development of a pathologic microenvironment. *Nat Med* 2010;**16**:1009-1017.

141. Boak AM, Roy R, Berk J, Taylor L, Polgar P, Goldstein RH, Kagan HM. Regulation of lysyl oxidase expression in lung fibroblasts by transforming growth factor-beta 1 and prostaglandin E2. *Am J Respir Cell Mol Biol* 1994;**11**:751-755.

142. Roy R, Polgar P, Wang Y, Goldstein RH, Taylor L, Kagan HM. Regulation of lysyl oxidase and cyclooxygenase expression in human lung fibroblasts: Interactions among TGF-beta, IL-1 beta, and prostaglandin E. *J Cell Biochem* 1996;**62**:411-417.

143. Engebretsen KV, Skardal K, Bjornstad S, Marstein HS, Skrbic B, Sjaastad I, Christensen G, Bjornstad JL, Tonnessen T. Attenuated development of cardiac fibrosis in left ventricular pressure overload by SM16, an orally active inhibitor of ALK5. *J Mol Cell Cardiol* 2014;**76**:148-157.

144. Adam O, Zimmer C, Hanke N, Hartmann RW, Klemmer B, Bohm M, Laufs U. Inhibition of aldosterone synthase (CYP11B2) by torasemide prevents atrial fibrosis and atrial fibrillation in mice. *J Mol Cell Cardiol* 2015;**85**:140-150.

145. Gonzalez GE, Rhaleb NE, Nakagawa P, Liao TD, Liu Y, Leung P, Dai X, Yang XP, Carretero OA. N-acetyl-seryl-aspartyl-lysyl-proline reduces cardiac collagen cross-linking and inflammation in angiotensin II-induced hypertensive rats. *Clin Sci* 2014;**126**:85-94.

146. Miguel-Carrasco JL, Beaumont J, San Jose G, Moreno MU, Lopez B, Gonzalez A, Zalba G, Diez J, Fortuno A, Ravassa S. Mechanisms underlying the cardiac antifibrotic effects of losartan metabolites. *Sci Rep* 2017;**7**:41865.

147. Lopez B, Querejeta R, Gonzalez A, Larman M, Diez J. Collagen cross-linking but not collagen amount associates with elevated filling pressures in hypertensive patients with stage C heart failure: Potential role of lysyl oxidase. *Hypertension* 2012;**60**:677-683.

148. Lopez B, Gonzalez A, Lindner D, Westermann D, Ravassa S, Beaumont J, Gallego I, Zudaire A, Brugnolaro C, Querejeta R, Larman M, Tschope C, Diez J. Osteopontin-mediated myocardial fibrosis in heart failure: A role for lysyl oxidase?. *Cardiovasc Res* 2013;**99**:111-120.

149. Herum KM, Lunde IG, Skrbic B, Louch WE, Hasic A, Boye S, Unger A, Brorson SH, Sjaastad I, Tonnessen T, Linke WA, Gomez MF, Christensen G. Syndecan-4 is a key determinant of collagen cross-linking and passive myocardial stiffness in the pressure-overloaded heart. *Cardiovasc Res* 2015;**106**:217-226.

150. Gao AE, Sullivan KE, Black LD, 3rd. Lysyl oxidase expression in cardiac fibroblasts is regulated by alpha2beta1 integrin interactions with the cellular microenvironment. *Biochem Biophys Res Commun* 2016;**475**:70-75.

151. Xiao Y, Nie X, Han P, Fu H, James Kang Y. Decreased copper concentrations but increased lysyl oxidase activity in ischemic hearts of rhesus monkeys. *Metallomics* 2016;**8**:973-980.

152. Beaumont J, Lopez B, Ravassa S, Hermida N, Jose GS, Gallego I, Valencia F, Gomez-Doblas JJ, de Teresa E, Diez J, Gonzalez A. MicroRNA-19b is a potential biomarker of increased myocardial collagen cross-linking in patients with aortic stenosis and heart failure. *Sci Rep* 2017;**7**:40696.

153. Schreckenberg R, Horn AM, da Costa Rebelo RM, Simsekyilmaz S, Niemann B, Li L, Rohrbach S, Schluter KD. Effects of 6-months' exercise on cardiac function, structure and metabolism in female hypertensive rats-the decisive role of lysyl oxidase and collagen III. *Front Physiol* 2017;**8**:556.

## Figure Legends

**Figure 1. Schematic representation of collagen biosynthesis and cross-linking.** Following translation, procollagen α-chains are imported into the endoplasmic reticulum (ER) and Golgi apparatus to form triple-helical procollagen (two α1-chains and one α2-chain). These immature collagen helices are secreted into the extracellular space and then converted to mature collagen through cleavage by procollagen N-proteinase (PNPase) and C-proteinase (PCPase). Mature collagen fibrils are self-assembled and then cross-linking is initiated by enzymatic (lysyl oxidase (LOX) family) and non-enzymatic (advanced glycation end products (AGEs)) processes.

**Figure 2. Structures of lysyl oxidase (LOX) and LOX-like proteins (LOXL-1, LOXL-2, LOXL-3 and LOXL-4).**

**Figure 3. Mechanism of collagen cross-linking as catalyzed by lysyl oxidase (LOX) enzymes.** (A) Sequences of peptidyl lysine and hydroxylysine in collagen. (B) Oxidation of peptidyl lysine and hydroxylysine to peptidyl aldehyde (allysyl and hydroxyallysyl) in collagen. (C) Condensation of peptidyl aldehyde (allysyl and hydroxyallysyl) and lysine to dehydrolysinonorleucine and aldol. (D) Maturation of dehydrolysinonorleucine and aldol condensation products to pyridinoline and pyrrole.

**Figure 4**. **Schematic representation of biosynthesis, secretion and activation of lysyl oxidase (LOX) enzyme in heart tissues.** LOX gene is transcribed in the nucleus, LOX mRNA is translated, pre-protein (pre-pro-LOX) enters the endoplasmic reticulum (ER), and is transported as a prolysyl oxidase (pro-enzyme) from the ER to the Golgi apparatus. In the Golgi apparatus, glycosylation occurs, followed by association with cellular copper and formation of a lysine tyrosylquinone (LTQ) cofactor. Prolysyl oxidase is cleaved between Gly168 and Asp169 at the surface of cardiac cells by procollagen C-proteinase (PCPase; bone morphogenetic protein 1 (BMP-1)) to form the active (mature) LOX (30 kDa) and LOX propeptide (18 kDa), which are then secreted into the extracellular matrix (ECM). Transforming growth factor beta (TGF-β) and prostaglandin E2 modulate LOX mRNA transcription.

**Figure 5. Schematic overview of the principal role of LOX-family enzymes in heart disease**.

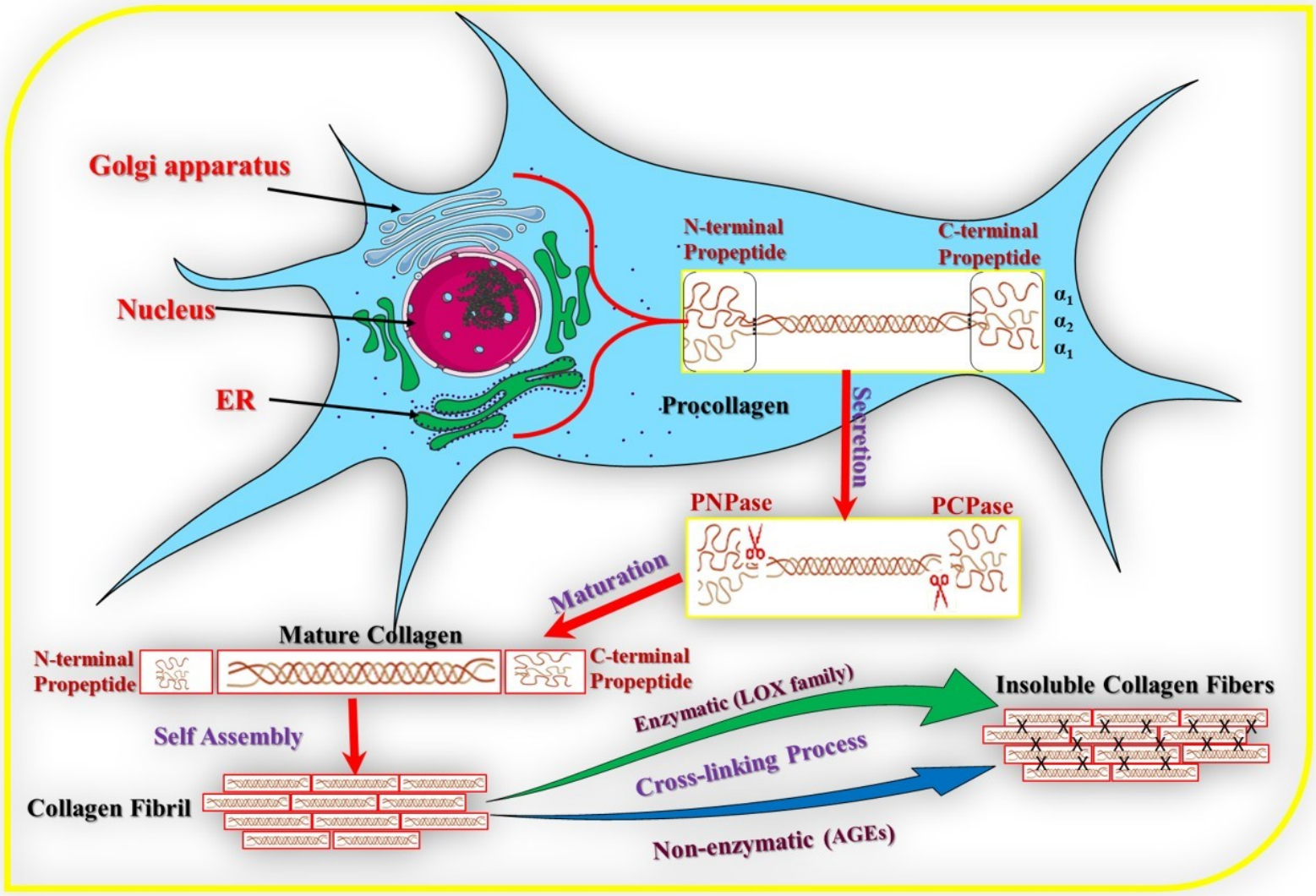
Golgi apparatus
Nucleus
ER
N-terminal
Propeptide
C-terminal
Propeptide
α1
α2
α1
Procollagen
Secretion
PNPase
PCPase
Maturation
Mature Collagen
N-terminal
Propeptide
C-terminal
Propeptide
Self Assembly
Collagen Fibril
Enzymatic (LOX family)
Cross-linking Process
Non-enzymatic (AGEs)
Insoluble Collagen Fibers

**Figure 1.**

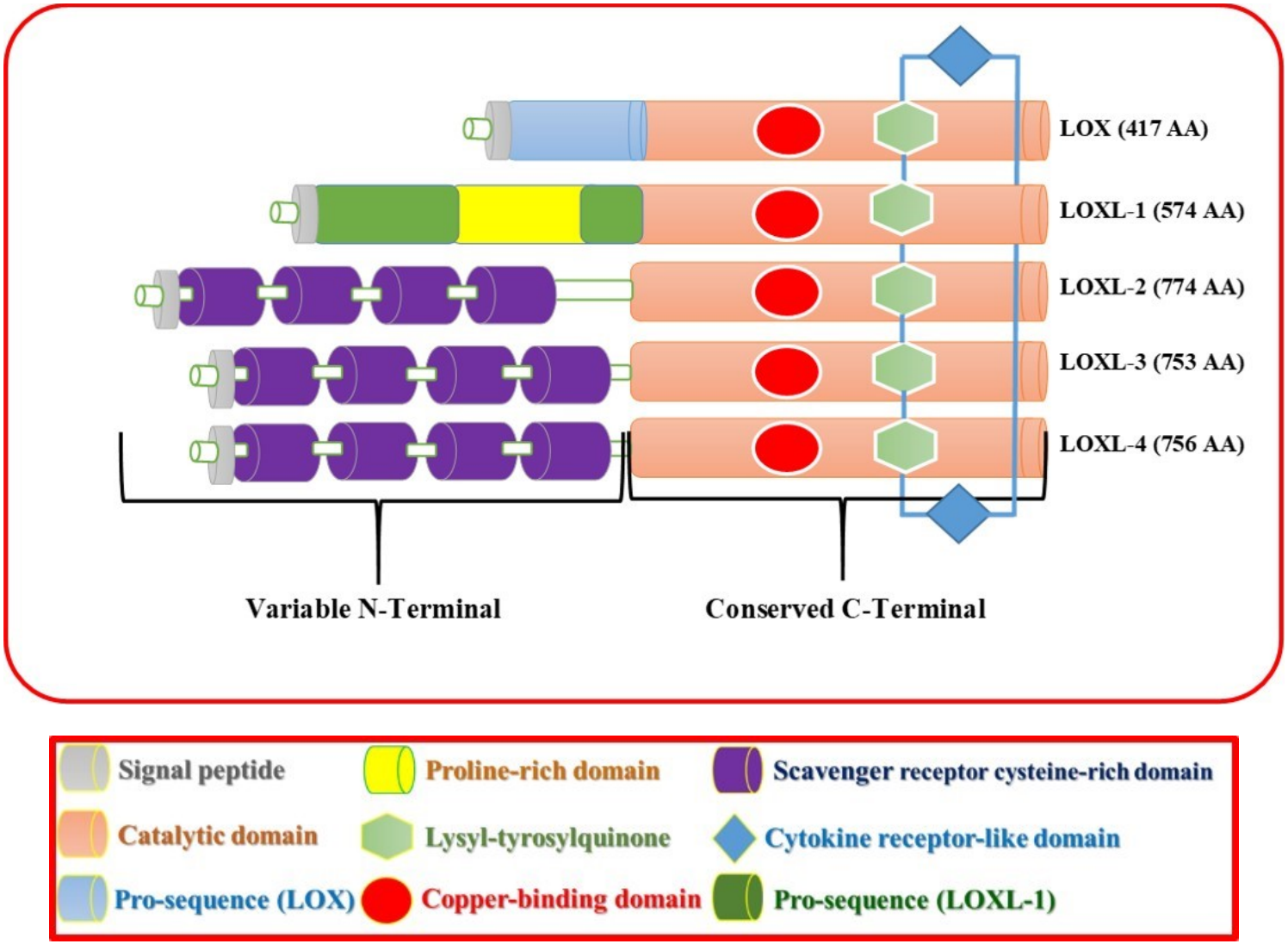
LOX (417 AA)
LOXL-1 (574 AA)
LOXL-2 (774 AA)
LOXL-3 (753 AA)
LOXL-4 (756 AA)
Variable N-Terminal
Conserved C-Terminal
Signal peptide
Proline-rich domain
Scavenger receptor cysteine-rich domain
Catalytic domain
Lysyl-tyrosylquinone
Cytokine receptor-like domain
Pro-sequence (LOX)
Copper-binding domain
Pro-sequence (LOXL-1)

**Figure 2.**

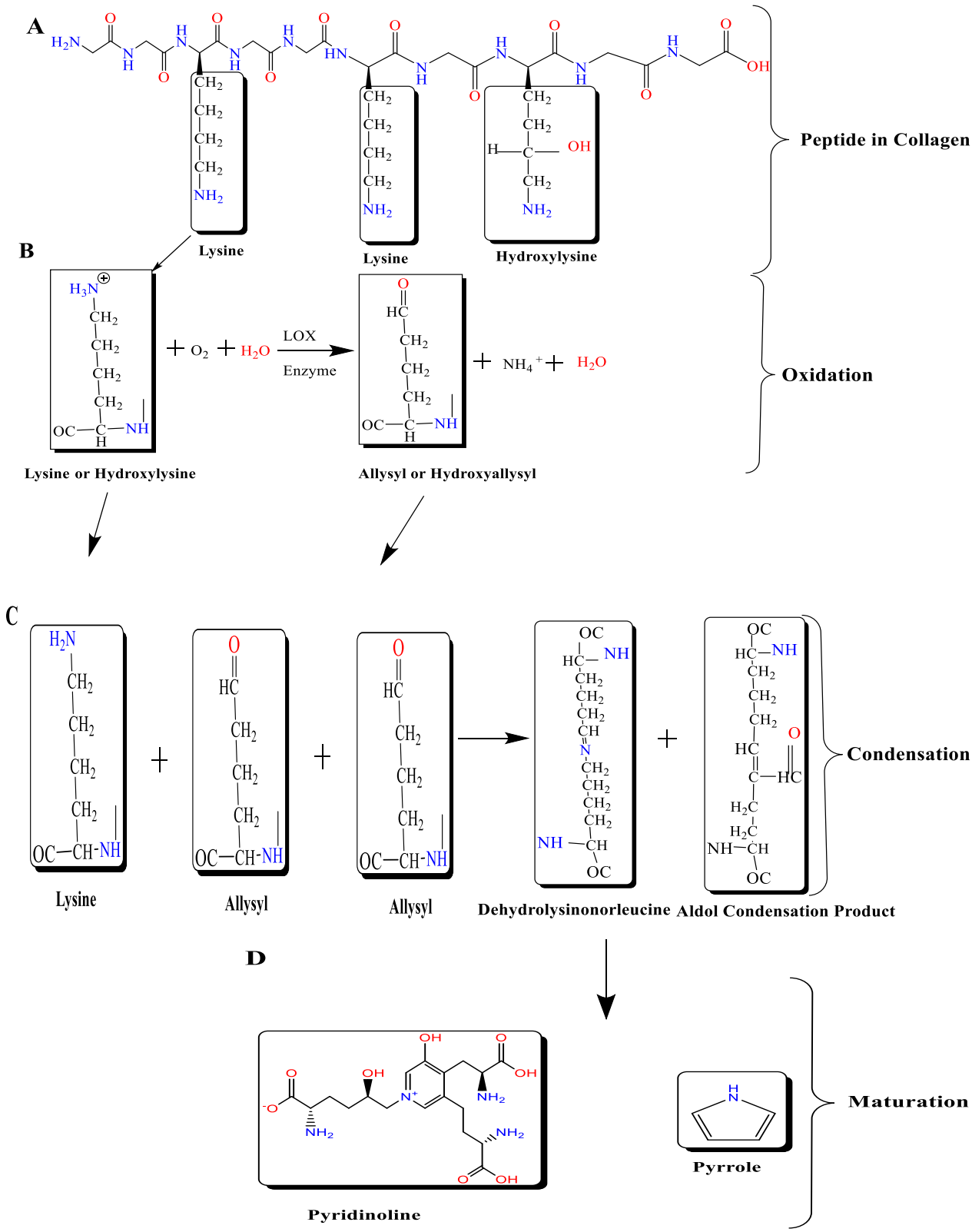
A
Peptide in Collagen
Lysine
Lysine
Hydroxylysine
B
Oxidation
LOX
Enzyme
Lysine or Hydroxylysine
Allysyl or Hydroxyallysyl
C
Condensation
Lysine
Allysyl
Allysyl
Dehydrolysinonorleucine
Aldol Condensation Product
D
Maturation
Pyrrole
Pyridinoline

**Figure 3.**

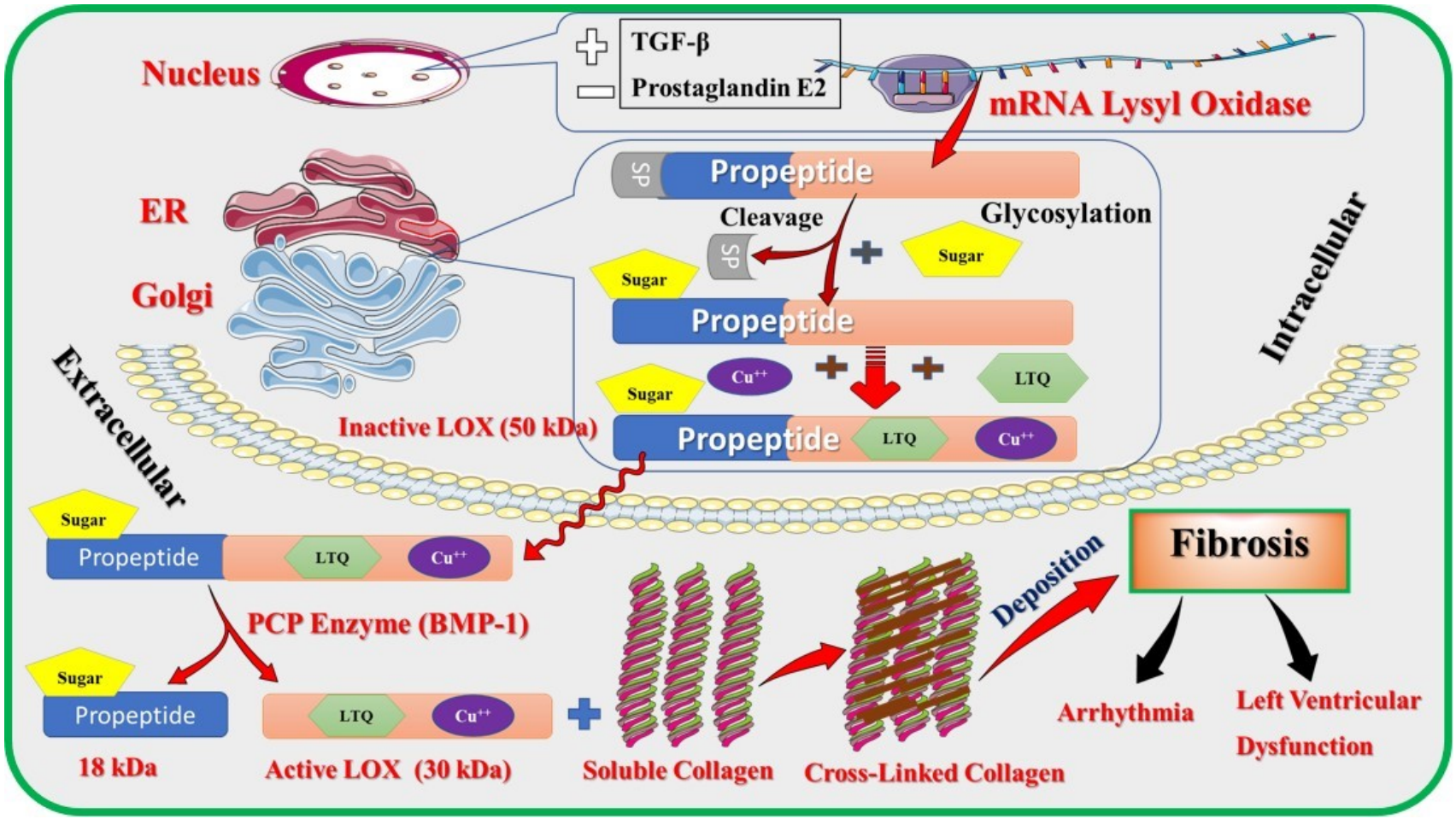
Nucleus
TGF-β
Prostaglandin E2
mRNA Lysyl Oxidase
ER
Golgi
SP
Propeptide
Cleavage
Glycosylation
Sugar
Propeptide
Cu++
LTQ
Propeptide
LTQ
Cu++
Inactive LOX (50 kDa)
Extracellular
Intracellular
Sugar
Propeptide
LTQ
Cu++
PCP Enzyme (BMP-1)
Sugar
Propeptide
18 kDa
LTQ
Cu++
Active LOX (30 kDa)
Soluble Collagen
Cross-Linked Collagen
Deposition
Fibrosis
Arrhythmia
Left Ventricular
Dysfunction

**Figure 4.**

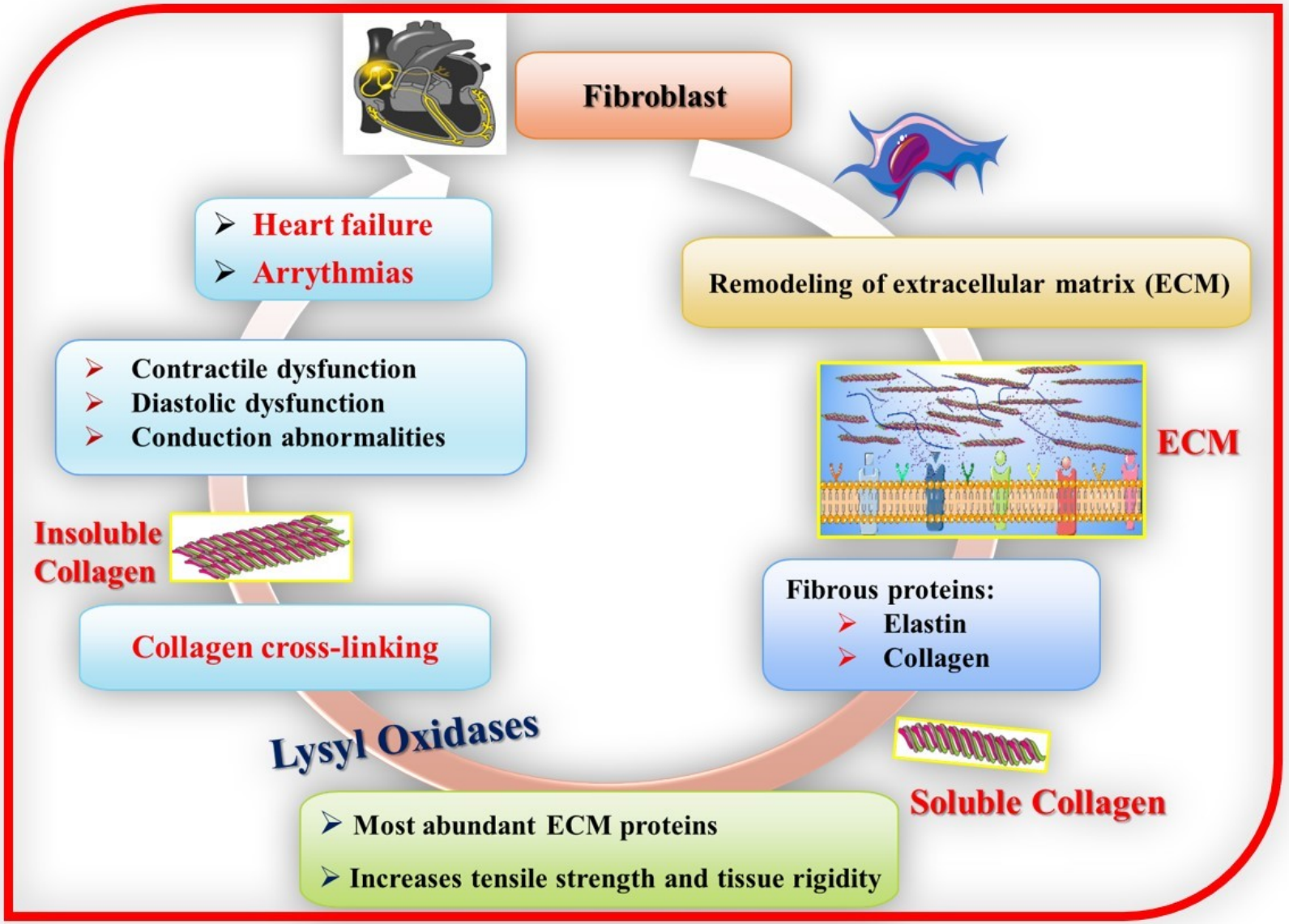
Fibroblast
Remodeling of extracellular matrix (ECM)
ECM
Fibrous proteins:
Elastin
Collagen
Soluble Collagen
Lysyl Oxidases
Most abundant ECM proteins
Increases tensile strength and tissue rigidity
Collagen cross-linking
Insoluble Collagen
Contractile dysfunction
Diastolic dysfunction
Conduction abnormalities
Heart failure
Arrythmias

**Figure 5.**

**Table 1:** Summary of investigations of LOX-family isoforms in heart failure (HF).

| Reference | Model | Species | Effects of LOX Inhibition | Cardiac Condition | LOX Inhibitor | Observations and Conclusions |
|---|---|---|---|---|---|---|
| **Sivakumar *et al.*** [92] | -DCM patients with HF | -Human | -Not studied | -HF due to DCM | -None used | -Increased collagen concentration and contents of MMP-2 and MMP-9 in LV tissues of DCM patients with HF<br>-Upregulation of transcript levels for LOX, cytokines (IFN, IL-6, TNF-α, and TGF-β), TIMP-1 and TIMP-2 in LV tissues of DCM patients with HF<br>-A significant role of LOX in cardiac dysfunction via modification the collagen structure |
| **Lopez *et al.*** [57] | -HF patients | -Human | -Declined LOX expression and collagen cross-linking in treated HF patients with torasemide<br>-Normalization of LV stiffness in treated HF patients with torasemide | -HF | -None used | -Increased LOX expression and collagen cross-linking in LV tissues of HF patients<br>-A strong correlation of collagen cross-linking with LOX expression and LV stiffness in HF patients<br>-LOX is a potential target for reduction the degree of collagen stiffness and improvement of LV mechanical properties in HF patients |
| **Lopez *et al.*** [147] | -Hypertensive patients with HF | -Human | -Not studied | -HF due to hypertension | -None used | -Increased LV stiffness, total collagen, collagen type I fibers, insoluble collagen, collagen cross-linking and LOX expression in LV tissues of hypertensive patients with HF<br>-LOX excessively induced collagen cross-linking, leading to increase LV stiffness and filling pressure in hypertensive patients with HF |
| **Lopez *et al.*** [148] | Hypertensive patients with HF | -Human | -Silencing of CTGF prevented osteopontin-induced upregulation of LOX activity and expression in cardiac fibroblasts | -HF due to hypertension | -None used | -Increased myocardial osteopontin expression is associated with upregulation of LOX, insoluble collagen, collagen type I and LV stiffness in HF patients with hypertension<br>-Increased LOX activity and expression in cardiac fibroblasts upon treatment with osteopontin<br>-Inhibition of osteopontin–LOX pathway may be a therapeutic target for myocardial fibrosis in HF patients with hypertension |
| **Gonzalez-Santamaria *et al.*** [95] | -HF induced by MI | -Mice | -BAPN decreased collagen content, collagen cross-linking, LV dilatation and improved cardiac function post-MI<br>-BAPN didn't change the expression of LOX isoforms in the LV infarcted area<br>-Anti-LOX antibody reduced collagen accumulation, scar area and LV dilatation | -HF | -BAPN<br>-Anti-LOX antibody | -Upregulation of mature collagen bundles, collagen cross-linking and LOX isoforms mRNA expressions in the LV infarcted area<br>-TGF-β and hypoxia induced an increase of LOX isoforms mRNA expressions except LOXL-1 in cultured fibroblasts<br>-LOX isoforms had a crucial role in cardiac remodeling post-MI |
| **Yang *et al.*** [84] | -Pressure overload induced by TAC<br>-HF patients with preserved ejection fraction, ischemia and idiopathic DCM | -Mice<br>-Human | -Anti-LOXL-2 antibody or genetic LOXL-2 disruption decreased cardiac fibrosis, chamber dilatation and improved systolic and diastolic functions | -HF | -Anti-LOXL-2 antibody<br>-Genetic LOXL-2 disruption by CRISPR/Cas9 | -Elevated LOXL-2 levels in the LV tissues of TAC mice and human with HF, ischemia and idiopathic DCM<br>-LOXL-2 promoted TGF-β2 production, differentiation of fibroblasts into myofibroblasts and cross-linking and deposition of collagen during stress<br>-LOXL-2 had an important role in the interstitial fibrosis and cardiac dysfunction during HF development |
| **El Hajj *et al.*** [97] | -HF induced by VO | -Rats | -BAPN attenuated VO-induced cardiac wall stress and dysfunction | -HF | -BAPN | -VO induced an increase of ventricular wall stress, chamber dilatation, collagen (type I and III) expressions and collagen cross-linking<br>-BAPN had cardioprotective effects and prevented HF progression in VO rats |

| | | | | | | |
|---|---|---|---|---|---|---|
| | | | -BAPN attenuated the increase in collagen (type I and III) expressions and collagen cross-linking in VO rats | | | |
| **El Hajj *et al.*** [98] | -HF induced by VO | -Rats | -BAPN attenuated cardiac dysfunction, collagen deposition and cross-linking in chronic VO rats | -HF | -BAPN | -Chronic VO induced an upregulation of LOX expression, LOX activity and collagen cross-linking during the shift from compensated to decompensated stage of HF (4 to 21 weeks post-surgery)<br>-Upregulation of LOX levels had a detrimental role in HF progression |
| **El Hajj *et al.*** [99] | -HF induced by VO | -Rats | -BAPN suppressed the LV wall stress and stiffness as well as improved the cardiac contractility in chronic VO rats<br>-BAPN decreased collagen (I and III), MMP-2, MMP-8, MMP-14, TIMP-1 and TIMP-2 protein expressions along with decrease in collagen cross-linking and interstitial fibrosis | -HF | -BAPN | -Chronic VO rats demonstrated an increase of cardiac wall stress, collagen cross-linking and interstitial fibrosis along with increase in collagen and MMPs expressions<br>-BAPN had a cardioprotective effects in chronic VO model |

LV, Left ventricle; DCM, Dilated cardiomyopathy; MMPs, Matrix metalloproteinases; BAPN, β-aminopropionitrile; LOX, Lysyl oxidase; LOXL, Lysyl oxidase like protein; CTGF, Connective tissue growth factor; ECM, Extracellular matrix; TAC, Transverse aortic constriction; MI, Myocardial infarction; HF, Heart failure; IFN, Interferon; IL-6, Interleukin 6; TNF-α, Tumor necrosis factor-α; TGF-β, Transforming growth factor β,TIMP, Tissue inhibitor of metalloproteinase; VO, Volume overload.

**Table 2:** Summary of investigations of LOX-family isoforms in hypertrophic cardiac conditions.

| Reference | Model | Species | Effects of LOX Inhibition | Cardiac Condition | LOX Inhibitor | Observations and Conclusions |
|---|---|---|---|---|---|---|
| **Ohmura *et al.*** [108] | -Neonatal rats<br>-Hypertrophy induced by abdominal aortic constriction<br>-Transgenic mice with LOXL-1 overexpression | -Rats<br>-Mice | -BAPN inhibited cardiac hypertrophy that was induced by Ang II *in vivo*<br>-BAPN inhibited leucine incorporation in cardiomyocyte that was induced by hypertrophic agonists | -Pressure overload<br>-Cardiomyocyte-specific overexpression of LOXL-1 | -BAPN | -Increased LOXL-1 expression and LOX activity in neonatal rat cardiomyocytes upon stimulation with hypertrophic agonists<br>-Elevated mRNA expression of LOXL-1 in rats after abdominal aortic constriction<br>-Transgenic mice expressing LOXL-1 showed an increase of brain natriuretic peptide expression, myocyte diameter, LV to body weight ratio and wall thickness<br>-A vital role of LOXL-1 in cardiac hypertrophy |
| **Gonzalez *et al.*** [145] | -Hypertension by Ang II infusion | -Rats | -Ac-SDKP prevented the increase of total and cross-linked collagen, LOX and LOXL-1 expressions | -Hypertension | -None used | -Ac-SDKP decreased LOX expression, leading to decrease the nuclear translocation of NF-κB, CD4+/CD8+ lymphocyte infiltration and CD68+ macrophage infiltration induced by Ang II<br>-Ac-SDKP decreased inflammation and fibrosis but failed to lower blood pressure or LV hypertrophy |
| **Herum *et al.*** [149] | -Hypertrophy induced by aortic banding in syndecan-4 knockout (syndecan-4$^{-/-}$) mice | -Mice | -Knockout of syndecan-4 decreased LOX and osteopontin expressions in cardiac fibroblasts | -Pressure overload | -None used | -Decreased LOX activity and expression, collagen cross-linking and osteopontin expression in LV from syndecan-4$^{-/-}$ mice<br>-Increased osteopontin expression in mechanically stretched fibroblasts as well as in fibroblasts overexpressing calcineurin, NFAT or syndecan-4<br>-Syndecan-4 induced collagen, LOX and osteopontin in cardiac fibroblasts via its cytosolic domain and NFAT signaling pathway |
| **Gao *et al.*** [150] | -Myocardial infarction (MI) | -Rats | -BTT3033 (α2β1 integrin inhibitor) decreased the expression of collagen 1A1 and LOX as well as cellular adhesion to collagen in cardiac fibroblasts | -Myocardial ischemia | -None used | -Increased expression of LOX, collagen 1A1, α-SMA and integrin β1 in cardiac fibroblasts from one-week post-MI LV tissue<br>-Upregulation of LOX and collagen I in cultured infarct cardiac fibroblasts on collagen I coated plates with or without TGF-β1; α2β1 integrin blocker reduced LOX, pro-LOX and collagen-1 expression<br>-Interactions of the α2β1 integrin to collagen I regulated LOX expression |
| **Xiao *et al.*** [151] | -Ischemia (occlusion-reperfusion) | -Monkeys | -Not studied | -Myocardial ischemia | -None used | -Reduced copper contents in tissues leads to increase the collagen deposition by LOX in the infarcted area<br>-Upregulation of mRNA expression of LOX and collagen (type I and III), protein expression of collagen (type I and III), LOX activity and collagen cross-linking in the infarcted area |
| **Martinez-Martinez *et al.*** [77] | -Rat fed with HFD | -Rats | -BAPN prevented the increase in circulating levels of leptin and body weight in HFD rats<br>-BAPN decreased cardiac hypertrophy without effect on blood pressure in HFD rats<br>-LOX knockdown reduced the effect of leptin-induced collagen I synthesis and inhibited leptin-induced ROS production and profibrotic mediators in cardiac fibroblasts and aortic VSMCs | -Metabolic syndrome | -BAPN<br>-LOX knockdown (siRNA) | -Interactions between leptin and LOX regulated downstream events that mediated cardiovascular fibrosis in obesity |

| | | | | | | |
|---|---|---|---|---|---|---|
| **Beaumont *et al.*** [152] | -AS patients with HF | -Human | -Anti miRNA-19b increased CTGF and LOX protein in human fibroblasts | -HF due to AS | -None used | -Increased total collagen, cross-linked collagen and LOX expression along with a decrease in expression of miRNA-19b and miRNA-133a in myocardial samples of AS patients with HF<br>-Inverse correlation of myocardial and serum miRNA-19b expression with myocardial collagen cross-linking, LV stiffness and LOX expression in AS patients with HF<br>-miR-19b inhibition increased CTGF and LOX expression in fibroblasts |
| **Schreckenberg *et al.*** [153] | -Exercise in spontaneous hypertension | -Rats | -Knocking down osteopontin decreased LOX expression in cardiac fibroblasts | -Hypertension | -None used | -Decreased heart rate with no effect on the systolic or diastolic blood pressure along with development of LV hypertrophy in exercised hypertensive rats<br>-Reduced expression of TGF-β1, CTGF, and FGF2 and increased expression of collagen III and LOX in exercised hypertensive rats |
| **Galan *et al.*** [109] | -TgLOX | -Mice | -Not studied | -LOX overexpression | -None used | -TgLOX mice showed higher collagen cross-linking and deposition along with increase of fibrotic markers (like α-actin, SM22α and collagen type I)<br>-Infusion of TgLOX mice with Ang II stimulated p38 MAPK, leading to concentric hypertrophy (increase of LV mass, HW/body weight ratio and cross-sectional area of myocytes)<br>-LOX induced age-dependent impairment of diastolic function and exacerbated Ang II-induced cardiac hypertrophy |
| **Miguel-Carrasco *et al.*** [146] | -Hypertension by L-NAME infusion | -Rats | -Losartan metabolite (EXP3179) inhibited the increase of LOX and CTGF expressions, collagen cross-linking and cardiac fibrosis | -Hypertension | -None used | -EXP3179 had anti-fibrotic effects through inhibition of CTGF and LOX levels without any change in blood pressure |

LV, Left ventricle; BAPN, β-aminopropionitrile; LOX, Lysyl oxidase; LOXL, Lysyl oxidase like protein; CTGF, Connective tissue growth factor; TgLOX, Transgenic mice with LOX overexpression; Ang II, Angiotensin II; HW, Heart weight; SM22α, Smooth muscle protein 22α; p38 MAPK, p38 mitogen-activated protein kinase; HFD, High-fat diet; VSMCs, Vascular smooth muscle cells; ROS, Reactive oxygen species; siRNA, Small interfering RNA; Ac-SDKP, N-acetyl-seryl-aspartyl-lysyl-proline; NF-κB, Nuclear factor-kappa β; TGF-β1, Transforming growth factor β1; NFAT, Nuclear factor of activated T-cells; MI, Myocardial infarction; α-SMA, α-smooth muscle actin; AS, Aortic stenosis; miRNA: MicroRNA; FGF2, Fibroblast growth factor-2.

**Table 3:** Summary of investigations of LOX-family isoforms in atrial disease and atrial fibrillation (AF).

| Reference | Model | Species | Effects of LOX Inhibition | Cardiac Condition | LOX Inhibitor | Observations and Conclusions |
|---|---|---|---|---|---|---|
| **Adam *et al.*** [91] | -Permanent AF patients<br>-RacET transgenic mice<br>-Neonatal rats | -Human<br>-Mice<br>-Rats | -Specific Rac1 inhibitor (NSC23766) prevented the increase of LOX expression by Ang II in cardiac fibroblasts<br>-Knockdown of CTGF completely inhibited the effect of Ang II on upregulation of LOX expression in cardiac fibroblasts<br>-Inhibition of Rac1 GTPase by statin decreased level of fibronectin, LOX, collagen cross-linking and AF prevalence *in vivo* | -AF<br>-RacET | -BAPN | -Increased fibronectin expression, collagen cross-linking and LOX expression in LA tissues of AF patients<br>-Ang II induced an increase of LOX and fibronectin expressions through stimulation of Rac1 GTPase and CTGF<br>-Inhibition of Rac1 signaling pathway could be a potential therapeutic target for prevention of atrial fibrosis and remodeling |
| **Adam *et al.*** [112] | -RacET transgenic mice<br>-Neonatal rats<br>-AF patients | -Mice | -BAPN inhibited the increase of miRNA-21 that is induced by CTGF or Ang II in cardiac fibroblasts | -RacET | -BAPN | -Elevation of miRNA-21 expression was associated with a decline of Sprouty1 protein expression and increase levels of Rac1 GTPase, CTGF and LOX expressions in LA tissues of AF patients<br>-Ang II increased miRNA-21 expression by stimulation of CTGF, Rac1 GTPase and LOX in cardiac fibroblasts<br>-Regulation of miRNA-21 may be a further potential target for atrial fibrosis |
| **Zhong *et al.*** [114] | -Persistent or permanent AF patients. | -Human | -Not studied | -AF | -None used | -Increased LOXL-2 expression in the RA of permanent AF patients<br>-Significant correlation between LOXL-2 expression and LA size in all AF patients<br>-Significant correlations of LOXL-2 expression with TGF-β1, collagen III, fibronectin or CTGF expression in all AF patients<br>-LOXL-2 may contribute to atrial fibrosis which is the main substrate for AF maintenance |
| **Lavall *et al.*** [113] | -Permanent AF patients<br>-Neonatal rats<br>-RacET transgenic mice | -Human<br>-Mice<br>-Rats | -Mineralocorticoid receptor antagonist (spironolactone) decreased hydroxyproline concentration, CTGF and LOX expressions in cardiac fibroblasts | -RacET | -None used | -Elevated hydroxyproline concentration, CTGF and LOX expressions in cardiac fibroblasts upon treatment with aldosterone<br>-Increased LOX, CTGF and miRNA-21 expressions, total collagen content and atrial fibrosis in AF patients<br>-Mineralocorticoid receptor signaling induced atrial fibrosis and remodeling |
| **Adam *et al.*** [144] | -RacET transgenic mice<br>-Neonatal rats | -Mice<br>-Rats | -SL242 (selective inhibitor of CYP11B2) decreased CTGF, LOX, and miRNA-21 expressions along with collagen content in cardiac fibroblasts<br>-Torasemide inhibited CYP11B2 activity and decreased atrial fibrosis, AF prevalence and CTGF, LOX and miRNA-21 expressions | -RacET | -None used | -Decreased CTGF, miRNA-21 and LOX expressions in cardiac fibroblast treated with torasemide<br>-Ang II treatment increased the collagen content and the expression of CTGF, LOX and miRNA-21 in cardiac fibroblasts<br>-Increased atrial fibrosis and protein expressions of CTGF, LOX and miRNA-21 in LA tissues of RacET mice |
| **Zhao *et al.*** [115] | -AF patients | -Human | -Not studied | -AF | -None used | -Upregulation of serum LOXL-2 levels in AF patients<br>-Significant correlations of serum LOXL-2 levels with LA size and atrial fibrosis in AF patients |

LV, Left ventricle; LA, Left atrium; RA, Right atrium; BAPN, β-aminopropionitrile; LOX, Lysyl oxidase; LOXL, Lysyl oxidase like protein; AF, Atrial fibrillation; CTGF, Connective tissue growth factor; Ang II, Angiotensin II; Rac 1 GTPase, Rac family small GTPase 1; TGF-β, Transforming growth factor β, miRNA, MicroRNA, RacET, Transgenic mice with Rac1 overexpression.

# Part III– Hypothesis and objectives

## 1. Thesis rationale

LOX and LOXL proteins have several intra- and extra-cellular functions in the body [334]. The extracellular function of LOX and LOXL proteins is mainly elastin and collagen cross-linking within the ECM. A variety of models in which animals are subjected to pressure or volume overload show cardiac fibrosis along with an increase in LOX activity, LOX expression and collagen cross-linking [335-339]. Apart from the extracellular role of LOX and LOXL proteins in the cross-linking of cardiac ECM proteins, the intracellular roles of LOX and LOXL proteins in regulating normal cardiac fibroblast and myocyte functions have not been studied yet. In other body organs, novel intracellular roles of LOX and LOXL proteins have been reported, such as cell apoptosis, cell proliferation and gene transcription [334]. Total and cross-linked collagens were increased in the LA tissues of AF patients [280]. The mechanism and role of LOX and LOXL proteins in atrial remodeling and AF are not fully elucidated and understood. No studies have been reported on the secretion of LOXL proteins from cardiomyocytes and fibroblasts or their roles in atrial remodeling. In the literature, the CHF model shows $Ca^{2+}$ handling abnormalities along with a decline in cardiomyocyte contractility [133]. No studies have been reported on the roles of LOX and LOXL proteins in cardiomyocyte contractility and $Ca^{2+}$ signaling. It is important to conduct further studies on the other intracellular roles of LOX and LOXL proteins in cardiac fibroblast and myocyte functions.

Recent studies showed that LOX inhibition can be a therapeutic approach in several cardiac diseases [340-342]. The inhibition of LOX by β-aminopropionitrile (BAPN) attenuated cardiac dysfunction and ventricular fibrosis in a volume overload model [340, 341]. No studies have been reported

on the effect of LOX and LOXL protein inhibition via BAPN on atrial fibrotic signaling pathways and AF.

## 2. Thesis hypotheses

The hypotheses of the current study were:

**(1)** LOX and LOXL proteins have roles in AF-related atrial fibrosis and AF.

**(2)** Distinct LOX family isoforms have distinct functions and roles.

**(3)** In addition to their well-recognized cross-linking function, LOX family proteins have intracellular functions and can modify important cellular properties.

## 3. Objectives

The above hypotheses were addressed by pursuing the following specific objectives:

**(1)** To investigate the potential of LOX family proteins as an upstream therapeutic target for atrial fibrosis and AF in well-established models of fibrosis-related AF (Chapter 2; Article 2).

**(2)** To address the expression levels of LOX and LOXL proteins in LA fibroblasts and cardiomyocytes and their changes with CHF (Chapter 3; Article 3).

**(3)** To evaluate the physiological roles of LOX and LOXL proteins in cardiac cells (isolated fibroblasts and cardiomyocytes), including matrix-dependent (collagen cross-linking) and matrix-independent (proliferation, $Ca^{2+}$ signaling and contractility) functions (Chapter 3; Article 3).

# Chapter 2: Targeting the lysyl oxidase protein signaling pathway in atrial fibrosis and fibrillation

## Article 2

## Title: Targeting the lysyl oxidase protein signaling pathway in atrial fibrosis and fibrillation

This article is in preparation for submission to Cardiovascular Research.

## Contributions of authors

**Doa'a Ghazi Al-u'datt** conceived, designed and carried out the experiments for MI rat model. Collected tissue samples from CHF dogs and MI rats, prepared pumps for BAPN administration in MI study, performed ECG, collagen, fibrous tissue, qPCR and Western blot analysis, analyzed and interpreted the data, performed statistical analysis, generated table and figures and wrote the whole draft of the manuscript.

**Roddy Hiram** performed the electrophysiology study, and animal handling and sacrifice.

**Natacha Daquette** performed the MI surgery for rats.

**Yanfen Shi and Jean-Claude Tardif** performed all echocardiographic measurements and analysis.

**Martin Sirois** supervised the histology part of this study.

**Bruce Allen** co-supervised the project, interpreted the biochemical analysis, participated in data analysis, provided intellectual input and edited the final draft of the manuscript.

**Stanley Nattel s**upervised the whole project, conceived, designed and provided intellectual ideas for the experiments, interpreted the data and edited the final draft of the manuscript.

# Targeting the lysyl oxidase protein signaling pathway in atrial fibrosis and fibrillation

**Doa'a Al-u'datt[1,2], Roddy Hiram[2], Natacha Daquette[2], Yanfen Shi[2], Jean-Claude Tardif[2,3], Martin G. Sirois[1,3], Bruce Allen[1,2,3,4], and Stanley Nattel[1,2,3,5*]**

[1]Department of Pharmacology and Physiology, Université de Montréal, Montreal, Quebec, Canada

[2]Montreal Heart Institute and Université de Montréal, Montreal, Quebec, Canada

[3]Department of Medicine, Montreal Heart Institute, Montreal, Quebec, Canada

[4]Department of Biochemistry and Molecular Medicine, Université de Montréal, Montreal, Quebec, Canada

[5]Department of Pharmacology and Therapeutics, McGill University, Montreal, Quebec, Canada

**Running head: Role of LOX and LOXL proteins in atrial fibrillation**

*Address correspondence to: Stanley Nattel, Montreal Heart Institute, 5000 Belanger Street East, Montreal, Quebec, H1T 1C8, Canada. Tel.: 514-376-3330; Fax: 514-376-1355. E-mail: stanley.nattel@icm-mhi.org.

## Abstract

**Aims:** The lysyl oxidase (LOX) enzyme has a vital role in the stability of the extracellular matrix (ECM) during remodeling in several heart diseases, such as heart failure (HF), fibrosis and atrial fibrillation (AF). Atrial fibrosis is a hallmark of atrial dysfunction and structural remodeling that affects the propagation and conduction of cardiac impulses promoting AF. This study was performed to address the roles of LOX and LOX-like (LOXL) proteins in signal transduction, leading to left atrial (LA) fibrosis and AF as a potential therapeutic target.

**Methods and results:** Congestive heart failure (CHF) was induced in adult mongrel dogs by ventricular tachypacing (VTP) for two weeks, followed by measuring the mRNA and protein expressions of LOX and LOXL proteins in the LA tissues. Our results revealed that the protein expression of LOX and LOXL-1 were significantly increased in the LA tissues of CHF dogs. Myocardial infarction (MI) was induced by ligation of the left anterior descending coronary artery in male Wistar rats, followed by the administration of a LOX inhibitor (β-aminopropionitrile; BAPN) via an osmotic pump. There was an upregulation in the mRNA abundance of LOX, LOXL-1, LOXL-2 and LOXL-3 along with an increase in the mRNA expression of COL 1A1, TGF-β1 and periostin in the LA tissues post-MI. AF inducibility, fibrosis and dilatation were increased in the LA post-MI. However, administration of BAPN post-MI decreased LOXL-1, LOXL-2, LOXL-3, COL 1A1, COL 3A1, TGF-β1, periostin and α-SMA mRNA expression, as well as fibrosis, AF inducibility and adverse remodeling in the LA. Nevertheless, there were no significant changes in LOX family mRNA expression, collagen cross-linking, fibrosis and adverse remodeling in the LV upon administration of BAPN post-MI. Furthermore, administration of BAPN post-MI decreased the correlations of wall motion score index (WMSI) with LA area, LA dimensions and fractional area change and had a modest effect on the correlations of WMSI with LV structural and functional parameters.

**Conclusions:** The major finding of this study was that the upregulation of LOX and LOXL protein expression in LA tissues plays an essential role in LA remodeling and AF maintenance post-MI. Inhibition of the LOX signaling pathway using BAPN has a potential therapeutic role in LA fibrosis and AF post-MI.

**Keywords** Myocardial infarction • Atrial fibrillation • Atrial fibrosis • Lysyl oxidase (LOX) • LOX-like (LOXL) protein • Left atrial remodeling • Correlations.

## 1. Introduction

Atrial fibrillation (AF), a common disorder, is accompanied by several complications that lead to high morbidity and mortality [1]. The incidence of AF increases from 0.5 % to 5-20 % of patients as age increased from 40-50 to 85 years old, respectively [2, 3]. The prevalence of AF ranges from 1 to 2 % of the population, and this percentage is predicted to increase in the future [3]. In the past two decades, the AF incidence increased to 13 % of the population [4]. AF is a common clinical dysrhythmia in which the atria beat in a rapid chaotic manner (350-600 bpm) and is prevalently among patients with diabetes mellitus, hypertension, sleep apnea, obesity, diastolic and systolic heart failure (HF), coronary artery diseases, myocardial infarction (MI) and valvular heart diseases [5-7]. Furthermore, 10 to 50 % of chronic HF cases develop AF with a poor prognosis [8, 9]. HF is associated with significant structural remodeling of the atria that can lead to increased AF susceptibility [10]. AF patients are characterized by increased atrial volume, atrial size and fibrosis than sinus rhythm patients [11, 12]. The key hallmarks of atrial structural remodeling are dilatation and fibrosis of the atrium, which later lead

to AF [11]. Atrial fibrosis disturbs the electrophysiological properties of the heart and stimulates the micro-reentry circles, leading to AF [7]. Cardiac fibrosis is a common pathological disorder characterized by deposition of extracellular matrix (ECM) proteins [13]. Excessive production of ECM proteins increases myocardial stiffness and changes cardiac mechanics, which contributes to the pathophysiology of HF. Myocardial stiffness has several beneficial roles at the early stages of collagen deposition, such as wound healing and prevention of myocardial infarct expansion before the development of a chronic pathological state (cardiac fibrosis) [14]. A total of 45 % of the total deaths per year worldwide are caused by fibrotic diseases [15]. Cardiac fibrosis causes a substantial proportion of deaths among all types of fibrosis. Cardiac fibrosis is initially an adaptive and protective mechanism. Nevertheless, prolonged cardiac fibrosis leads to adverse remodeling and distinct impairment of ventricular function [13, 15]. In the heart, increased deposition of ECM proteins is caused by several pathological conditions, such as pressure overload, MI, diabetes and cardiomyopathy [16]. The lysyl oxidase (LOX) family, a copper-dependent amine oxidase, has a dynamic function in the genesis of connective tissue matrices by catalyzing the oxidation of lysine in elastin and collagen to form cross-linked molecules [17]. The LOX family consists of five members, namely LOX and LOX-like proteins (LOXL-1, LOXL-2, LOXL-3 and LOXL-4) [18]. The LOX family oxidizes the ε-amino group of peptidyl lysine to peptidyl aldehyde in elastin and collagen to produce peptidyl α-aminoadipic γ-semialdehydes, followed by continuous condensation of semialdehydes with neighboring amino acids or peptidyl aldehydes to form cross-linked (insoluble) collagen and elastin fibers [17, 19, 20]. The LOX family has an important function in the stability of ECM proteins during various cardiac diseases [21-23]. A variety of models in which animals are subjected to pressure or volume overload show cardiac fibrosis, which is associated with an increase in LOX activity/expression and collagen cross-linking [22, 24]. The mechanisms of cardiac fibrosis underlying the development of AF are not well understood. To date, there are no effective drugs to reverse

cardiac fibrosis. Understanding the common signaling mechanisms in the progression of cardiac fibrosis is necessary for the development of more effective means of prevention and treatment. The main objective of this study was to address the roles of LOX and LOXL proteins in signal transduction, leading to atrial fibrosis, atrial remodeling and AF in a MI rat model.

## 2. Methods

### 2.1 Animal Models

#### 2.1.1 Dog model

Adult mongrel dogs (20-30 kg) were divided into two groups, namely non-paced controls and dogs with congestive heart failure (CHF) induced by ventricular tachypacing (VTP) according to the method described by Dawson *et al.* [25]. Dogs were sedated with 0.25 mg/kg of diazepam, 5.0 mg/kg of ketamine and 1.0-2.0 % of halothane for pacemaker implantation. Following sedation of the dogs, tachypacemakers (model 8084, Medtronic) were subcutaneously implanted in the neck and connected to ventricular pacing leads in the right ventricular (RV) apex via left jugular vein under fluoroscopy. After 24 hrs post-operative recovery, the pacemakers were programmed to stimulate the RV for two weeks at 240 bpm inducing CHF. Clinical signs (edema, dyspnea and lethargy) and *in vivo* hemodynamic measurements were assessed to confirm CHF. Two weeks later, the dogs were sedated with 2.0 mg/kg of morphine and 120 mg/kg of α-chloralose, and the hearts were then excised. Left atrial (LA) tissues were kept at -80°C for further experiments. The Ethics Committee of the Animals Research in the Montreal Heart Institute approved the animal care and handling procedures according to the Animal Care guidelines of the Canadian Council (NIH Publication 65-23, revised 1996).

### 2.1.2 Rat model

Male Wistar rats (150-175 g) were obtained from Charles River Inc. (Saint-Constant, Quebec, Canada). A standard laboratory diet was used to feed the rats (normal rat chow diet; 2018 Harlan). Rats were housed in the animal care unit of the Montreal Heart Institute (University of Montreal, Montreal, Quebec, Canada) with a 12 hr light/dark cycle under controlled environmental conditions, with a temperature of 21±2°C and 50 % humidity level. All rats had free access to drinking water and food. All aspects of animal experiments were carried out and approved by the Animal Ethical Committee of the Montreal Heart Institute (University of Montreal, Montreal, Quebec, Canada) according to the procedures and guidelines of the Canadian Council of Animal Care. The rats were randomly classified into four groups, namely Sham (control+saline vehicle), MI (MI+saline vehicle), Sham+BAPN and MI+BAPN. BAPN infusion was initiated week after the MI surgery and continued for 3 consecutive weeks at 100 mg/kg/day (Santa Cruz Biotechnology, Dallas, TX, USA) using a subcutaneously implanted osmotic mini-pump (Alzet, Cupertino, CA). Buprenorphine (0.03 mg/kg) was subcutaneously administered in two doses; before implantation of the pump and 24 hr after implantation of the pump. Figure 1 illustrates the experimental timeline for echocardiography and electrophysiological assessment.

### 2.2 MI surgery

The MI protocol was performed according to the method described by Cardin *et al.* [26]. Rats were sedated using 3 % isoflurane under ventilation. A dose of 0.03 mg/kg buprenorphine was injected subcutaneously before MI surgery. The thoracic hair of the rat was shaved, followed by sterilization with 2 % chlorhexidine gluconate and 70 % isopropyl alcohol. The left thoracotomy and pericardial incision were performed under an artificial respirator. The left anterior descending coronary artery was ligated with a 5-0 silk suture. The heart was returned to the normal position,

and the chest was then closed with a 4-0 silk suture, followed by skin closure with autoclips. The rat was placed on a thermal plate during the surgery to maintain a steady body temperature. The artificial respirator was disconnected post-surgery after rat recovery. Buprenorphine (0.03 mg/kg) was subcutaneously administered in two doses at 6 and 12 hr post-surgery.

### 2.3 Assessment of transthoracic echocardiography

Transthoracic echocardiographic measurements (cardiac dimensions and functions) were performed according to the method described by Cardin *et al.* [26] and Reffelmann and Kloner [27] before MI surgery and at day 7 and 27 post-MI by using a Vivid 7 Dimension system (GE Healthcare Ultrasound, Horten, Norway) and a phased-array 10S probe (4.5-11.5 Megahertz). Rats were anesthetized with 3 % isoflurane, and two-dimensional echocardiography was then used to visualize the left ventricular (LV) myocardial infarct. LV myocardial infarct areas were assessed by viewing the short-axis of the LV at the papillary muscle level. The wall motion of the LV was scored as follows: 1 (normal), 2 (hypokinesis), 3 (akinesis), 4 (dyskinesis) or 5 (aneurysmal). Sections of the LV were used to evaluate the wall motion score index (WMSI). The WMSI was measured by calculating the average wall motion score for multiple LV segments. The M-mode spectrum of the LV was analyzed in the short-axis view at the papillary muscle level. Dimensions (D) of the LV were evaluated at the end of cardiac systole (s) and diastole (d) and described as LVDs and LVDd, respectively. The thickness of the LV was measured at the posterior (P) and anterior (A) walls (W) and described as LVPW and LVAW, respectively. Fractional shortening (FS) of the LV was measured according to equation 1:

$$FS_{LV} = \left(\frac{LVDd - LVDs}{LVDd}\right) * 100\ \% \qquad (1)$$

Doppler imaging of tissues was used to measure lateral (L) and septal (S) mitral annulus movement

velocities in systole ($S_L$ and $S_S$, respectively). The ejection fraction (EF) of the LV was calculated by the manipulated formula in the Vivid 7-dimensional system. LV mass was calculated using the formula suggested by Reffelmann and Kloner [27]. Furthermore, LV structural remodeling was evaluated by calculating the ratios of LV mass to body weight (BW), LVDd to BW, and LV mass to LVDd. An M-mode spectrum of LA and right atrium (RA) in the view of the parasternal long axis view at the aortic valve level was obtained. Atrial dimensions were measured at the end of cardiac diastole (LADd) and systole (LADs and RADs, respectively). FS of the LA was calculated based on equation 2.

$$FS_{LA} = \left(\frac{LADd - LADs}{LADd}\right) * 100\ \% \quad (2)$$

Heart rate and R-R interval were measured at the time of electrocardiogram (ECG) recording. The 4-chamber apical view was obtained, and areas (A) of the LA were then measured at the end of cardiac diastole ($LAA_d$) and systole ($LAA_s$). Fractional area changing (FAC) of the LA and RA was estimated according to equations 3 and 4:

$$FAC_{LA} = \left(\frac{LAAs - LAAd}{LAAs}\right) * 100\ \% \quad (3)$$

$$FAC_{RA} = \left(\frac{RAAs - RAAd}{RAAs}\right) * 100\ \% \quad (4)$$

Pulsed wave (PW) Doppler was also performed to estimate the transmitral flow (TMF) in the apical four-chamber view. Early peak velocity filling (E wave), E wave deceleration time (EDT), peak velocity during atrial filling (A wave) and E/A ratio were measured in the TMF. The mitral annulus moving velocity during early (e') filling and atrial (a') filling as well as the e'/ a' ratio were measured in both lateral and septal views. The PW in the apical five-chamber view was used to obtain the transaortic flow. The time interval from mitral valve (MV) closing to opening (MVco)

and the LV ejection time (LVET) were measured. The myocardial performance index (MPI) of the LV was calculated according to equation 5:

$$MPI_{Global}=\left(\frac{MVco-LVET}{LVET}\right)*100\ \% \quad (5)$$

$MPI_{Lateral}$ and $MPI_{Septal}$ were calculated according to equation 6:

$$MPI_{Septal}\text{ or }MPI_{Lateral}=\left(\frac{B-A}{A}\right)*100\ \% \quad (6)$$

B: Time interval from the end of a' to the beginning of e' based on the lateral and septal views.

A: Time interval from the beginning to the end of $S_L/S_S$.

The averages of 3 to 6 consecutive cardiac cycles were used to obtain the structural and functional parameters. Great attention was taken in order to obtain similar images for measurements of echocardiographic parameters. All of the echocardiographic measurements were performed by the same echocardiographer who was blinded to the experimental design.

### 2.4 *In vivo* electrophysiological study via trans-jugular stimulation

The electrophysiological study was performed according to the method described by Iwasaki *et al.* [28]. Rats were anesthetized by inhalation of 3 % isoflurane. Once under anesthesia, rats were intubated and mechanically ventilated with 100 % $O_2$. A quadripolar catheter (i.d. 1 mm; Sonde 4F Supreme, St-Judr Medical 401993) was inserted into the RA through the jugular vein to induce programmed atrial stimulation. The coincidence of the catheter position in the RA and the P wave on the surface ECG were monitored to assure the exact position of the catheter in the RA. Automated RA stimulation was induced with a 150 ms cycle length (2-ms pulse width, 2x

threshold current) to determine the effective refractory periods (ERPs). Atrial ERPs were well-defined as the longest S1-S2 coupling interval failing to generate a propagated beat. Burst pacing (25-Hz, 4x threshold current, pulse width 2 ms) was applied for 3 sec, with 3 sec of six burst cycles (disconnected by 1-sec intervals) to estimate the atrial arrhythmia inducibility. A rapid irregular atrial rhythm with varying electrogram morphology (missing P-waves) for more than 1 sec after the 6 burst cycle protocol was classified as AF. Burst pacing was deferred to avoid interfering with the progress of AF in case AF was initiated after less than 6 burst pacing cycles. The duration of AF was measured for each rat as the average duration in seconds for all AF occurrences. Stimulus artifacts, intracardiac electrograms and surface ECG were monitored and analyzed by IOX2 software (Version 2.8.0.13; EMKA technologies, Paris, France).

**2.5 Fibrosis quantification by Masson's trichrome staining**

Fibrosis in cardiac tissues was quantified as described by Cardin *et al.* [26] and Yang *et al.* [29]. Hearts from 28-day post-MI rats were fixed in 10 % formalin for structural preservation. Hearts were dehydrated with xylene and then embedded in paraffin. Several transverse cross-sections of 6 μm thickness from LA and LV tissues were obtained every 500 μm. LA and LV tissues were rehydrated with xylene (4 X 5 min), followed by a sequential series of ethanol dilutions: 100 % (2 X 3 min), 95 % (1 X 3 min), 70 % (1 X 3 min) and 0 % (2 X 2 min). Tissue sections were stained with Masson's trichrome for fibrosis quantification. The slides were incubated with Bouin's solution overnight at room temperature. The slides were washed with running tap water to eliminate the yellow color from slide sections. Slide sections were immersed in Weigert's Iron Haematoxylin solution for 10 min, followed by multiple washings with running tap water. The slides were immersed in Biebrich Scarlet-acid Fucshin for 15 min and then rinsed with distilled water. The slides were immersed in Phosphotungstic/Phosphomolybdic acid solution for 8 min

and Aniline Blue solution for 7 min, followed by washing with distilled water and 1 % acetic acid for 3 min. Finally, the slides were dehydrated with 95 % (2 X 30 sec) ethanol, 100 % (2 X 30 sec) ethanol and 100 % xylene (2 X 2 min). Stained LA and LV sections were analyzed with software (Image-Pro 9.3) at 10x magnification. Collagen around the blood vessels was excluded during the fibrosis quantification. Whole LVs were stained with Masson's trichrome and used for measurement of total areas of LV and infarct (scar area; blue stained) at 1.25x magnification using Image-Pro 9.3 software. Scar area was calculated as the percentage of LV infarct area to total LV area. Fibrous tissue contents of atrial and ventricular tissues were represented as the percentage of collagen in each region and the average of all five regions for each rat in the four groups, as described in equation 7.

$$\text{Fibrous tissue content} = \left(\frac{Area\ covered\ by\ collagen}{Total\ area\ of\ the\ field}\right) * 100\ \% \qquad (7)$$

**2.6 RNA extraction, reverse transcription (RT) and quantitative real-time polymerase chain reaction (qPCR)**

RNA extraction was performed according to the method previously described by Duong *et al.* [30]. Frozen tissues from the LA and LV were mixed with Trizol reagent (Invitrogen, Carlsbad, CA, US) and homogenized with polytron. RNA was extracted from homogenized samples with the miRNeasy Mini Kit (Qiagen, MD, Germany). Quantification and qualification of RNA were estimated using a Nanodrop spectrophotometer. cDNA was synthesized from 250 ng of total RNA with a High Capacity cDNA Reverse Transcription Kit (SuperArray, Applied Biosystems, Foster City, CA, US). Real-time qPCR was performed with TaqMan Universal Master Mix (Applied Biosystems, Foster City, CA, US) and SuperArray SYBR Green PCR kits (Applied Biosystems, Foster City, CA, US), custom-made SYBR Green primers (glucose 6-phosphate dehydrogenase

(G6PD), β2 microglobulin (B2m), matrix metalloproteinase 2 (MMP-2), MMP-9, α-smooth muscle actin (α-SMA), periostin, connexin 43 (Cx 43), transforming growth factor β1 (TGF-β1), connective tissue growth factor (CTGF), LOX, LOXL-1, LOXL-2, LOXL-3 and LOXL-4; Applied Biosystems, Foster City, CA, US; Supplementary Table S1) and rat TaqMan probes (LOX (Assay ID: Rn01491829), glyceraldehyde 3-phosphate dehydrogenase (GAPDH; Assay ID: Rn01775763_g1), collagen 1A1 (Col 1A1; Assay ID: Rn01463848_m1), collagen 3A1 (Col 3A1; Assay ID: Rn01437681_m1) and Fibronectin 1 (FN 1; Assay ID: Rn00569575_m1); Applied Biosystems, Foster City, CA). A rat SYBR primer for LOXL-4 (Assay ID: qRnoCID0018064) was purchased from Bio-Rad (CA, US). The relative quantifications of all samples were calculated with the comparative threshold cycle ($2^{-\Delta\Delta Ct}$) method [31] . B2m and G6PD were used as internal standards for rats and dogs, respectively.

**2.7 Protein quantification using immunoblot analysis**

Protein expression was quantified by Western blot analysis according to the method described by Surinkaew *et al.* [32]. Snap-frozen LA and LV tissues were immersed in lysis sample buffer and then homogenized by polytron. The lysis sample buffer was prepared by mixing 0.3 ml of 5.0 M NaCl, 0.5 ml of 1.0 M Tris HCl (pH 7.5), 0.05 ml of 20 % sodium dodecyl sulfate (SDS), 0.01 ml of 10 % Triton, 1.0 ml of 100 % glycerol, 20.0 µl of 0.5 M phenylmethanesulfonyl fluoride (PMSF) and one tablet of protease and phosphatase inhibitor cocktail with 8.14 ml of distilled water. The homogenized samples were kept for 30 min in an ice bath and then centrifuged at 8,000 rpm for 10 min at 4°C. Supernatants of the samples were subjected to protein quantification by the Bradford assay to adjust the amount of proteins in the samples. Twenty micrograms of proteins from lysed samples were mixed with loading buffer and then denatured for 5 min at 95°C. Loading buffer was prepared by mixing 4.5 ml of 0.5 M Tris HCl (pH 6.8), 1.0 ml of 20 % SDS, 5.0 ml of

100 % glycerol, 0.5 g of dithiothreitol (DTT), and 1.0 ml of 0.3 % bromophenol blue. Protein samples were separated by SDS polyacrylamide gel electrophoresis (SDS-PAGE; 4-20 % gradient gels) and then transferred onto 0.45 μm polyvinylidene difluoride membranes (PVDF, EMD Millipore, Billerica, MA, US). The membranes were immersed in blocking solution (0.1 ml of Tween 20 and 5.0 g of non-fat dry milk (NFDM) in 100 ml of Tris-buffered saline (TBS)) for 1.5 hr and then incubated with primary antibody, with continuous mixing overnight at 4°C. The membranes were washed with 0.1 % Tween 20 in TBS (v/v; 3 X 15 min) and then incubated with secondary antibodies conjugated to horseradish peroxidase (HRP) with continuous mixing for 1 hr at room temperature. The membranes were washed with 0.1 % Tween 20 in TBS (v/v; 3 X 15 min), and immunoreactive protein bands were then visualized using Western Lightning Plus ECL reagent (PerkinElmer, Waltham, MA, US) and Kodak film. Protein bands were quantified with ImageJ software and normalized to glyceraldehyde 3-phosphate dehydrogenase (GAPDH) and Tubulin densities from the same samples and membranes. The blots were reacted with antibodies of anti-LOX (1:5000, ab174316, Abcam), anti-LOXL-1 (1:2000, PA5-44213, Thermo Fisher), anti-LOXL-2 (1:2000, ab96233; Abcam), anti-LOXL-3 (1:2000, PA5-45074, Thermo Fisher), anti-LOXL-4 (1:1000, ab88186, Abcam), anti-GAPDH (1:10,000, 10R-G109A, Fitzgerald) and anti-alpha Tubulin (1:10,000, ab7291, Abcam). HRP-conjugated secondary antibodies (goat anti-rabbit, donkey anti-rabbit and donkey anti-mouse) were used at a dilution of 1:10,000 (Jackson ImmunoResearch Laboratories, West Grove, PA, US).

**2.8 Soluble, insoluble and cross-linking collagen analysis**

The soluble and insoluble collagens were determined by a colorimetric method using a total collagen assay kit (QuickZyme BioSciences, Leiden, Netherlands) [33]. Frozen LV and LA tissues were immersed in 0.5 M acetic acid (10 % w/v) and then extensively minced with scissors and

homogenized by polytron in an ice bath. Homogenized tissues were kept at 4°C/48 hr with continuous shaking to liberate soluble collagen, followed by centrifugation at 37,000 g for 60 min at 4°C. The supernatants and pellets were recovered as soluble and insoluble collagens, respectively. Soluble and insoluble collagens were determined as hydroxyproline contents in supernatants and pellets, respectively. The supernatants and pellets were hydrolyzed with diluted HCI (12.0 M and 6.0 M, respectively) for 21 hr at 95°C. Hydroxyproline contents were quantified from hydrolyzed supernatants and pellets by using the QuickZyme assay kit. The absorbance of samples was monitored at a wavelength of 570 nm. The soluble and insoluble collagens are expressed as μg/mg wet tissue according to the standard curve of hydroxyproline contents of the collagen stock solution (QuickZyme assay kit). The degree of collagen cross-linking was calculated as the ratio of insoluble collagen to total collagen.

**2.9 Statistical analysis**

Results are presented as the means ± standard error of the mean (SEM). Statistical analysis was carried out using GraphPad Prism 7 (GraphPad Software, La Jolla, CA). Unpaired Student's *t*-tests were performed to compare two groups. One-way analysis of variance (ANOVA) followed by Bonferroni's multiple comparisons test was performed between more than two groups. Fisher's exact tests were performed to compare AF inducibility. One-way ANOVA followed by the Kruskal-Wallis's multiple comparisons test was performed for AF duration. Two-way ANOVA followed by Bonferroni's multiple comparisons test was applied for two independent variables. Linear regression analysis was carried out to assess the relationship between the WMSI and echocardiographic parameters, including structural and functional parameters of the LA and LV in the MI and MI+BAPN groups; $*P < 0.05$; $**P < 0.01$; $***P < 0.001$.

## 3. Results

### 3.1 Increased LOX family expression in LA tissues of CHF dogs

Several changes occur in CHF, including an increase in atrial fibrosis and AF susceptibility [1]. This part of the study examined the mRNA and protein levels of the LOX family (LOX and LOXL-1, 2, 3 and 4) in the LA tissues from control and CHF dogs by qPCR and Western blot analysis, respectively (Figure 2; Supplementary Figure S1). The mRNA and protein levels of the LOX family were increased at different levels in the LA tissues of CHF dogs compared with control (Figure 2; Supplementary Figure S1). mRNA and protein expression levels of LOXL-1 were significantly increased in the LA tissues of CHF dogs ($P$ = 0.001 and $P$ = 0.02, respectively) compared with controls (Supplementary Figure S1B; Figure 2A and C). LOX protein expression was significantly increased in the LA tissues of CHF dogs compared with controls ($P$ = 0.01; Figure 2A and B); however, the abundance of LOX mRNA did not change significantly ($P$ = 0.05; Supplementary Figure S1A). The upregulation of LOX and LOXL-1 in the LA tissues of the CHF dog model suggested that these isoforms may have roles in the LA fibrotic response and atrial remodeling during CHF development.

### 3.2 Administration of BAPN post-MI in rats decreased the P-wave duration, AF duration and AF inducibility

MI is commonly accompanied by AF and a higher risk for death [34, 35]. We used an MI rat model to further investigate the role of the LOX family in LA remodeling post-MI. The MI group exhibited a significant increase in AF inducibility compared with the Sham group, with values of 77.8 and 11.1 %, respectively (Figure 3A). Additionally, AF inducibility was significantly decreased in the MI+BAPN group (40.0 %) compared with the MI group (77.8 %; Figure 3A). The AF duration in the

MI group was significantly higher than that in the Sham or MI+BAPN group, with values of 2.4±0.8, 0.21±0.11 and 0.61±0.20 sec, respectively (Figure 3B). The AF duration in the MI+BAPN group (0.61±0.20 sec) was significantly longer than that in the Sham+BAPN group (0.16±0.07 sec) (Figure 3B). Regarding ERP values, there were no significant differences between the four groups (Figure 3C). The P-wave duration in the MI group (28.7±0.7 ms) was significantly longer than those in the Sham group (23.7±0.5 ms) or the MI+BAPN group (25.2±0.8 ms; Figure 3D). The values of the P-P interval, P-R interval, QRS and QT were significantly longer in the MI group (186.1±4.7, 61.7±1.4, 34.9±1.2 and 88.3±2.6 ms, respectively; Figure 3E-H) than the Sham group (162.9±4.6, 56.2±1.3, 29.4±1.1 and 75.5±2.6 ms respectively; Figure 3E-H). There were no significant differences in the P-P interval, P-R interval, QRS and QT between the MI+BAPN and MI groups. Supplementary Figure S2 illustrates examples of surface ECG and recording of burst pacing-induced AF in four rat groups (Sham, Sham+BAPN, MI and MI+BAPN) at day 28 post-MI. The results revealed that MI increased the P-wave duration, AF duration and AF inducibility, whereas administration of BAPN post-MI reduced these values significantly.

### 3.3 Administration of BAPN post-MI in rats attenuated LA fibrosis without changing LV fibrosis

The fibrous contents of the LA and LV (remote (Rem) and infarct (Inf) areas) in the four groups (Sham, MI, Sham+BAPN and MI+BAPN) were evaluated with Masson's trichrome staining. The percentage of LA fibrous tissue in the MI group was significantly higher than that in the Sham group, with values of 14.6±1.8 % and 5.5±1.1 %, respectively (Figure 4A-B). However, administration of BAPN post-MI significantly decreased the percentage of LA fibrous tissues from 14.6±1.8 % to 9.46±0.68 % (Figure 4A-B). However, there were no significant changes in LA fibrous tissue content between the Sham (5.5±1.1 %; Figure 4A-B) and Sham+BAPN (5.9±0.7 %; Figure 4A-B) groups.

The infarcted area of the LV in the MI group demonstrated a significant increase in fibrous tissue percentage compared with that in the remote area of the LV in the MI and Sham groups, with values of 55.1±5.2, 2.9±0.5 and 2.3±0.5 %, respectively (Figure 4A and C). The infarcted area of the LV in the MI+BAPN group exhibited a significant increase in fibrous tissue percentage compared with those in the remote area of the LV in the MI+BAPN or Sham+BAPN groups, with values of 55.2±6.3, 1.7±0.4 and 2.1±0.3 %, respectively (Figure 4A and C). However, there were no significant differences in the LV fibrous tissue contents in the MI-Inf vs MI+BAPN-Inf, MI-Rem vs MI+BAPN-Rem or Sham vs Sham+BAPN groups (Figure 4A and C). Additionally, no significant differences were found in the percentage of scarred areas between the MI and MI+BAPN groups (Figure 4D).

### 3.4 BAPN administration decreased MI-induced LA remodeling in rats

The values of $LAD_s$ and $LAD_d$ in the MI group (6.5±0.2 and 5.4±0.2 mm, respectively) were significantly higher than those in the Sham (5.7±0.2 and 4.2±0.2 mm, respectively) or MI+BAPN (5.7±0.2 and 4.5±0.2 mm, respectively) groups (Figure 5A-B and Table 1). The values of $LAD_s$ and $LAD_d$ in the MI+BAPN group (5.7±0.2 and 4.5±0.2 mm, respectively) were significantly higher than those in the Sham+BAPN group (5.0±0.1 and 3.6±0.1 mm, respectively; Figure 5A-B and Table 1). Additionally, the MI group had a significant decrease in FS of the LA compared with the Sham or MI+BAPN group, with values of 17.7±1.3, 27.4±1.0 and 22.6±1.4 %, respectively (Figure 5C and Table 1). For FS of the LA, the MI+BAPN group (22.6±1.4 %) had a significant decrease compared with that of the Sham+BAPN group (28.7±1.3 %; Figure 5C and Table 1). The values of $LAA_s$ and $LAA_d$ were significantly decreased in the MI+BAPN group compared with the MI group (Supplementary Figure S3A-B and Table 1), while there were no significant changes in $FAC_{LA}$ between the MI and MI+BAPN groups (Supplementary Figure S3C and Table 1). In the MI group, WMSI was positively and significantly correlated with $LAD_s$ ($R^2 = 0.503$; $P < 0.001$; Figure 5D),

$LAD_d$ ($R^2$ = 0.563; $P$ < 0.001; Figure 5E), $LAA_s$ ($R^2$ = 0.396; $P$ = 0.001; Supplementary Figure S3D) and $LAA_d$ ($R^2$ = 0.464; $P$ < 0.001; Supplementary Figure S3E), while the administration of BAPN post-MI decreased the significance of the correlation between WMSI and $LAD_s$ ($R^2$ = 0.150; $P$ = 0.08; Figure 5D), $LAD_d$ ($R^2$ = 0.219; $P$ = 0.03; Figure 5E), $LAA_s$ ($R^2$ = 0.099; $P$ = 0.15; Supplementary Figure S3D) or $LAA_d$ ($R^2$ = 0.225; $P$ = 0.03; Supplementary Figure S3E). The administration of BAPN had no effect on the correlation between the WMSI and FS of the LA post-MI (Figure 5F). However, the MI+BAPN group exhibited a significant decrease in the correlation between WMSI and $FAC_{LA}$ ($R^2$ = 0.262; $P$ = 0.01; Supplementary Figure S3F) compared with that in the MI group ($R^2$ = 0.357; $P$ = 0.003; Supplementary Figure S3F). Regarding the correlation of LA echocardiographic parameters, there were no significant differences between the slopes of MI and MI+BAPN groups (Table S2). Moreover, the value of Y-intercepts for $LAD_d$, $LAD_s$, $LAA_d$, $LAA_s$ and FS were significantly varied between the MI and MI+BAPN were significantly differed (Table S2). The results demonstrated that MI induced dilatation and impaired LA functions; however, the administration of BAPN post-MI attenuated the adverse LA remodeling.

### 3.5 BAPN administration had no effect on MI-induced LV remodeling in rats

The $LVD_s$, $LVD_d$, LV mass and WMSI values were significantly increased in the MI group (7.2±0.3 mm, 9.8±0.2 mm, 1259.0±36.7 mg and 1.7±0.1, respectively) vs Sham group (3.6±0.1 mm, 7.9±0.1 mm, 897.6±20.1 mg and 1.0±0.0 mm, respectively) or MI+BAPN group (6.6±0.4 mm, 9.3±0.2 mm, 1124.0±43.3 mg and 1.6±0.1, respectively) vs Sham+BAPN group (3.64±0.1 mm, 7.6±0.1 mm, 787.0±29.5 mg and 1.0±0.0 mm, respectively; Table 1 and Figure 6A-C and I). However, there were no significant changes in $LVD_s$, $LVD_d$ and WMSI values in the MI group compared with those in the MI+BAPN group. Furthermore, the MI+BAPN group showed a significant decrease in EF and FS of the LV (60.1±3.6 and 30.8±2.1 %, respectively) compared with

those in the Sham+BAPN group (87.0 ±1.0 % and 52.0±1.2, respectively; Table 1, Figure 6H and Supplementary Figure S4P). MI rats had significantly lower values of EF, FS, $S_s$ and $S_L$ in the LV (57.1±2.9 %, 27.4±1.8 %, 4.4±0.2 cm/s and 4.7±0.2 cm/s, respectively) compared with the Sham group (88.9±0.8 %, 54.7±1.2 %, 5.2±0.2 cm/s and 5.6±0.2 cm/s, respectively; Table 1, Figure 6H and Supplementary Figure S4P-R). The LVmass/$LVD_d$, E/e'$_{Septal}$, E/e'$_{Lateral}$, $LVV_d$, $LVV_s$ and $MPI_{Global}$ values were significantly increased in the MI vs Sham group or MI+BAPN vs Sham+BAPN group (Table 1 and Supplementary Figure S4C-E, N-O and S). The WMSI of the MI group showed positive significant correlations with $LVD_s$ ($R^2 = 0.897$; $P < 0.001$; Figure 6D), $LVD_d$ ($R^2 = 0.657$; $P<0.001$; Figure 6E), $LVV_s$ ($R^2 = 0.869$; $P < 0.001$; Supplementary Figure S4U), $LVV_d$ ($R^2= 0.675$; $P<0.001$; Supplementary Figure S4T), E/e'$_{Septal}$ ($R^2 = 0.584$; $P < 0.001$; Supplementary Figure S4K), E/e'$_{Lateral}$ ($R^2 = 0.446$; $P < 0.001$; Supplementary Figure S4L) and $MPI_{Global}$ ($R^2 = 0.475$; $P<0.001$; Supplementary Figure S4Y), whereas the regression analysis in the MI group revealed negative significant correlations of WMSI with EF ($R^2 = 0.891$; $P < 0.001$; Figure 6K) and FS ($R^2 = 0.871$; $P < 0.001$; Supplementary Figure S4V). However, the correlations of WMSI with LVAW, LVPW, LV mass/$LVD_d$ and EDT were weak and non-significant in the MI group (Supplementary Figure S4G-I and M). The correlation of LV echocardiographic parameters, there were no significant differences between the slopes of MI and MI+BAPN groups (Table S2) except for E/A and E/e' $_{Septal}$ which had significant differences between the slopes of MI and MI+BAPN groups ($P = 0.02$ and $P = 0.04$, respectively; Table S2). The values of Y-intercept for $LVPW_d$, LV mass, $S_L$ and $MPI_{Global}$ were significantly differed between the MI and MI+BAPN groups (Table S2). The administration of BAPN post-MI had little effect on the strength and significance of WMSI correlations with LV structural and functional parameters. The results demonstrated that MI impaired LV structure and function; however, the administration of BAPN post-MI did not significantly affect the adverse LV remodeling.

### 3.6 Administration of BAPN post-MI in rats attenuated LA collagen cross-linking without a change in LV collagen cross-linking

The soluble collagen content in the LA tissues of the Sham+BAPN (2.34±0.33 μg/mg) and MI+BAPN (2.75±0.49 μg/mg) groups was significantly increased compared with that in the Sham (0.36±0.05 μg/mg) and MI (0.48±0.07 μg/mg) groups, respectively (Figure 7A). However, there were no significant changes in the content of insoluble collagen in the LA tissues between the groups (Figure 7B). The ratios of collagen cross-linking in the LA tissues of the Sham+BAPN (0.69±0.03) and MI+BAPN (0.65±0.02) groups were significantly lower than those in the Sham (0.92±0.01) and MI (0.92±0.01) groups, respectively (Figure 7C). The content of soluble collagen in the LV tissues of the MI+BAPN-Inf group (5.35±1.30 μg/mg) was significantly higher than that in the MI-Inf group (2.42±0.13 μg/mg) (Figure 7D). Furthermore, the insoluble collagen contents in the LV tissues of the MI-Inf (14.02±3.84 μg/mg) and MI+BAPN-Inf (13.87±2.91 μg/mg) groups were significantly increased compared with those in the Sham (1.59±0.35 μg/mg) and Sham+BAPN (2.68±0.65 μg/mg) groups, respectively (Figure 7E). No significant changes were found in the soluble and insoluble collagen contents in the LV tissues of the MI-Rem vs MI+BAPN-Rem or Sham vs Sham+BAPN groups (Figure 7D-E). Nevertheless, collagen cross-linking ratios in the LV tissues were not significantly different between the groups (Figure 7F). The results revealed that the administration of BAPN post-MI decreased the collagen cross-linking ratios in the LA tissues without changing the values in the LV tissues.

### 3.7 Administration of BAPN post-MI in rats decreased the mRNA expression of some profibrotic markers in the LA tissues

The mRNA expression levels of LOXL-1, LOXL-3, COL 1A1, TGF-β1 and periostin were significantly increased in the LA tissues of the MI group (1.6±0.1, 1.4±0.1, 2.0±0.2, 1.4±0.1 and

4.6±1.6-fold change, respectively) compared with those in the Sham group (1.0±0.1, 1.0±0.1, 1.0±0.1, 1.00±0.1 and 1.0±0.3-fold change, respectively; Figure 8B, D, F, H and J). mRNA expression levels of LOXL-1, LOXL-2, LOXL-3, COL 1A1, COL 3A1, TGF-β1, periostin and α-SMA were significantly lower in the LA tissues of the MI+BAPN group (0.5±0.0, 0.7±0.0, 0.8±0.0, 0.6±0.1, 0.4±0.3, 1.0±0.1, 0.9±0.2 and 0.7±0.1-fold change, respectively) than those in the MI group (1.6±0.1, 1.6±0.3, 1.4±0.1, 2.0±0.2, 3.2±0.6, 1.4±0.1, 4.6±1.6 and 1.9±0.3-fold change, respectively; Figure 8B-D, F-H and J-K). However, the mRNA expression of LOX, LOXL-4, CTGF, FN 1, Cx 43, MMP-2 and MMP-9 in the LA tissues was not significantly different between the groups (Figure 8A, E and I, and Supplementary Figure S5A-D).

### 3.8 Administration of BAPN post-MI in rats had no effect on the mRNA expression of profibrotic markers in LV tissues

The abundance of LOX, LOXL-1, LOXL-2, LOXL-3, LOXL-4, COL 1A1, FN 1, TGF-β1, CTGF, periostin, α-SMA and MMP-2 mRNA was significantly higher in the LV tissues of the MI-Inf group than those in the MI-Rem or Sham (Supplementary Figure S6A-F, H-K and M-N) groups. Moreover, the mRNA expression levels of LOX, LOXL-1, LOXL-2, LOXL-3, FN 1, TGF-β1, CTGF, α-SMA and MMP-2 were significantly higher in the LV tissues of MI+BAPN-Inf than those in the MI+BAPN-Rem or Sham+BAPN (Supplementary Figure S6A-D, H-J and M-N) groups. The mRNA expression of Cx 43 was significantly reduced in the LV tissues of the MI-Inf group (0.2±0.1-fold change) compared with those in the MI-Rem (0.6±0.1-fold change) or Sham (1.0±0.1-fold change; Supplementary Figure S6L) groups. Additionally, Cx 43 mRNA expression was significantly decreased in the LV tissues of the MI+BAPN-Inf group (0.2±0.0-fold change) compared with the Sham+BAPN group (0.8±0.1-fold change; Supplementary Figure S6L). Administration of BAPN post-MI showed no significant changes in the mRNA expressions of profibrotic markers.

### 3.9 Administration of BAPN post-MI in rats had no effect on the protein expression of LOX and LOXL proteins in LA and LV tissues

Protein expression of all LOX isoforms in the LA tissues was not significantly different between the four groups (Supplementary Figure S7A-F). The protein expression levels of active LOX, LOXL-3 and LOXL-4 in the LV tissues of the MI-Inf group (12.2±1.5, 3.0±0.5 and 4.3±1.3-fold change) were significantly increased compared with those in the MI-Rem (1.7±0.9, 1.1±0.2 and 1.3±0.2-fold change) or Sham (1.0±0.5, 1.0±0.1 and 1.0±0.2-fold change; Supplementary Figure S8A and D-F) groups. Furthermore, the protein expression level of active LOX (32 kDa) was significantly higher in the LV tissue of the MI+BAPN-Inf group (12.6±2.1-fold change) than in the MI+BAPN-Rem (4.5±1.8-fold change) or Sham+BAPN (0.9±0.1-fold change; Supplementary Figure S8A and F) groups. Administration of BAPN post-MI yielded no significant changes in the protein expression of LOX isoforms.

## 4. Discussion

MI induces cardiomyocyte death and ECM remodeling [36]. Following MI, there is progressive LV remodeling, including replacement of dead cells by scars, thickening of non-infarcted areas, dilatation of the LV and thinning of the infarct wall [36]. The enlargement of the LV chamber occurs during the early phase of MI due to the infarct expansion [37]. Cardiac fibrosis is initiated after 3 to 5 days post-MI [38]. Weber *et al.* [39] reported that the upregulated profibrotic molecules in the infarcted area induced upregulation of their levels in the non-infarcted area, leading to interstitial fibrosis through the increased collagen deposition. LOX isoforms play an essential function in the structural stability of cardiac ECM [17]. Several animal models were used to study the roles of LOX in collagen cross-linking and cardiac fibrosis following pressure or volume overload [23, 40-44]. This is the first study

that focused on the role of LOX isoforms in mediating the LA fibrotic response, leading to AF in the MI rat model. Furthermore, the novel contribution of this study was to evaluate the alterations in the properties of atrial tissues and arrhythmia susceptibility following inhibition of LOX isoforms by BAPN post-MI as a key mechanism for collagen remodeling. The main findings of this study were the following: (a) LOX and LOXL-1 expression in the LA tissues was upregulated in the CHF model, (b) administration of BAPN post-MI reduced the MI-mediated LA electrical remodeling, (c) administration of BAPN post-MI decreased LA fibrosis and improved LA remodeling without any change in LV fibrosis and remodeling, (d) administration of BAPN in MI rats attenuated the collagen cross-linking in LA tissues without changing of that in the LV tissues and (e) administration of BAPN post-MI decreased the mRNA expression of some profibrotic markers in LA tissues without changing of those in the LV tissues.

Recent studies reported that LOX has a vital role in LV fibrosis in several HF models [40-44]. The mRNA and protein expression of LOX isoforms in LV tissues is upregulated in HF animal models induced by volume overload, pressure overload and MI [21-23]. Adam *et al.* [45] reported that LOX protein expression was significantly increased in the LA tissues of AF patients compared with that in sinus rhythm patients. Our results from LA tissues of a CHF dog model showed an increase in the mRNA expression of all LOX isoforms and a significant increase in the protein expression of LOX and LOXL-1. These results indicated that LOX and LOXL-1 may substantially contribute to LA remodeling and AF in CHF. P-wave duration, AF duration and AF inducibility increased in MI rats, and administration of BAPN post-MI effectively decreased this electrical remodeling. However, the underlying mechanisms of AF in MI patients have not been well studied. Electrical and structural remodeling are important mediators of AF [46]. Our results were consistent with the results of Tse and Yeo [47], who found that LA interstitial fibrosis and LV replacement fibrosis are important signs for structural remodeling that disturb the normal electrical conduction, leading to AF. Increases in the P-

P interval and P-wave duration post-MI may reflect a delay in the atrial conduction due to the progression of LA fibrosis. Our QRS results were consistent with previous findings that showed a strong association between prolonged QRS duration post-MI and LV dysfunction, such as reduced systolic function and increased ventricular volume [48]. Furthermore, the QRS and QT prolongation resulted from slowed conduction of the ventricles due to the increase in myocardial fibrosis post-MI. The prolonged P-R interval post-MI in our study indicated a disturbance in atrial and atrioventricular nodal conduction, which is associated with a high risk for AF as reported by Cheng *et al.* [49].

Our results indicated that the administration of BAPN post-MI decreased LA fibrosis without changing LV fibrosis. LA fibrosis and AF duration were increased in rats at 2, 4 and 8 weeks post-MI [26]. Previous studies showed that administration of BAPN in volume overloaded rats decreased LV fibrosis [42]. Gonzalez-Santamaria *et al.* [21] reported that administration of BAPN post-MI in mice decreased the LV fibrosis and scar area. Following MI, there is progressive cardiac remodeling in the remote and infarcted myocardium, leading to LV and LA dysfunction and dilatation [26, 32, 50, 51]. Yamada *et al.* [52] reported that the ventricular remodeling mediated remodeling of the LA due to movement of the blood from the LA to LV. We found that the administration of BAPN post-MI may be intensely effective in attenuating the progression of LA remodeling and AF. Dayeh *et al.* [53] noted that the increase in WMSI after MI reflects cardiac damage and can be an indicator of adverse cardiac consequences. The correlations of infarct size were positive and significant with LV volume and mass, whereas the correlation of infarct size was inverse and significant with EF in MI mice [37]. Numerous studies demonstrated weak correlations of infarct size with LV volume and FS, and there were no correlations of infarct size with LV mass and dimension at the end of diastole in MI mice [54, 55]. No studies have been reported on the effect of BAPN administration post-MI on cardiac remodeling through evaluating the relationship of infarct size with LA and LV structural and functional parameters. The study results illustrated that administration of BAPN disturbed the

correlations between the WMSI and the degree of LA remodeling at four weeks post-MI. Herein, we found that the administration of BAPN post-MI reduced the impact of the relationships of WMSI with LA dimensions, areas and FAC, while BAPN administration post-MI had little effect on the correlations of WMSI with LV structural and functional parameters.

Following MI, the number of myofibroblasts in the infarcted area was found to be higher than that in the non-infarcted area and was associated with the production of more collagen [56]. The stabilization of ECM through collagen cross-linking induces the deposition of insoluble collagen during cardiac injury. Cleutjens *et al.* [56] demonstrated that the mechanisms of collagen synthesis in the infarcted and non-infarcted areas were different in MI rats. Our results indicated that the administration of BAPN after the early stage of MI had beneficial effects on LA interstitial fibrosis and remodeling without affecting LV replacement fibrosis and remodeling due to the following reasons: (1) the progression ratio of LV replacement fibrosis was higher than that of LA and LV interstitial fibrosis, and (2) LV replacement fibrosis occurs before LA and LV interstitial fibrosis. In our study, BAPN was administered to rats after the early phase of MI. During this phase, BAPN started to decrease the LV and LA interstitial fibrosis, which was already present to a decreased degree and not as developed as LV replacement fibrosis. BAPN affected collagen synthesis via inhibition of the cross-linking process [23]. Bing *et al.* [57] reported that BAPN increased the content of soluble collagen in Sham and aortic constricted rats. The increase in the contents of soluble collagen was due to the inhibition of collagen cross-linking to compensate for the loss of insoluble collagen content [57]. We found that the administration of BAPN post-MI yielded no significant changes in the ratio of collagen cross-linking in LV tissues because BAPN had no significant changes in the soluble and insoluble collagen content compared with that in MI. However, the administration of BAPN post-MI yielded a significant decrease in the collagen cross-linking ratio as a result of a significant increase in the soluble collagen content without a significant decrease in the content of insoluble collagen in

LA tissues compared with that in MI. Our results were not consistent with the results of Gonzalez-Santamaria *et al.* [21], who reported that the administration of BAPN post-MI in mice decreased the degree of collagen cross-linking and fibrosis in the infarcted area of the LV. The variations in collagen cross-linking and fibrosis after administration of BAPN between our study and that by Gonzalez-Santamaria *et al.* [21] could be related to differences in the animal model, the method of BAPN administration and the dose of BAPN. Liu *et al.* [58] reported that the administration of BAPN decreased the ratio of collagen cross-linking in fibrotic hepatic mice. Additionally, there were no significant changes in the soluble and insoluble collagen contents and collagen cross-linking in the MI-Rem group compared with the Sham group. Our results were consistent with the results of Xiao *et al.* [43], who found no changes in the contents of soluble and insoluble collagen as well as the collagen cross-linking ratio between the MI-Rem and Sham groups in a monkey model. The effect of BAPN administration post-MI on LA fibrosis in the rat model was first investigated by this study. The results provide further evidence that AF is associated with LA interstitial fibrosis and electrical remodeling post-MI. The extension of LA fibrosis and structural remodeling in the MI rats was significantly suppressed upon administration of BAPN. Cardiac fibroblasts are the main cells that mediate cardiac fibrosis upon stressful conditions, such as MI or pressure overload. Cardiac fibroblasts play a significant role in ECM homeostasis, which is important for the structural stability of the heart [59]. Cardiac fibroblasts differentiate into myofibroblasts, which play an essential role in cardiac fibrosis in parallel with other heart cells [60]. There are several profibrotic signaling molecules that are synthesized by myofibroblasts after MI, including COL 1, COL 3, TGF-β, LOX isoforms, MMP, CTGF, FN, α-SMA, and periostin [1, 15, 59, 61, 62]. LOX isoforms are cross-linkers of intramolecular and intermolecular ECM collagens in the heart [20, 63]. We demonstrated that upregulation of LOX family mRNA expression occurred along with upregulation of the mRNA expression of COL 1A1, FN 1, TGF-β1, CTGF, periostin, α-SMA and MMP-2 and with reduction of Cx 43 mRNA expression in

the infarcted area of the LV in MI rats. Our results were consistent with those of previous studies that showed an increase in mRNA expression of LOX isoforms in parallel with an increase in mRNA expression of COLA 1A, COL 3A and α-SMA in the LV of transverse aortic constriction mice [22] and of MMP-2 in the infarcted area of LV in MI mice [21]. Treatment of cultured cardiac fibroblasts with TGF-β1 increased the mRNA expression of LOX isoforms [21, 64]. We found upregulation of mRNA expression of LOXL-1, LOXL-3, COL 1A1, TGF-β1 and periostin in LA tissues of the MI group compared with those of the Sham group. For infarcted and remote areas of the LV, BAPN administration had no effects on the mRNA expression of all studied profibrotic markers, while administration of BAPN post-MI showed suppression in mRNA expression of LOXL-1, LOXL-2, LOXL-3, COL 1A1, COL 3A1, TGF-β1, periostin and α-SMA without any effects on the mRNA expression of LOX, LOXL-4, CTGF, FN 1, Cx 43, MMP-2 and MMP-9 in LA tissues. Gonzalez-Santamaria *et al.* [21] reported that BAPN administration had no effect on the mRNA expression of LOX isoforms, MMP-2 and MMP-9 in infarcted area of the LV. The mRNA expression of TGF-β1 and COL 1A1 was suppressed upon BAPN administration in fibrotic hepatic mice. We found an upregulation in the protein expression of active LOX, LOXL-3 and LOXL-4 in the infarcted area of the LV. However, administration of BAPN post-MI had no effects on the protein expression of LOX isoforms in LA and LV tissues. Our results revealed that mRNA expression of LOXL-1, LOXL-2 and LOXL-3 in LA tissues was significantly decreased without a significant decrease in the protein expression of each LOX isoform upon administration of BAPN post-MI. The accumulation of non-significant decreases in the protein expressions of all LOX isoforms may result in a significant attenuation of cardiac fibrosis. In this study, we revealed that administration of BAPN post-MI decreased the synthesis of mRNA LOX isoforms, collagen cross-linking and fibrosis in LA; However, there were no significant changes in mRNA expression of LOX isoforms, collagen cross-linking or fibrosis in the remote area of the LV. Yue *et al.* [65] found that the atrial fibroblasts had a

higher proliferative response compared with the ventricular fibroblasts upon exposure to stimuli. Many studies reported that atria are more prone to fibrosis than ventricles [66, 67]. We noted that BAPN was not specific to one LOX isoform and was more likely to attenuate LA fibrosis compared with that affinity in the remote area of the LV, which may be due to the higher sensitivity of LA fibroblasts. The current study provides novel insight into the activation and suppression of the LOX pathway in LA fibrosis and AF. In this study, the positive effects of BAPN administration on LA electrical and structural remodeling in the MI rat model provide further evidence that the LOX signaling pathway may contribute to LA fibrosis and later AF development.

## 5. Conclusions

The current study investigated the role of LOX isoforms in the pathogenesis of LA fibrosis and AF and provided new information on the progress of potential therapeutic treatments of LA fibrosis and AF through inhibition of the LOX signaling pathway. The ischemic model could mediate electrical and structural atrial remodeling, which increases AF inducibility. BAPN attenuated LA fibrosis and arrhythmogenesis through inhibiting the signaling pathway of LOX isoforms in the MI rat model. The inhibition of the LOX signaling pathway may lead to suppression of LA fibrosis and AF development.

## References


1. Nattel S, Burstein B, Dobrev D. Atrial remodeling and atrial fibrillation: Mechanisms and implications. *Circ Arrhythm Electrophysiol* 2008;**1**:62-73.

2. Heeringa J, van der Kuip DA, Hofman A, Kors JA, van Herpen G, Stricker BH, Stijnen T, Lip GY, Witteman JC. Prevalence, incidence and lifetime risk of atrial fibrillation: The Rotterdam study. *Eur Heart J* 2006;**27**:949-953.

3. Stewart S, Hart CL, Hole DJ, McMurray JJ. Population prevalence, incidence, and predictors of atrial fibrillation in the Renfrew/Paisley study. *Heart* 2001;**86**:516-521.

4. Camm AJ, Kirchhof P, Lip GYH, Schotten U, Savelieva I, Ernst S, Van Gelder IC, Al-Attar N, Hindricks G, Prendergast B, Heidbuchel H, Alfieri O, Angelini A, Atar D, Colonna P, De Caterina R, De Sutter J, Goette A, Gorenek B, Heldal M, Hohloser SH, Kolh P, Le Heuzey J-Y, Ponikowski P, Rutten FH, Guidelines ESCCfP, Vahanian A, Auricchio A, Bax J, Ceconi C, Dean V, Filippatos G, Funck-Brentano C, Hobbs R, Kearney P, McDonagh T, Popescu BA, Reiner Z, Sechtem U, Sirnes PA, Tendera M, Vardas PE, Widimsky P, Document R, Vardas PE, Agladze V, Aliot E, Balabanski T, Blomstrom-Lundqvist C, Capucci A, Crijns H, Dahlöf B, Folliguet T, Glikson M, Goethals M, Gulba DC, Ho SY, Klautz RJM, Kose S, McMurray J, Perrone Filardi P, Raatikainen P, Salvador MJ, Schalij MJ, Shpektor A, Sousa J, Stepinska J, Uuetoa H, Zamorano JL, Zupan I. Guidelines for the management of atrial fibrillation: The task force for the management of atrial fibrillation of the European Society of Cardiology (ESC). *Eur Heart J* 2010;**31**:2369-2429.

5. Allessie MA, Boyden PA, Camm AJ, Kleber AG, Lab MJ, Legato MJ, Rosen MR, Schwartz PJ, Spooner PM, Van Wagoner DR, Waldo AL. Pathophysiology and prevention of atrial fibrillation. *Circulation* 2001;**103**:769-777.

6. Rose-Jones LJ, Bode WD, Gehi AK. Current approaches to antiarrhythmic therapy in heart failure. *Heart Fail Clin* 2014;**10**:635-652.

7. Miyazaki S, Shah AJ, Scherr D, Haïssaguerre M. Atrial fibrillation: Pathophysiology and current therapy. *Ann Med* 2011;**43**:425-436.

8. Maisel WH, Stevenson LW. Atrial fibrillation in heart failure: Epidemiology, pathophysiology, and rationale for therapy. *Am J Cardiol* 2003;**91**:2d-8d.

9. Hunt SA, Abraham WT, Chin MH, Feldman AM, Francis GS, Ganiats TG, Jessup M, Konstam MA, Mancini DM, Michl K, Oates JA, Rahko PS, Silver MA, Stevenson LW, Yancy CW. Focused update incorporated into the ACC/AHA 2005 Guidelines for the Diagnosis and Management of Heart Failure in Adults: A report of the American College of Cardiology Foundation/American Heart Association Task Force on Practice Guidelines: Developed in collaboration with the International Society for Heart and Lung Transplantation. *Circulation* 2009;**119**:e391-479.

10. Burashnikov A, Di Diego JM, Sicouri S, Doss MX, Sachinidis A, Barajas-Martinez H, Hu D, Minoura Y, Sydney Moise N, Kornreich BG, Chi L, Belardinelli L, Antzelevitch C. A temporal window of vulnerability for development of atrial fibrillation with advancing heart failure. *Eur J Heart Fail* 2014;**16**:271-280.

11. Goette A, Kalman JM, Aguinaga L, Akar J, Cabrera JA, Chen SA, Chugh SS, Corradi D, D'Avila A, Dobrev D, Fenelon G, Gonzalez M, Hatem SN, Helm R, Hindricks G, Ho SY, Hoit B, Jalife J, Kim YH, Lip GY, Ma CS, Marcus GM, Murray K, Nogami A, Sanders P, Uribe W, Van Wagoner DR, Nattel S. EHRA/HRS/APHRS/SOLAECE expert consensus on atrial

cardiomyopathies: Definition, characterization, and clinical implication. *Heart Rhythm* 2017;**14**:e3-e40.

12. Melenovsky V, Hwang SJ, Redfield MM, Zakeri R, Lin G, Borlaug BA. Left atrial remodeling and function in advanced heart failure with preserved or reduced ejection fraction. *Circ Heart Fail* 2015;**8**:295-303.

13. Krenning G, Zeisberg EM, Kalluri R. The origin of fibroblasts and mechanism of cardiac fibrosis. *J Cell Physiol* 2010;**225**:631-637.

14. Berk BC, Fujiwara K, Lehoux S. ECM remodeling in hypertensive heart disease. *J Clin Invest* 2007;**117**:568-575.

15. Murtha LA, Schuliga MJ, Mabotuwana NS, Hardy SA, Waters DW, Burgess JK, Knight DA, Boyle AJ. The processes and mechanisms of cardiac and pulmonary fibrosis. *Front Physiol* 2017;**8**:777.

16. Cieslik KA, Trial J, Crawford JR, Taffet GE, Entman ML. Adverse fibrosis in the aging heart depends on signaling between myeloid and mesenchymal cells; role of inflammatory fibroblasts. *J Mol Cell Cardiol* 2014;**70**:56-63.

17. Smith-Mungo LI, Kagan HM. Lysyl oxidase: Properties, regulation and multiple functions in biology. *Matrix Biol* 1998;**16**:387-398.

18. Miana M, Galan M, Martinez-Martinez E, Varona S, Jurado-Lopez R, Bausa-Miranda B, Antequera A, Luaces M, Martinez-Gonzalez J, Rodriguez C, Cachofeiro V. The lysyl oxidase inhibitor beta-aminopropionitrile reduces body weight gain and improves the metabolic profile in diet-induced obesity in rats. *Dis Model Mech* 2015;**8**:543-551.

19. Lucero HA, Kagan HM. Lysyl oxidase: An oxidative enzyme and effector of cell function. *Cell Mol Life Sci* 2006;**63**:2304-2316.

20. Rodriguez C, Martinez-Gonzalez J, Raposo B, Alcudia JF, Guadall A, Badimon L. Regulation of lysyl oxidase in vascular cells: Lysyl oxidase as a new player in cardiovascular diseases. *Cardiovasc Res* 2008;**79**:7-13.

21. Gonzalez-Santamaria J, Villalba M, Busnadiego O, Lopez-Olaneta MM, Sandoval P, Snabel J, Lopez-Cabrera M, Erler JT, Hanemaaijer R, Lara-Pezzi E, Rodriguez-Pascual F. Matrix cross-linking lysyl oxidases are induced in response to myocardial infarction and promote cardiac dysfunction. *Cardiovasc Res* 2016;**109**:67-78.

22. Yang, Savvatis K, Kang JS, Fan P, Zhong H, Schwartz K, Barry V, Mikels-Vigdal A, Karpinski S, Kornyeyev D, Adamkewicz J, Feng X, Zhou Q, Shang C, Kumar P, Phan D, Kasner M, Lopez B, Diez J, Wright KC, Kovacs RL, Chen PS, Quertermous T, Smith V, Yao L, Tschope C, Chang CP. Targeting LOXL2 for cardiac interstitial fibrosis and heart failure treatment. *Nat Commun* 2016;**7**:13710.

23. El Hajj EC, El Hajj MC, Ninh VK, Gardner JD. Inhibitor of lysyl oxidase improves cardiac function and the collagen/MMP profile in response to volume overload. *Am J. Physiol Heart Circ Physiol* 2018;**315**:H463-h473.

24. El Hajj EC, El Hajj MC, Ninh VK, Gardner JD. Cardioprotective effects of lysyl oxidase inhibition against volume overload-induced extracellular matrix remodeling. *Exp Biol Med* 2016;**241**:539-549.

25. Dawson K, Wakili R, Ordog B, Clauss S, Chen Y, Iwasaki Y, Voigt N, Qi XY, Sinner MF, Dobrev D, Kaab S, Nattel S. MicroRNA29: A mechanistic contributor and potential biomarker in atrial fibrillation. *Circulation* 2013;**127**:1466-1475.

26. Cardin S, Guasch E, Luo X, Naud P, Le Quang K, Shi Y, Tardif JC, Comtois P, Nattel S. Role for MicroRNA-21 in atrial profibrillatory fibrotic remodeling associated with experimental postinfarction heart failure. *Circ Arrhythm Electrophysiol* 2012;**5**:1027-1035.

27. Reffelmann T, Kloner RA. Transthoracic echocardiography in rats. Evalution of commonly used indices of left ventricular dimensions, contractile performance, and hypertrophy in a genetic model of hypertrophic heart failure (SHHF-Mcc-facp-Rats) in comparison with Wistar rats during aging. *Basic Res Cardiol* 2003;**98**:275-284.

28. Iwasaki YK, Kato T, Xiong F, Shi YF, Naud P, Maguy A, Mizuno K, Tardif JC, Comtois P, Nattel S. Atrial fibrillation promotion with long-term repetitive obstructive sleep apnea in a rat model. *J Am Coll Cardiol* 2014;**64**:2013-2023.

29. Yang J, Savvatis K, Kang JS, Fan P, Zhong H, Schwartz K, Barry V, Mikels-Vigdal A, Karpinski S, Kornyeyev D, Adamkewicz J, Feng X, Zhou Q, Shang C, Kumar P, Phan D, Kasner M, Lopez B, Diez J, Wright KC, Kovacs RL, Chen PS, Quertermous T, Smith V, Yao L, Tschope C, Chang CP. Targeting LOXL2 for cardiac interstitial fibrosis and heart failure treatment. *Nat Commun* 2016;**7**:13710.

30. Duong E, Xiao J, Qi XY, Nattel S. MicroRNA-135a regulates sodium-calcium exchanger gene expression and cardiac electrical activity. *Heart Rhythm* 2017;**14**:739-748.

31. Livak KJ, Schmittgen TD. Analysis of relative gene expression data using real-time quantitative PCR and the $2^{-\Delta\Delta CT}$ Method. *Methods* 2001;**25**:402-408.

32. Surinkaew S, Aflaki M, Takawale A, Chen Y, Qi XY, Gillis MA, Shi YF, Tardif JC, Chattipakorn N, Nattel S. Exchange-protein activated by cyclic-AMP (EPAC) regulates atrial fibroblast function and controls cardiac remodeling. *Cardiovasc Res* 2019;**115**:94-106.

33. Chang K, Uitto J, Rowold EA, Grant GA, Kilo C, Williamson JR. Increased collagen cross-linkages in experimental diabetes: Reversal by beta-aminopropionitrile and D-penicillamine. *Diabetes* 1980;**29**:778-781.

34. Jabre P, Jouven X, Adnet F, Thabut G, Bielinski SJ, Weston SA, Roger VL. Atrial fibrillation and death after myocardial infarction: A community study. *Circulation* 2011;**123**:2094-2100.

35. Mehta RH, Dabbous OH, Granger CB, Kuznetsova P, Kline-Rogers EM, Anderson FA, Jr., Fox KA, Gore JM, Goldberg RJ, Eagle KA. Comparison of outcomes of patients with acute coronary syndromes with and without atrial fibrillation. *Am J Cardiol* 2003;**92**:1031-1036.

36. Pfeffer MA, Braunwald E. Ventricular remodeling after myocardial infarction. Experimental observations and clinical implications. *Circulation* 1990;**81**:1161-1172.

37. Kanno S, Lerner DL, Schuessler RB, Betsuyaku T, Yamada KA, Saffitz JE, Kovacs A. Echocardiographic evaluation of ventricular remodeling in a mouse model of myocardial infarction. *J Am Soc Echocardiogr* 2002;**15**:601-609.

38. Kurose H, Mangmool S. Myofibroblasts and inflammatory cells as players of cardiac fibrosis. *Arch Pharm Res* 2016;**39**:1100-1113.

39. Weber KT, Sun Y, Bhattacharya SK, Ahokas RA, Gerling IC. Myofibroblast-mediated mechanisms of pathological remodelling of the heart. *Nat Rev Cardiol* 2013;**10**:15-26.

40. Miguel-Carrasco JL, Beaumont J, San Jose G, Moreno MU, Lopez B, Gonzalez A, Zalba G, Diez J, Fortuno A, Ravassa S. Mechanisms underlying the cardiac antifibrotic effects of losartan metabolites. *Sci Rep* 2017;**7**:41865.

41. Galan M, Varona S, Guadall A, Orriols M, Navas M, Aguilo S, de Diego A, Navarro MA, Garcia-Dorado D, Rodriguez-Sinovas A, Martinez-Gonzalez J, Rodriguez C. Lysyl oxidase overexpression accelerates cardiac remodeling and aggravates angiotensin II-induced hypertrophy. *FASEB J* 2017;**31**:3787-3799.

42. El Hajj EC, El Hajj MC, Ninh VK, Bradley JM, Claudino MA, Gardner JD. Detrimental role of lysyl oxidase in cardiac remodeling. *J Mol Cell Cardiol* 2017;**109**:17-26.

43. Xiao Y, Nie X, Han P, Fu H, James Kang Y. Decreased copper concentrations but increased lysyl oxidase activity in ischemic hearts of rhesus monkeys. *Metallomics* 2016;**8**:973-980.

44. Gonzalez GE, Rhaleb NE, Nakagawa P, Liao TD, Liu Y, Leung P, Dai X, Yang XP, Carretero OA. N-acetyl-seryl-aspartyl-lysyl-proline reduces cardiac collagen cross-linking and inflammation in angiotensin II-induced hypertensive rats. *Clin Sci* 2014;**126**:85-94.

45. Adam O, Theobald K, Lavall D, Grube M, Kroemer HK, Ameling S, Schafers HJ, Bohm M, Laufs U. Increased lysyl oxidase expression and collagen cross-linking during atrial fibrillation. *J Mol Cell Cardiol* 2011;**50**:678-685.

46. Lip GY, Lane DA. Stroke prevention in atrial fibrillation: A systematic review. *Jama* 2015;**313**:1950-1962.

47. Tse G, Yeo JM. Conduction abnormalities and ventricular arrhythmogenesis: The roles of sodium channels and gap junctions. *Int J Cardiol Heart and Vasc* 2015;**9**:75-82.

48. Yerra L, Anavekar N, Skali H, Zelenkofske S, Velazquez E, McMurray J, Pfeffer M, Solomon SD. Association of QRS duration and outcomes after myocardial infarction: The VALIANT trial. *Heart Rhythm* 2006;**3**:313-316.

49. Cheng S, Keyes MJ, Larson MG, McCabe EL, Newton-Cheh C, Levy D, Benjamin EJ, Vasan RS, Wang TJ. Long-term outcomes in individuals with prolonged PR interval or first-degree atrioventricular block. *Jama* 2009;**301**:2571-2577.

50. Yamani M, Massie BM. Congestive heart failure: Insights from epidemiology, implications for treatment. *Mayo Clin Pro* 1993;**68**:1214-1218.

51. Ho KK, Anderson KM, Kannel WB, Grossman W, Levy D. Survival after the onset of congestive heart failure in Framingham Heart Study subjects. *Circulation* 1993;**88**:107-115.

52. Yamada S, Fong MC, Hsiao YW, Chang SL, Tsai YN, Lo LW, Chao TF, Lin YJ, Hu YF, Chung FP, Liao JN, Chang YT, Li HY, Higa S, Chen SA. Impact of renal denervation on atrial arrhythmogenic substrate in ischemic model of heart failure. *J Am Heart Assoc* 2018;**7**.

53. Dayeh NR, Tardif JC, Shi Y, Tanguay M, Ledoux J, Dupuis J. Echocardiographic validation of pulmonary hypertension due to heart failure with reduced ejection fraction in mice. *Sci Rep* 2018;**8**:1363.

54. Patten RD, Aronovitz MJ, Deras-Mejia L, Pandian NG, Hanak GG, Smith JJ, Mendelsohn ME, Konstam MA. Ventricular remodeling in a mouse model of myocardial infarction. *Am J Physiol* 1998;**274**:H1812-1820.

55. Gao XM, Dart AM, Dewar E, Jennings G, Du XJ. Serial echocardiographic assessment of left ventricular dimensions and function after myocardial infarction in mice. *Cardiovasc Res* 2000;**45**:330-338.

56. Cleutjens JP, Verluyten MJ, Smiths JF, Daemen MJ. Collagen remodeling after myocardial infarction in the rat heart. *Am J Pathol* 1995;**147**:325-338.

57. Bing OH, Fanburg BL, Brooks WW, Matsushita S. The effect of lathyrogen beta-amino proprionitrile (BAPN) on the mechanical properties of experimentally hypertrophied rat cardiac muscle. *Circ Res* 1978;**43**:632-637.

58. Liu SB, Ikenaga N, Peng Z-W, Sverdlov DY, Greenstein A, Smith V, Schuppan D, Popov Y. Lysyl oxidase activity contributes to collagen stabilization during liver fibrosis progression and limits spontaneous fibrosis reversal in mice. *FASEB J* 2016;**30**:1599-1609.

59. Talman V, Ruskoaho H. Cardiac fibrosis in myocardial infarction—from repair and remodeling to regeneration. *Cell Tissue Res* 2016;**365**:563-581.

60. Moore-Morris T, Cattaneo P, Puceat M, Evans SM. Origins of cardiac fibroblasts. *J Mol Cell Cardiol* 2016;**91**:1-5.

61. Frangogiannis NG. Regulation of the inflammatory response in cardiac repair. *Circ Res* 2012;**110**:159-173.

62. Stefanon I, Valero-Munoz M, Fernandes AA, Ribeiro RF, Jr., Rodriguez C, Miana M, Martinez-Gonzalez J, Spalenza JS, Lahera V, Vassallo PF, Cachofeiro V. Left and right ventricle late remodeling following myocardial infarction in rats. *PloS One* 2013;**8**:e64986.

63. Lopez B, Gonzalez A, Hermida N, Valencia F, de Teresa E, Diez J. Role of lysyl oxidase in myocardial fibrosis: From basic science to clinical aspects. *Am J Physiol Heart and Circ Physiol* 2010;**299**:H1-9.

64. Sethi A, Mao W, Wordinger RJ, Clark AF. Transforming growth factor-beta induces extracellular matrix protein cross-linking lysyl oxidase (LOX) genes in human trabecular meshwork cells. *Inves Ophthalmol Vis Sci* 2011;**52**:5240-5250.

65. Yue L, Xie J, Nattel S. Molecular determinants of cardiac fibroblast electrical function and therapeutic implications for atrial fibrillation. *Cardiovasc Res* 2011;**89**:744-753.

66. Xiao HD, Fuchs S, Campbell DJ, Lewis W, Dudley SC, Jr., Kasi VS, Hoit BD, Keshelava G, Zhao H, Capecchi MR, Bernstein KE. Mice with cardiac-restricted angiotensin-converting enzyme (ACE) have atrial enlargement, cardiac arrhythmia, and sudden death. *Am J Pathol* 2004;**165**:1019-1032.

67. Nakajima H, Nakajima HO, Salcher O, Dittie AS, Dembowsky K, Jing S, Field LJ. Atrial but not ventricular fibrosis in mice expressing a mutant transforming growth factor-beta (1) transgene in the heart. *Circ Res* 2000;**86**:571-579.

## Figure Legends

**Figure 1. *In vivo* experimental timeline.** β-aminopropionitrile (BAPN) was administered to rats on day 8 post-MI. Echocardiographic measurements were recorded at baseline, day 7 and day 27 post-MI. All animals were subjected to electrophysiological study prior to sacrifice.

**Figure 2. Increased protein expressions of lysyl oxidase (LOX) and LOX-like protein 1 (LOXL-1) in the left atrial (LA) tissues of congestive heart failure (CHF) dogs.** Basal relative protein expressions of LOX isoforms in the LA tissues (n = 5) of a CHF (2 weeks of ventricular tachypacing (VTP)) model were quantified by Western blot analysis, including (A) band intensities of Western blot images were normalized to glyceraldehyde 3-phosphate dehydrogenase (GAPDH), (B) LOX, (C) LOXL-1, (D) LOXL-2, (E) LOXL-3 and (F) LOX-4. The results are the means ± SEM; unpaired Student's *t*-tests were performed. $*P < 0.05$; $**P < 0.01$; $***P < 0.001$.

**Figure 3. Administration of β-aminopropionitrile (BAPN) post-myocardial infarction (MI) in rats decreased P-wave duration, atrial fibrillation (AF) duration and AF inducibility.** Electrophysiological (A-C) and electrocardiogram (ECG; D-H) measurements for four rat groups (Sham; n = 16-18, Sham+BAPN; n = 16-18, MI; n = 16-22; MI+BAPN; n = 16-18) were assessed at day 28 post-surgery, including (A) AF inducibility, (B) AF duration, (C) effective refractory period (ERP), (D) P-wave duration, (E) P-P interval, (F) P-R interval, (G) QRS duration and (H) QT duration. The results are the means ± SEM; one-way ANOVA followed by the Bonferroni's multiple comparisons test (C-H) was performed. Fisher's exact test for AF inducibility was performed. One-way ANOVA followed by the Kruskal-Wallis's multiple comparisons test for AF duration was performed. $*P < 0.05$; $**P < 0.01$; $***P < 0.001$.

**Figure 4. Administration of β-aminopropionitrile (BAPN) post-myocardial infarction (MI) in rats attenuated left atrial (LA) fibrosis without changing the left ventricular (LV) fibrosis.** LA and LV fibrosis in four rat groups (Sham; n = 6, Sham+BAPN; n = 6, MI from remote (Rem) and infarct (Inf) areas (MI, MI-Rem and MI-Inf; n = 5) and MI+BAPN (MI+BAPN, MI+BAPN-Rem and MI+BAPN-Inf; n = 6)) was evaluated on day 28 post-surgery, including (A) representative Masson's trichrome staining images of LA and LV tissue sections for fibrosis quantification, (B) LA fibrous tissue quantification, (C) LV fibrous tissue quantification and (D) LV scar area. The results are the means ± SEM; unpaired Student's *t*-tests for scar area were

performed; one-way ANOVA followed by the Bonferroni's multiple comparisons test was performed. *$P < 0.05$; **$P < 0.01$; ***$P < 0.001$.

**Figure 5. β-aminopropionitrile (BAPN) administration decreased myocardial infarction (MI)-induced left atrial (LA) remodeling in rats.** LA structural and functional remodeling in four rat groups was assessed by echocardiography, including Sham (n = 21), Sham+BAPN (n = 18-20), MI (n = 23-24) and MI+BAPN (n = 22), on day 27 post-MI. (A) LA diameter at end systole ($LAD_s$), (B) LA diameter at end diastole ($LAD_d$), and (C) fractional shortening (FS). Comparison between echocardiographic assessment of the wall motion score index (WMSI) and LA structural and functional parameters in MI rats treated with vehicle or BAPN on day 27 post-surgery. Linear correlations of WMSI with (D) $LAD_s$, (E) $LAD_d$, and (F) FS. The results are the means ± SEM; one-way ANOVA followed by the Bonferroni's multiple comparisons test (A-C) was performed. *$P < 0.05$; **$P < 0.01$; ***$P < 0.001$; $R^2$: correlation coefficient; in the equation, (x) represents the WMSI and (Y) represents structural and functional parameters.

**Figure 6. β-aminopropionitrile (BAPN) administration had no effect on myocardial infarction (MI)-induced left ventricular (LV) remodeling in rats.** LV structural and functional remodeling in four rat groups was assessed by echocardiography, including Sham (n = 17-21), Sham+BAPN (n = 18-20), MI (n = 18-24) and MI+BAPN (n = 14-22), on day 27 post-surgery. (A) LV diameter at end systole ($LVD_s$), (B) LV diameter at end diastole ($LVD_d$), (C) LV mass, (G) ratio of early diastolic transmitral filling velocity (E) to atrial transmitral filling velocity (A), (H) ejection fraction (EF) and (I) wall motion score index (WMSI). Comparison between echocardiographic assessment of the WMSI and LV structural and functional parameters in MI rats treated with vehicle or BAPN on day 27 post-MI. Linear correlations of WMSI with (D) $LVD_s$, (E) $LVD_d$, (F) LV mass, (J) ratio of E/A and (K) EF. The results are the means ± SEM; one-way ANOVA followed by the Bonferroni's multiple comparisons test (A-C and G-I) was performed. *$P < 0.05$; **$P < 0.01$; ***$P < 0.001$; $R^2$: correlation coefficient; in the equation, (x) represents the WMSI and (Y) represents structural and functional parameters.

**Figure 7. Administration of β-aminopropionitrile (BAPN) post-myocardial infarction (MI) in rats attenuated collagen cross-linking in the left atrium (LA) without changing that in the left ventricle (LV).** Collagen content in the LA and LV from four rat groups (Sham; n = 6, Sham+BAPN; n = 6, MI from remote (Rem) and infarct (Inf) areas (MI, MI-Rem and MI-Inf; n = 6) and MI+BAPN

(MI+BAPN, MI+BAPN-Rem and MI+BAPN-Inf; n = 6)) was measured by the QuickZyme assay on day 28 post-surgery, including (A) soluble collagen in LA tissues, (B) insoluble collagen in LA tissues, (C) collagen cross-linking ratio in LA tissues, (D) soluble collagen in LV tissues, (E) insoluble collagen in LV tissues and (F) collagen cross-linking ratio in LV tissues. The results are the means ± SEM; one-way ANOVA followed by the Bonferroni's multiple comparisons test was performed. *$P < 0.05$; **$P < 0.01$; ***$P < 0.001$.

**Figure 8. Administration of β-aminopropionitrile (BAPN) post-myocardial infarction (MI) in rats decreased the mRNA expression of several profibrotic markers in left atrial (LA) tissues.** mRNA expression levels of profibrotic markers in the LA tissues from four rat groups (Sham; n = 6, Sham+BAPN; n = 6, MI; n = 6 and MI+BAPN; n = 6) were quantified by qPCR on day 28 post-surgery, including (A) lysyl oxidase (LOX), (B) LOX-like protein-1 (LOXL-1), (C) LOXL-2, (D) LOXL-3, (E) LOXL-4, (F) collagen 1A1 (COL 1A1), (G) collagen 3A1 (COL 3A1), (H) transforming growth factor β1 (TGF-β1), (I) connective tissue growth factor (CTGF), (J) periostin, and (K) α-smooth muscle actin (α-SMA). The results are the means ± SEM; one-way ANOVA followed by the Bonferroni's multiple comparisons test was performed. *$P < 0.05$; **$P < 0.01$; ***$P < 0.001$.

**Table 1:** Effect of BAPN administration on echocardiographic parameters (ventricular and atrial structural and functional remodeling) post-MI in rats.

| | Sham | | | MI | | | Sham+BAPN | | | MI+BAPN | | |
|---|---|---|---|---|---|---|---|---|---|---|---|---|
| | Baseline | 7 days post-MI | 27 days post-MI | Baseline | 7 days post-MI | 27 days post-MI | Baseline | 7 days post-MI | 27 days post-MI | Baseline | 7 days post-MI | 27 days post-MI |
| **LV structural function** | | | | | | | | | | | | |
| $LVAW_d$ (mm) | 1.4±0.0 | 1.6±0.0 | 1.7±0.0 | 1.4±0.0 | 1.6±0.1 | 1.6±0.1 | 1.4±0.0 | 1.6±0.0 | 1.6±0.0 | 1.4±0.0 | $1.7±0.1^{*}$ | 1.6±0.1 |
| $LVPW_d$ (mm) | 1.4±0.0 | 1.5±0.0 | $1.6±0.0^{*}$ | 1.4±0.0 | $1.6±0.1^{*}$ | $1.8±0.1^{*}$ | 1.4±0.0 | 1.5±0.0 | 1.5±0.0 | 1.4±0.0 | 1.6±0.0 | $1.7±0.1^{*}$ |
| $LVD_d$ (mm) | 7.1±0.1 | 7.4±0.1 | $7.9±0.1^{*}$ | 7.2±0.1 | $8.5±0.2^{*\$}$ | $9.8±0.2^{*}$ | 7.3±0.1 | 7.7±0.1 | 7.6±0.1 | 7.0±0.1 | $8.3±0.1^{*\#}$ | $9.3±0.2^{*\#}$ |
| $LVD_s$ (mm) | 3.6±0.1 | 3.7±0.1 | 3.6±0.1 | 3.6±0.1 | $6.1±0.2^{*\$}$ | $7.2±0.3^{*\$}$ | 3.5±0.1 | 3.6±0.1 | 3.6±0.1 | 3.5±0.1 | $5.6±0.2^{*\#}$ | $6.6±0.4^{*\#}$ |
| LV mass (mg) | 638 ±16 | 766±13 | $898±20^{*}$ | 662±11 | $935±30^{*\$}$ | $1259±37^{*\$\S}$ | 683±15 | 799±22 | 787±30 | 655±16 | $975±35^{*\#}$ | $1124±43^{*\#}$ |
| LV mass/$LVD_d$ (mg/mm) | 89.9±1.7 | $103.1±1.7^{*}$ | $113.2±2.0^{*}$ | 92.3±1.3 | $110.8±3.4^{*}$ | $129.3±3.8^{*\$}$ | 94.1±1.7 | 104.4±1.9 | 103.8±2.6 | 93.0±1.6 | $117.0±3.7^{*}$ | $120.7±2.8^{*\#}$ |
| LV mass/BW (mg/g) | 2.7±0.1 | 2.7±0.0 | $2.2±0.0^{*}$ | 2.8±0.0 | $3.4±0.1^{*\$}$ | $3.1±0.1^{\$}$ | 2.8±0.1 | 2.8±0.1 | $2.7±0.1^{\dagger}$ | 2.7±0.1 | $3.5±0.1^{*\#}$ | $3.8±0.2^{\S\#}$ |
| **LV systolic function** | | | | | | | | | | | | |
| $LVV_d$ (ml) | 0.8±0.0 | 0.9±0.0 | 1.1±0.03 | 0.8±0.0 | $1.3±0.1^{*\$}$ | $2.0±0.1^{*\$}$ | 0.9±0.0 | 1.0±0.0 | 1.0±0.05 | 0.8±0.0 | $1.27±0.1^{*}$ | $1.73±0.12^{*\#}$ |
| $LVV_s$ (ml) | 0.1±0.0 | 0.1±0.0 | 0.1±0.0 | 0.1±0.0 | $0.6±0.1^{*\$}$ | $0.9±0.1^{*\$}$ | 0.1±0.0 | 0.1±0.0 | 0.1±0.02 | 0.1±0.0 | $0.5±0.1^{*\#}$ | $0.75±0.12^{*\#}$ |
| FS (%) | 49.5±1.3 | $50.2±1.3^{\$}$ | $54.7±1.2^{\$}$ | 49.1±0.9 | $29.0±1.7^{*}$ | $27.4±1.8^{*}$ | 52.4±1.3 | $53.4±1.3^{\#}$ | $52.0±1.2^{\#}$ | 50.6±1.4 | $33.3±2.0^{*}$ | $29.8±2.3^{*}$ |
| EF (%) | 84.9±1.2 | $85.5±1.1^{\$}$ | $88.9±0.8^{\$}$ | 84.9±0.8 | $60.0±2.7^{*}$ | $57.1±2.9^{*}$ | 83.3±4.3 | $87.9±0.9^{\#}$ | $87.0±1.0^{\#}$ | 85.8±1.2 | $66.0±2.9^{*}$ | $60.1±3.6^{*}$ |
| WMSI | 1.0±0.0 | 1.0±0.0 | 1.0±0.0 | 1.0±0.0 | $1.7±0.1^{*\$}$ | $1.7±0.1^{*\$}$ | 1.0±0.0 | 1.0±0.0 | 1.0±0.0 | 1.0±0.0 | $1.6±0.1^{*\#}$ | $1.6±0.1^{*\#}$ |
| $S_L$ (cm/s) | 5.0±0.2 | $4.9±0.2^{\$}$ | 5.6±0.2 | 5.3±0.2 | $3.7±0.2^{*}$ | 4.7±0.2 | 4.9±0.2 | $5.1±0.2^{\#}$ | 4.7±0.2 | 5.5±0.2 | $3.8±0.1^{*}$ | $3.9±0.3^{*}$ |
| $S_S$ (cm/s) | 4.7±1.7 | $4.8±0.2^{\$}$ | $5.2±0.2^{\$}$ | 4.8±0.1 | $3.7±0.2^{*}$ | 4.4±0.2 | 4.7±0.1 | $5.0±0.2^{\#}$ | 4.7±0.2 | 4.8±0.1 | $4.0±0.1^{*}$ | 4.1±0.2 |
| **LV diastolic function** | | | | | | | | | | | | |
| E Velocity (cm/s) | 107.6±3.2 | 102.8±2.9 | $107.0±3.3^{\dagger}$ | 110.7±2.6 | 105±2.9 | $118.2±3.3^{\S}$ | 106.3±1.7 | 104.2±1.9 | $85.0±2.9^{*}$ | 108.3±3.6 | 107.4±2.7 | $101.7±3.4^{\#}$ |
| A (cm/s) | 84.2±4.3 | 76.7±4.0 | 80.1±3.8 | 89.6±2.7 | 78.8±4.8 | 92.3±5.6 | 89.4±3.2 | 87.0±3.8 | 75.6±3.7 | 89.2±2.8 | 68.4±6.7 | 86.4±3.7 |
| E/A | 1.2±0.1 | 1.3±0.1 | 1.3±0.1 | 1.2±0.0 | 1.4±0.1 | 1.4±0.2 | 1.2±0.1 | 1.2±0.0 | 1.2±0.1 | 1.2±0.1 | 1.6±0.2 | 1.2±0.0 |
| E/e' $_{Lateral}$ | 16.8±0.8 | 16.3±0.6 | 17.6±0.8 | 16.8±0.7 | 20.7±1.3 | $25.9±2.1^{*\$}$ | 17.2±0.8 | 16.2±1.1 | 15.6±0.9 | 15.5±0.9 | $27.0±1.6^{*\#}$ | $24.6±2.4^{*\#}$ |
| E/e' $_{Septal}$ | 16.8±1.0 | 18.0±1.3 | 15.5±0.7 | 18.6±1.3 | 19.4±1.5 | $25.3±2.0^{*\$}$ | 17.3±0.8 | 18.4±1.1 | 14.7±1.0 | 16.8±1.0 | $27.7±2.5^{*\#}$ | 21.4±1.4 |
| Heart rate | 375±6.5 | 361±6.6 | 362±9.5 | 371±6.0 | 358±8.0 | 357±9.2 | 369±4.6 | 362±8.8 | 339±10.9 | $380±5.5^{*}$ | 347±7.7 | 329±8.8 |
| **Myocardial performance index (%)** | | | | | | | | | | | | |
| $MPI_{Septal}$ | 52.3±2.0 | 53.8±2.3 | 51.0±1.9 | 54.8±1.9 | $66.2±2.1^{*\$}$ | 61.6±2.8 | 53.4±1.9 | 53.4±2.1 | 57.3±2.3 | 52.8±1.4 | 59.7±2.2 | $67.6±3.1^{*}$ |
| $MPI_{Lateral}$ | 50.3±2.4 | 52.9±1.8 | 50.7±1.8 | 53.3±2.1 | $64.0±2.1^{*\$}$ | $63.7±2.4^{*\$}$ | 50.4±2.0 | 53.3±2.2 | 58.3±2.3 | 49.7±1.6 | 59.9±2.1 | $66.3±2.9^{*}$ |
| $MPI_{Global}$ | 39.3±1.8 | 41.1±1.5 | 38.4±1.8 | 44.9±1.6 | $53.8±2.1^{\$}$ | $52.1±2.9^{\$}$ | 39.0±2.1 | 40.2±1.7 | 43.5±2.2 | 42.3±1.5 | 49.1±1.4 | $59.0±3.1^{*\#}$ |
| **Atrial remodeling (LA and RA)** | | | | | | | | | | | | |
| $LAD_d$ (mm) | 3.8±0.1 | 3.9±0.1 | 4.2±0.2 | 3.8±0.2 | $4.9±0.2^{*\$}$ | $5.4±0.2^{*\$\S}$ | 3.8±0.1 | 3.9±0.2 | 3.6±0.1 | 3.9±0.1 | $4.9±0.2^{*\#}$ | $4.5±0.2^{\#}$ |
| $LAD_s$ (mm) | 5.1±0.1 | 5.2±0.1 | 5.7±0.2 | 5.1±0.1 | $6.1±0.1^{*\$}$ | $6.5±0.2^{*\$\S}$ | 5.1±0.1 | 5.3±0.1 | 5.0±0.1 | 5.1±0.1 | $6.0±0.2^{*\#}$ | 5.7±0.2 |
| $LAA_d$ ($mm^2$) | 14.0±0.5 | $14.4±0.6^{*}$ | $16.3±1.0^{*}$ | 14.3±0.6 | $21.7±1.4^{*\$}$ | $22.4±1.6^{*\$\S}$ | 12.8±0.5 | 12.9±0.7 | 11.7±1.0 | 14.0±0.5 | $21.3±1.3^{*\#}$ | 16.8±1.4 |
| $LAA_s$ ($mm^2$) | 25.9±0.7 | 26.5±0.8 | $30.9±1.3^{*\dagger}$ | 26.1±0.7 | $31.5±1.7^{*\$}$ | $34.9±1.3^{*\S}$ | 24.8±0.7 | 25.4±0.9 | 23.2±1.0 | 26.0±0.9 | $31.6±1.0^{*\#}$ | $28.5±1.1^{\#}$ |
| FS (%) | 26.2±1.1 | $25.6±1.0^{\$}$ | $27.4±1.0^{\$}$ | 26.0±1.6 | $19.7±1.2^{*}$ | $17.7±1.3^{*}$ | 26.4±1.3 | $26.2±1.1^{\#}$ | $28.7±1.3^{\#}$ | 24.8±1.0 | $18.5±1.0^{*}$ | 22.6±1.4 |
| $FAC_{LA}$ (%) | 45.9±1.2 | $45.9±1.3^{\$}$ | $47.8±1.3^{\$}$ | 45.5±1.4 | $32.1±2.3^{*}$ | 37.0±2.5 | 48.5±1.3 | $49.6±1.7^{\#}$ | $50.8±2.3^{\#}$ | 46.0±1.0 | $33.8±2.5^{*}$ | 42.5±2.6 |
| $RAD_s$ (mm) | 4.3±0.1 | 4.5±0.1 | 4.7±0.1 | 4.3±0.1 | 4.8±0.1 | $5.1±0.2^{*}$ | 4.2±0.1 | 4.3±0.1 | 4.2±0.1 | 4.4±0.1 | 4.8±0.1 | 4.7±0.1 |
| $RAA_d$ ($mm^2$) | 10.5±0.4 | 11.1±0.5 | $12.8±0.7^{\dagger}$ | 10.8±0.4 | $13.6±0.5^{*}$ | $15.2±0.9^{*\S}$ | 9.8±0.4 | 10.8±0.6 | 9.1±0.7 | 10.7±0.5 | $14.5±0.7^{*\#}$ | 11.1±0.6 |
| $RAA_s$ ($mm^2$) | 18.5±0.5 | 21.5±0.8 | $22.7±1.0^{*\dagger}$ | 19.6±0.6 | 21.8±0.7 | $25.4±0.8^{*\S}$ | 18.4±0.4 | 20.5±0.8 | 17.0±0.9 | 19.7±0.7 | 22.8±0.9 | 20.0±0.6 |
| $FAC_{RA}$ (%) | 43.2±1.7 | $48.6±1.2^{\$}$ | 43.6±1.3 | 44.7±1.4 | 37.7±1.6 | 40.8±2.1 | 46.9±1.5 | $47.1±1.8^{\#}$ | 47.2±2.3 | $45.7±1.5^{*}$ | 36.5±1.7 | 44.6±1.8 |

Results are expressed as means ± SEM; Myocardial infarction (MI); β-aminopropionitrile (BAPN); Left ventricle (LV); Left atrium (LA); Right atrium (RA); LV anterior wall thickness at end diastole ($LVAW_d$); LV posterior wall thickness at end diastole ($LVPW_d$); LV and LA diameter at end diastole ($LVD_d$ and $LAD_d$); Body weight (BW); LV, LA and RA diameter at end systole ($LVD_s$, $LAD_s$ and $RAD_s$); LV volume at end diastole ($LVV_d$); LV volume at end systole ($LVV_s$); Fractional shortening (FS); Ejection fraction (EF); Wall motion score index (WMSI); Lateral wall systolic contractility ($S_L$); Septal systolic contractility ($S_S$); Early diastolic transmitral filling velocity (E); Atrial transmitral filling velocity (A); Mitral annulus moving velocity during early filling (e'); Myocardial performance index (MPI); LA and RA area at the end diastole ($LAA_d$ and $RAA_d$); LA and RA area at end systole ($LAA_s$ and $RAA_s$); Fractional area changing of LA and RA ($FAC_{LA}$ and $FAC_{RA}$). For statistical analysis, Two-way ANOVA followed by Bonferroni's multiple-comparison test was applied. $^{*}P < 0.05$ vs. baseline; $^{\$}P < 0.05$ for Sham vs. MI; $^{\#}P < 0.05$ for Sham+BAPN vs. MI+BAPN; $^{\S}P < 0.05$ for MI vs. MI+BAPN; $^{\dagger}P < 0.05$ for Sham vs. Sham+BAPN.

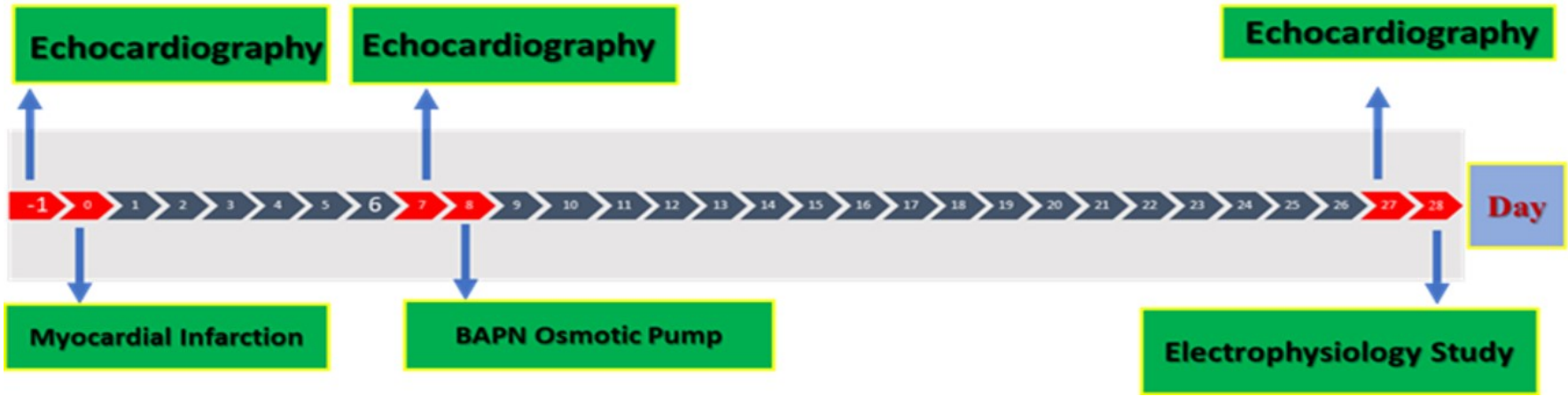
Echocardiography
Echocardiography
Echocardiography
-1
0
1
2
3
4
5
6
7
8
9
10
11
12
13
14
15
16
17
18
19
20
21
22
23
24
25
26
27
28
Day
Myocardial Infarction
BAPN Osmotic Pump
Electrophysiology Study

**Figure 1.**

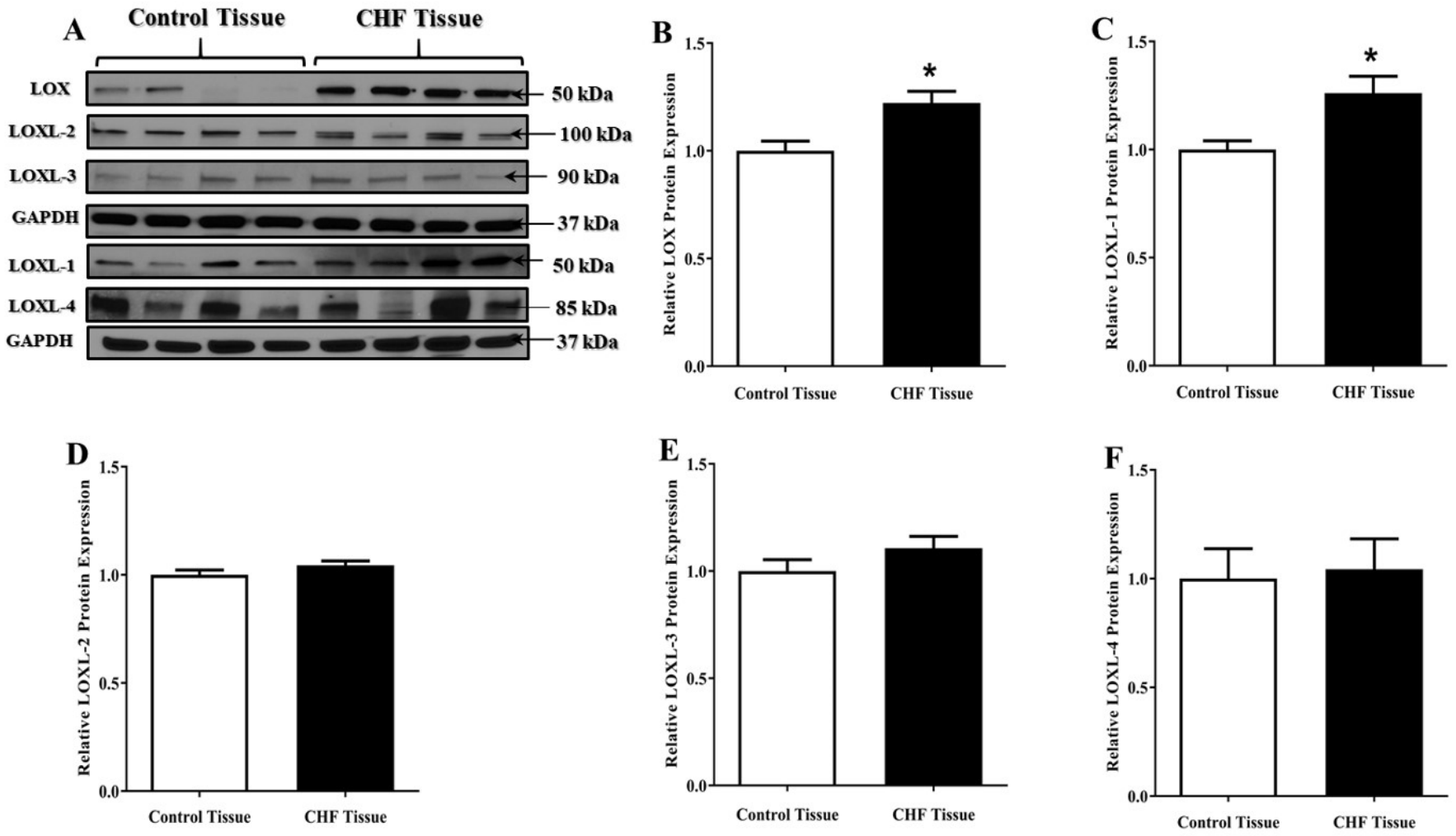
A
Control Tissue
CHF Tissue
LOX
LOXL-2
LOXL-3
GAPDH
LOXL-1
LOXL-4
GAPDH
50 kDa
100 kDa
90 kDa
37 kDa
50 kDa
85 kDa
37 kDa
B
Relative LOX Protein Expression
C
Relative LOXL-1 Protein Expression
D
Relative LOXL-2 Protein Expression
E
Relative LOXL-3 Protein Expression
F
Relative LOXL-4 Protein Expression
1.5
1.0
0.5
0.0
*
Control Tissue
CHF Tissue

**Figure 2.**

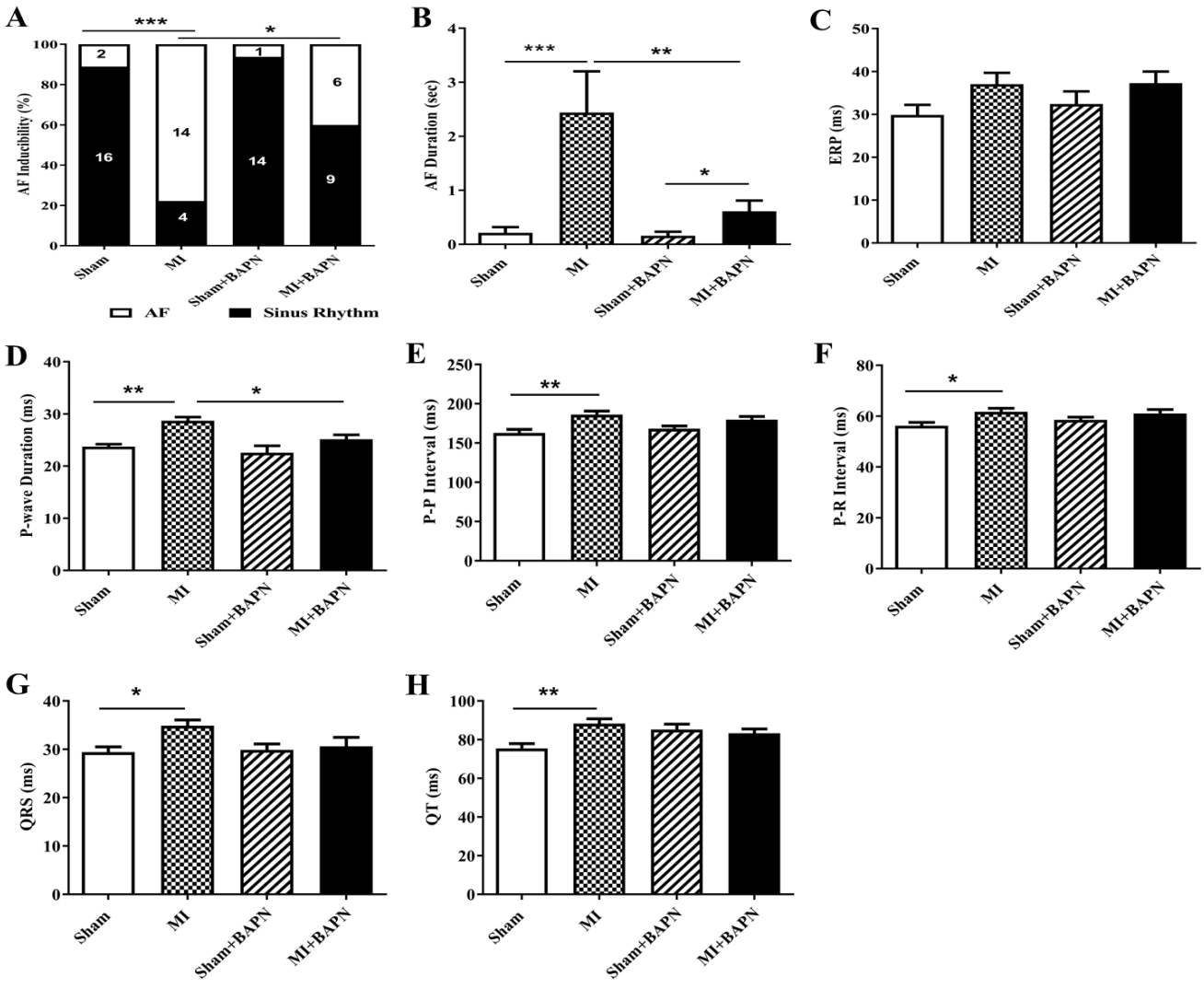
A
B
C
D
E
F
G
H
AF Inducibility (%)
AF Duration (sec)
ERP (ms)
P-wave Duration (ms)
P-P Interval (ms)
P-R Interval (ms)
QRS (ms)
QT (ms)
Sham
MI
Sham+BAPN
MI+BAPN
AF
Sinus Rhythm

**Figure 3.**

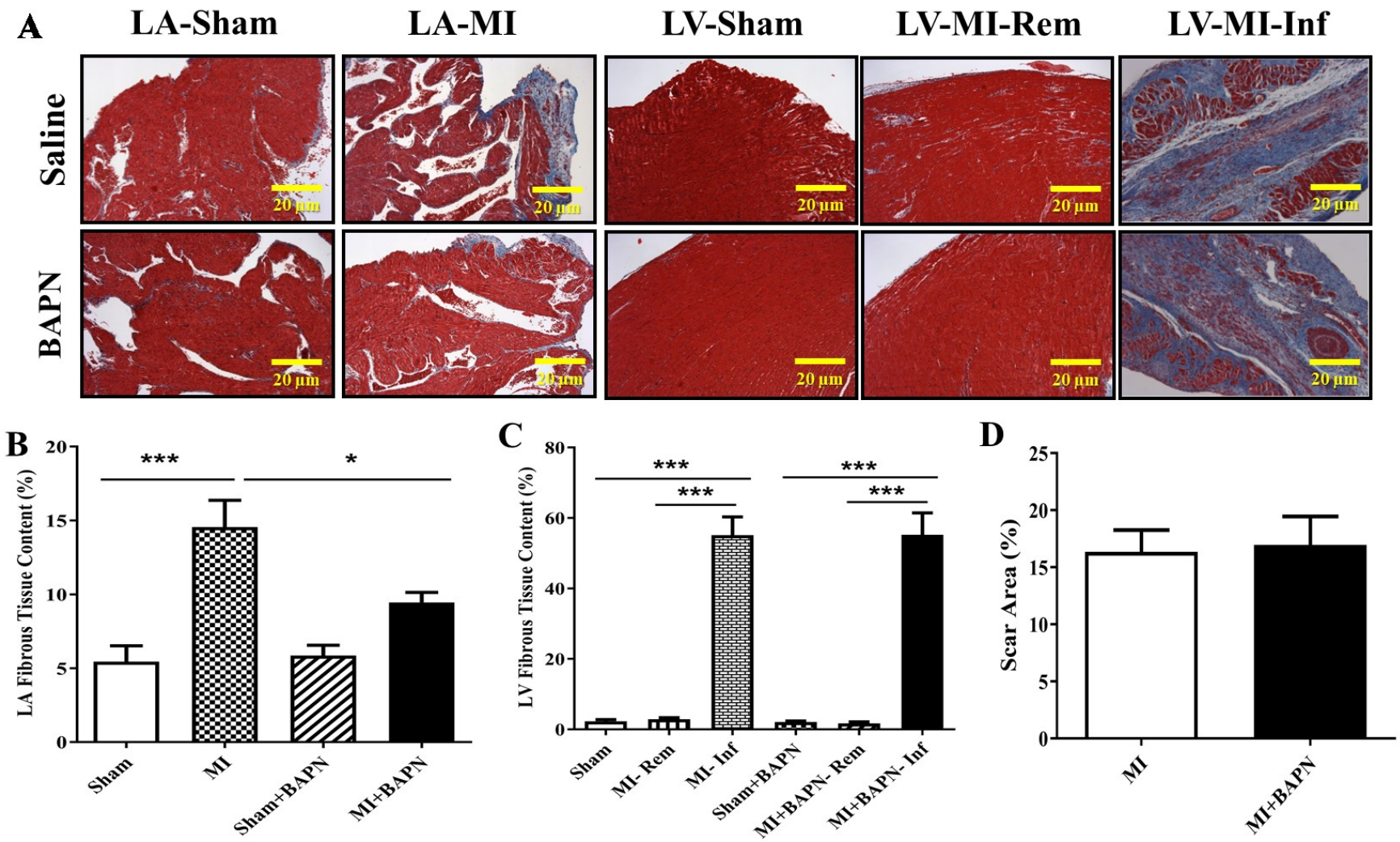
A
LA-Sham
LA-MI
LV-Sham
LV-MI-Rem
LV-MI-Inf
Saline
BAPN
20 µm
B
LA Fibrous Tissue Content (%)
***
*
Sham
MI
Sham+BAPN
MI+BAPN
C
LV Fibrous Tissue Content (%)
***
***
***
***
Sham
MI- Rem
MI- Inf
Sham+BAPN
MI+BAPN- Rem
MI+BAPN- Inf
D
Scar Area (%)
MI
MI+BAPN

**Figure 4.**

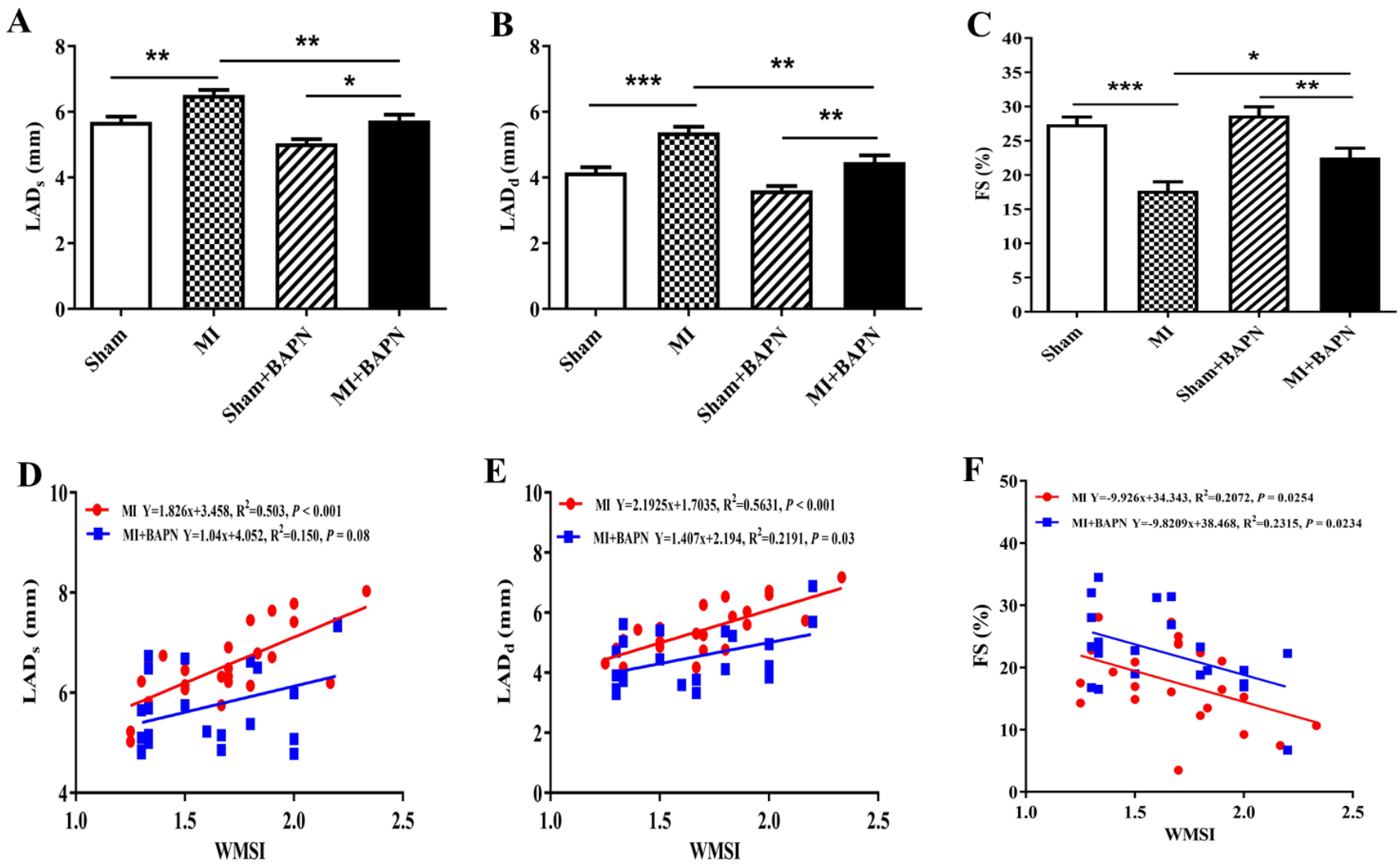
A
B
C
D
E
F
LADs (mm)
LADd (mm)
FS (%)
Sham
MI
Sham+BAPN
MI+BAPN
WMSI
MI Y=1.826x+3.458, R2=0.503, P < 0.001
MI+BAPN Y=1.04x+4.052, R2=0.150, P = 0.08
MI Y=2.1925x+1.7035, R2=0.5631, P < 0.001
MI+BAPN Y=1.407x+2.194, R2=0.2191, P = 0.03
MI Y=-9.926x+34.343, R2=0.2072, P = 0.0254
MI+BAPN Y=-9.8209x+38.468, R2=0.2315, P = 0.0234

**Figure 5.**

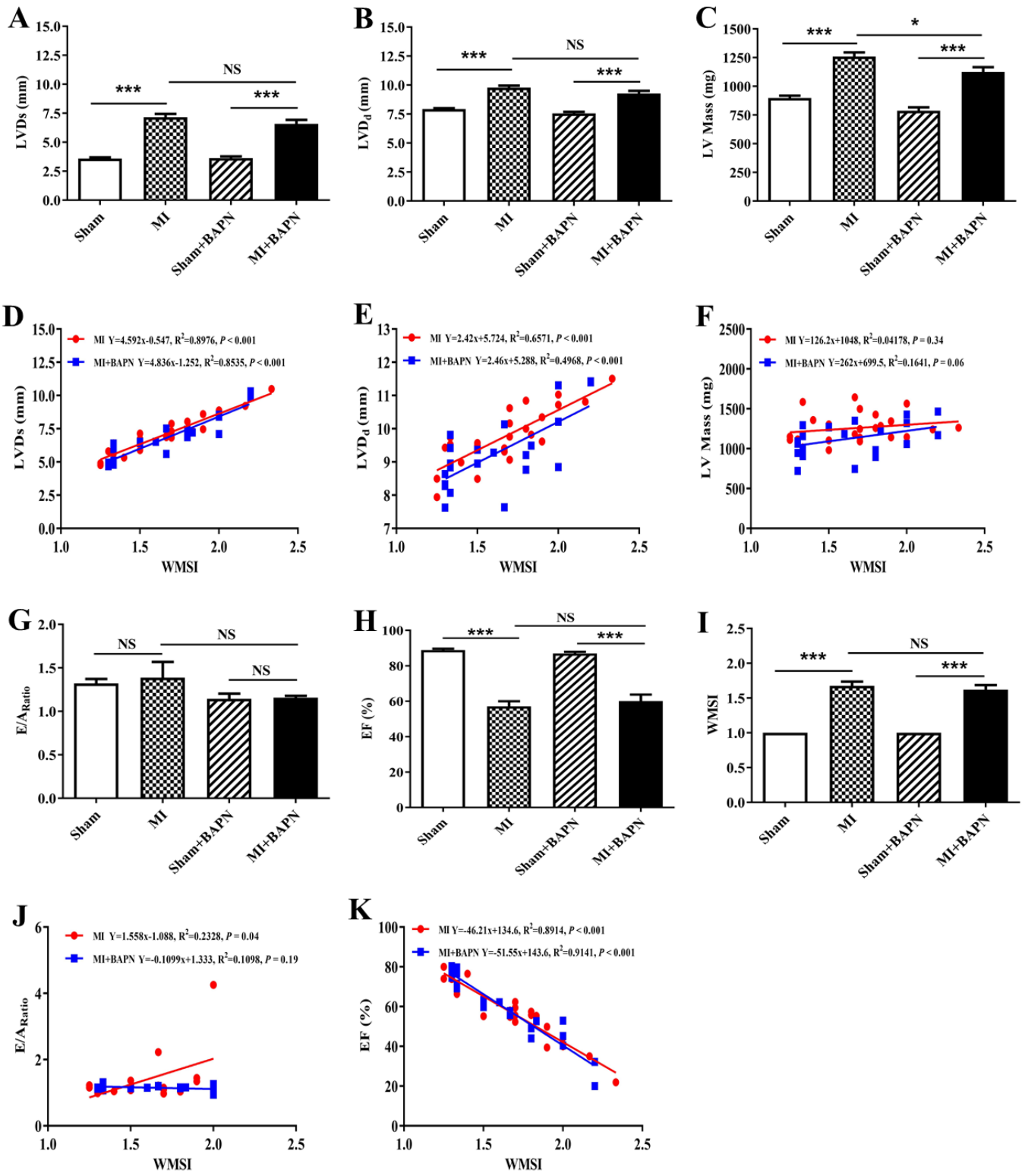
A
LVDs (mm)
***
NS
***
Sham
MI
Sham+BAPN
MI+BAPN
B
LVDd (mm)
***
NS
***
C
LV Mass (mg)
***
*
***
D
MI Y=4.592x-0.547, R²=0.8976, P < 0.001
MI+BAPN Y=4.836x-1.252, R²=0.8535, P < 0.001
WMSI
E
MI Y=2.42x+5.724, R²=0.6571, P < 0.001
MI+BAPN Y=2.46x+5.288, R²=0.4968, P < 0.001
F
MI Y=126.2x+1048, R²=0.04178, P = 0.34
MI+BAPN Y=262x+699.5, R²=0.1641, P = 0.06
G
E/ARatio
NS
NS
NS
H
EF (%)
***
NS
***
I
WMSI
***
NS
***
J
MI Y=1.558x-1.088, R²=0.2328, P = 0.04
MI+BAPN Y=-0.1099x+1.333, R²=0.1098, P = 0.19
K
MI Y=-46.21x+134.6, R²=0.8914, P < 0.001
MI+BAPN Y=-51.55x+143.6, R²=0.9141, P < 0.001

**Figure 6.**

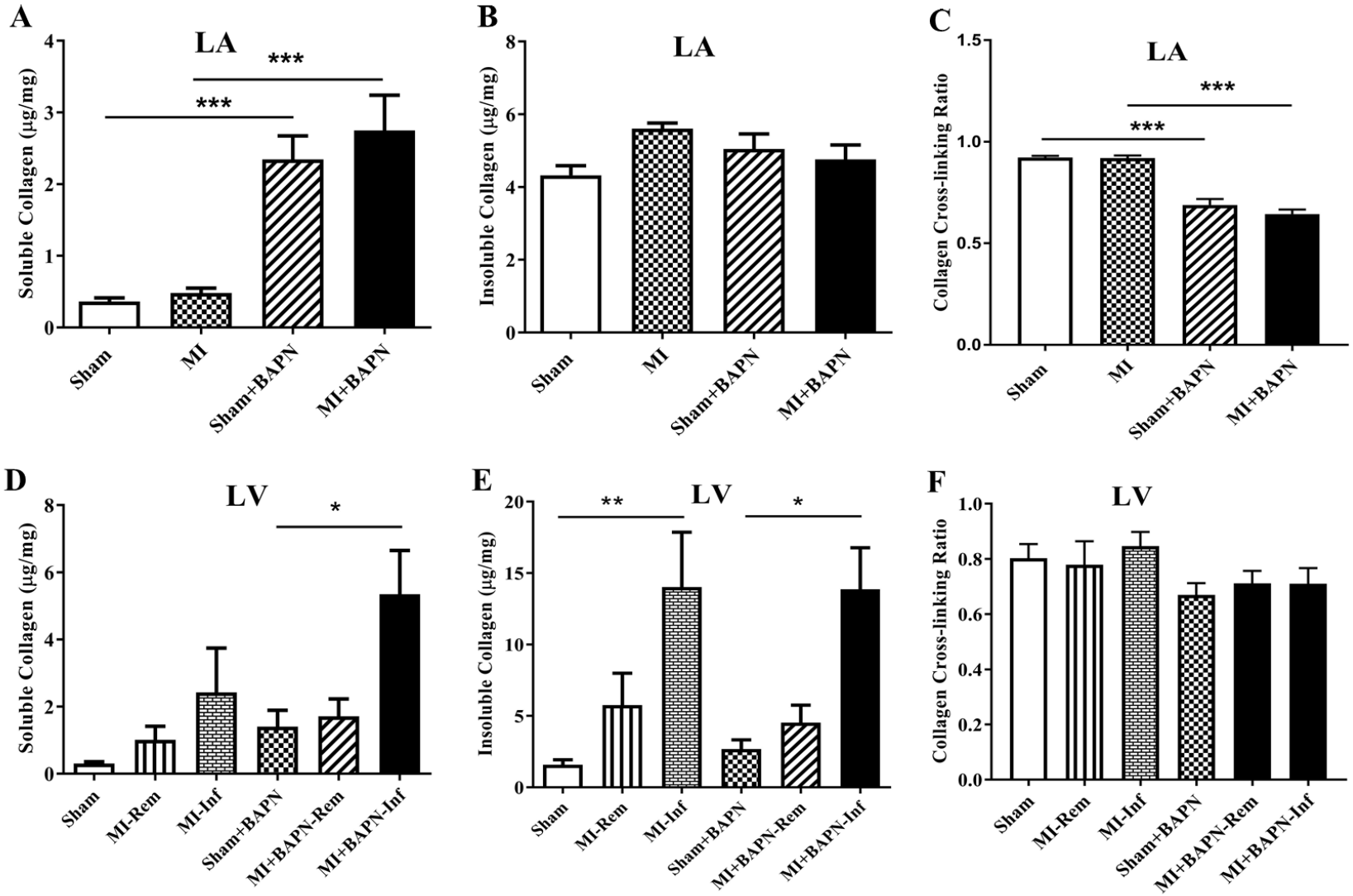
A
LA
Soluble Collagen (µg/mg)
***
***
Sham
MI
Sham+BAPN
MI+BAPN
B
LA
Insoluble Collagen (µg/mg)
Sham
MI
Sham+BAPN
MI+BAPN
C
LA
Collagen Cross-linking Ratio
***
***
Sham
MI
Sham+BAPN
MI+BAPN
D
LV
Soluble Collagen (µg/mg)
*
Sham
MI-Rem
MI-Inf
Sham+BAPN
MI+BAPN-Rem
MI+BAPN-Inf
E
LV
Insoluble Collagen (µg/mg)
**
*
Sham
MI-Rem
MI-Inf
Sham+BAPN
MI+BAPN-Rem
MI+BAPN-Inf
F
LV
Collagen Cross-linking Ratio
Sham
MI-Rem
MI-Inf
Sham+BAPN
MI+BAPN-Rem
MI+BAPN-Inf

**Figure 7.**

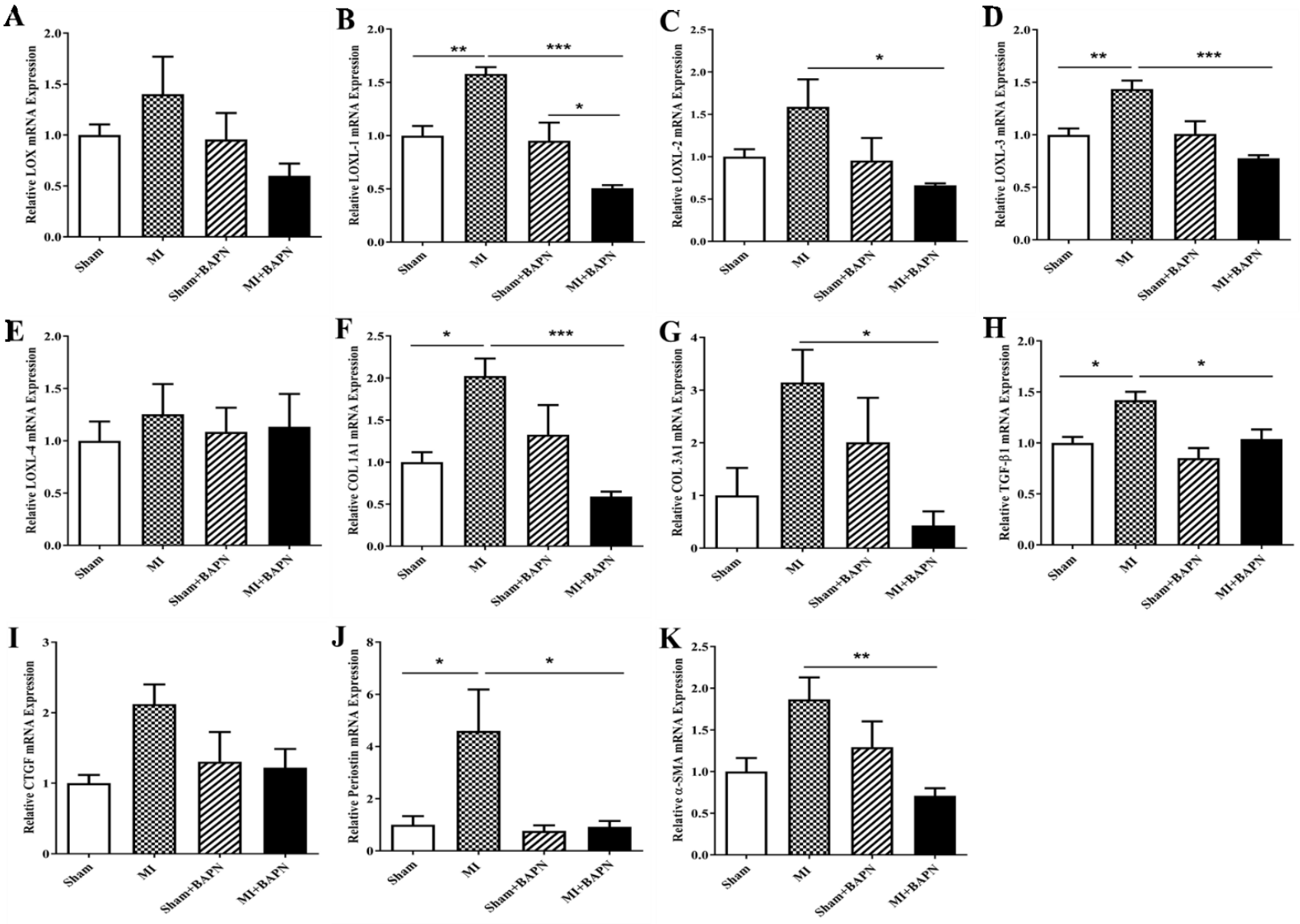
A
Relative LOX mRNA Expression
B
Relative LOXL-1 mRNA Expression
C
Relative LOXL-2 mRNA Expression
D
Relative LOXL-3 mRNA Expression
E
Relative LOXL-4 mRNA Expression
F
Relative COL 1A1 mRNA Expression
G
Relative COL 3A1 mRNA Expression
H
Relative TGF-β1 mRNA Expression
I
Relative CTGF mRNA Expression
J
Relative Periostin mRNA Expression
K
Relative α-SMA mRNA Expression
Sham
MI
Sham+BAPN
MI+BAPN

**Figure 8.**

## Supplementary Figure Legends

**Figure S1. Increased mRNA expressions of lysyl oxidase (LOX) isoforms in the left atrial (LA) tissues of congestive heart failure (CHF) dogs.** Basal relative mRNA (A-E) expressions of LOX isoforms in the LA tissues (n = 5) of CHF (2 weeks of ventricular tachypacing (VTP)) model were quantified by qPCR, including (A) LOX, (B) LOX-like protein 1 (LOXL-1), (C) LOXL-2, (D) LOXL-3 and (E) LOX-4. mRNA expression was normalized to glucose 6-phosphate dehydrogenase (G6PD). The results are the means ± SEM; unpaired Student's *t*-tests were performed. **P* < 0.05; ***P* < 0.01; ****P* < 0.001.

**Figure S2. Effect of β-aminopropionitrile (BAPN) administration post-myocardial infarction (MI) on the surface electrocardiogram (ECG) and atrial fibrillation (AF) induction.** (A) representative surface ECG recording and (B) representative recording of burst pacing-induced AF in four rat groups (Sham, Sham+BAPN, MI and MI+BAPN) at day 28 post-surgery.

**Figure S3. β-aminopropionitrile (BAPN) administration decreased myocardial infarction (MI)-induced left atrial (LA) remodeling in rats.** LA structural and functional remodeling in four rat groups was assessed by echocardiography, including Sham (n = 21), Sham+BAPN (n = 18-20), MI (n = 23-24) and MI+BAPN (n = 22) on day 27 post-surgery. (A) LA area at end systole ($LAA_s$), (B) LA area at end diastole ($LAA_d$) and (C) fractional area changing of LA ($FAC_{LA}$). Comparison between echocardiographic assessment of the wall motion score index (WMSI) and LA structural and functional parameters in MI rats treated with vehicle or BAPN on day 27 post-MI. Linear correlations of WMSI with (D) $LAA_s$, (E) $LAA_d$, and (F) $FAC_{LA}$. The results are the means ± SEM; one-way ANOVA followed by the Bonferroni's multiple comparisons test (A-C) was performed. **P* < 0.05; ***P* < 0.01; ****P* < 0.001; $R^2$: correlation coefficient; in the equation, (x) represents the WMSI and (Y) represents structural and functional parameters.

**Figure S4. β-aminopropionitrile (BAPN) had no effect on myocardial infarction (MI)-induced left ventricular (LV) remodeling in rats.** LV structural and functional remodeling in four rat groups was assessed by echocardiography, including Sham (n = 17-21), Sham+BAPN (n = 18-20), MI (n = 18-24) and MI+BAPN (n = 14-22) on day 27 post-surgery. (A) LV anterior wall thickness at end diastole ($LVAW_d$), (B) LV posterior wall thickness at end diastole ($LVPW_d$), (C) ratio of LV mass

to LV diameter at end diastole ($LVD_d$), (D) ratio of early diastolic transmitral filling velocity (E) to mitral annulus moving velocity during early filling at septal wall ($e'_{Septal}$,), (E) ratio of E to mitral annulus moving velocity during early filling at lateral wall ($e'_{Lateral}$), (F) E wave deceleration time (EDT), (N) LV volume at end diastole ($LVV_d$), (O) LV volume at end systole ($LVV_s$), (P) fractional shortening (FS), (Q) septal systolic contractility ($S_S$), (R) lateral wall systolic contractility ($S_L$) and (S) myocardial performance index ($MPI_{Global}$). Comparison between echocardiographic assessment of the wall motion score index (WMSI) and LV structural and functional parameters in MI rats treated with vehicle or BAPN on day 27 post-MI. Linear correlations of WMSI with (G) $LVAW_d$, (H) $LVPW_d$, (I) ratio of LV mass to $LVD_d$, (K) ratio of E to $e'_{Septal}$ (L) ratio of E to $e'_{Lateral}$, (M) EDT, (T) $LVV_d$, (U) $LVV_s$, (V) FS, (W) $S_S$, (X) $S_L$ and (Y) $MPI_{Global}$. The results are the means ± SEM; one-way ANOVA followed by the Bonferroni's multiple comparisons test (A-F and N-S) was performed. $*P < 0.05$; $**P < 0.01$; $***P < 0.001$; $R^2$: correlation coefficient; in the equation, (x) represents the WMSI and (Y) represents structural and functional parameters.

**Figure S5. Administration of β-aminopropionitrile (BAPN) post-myocardial infarction (MI) in rats decreased the mRNA expression profibrotic markers in the left atrial (LA) tissues.** Transcript levels of profibrotic markers in the LA tissues from four rat groups, including Sham (n = 6), Sham+BAPN (n = 6), MI (n = 6) and MI+BAPN (n = 6) were quantified by qPCR on day 28 post-surgery. (A) fibronectin 1 (FN 1), (B) connexin 43 (Cx 43), (C) matrix metalloproteinase 2 (MMP-2) and (D) MMP-9. The results are the means ± SEM; one-way ANOVA followed by the Bonferroni's multiple comparisons test was performed. $*P < 0.05$; $**P < 0.01$; $***P < 0.001$.

**Figure S6. Administration of β-aminopropionitrile (BAPN) post-myocardial infarction (MI) in rats had no effect on the abundance of transcripts for profibrotic markers in left ventricular (LV) tissues.** mRNA levels of profibrotic markers in the LV tissues from four rat groups (Sham; n = 6, Sham+BAPN; n = 6, MI from remote (Rem) and infarct (Inf) areas (MI-Rem and MI-Inf; n = 6) and MI+BAPN (MI+BAPN-Rem and MI+BAPN-Inf; n = 6)) were quantified by qPCR on day 28 post-surgery, including (A) lysyl oxidase (LOX), (B) LOX-like protein-1 (LOXL-1), (C) LOXL-2, (D) LOXL-3, (E) LOXL-4, (F) collagen 1A1 (COL 1A1), (G) collagen 3A1 (COL 3A1), (H) fibronectin 1 (FN 1), (I) transforming growth factor β1 (TGF-β1), (J) connective tissue growth factor (CTGF), (K) periostin, (L) connexin 43 (Cx 43), (M) α-smooth muscle actin (α-SMA), (N) matrix metalloproteinase-2 (MMP-2) and (O) MMP-9. The results are the means ± SEM; one-way ANOVA

followed by the Bonferroni's multiple comparisons test was performed. *$P < 0.05$; **$P < 0.01$; ***$P < 0.001$.

**Figure S7. Administration of β-aminopropionitrile (BAPN) post-myocardial infarction (MI) in rats had no effect on the protein expression of lysyl oxidase (LOX) isoforms in left atrial (LA) tissues.** Western blot analysis was used to evaluate the protein expression of LOX isoforms in the LA tissues from four rat groups, including Sham (n = 6), Sham+BAPN (n = 6), MI (n = 6) and MI+BAPN (n = 6) on day 28 after surgery. (A) LOX, (B) LOX-like protein-1 (LOXL-1), (C) LOXL-2, (D) LOXL-3, (E) LOXL-4 and (F) representative immunoblot images of protein quantification. Band intensities of Western blot images were normalized to glyceraldehyde 3-phosphate dehydrogenase (GAPDH). Active and inactive LOX represent the bands at the molecular weight of 32 and 50 kDa, respectively. The results are the means ± SEM; one-way ANOVA followed by the Bonferroni's multiple comparisons test was performed. *$P < 0.05$; **$P < 0.01$; ***$P < 0.001$.

**Figure S8. Administration of β-aminopropionitrile (BAPN) post-myocardial infarction (MI) in rats had no effect on the amount of lysyl oxidase (LOX) isoform immunoreactivity in left ventricular (LV) tissues.** Western blot analysis was used to evaluate the LOX isoform immunoreactivity in the LV tissues from four rat groups, including Sham (n = 4), Sham+BAPN (n = 4), MI from remote (Rem) and infarct (Inf) areas (MI-Rem and MI-Inf; n = 4) and MI+BAPN (MI+BAPN-Rem and MI+BAPN-Inf; n = 4) on day 28 after surgery. (A) LOX, (B) LOX-like protein-1 (LOXL-1), (C) LOXL-2, (D) LOXL-3, (E) LOXL-4 and (F) representative immunoblot images of protein quantification. Band intensities of Western blot images were normalized to Tubulin. Active and inactive LOX represent the bands at the molecular weight of 32 and 50 kDa, respectively. The results are the means ± SEM; one-way ANOVA followed by the Bonferroni's multiple comparisons test was performed. *$P < 0.05$; **$P < 0.01$; ***$P < 0.001$.

**Table S1:** Sequences of custom-made SYBR Green primers used in this study.

| Gene Name | Species | Abbreviation | | Primer sequence (5′ to 3′) |
|---|---|---|---|---|
| Lysyl oxidase like-1 | Rat | LOXL-1 | **F:** | AGGGCCGTCTCAGCGTGGGTAGT |
| | | | **R:** | ATGCCTGCACGTAGTTGGGATCTGG |
| Lysyl oxidase like-2 | Rat | LOXL-2 | **F:** | GGCCAGCTTCTGCTTGGAGGACAC |
| | | | **R:** | GCCTTGTTCTCCGAAGTTGGCACAC |
| Lysyl oxidase like-3 | Rat | LOXL-3 | **F:** | ACCCACAGTGCCAAATACGG |
| | | | **R:** | TTGCAGATGACCCCAGCATC |
| Transforming growth factor-β1 | Rat | TGF-β1 | **F:** | CCATGACATGAACCGACCCT |
| | | | **R:** | TGCCGTACACAGCAGTTCTT |
| Matrix metalloproteinase-2 | Rat | MMP-2 | **F:** | AAGAGGCCTGGTTACCCTGT |
| | | | **R:** | AAGTAGCACCTGGGAGGGAT |
| Matrix metalloproteinase-9 | Rat | MMP-9 | **F:** | TCCAGTAGACAATCCTTGCAATGTG |
| | | | **R:** | CTCCGTGATTCGAGAACTTCCAATA |
| Gap junction protein connexin 43 | Rat | GJA1 Cx 43 | **F:** | AGGCGTGAGGAAAGTACCAA |
| | | | **R:** | GCACTCCAGTCACCCATGTC |
| Periostin | Rat | Periostin | **F:** | CTGCCCCGGCTATATGAGAA |
| | | | **R:** | TGTTGAGTGGTCGTGGCTC |
| β2 microglobulin | Rat | B2m | **F:** | CCGTGATCTTTCTGGTGCTT |
| | | | **R:** | GTGGAACTGAGACACGTAGC |
| Connective tissue growth factor | Rat | CTGF | **F:** | CAAGGGTCTCTTCTGCGACT |
| | | | **R:** | GTACACGGACCCACCGAAG |
| α-smooth muscle actin | Rat | α-SMA | **F:** | AGCCAGTCGCCATCAGGAAC |
| | | | **R:** | CCGGAGCCATTGTCACACAC |
| Lysyl oxidase | Dog | LOX | **F:** | CGTACTACATCCAGGCGTCC |
| | | | **R:** | GGGAATCTTAGCAGCACCCT |
| Lysyl oxidase like-1 | Dog | LOXL-1 | **F:** | AGCCCGGGAACTACATCCT |
| | | | **R:** | GTAGTGGATGTTGCAACGCA |
| Lysyl oxidase like-2 | Dog | LOXL-2 | **F:** | GGAGAAGACGTACAACGCCA |
| | | | **R:** | GAGATATGAGCCTCCGTGCC |
| Lysyl oxidase like-3 | Dog | LOXL-3 | **F:** | CAGGATGCTGGAGTCCGATG |
| | | | **R:** | CCCCAGTCATCCCCACAAAT |
| Lysyl oxidase like-4 | Dog | LOXL-4 | **F:** | AGAGAACTGCCTCTCCCAGT |
| | | | **R:** | GAAGACCTCGATGCTGTGGT |
| Glucose 6-phosphate dehydrogenase | Dog | G6PD | **F:** | GGCGGTCACCAAGAACATCC |
| | | | **R:** | GCTTCTCCACGATGACACGG |

**F: Forward, R: Reverse.**

**Table S2:** Statistical linear regression comparison (slopes and Y-intercepts) between WMSI and echocardiographic parameters in MI and MI+BAPN rats.

| Echocardiographic Parameters | Slope | | | Y-intercept | | |
|---|---|---|---|---|---|---|
| | **MI** | **MI+BAPN** | ***P*-value** | **MI** | **MI+BAPN** | ***P*-value** |
| **LV structural function** | | | | | | |
| $LVAW_d$ | -0.5823 | -0.2998 | 0.43 | 2.571 | 2.100 | 0.96 |
| $LVPW_d$ | -0.173 | -0.114 | 0.80 | 2.087 | 1.832 | **0.03** |
| $LVD_d$ | 2.42 | 2.46 | 0.95 | 5.724 | 5.288 | 0.07 |
| $LVD_s$ | 4.592 | 4.836 | 0.66 | -0.547 | -1.252 | 0.07 |
| LV mass | 126.2 | 262.0 | 0.47 | 1048.0 | 699.5 | **0.03** |
| LV mass/$LVD_d$ | -18.10 | -2.93 | 0.36 | 159.6 | 125.4 | 0.06 |
| **LV systolic function** | | | | | | |
| $LVV_d$ | 1.323 | 1.330 | 0.98 | -0.2465 | -0.4254 | 0.10 |
| $LVV_s$ | 1.574 | 1.563 | 0.96 | -1.744 | -1.783 | 0.37 |
| FS | -28.37 | -31.97 | 0.28 | 75.00 | 81.58 | 0.52 |
| EF | -46.21 | -51.55 | 0.29 | 134.6 | 143.6 | 0.87 |
| $S_L$ | -1.703 | -0.846 | 0.43 | 7.571 | 5.276 | **0.009** |
| $S_S$ | -1.927 | -0.367 | 0.07 | 7.643 | 4.710 | 0.19 |
| **LV diastolic function** | | | | | | |
| E/A | 1.558 | -1.099 | **0.02** | -1.088 | 1.333 | ND |
| E/e' $_{Lateral}$ | 23.46 | 18.56 | 0.59 | -12.960 | -5.906 | 0.69 |
| E/e' $_{Septal}$ | 24.540 | 9.979 | **0.04** | -15.330 | 5.584 | ND |
| EDT | 0.158 | -4.028 | 0.48 | 27.88 | 34.04 | 0.67 |
| **MPI** | | | | | | |
| $MPI_{Global}$ | 36.81 | 31.09 | 0.62 | -8.584 | 8.641 | **0.02** |
| **LA remodeling** | | | | | | |
| $LAD_d$ | 2.193 | 1.407 | 0.28 | 1.704 | 2.194 | **<0.001** |
| $LAD_s$ | 1.826 | 1.040 | 0.25 | 3.458 | 4.052 | **0.001** |
| $LAA_d$ | 17.907 | 10.024 | 0.19 | -7.4898 | 0.5734 | **0.009** |
| $LAA_s$ | 13.225 | 5.231 | 0.12 | 12.787 | 20.055 | **<0.001** |
| FS | -9.926 | -9.821 | 0.986 | 34.343 | 38.468 | **0.0147** |
| $FAC_{LA}$ | -24.11 | -20.20 | 0.71 | 77.28 | 75.18 | 0.17 |

Myocardial infarction (MI); β-aminopropionitrile (BAPN); Left ventricle (LV); Left atrium (LA); LV anterior wall thickness at end diastole ($LVAW_d$); LV posterior wall thickness at end diastole ($LVPW_d$); LV and LA diameter at end diastole ($LVD_d$ and $LAD_d$); LV and LA diameter at end systole ($LVD_s$ and $LAD_s$); LV volume at end diastole ($LVV_d$); LV volume at end systole ($LVV_s$); Fractional shortening (FS); Ejection fraction (EF); Wall motion score index (WMSI); Lateral wall systolic contractility ($S_L$); Septal systolic contractility ($S_s$); Early diastolic transmitral filling velocity (E); Atrial transmitral filling velocity (A); Mitral annulus moving velocity during early filling (e'); E wave deceleration time (EDT); Myocardial performance index (MPI); LA area at the end diastole ($LAA_d$); LA area at end systole ($LAA_s$); Fractional area changing of LA ($FAC_{LA}$). Linear regression analysis was carried out to assess the relationship between the WMSI and echocardiographic parameters. **Bold** values indicated statistical significance; ND: non determined (the slopes differ so much).

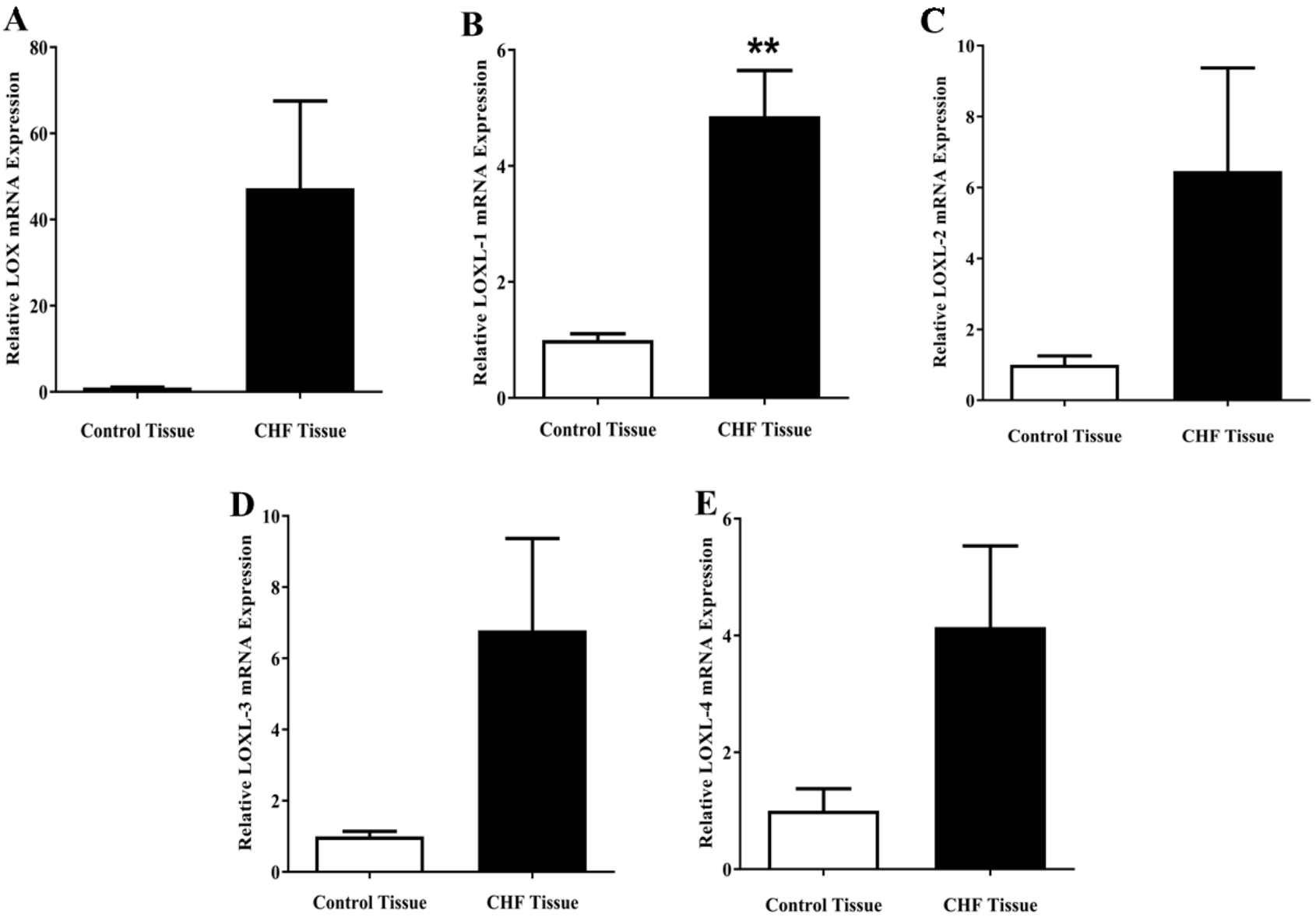
A
Relative LOX mRNA Expression
80
60
40
20
0
Control Tissue
CHF Tissue
B
**
Relative LOXL-1 mRNA Expression
6
4
2
0
Control Tissue
CHF Tissue
C
Relative LOXL-2 mRNA Expression
10
8
6
4
2
0
Control Tissue
CHF Tissue
D
Relative LOXL-3 mRNA Expression
10
8
6
4
2
0
Control Tissue
CHF Tissue
E
Relative LOXL-4 mRNA Expression
6
4
2
0
Control Tissue
CHF Tissue

**Figure S1.**

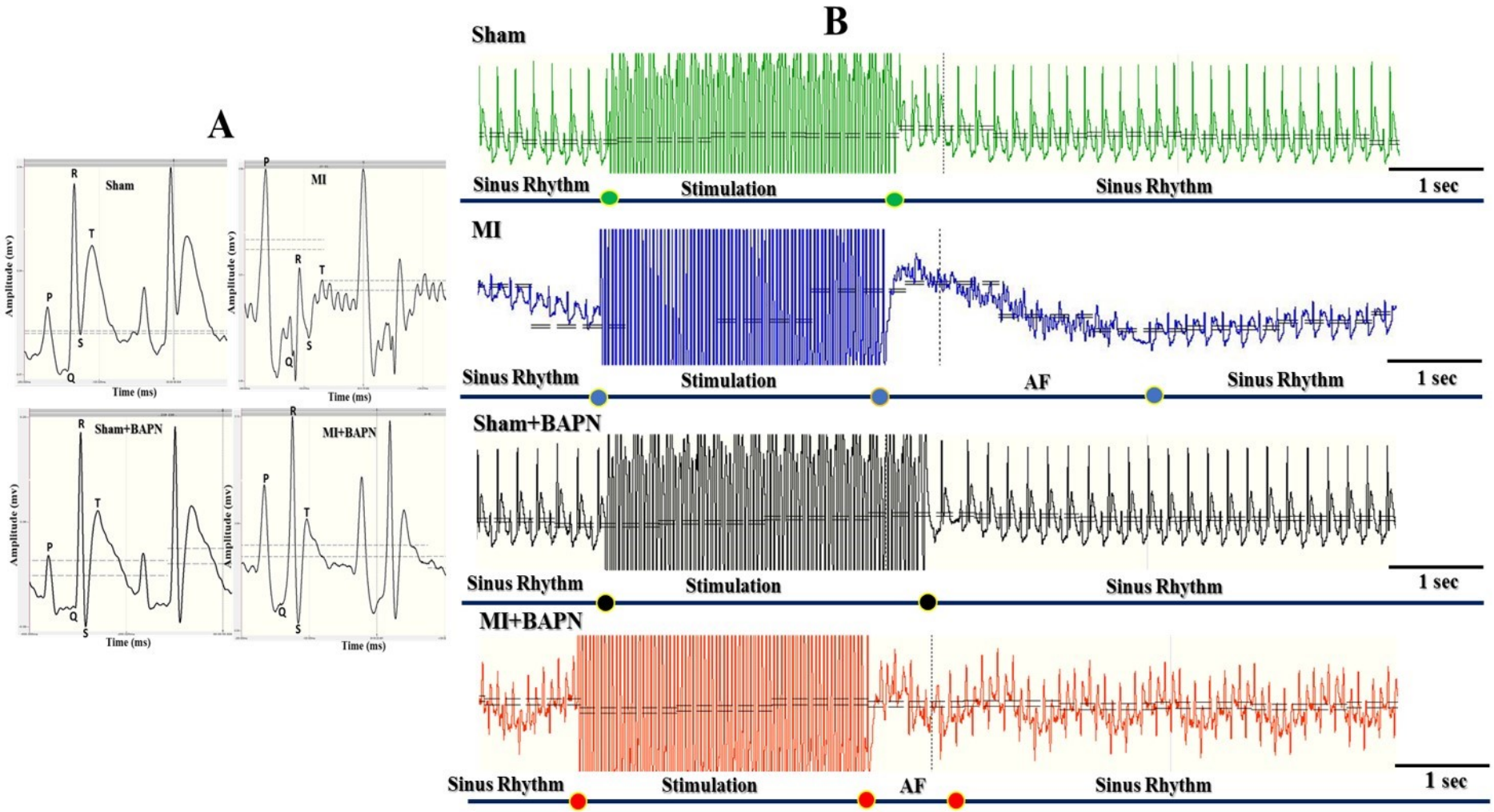
A
Sham
MI
Sham+BAPN
MI+BAPN
Amplitude (mv)
Time (ms)
P
Q
R
S
T
B
Sham
MI
Sham+BAPN
MI+BAPN
Sinus Rhythm
Stimulation
AF
1 sec

**Figure S2.**

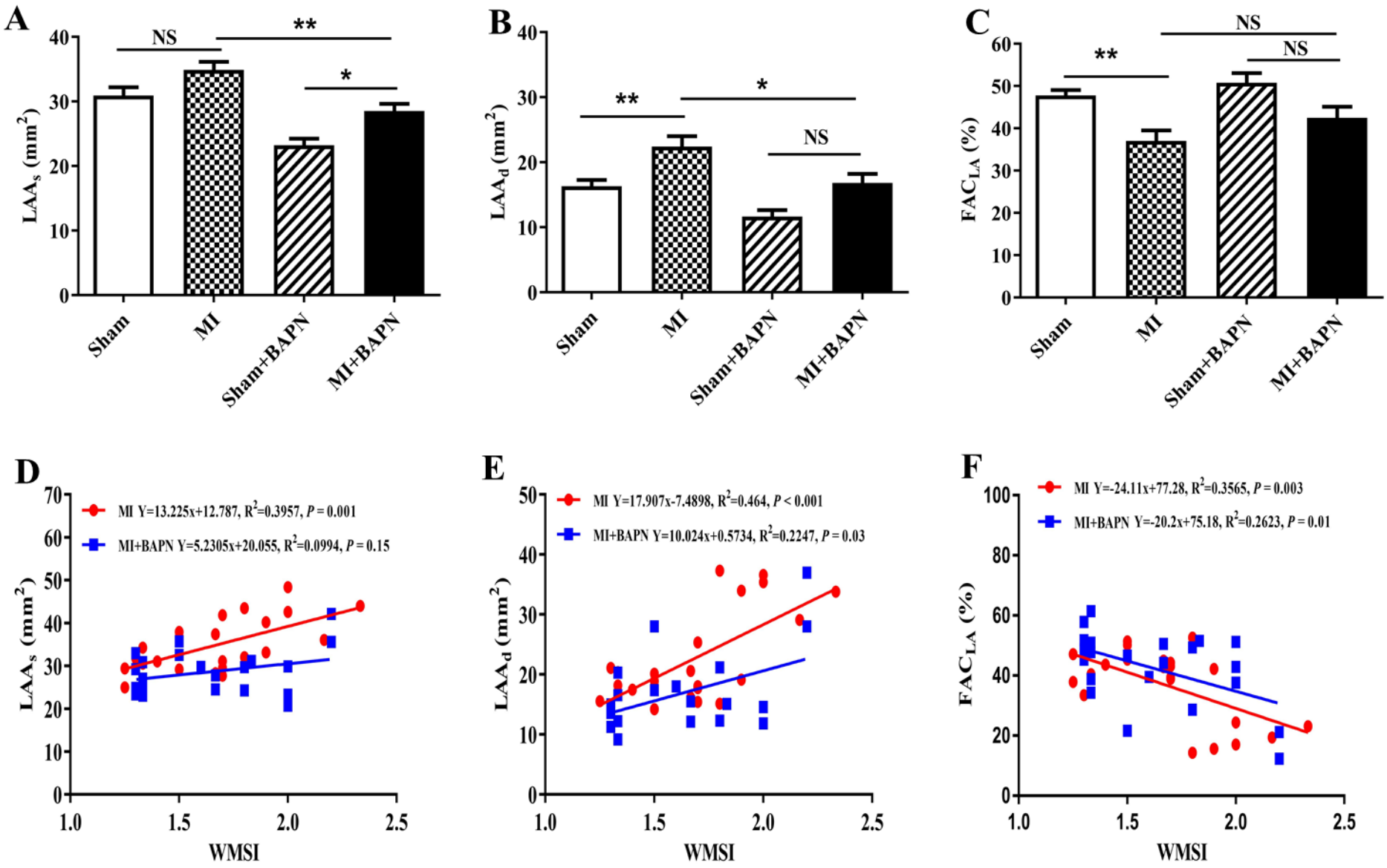
A
B
C
D
E
F
NS
**
*
Sham
MI
Sham+BAPN
MI+BAPN
LAAs (mm2)
LAAd (mm2)
FACLA (%)
WMSI
MI Y=13.225x+12.787, R2=0.3957, P = 0.001
MI+BAPN Y=5.2305x+20.055, R2=0.0994, P = 0.15
MI Y=17.907x-7.4898, R2=0.464, P < 0.001
MI+BAPN Y=10.024x+0.5734, R2=0.2247, P = 0.03
MI Y=-24.11x+77.28, R2=0.3565, P = 0.003
MI+BAPN Y=-20.2x+75.18, R2=0.2623, P = 0.01

**Figure S3.**

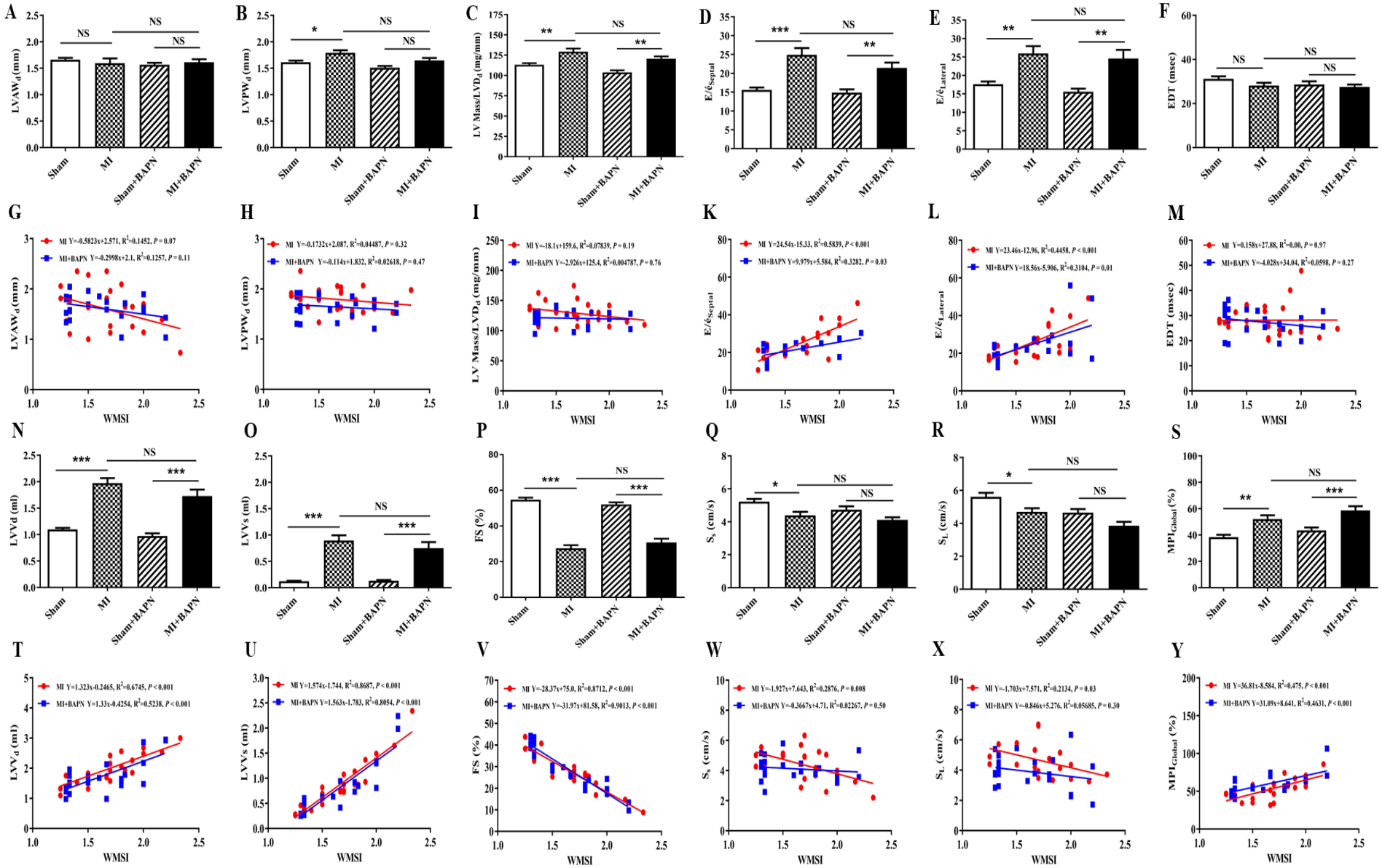
A
B
C
D
E
F
G
H
I
K
L
M
N
O
P
Q
R
S
T
U
V
W
X
Y
Sham
MI
Sham+BAPN
MI+BAPN
NS
WMSI

**Figure S4.**

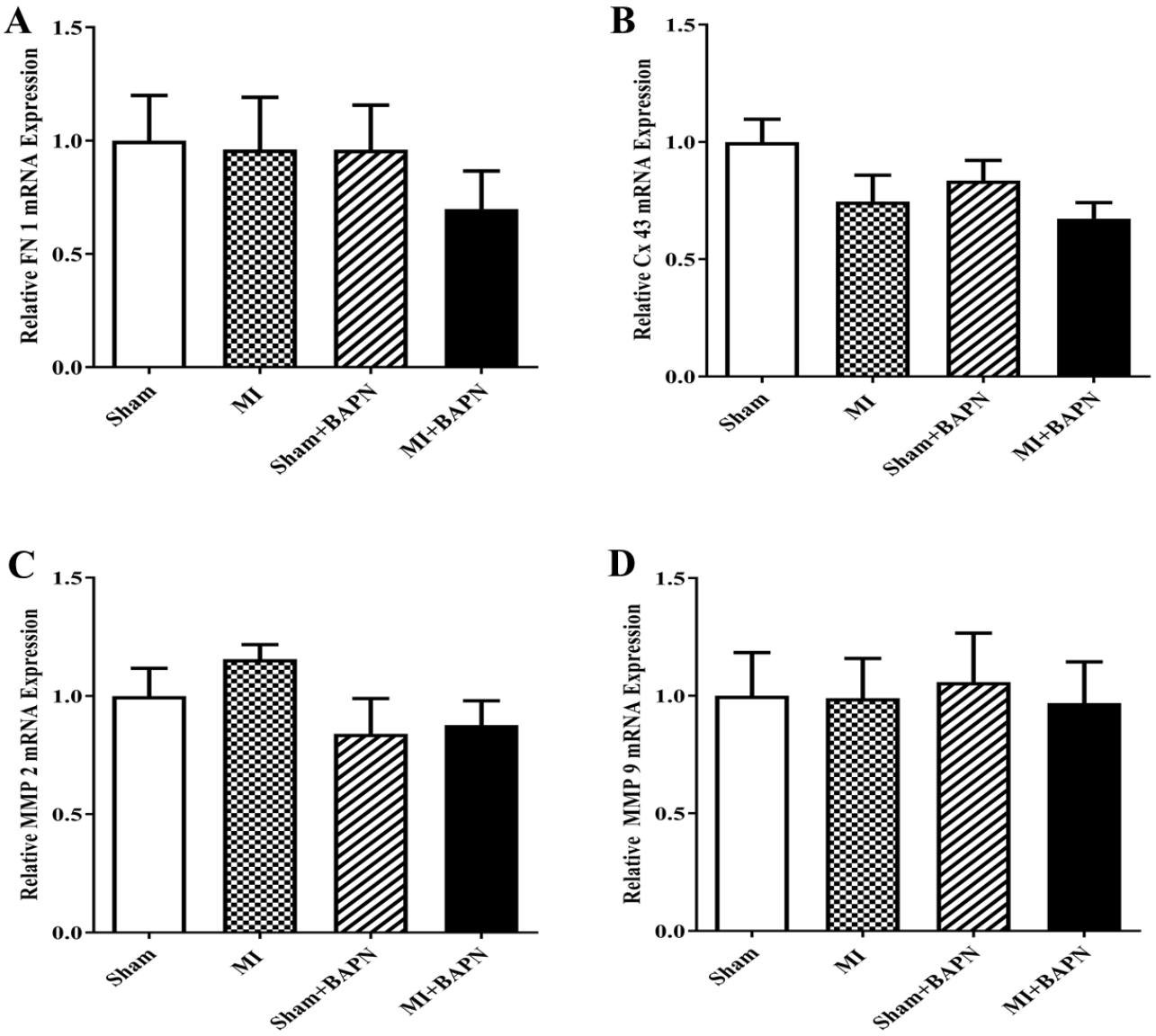
A
Relative FN 1 mRNA Expression
1.5
1.0
0.5
0.0
Sham
MI
Sham+BAPN
MI+BAPN
B
Relative Cx 43 mRNA Expression
1.5
1.0
0.5
0.0
Sham
MI
Sham+BAPN
MI+BAPN
C
Relative MMP 2 mRNA Expression
1.5
1.0
0.5
0.0
Sham
MI
Sham+BAPN
MI+BAPN
D
Relative MMP 9 mRNA Expression
1.5
1.0
0.5
0.0
Sham
MI
Sham+BAPN
MI+BAPN

**Figure S5.**

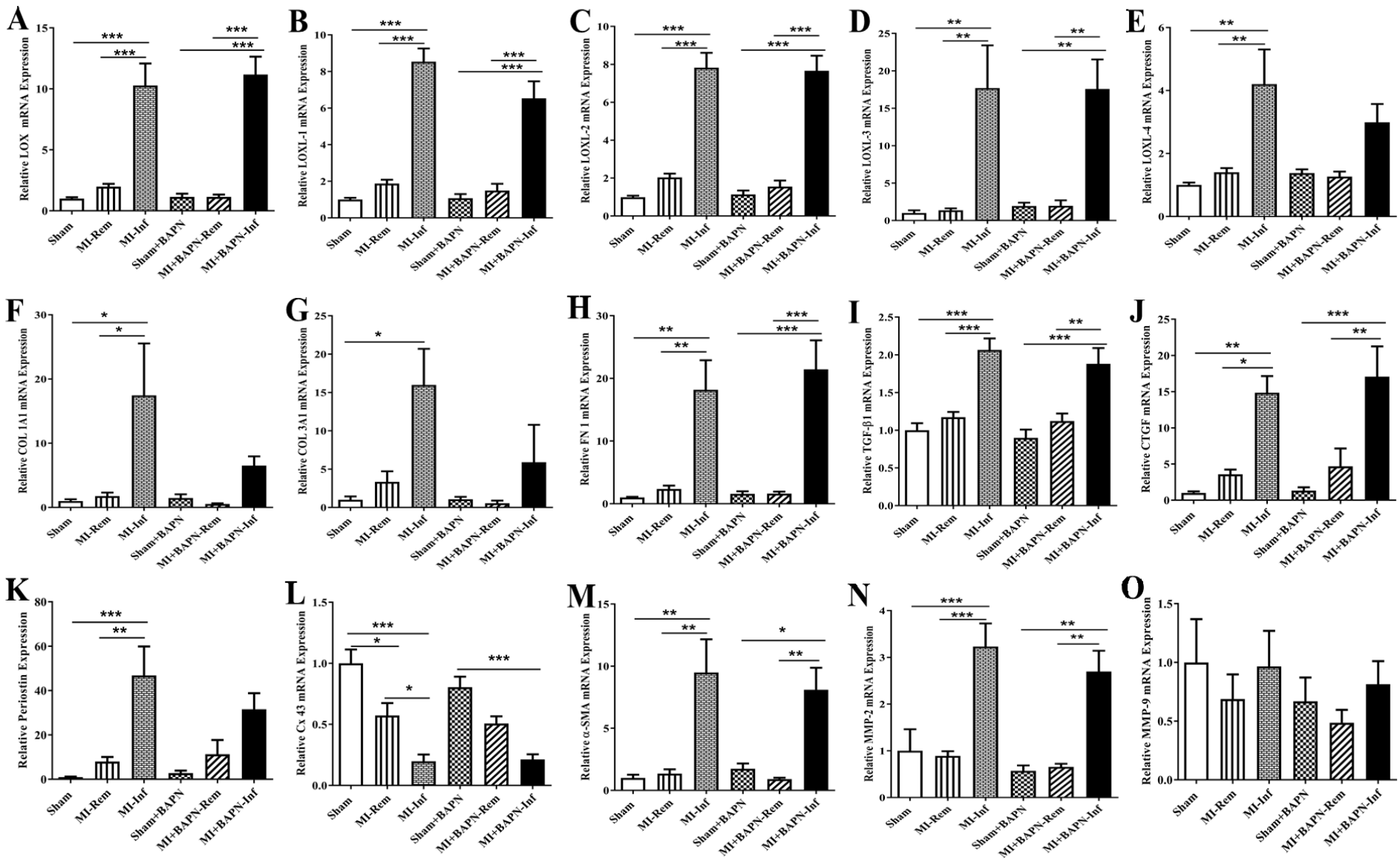
A
Relative LOX mRNA Expression
B
Relative LOXL-1 mRNA Expression
C
Relative LOXL-2 mRNA Expression
D
Relative LOXL-3 mRNA Expression
E
Relative LOXL-4 mRNA Expression
F
Relative COL 1A1 mRNA Expression
G
Relative COL 3A1 mRNA Expression
H
Relative FN 1 mRNA Expression
I
Relative TGF-β1 mRNA Expression
J
Relative CTGF mRNA Expression
K
Relative Periostin Expression
L
Relative Cx 43 mRNA Expression
M
Relative α-SMA mRNA Expression
N
Relative MMP-2 mRNA Expression
O
Relative MMP-9 mRNA Expression
Sham
MI-Rem
MI-Inf
Sham+BAPN
MI+BAPN-Rem
MI+BAPN-Inf

**Figure S6.**

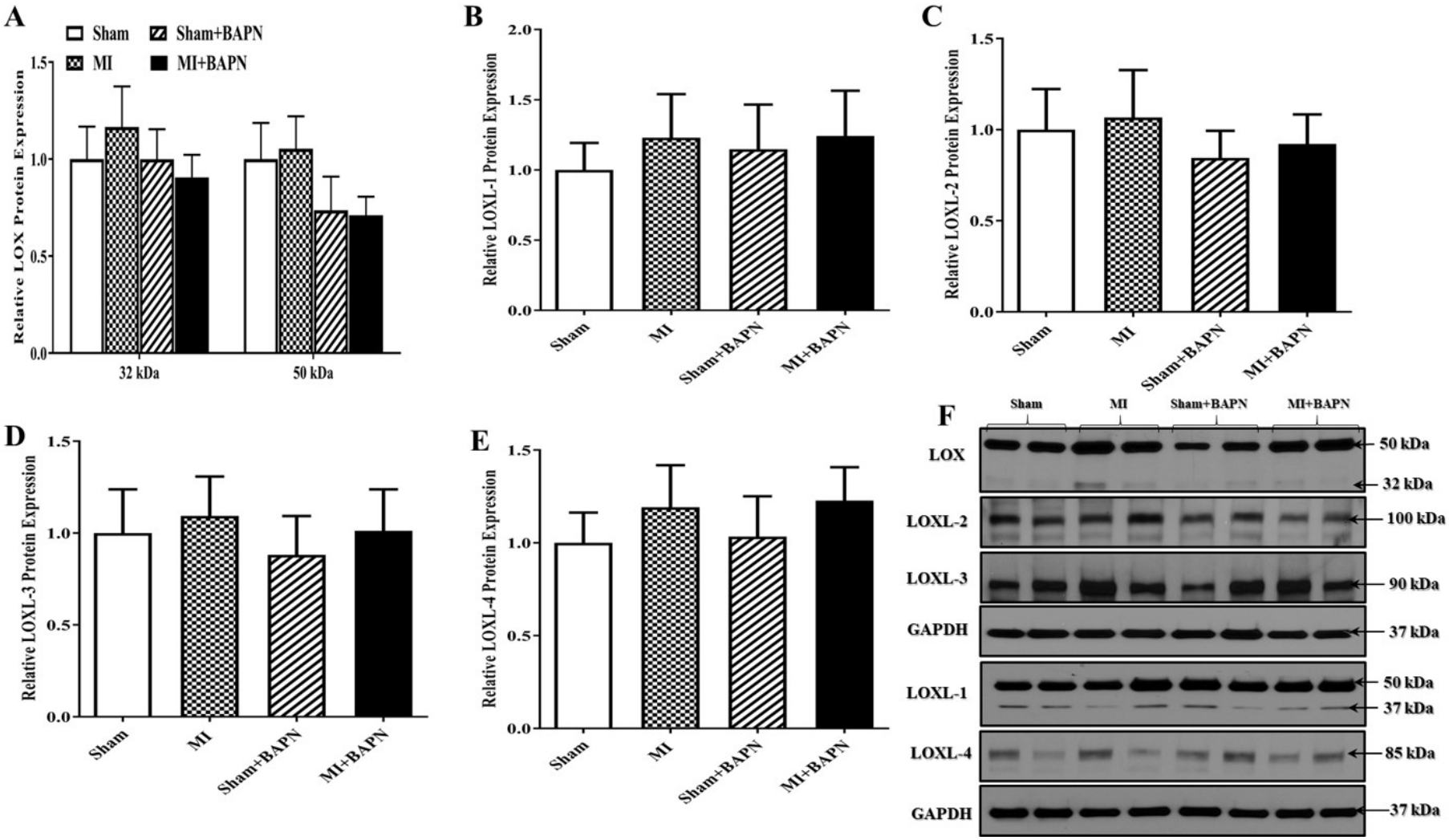
A
Sham
Sham+BAPN
MI
MI+BAPN
Relative LOX Protein Expression
1.5
1.0
0.5
0.0
32 kDa
50 kDa
B
Relative LOXL-1 Protein Expression
2.0
1.5
1.0
0.5
0.0
Sham
MI
Sham+BAPN
MI+BAPN
C
Relative LOXL-2 Protein Expression
1.5
1.0
0.5
0.0
Sham
MI
Sham+BAPN
MI+BAPN
D
Relative LOXL-3 Protein Expression
1.5
1.0
0.5
0.0
Sham
MI
Sham+BAPN
MI+BAPN
E
Relative LOXL-4 Protein Expression
1.5
1.0
0.5
0.0
Sham
MI
Sham+BAPN
MI+BAPN
F
Sham
MI
Sham+BAPN
MI+BAPN
LOX
50 kDa
32 kDa
LOXL-2
100 kDa
LOXL-3
90 kDa
GAPDH
37 kDa
LOXL-1
50 kDa
37 kDa
LOXL-4
85 kDa
GAPDH
37 kDa

**Figure S7.**

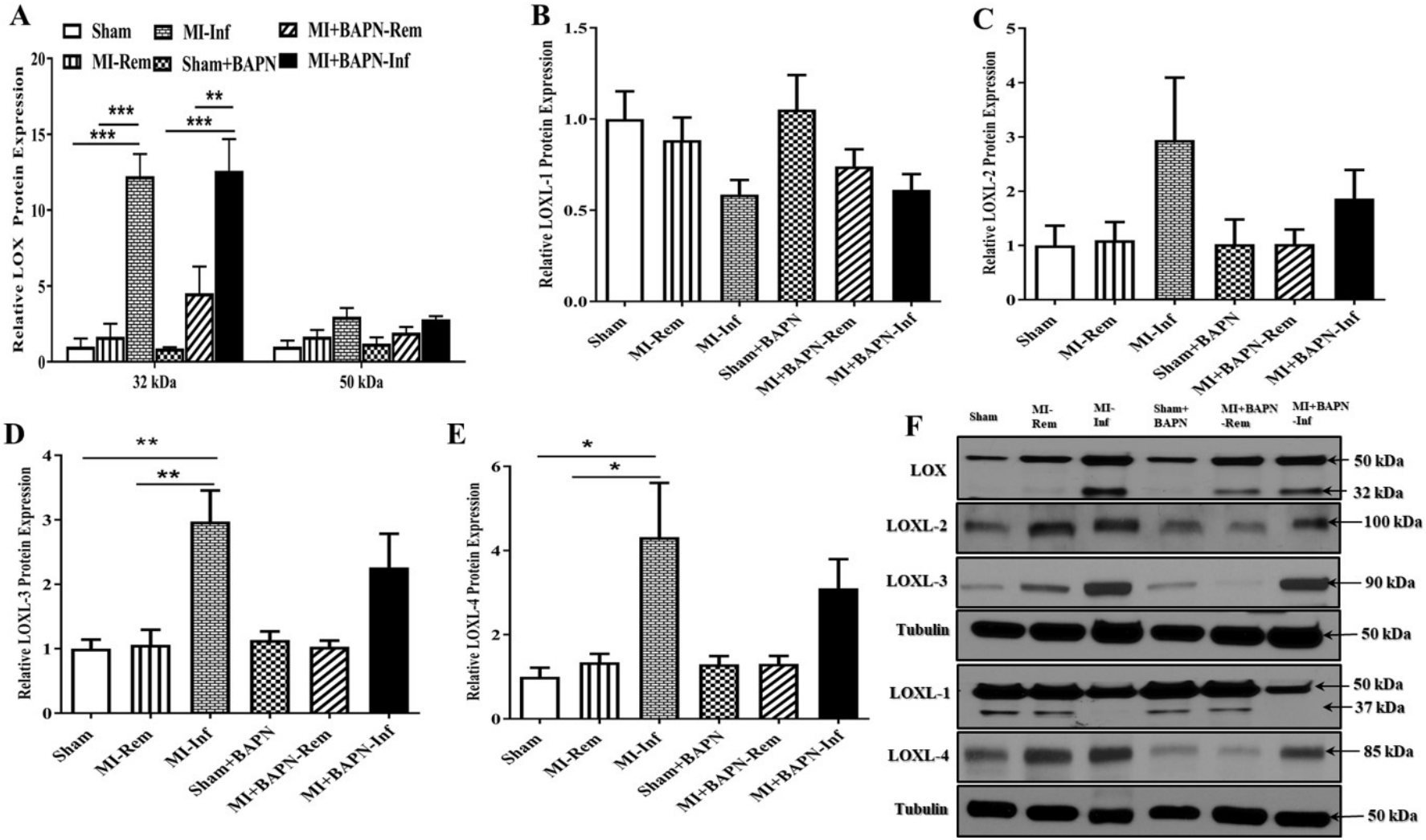
A
Sham
MI-Inf
MI+BAPN-Rem
MI-Rem
Sham+BAPN
MI+BAPN-Inf
Relative LOX Protein Expression
32 kDa
50 kDa
B
Relative LOXL-1 Protein Expression
C
Relative LOXL-2 Protein Expression
D
Relative LOXL-3 Protein Expression
E
Relative LOXL-4 Protein Expression
F
LOX
LOXL-2
LOXL-3
Tubulin
LOXL-1
LOXL-4
50 kDa
32 kDa
100 kDa
90 kDa
37 kDa
85 kDa

**Figure S8.**

# Chapter 3: Characterization of matrix-dependent and matrix-independent roles for lysyl oxidase (LOX) and LOX-like (LOXL) proteins in regulating cardiac fibroblast and myocyte functions

## Article 3

## Title: Characterization of matrix-dependent and matrix-independent roles for lysyl oxidase (LOX) and LOX-like proteins (LOXL) in regulating cardiac fibroblast and myocyte functions

This article is in preparation for submission to Cardiovascular Research.

## Contributions of authors

**Doa'a Ghazi Al-u'datt** conceived, designed and carried out all the experiments. Isolated cardiac myocytes and fibroblasts from dogs and neonatal rats, cultured cells and treated with angiotensin II (Ang II) and β-aminopropionitrile (BAPN), transfected cells with siRNA for LOX isoforms and LOX adenovirus, performed proliferation, collagen, cell shortening, $Ca^{2+}$ transient, qPCR and Western blot analysis, analyzed and interpreted the data, performed statistical analysis, generated figures and wrote the draft of manuscript.

**Jiening Xiao** constructed recombinant adenoviruses and helped in Western blot analysis.

**Patrice Naud** designed primers and helped in writing *in vitro* neonatal rat protocols and culturing canine cardiomyocytes.

**Bruce Allen** co-supervised the project, interpreted the biochemical analysis, participated in data analysis, provided intellectual input and edited the final draft of the manuscript.

**Stanley Nattel s**upervised the whole project, conceived, designed and provided intellectual ideas for the experiments, interpreted the data and edited the final draft of the manuscript.

# Characterization of matrix-dependent and matrix-independent roles for lysyl oxidase (LOX) and LOX-like proteins (LOXL) in regulating cardiac fibroblast and myocyte functions

**Doa'a Al-u'datt[1,2], Jiening Xiao[2], Patrice Naud[2] , Bruce Allen[1,2,3,4], and Stanley Nattel[1,2,3,5*]**

[1]Department of Pharmacology and Physiology, Université de Montréal, Montreal, Quebec, Canada

[2]Montreal Heart Institute and Université de Montréal, Montreal, Quebec, Canada

[3]Department of Medicine, Montreal Heart Institute, Montreal, Quebec, Canada

[4]Department of Biochemistry and Molecular Medicine, Université de Montréal, Montreal, Quebec, Canada

[5]Department of Pharmacology and Therapeutics, McGill University, Montreal, Quebec, Canada

**Running head: Role of LOX and LOXL proteins in cardiac cell functions**

*Address correspondence to: Stanley Nattel, Montreal Heart Institute, 5000 Belanger Street East, Montreal, Quebec, H1T 1C8, Canada. Tel.: 514-376-3330; Fax: 514-376-1355. E-mail: stanley.nattel@icm-mhi.org.

## Abstract

**Aims:** Lysyl oxidase (LOX) isoforms have numerous intra- and extra-cellular functions, including collagen and elastin cross-linking, motility and migration of fibroblasts, monocytes and smooth muscle cells, transcriptional regulation, apoptosis and proliferation. LOX secreted by cardiac fibroblasts has a vital role in the stability of the extracellular matrix (ECM) through elastin and collagen cross-linking. Excessive accumulation of cross-linked collagen leads to increase myocardial stiffness and fibrosis. This study was to investigate the matrix-dependent and matrix-independent roles of LOX and LOX-like (LOXL) proteins in regulating cardiac fibroblast and myocyte functions.

**Methods and results:** The expression of LOX and LOXL-2 in fibroblasts and LOX, LOXL-1, LOXL-3 and LOXL-4 in myocytes of left atria (LA) was upregulated in dogs with ventricular tachypacing (VTP)-induced congestive heart failure (CHF). Extracellular secretion of LOX and LOXL-2 from cultured neonatal rat ventricular fibroblasts and myocytes was increased upon stimulation with angiotensin II (Ang II) in a dose-dependent manner. Ang II induced collagen cross-linking in cultured neonatal rat ventricular fibroblasts. Upon knockdown of LOX isoforms by the siRNA approach in cultured neonatal rat ventricular fibroblasts and myocytes, LOXL-2, LOXL-3 and LOXL-4 had possible roles in fibroblast proliferation and collagen synthesis, while LOXL-4 might have a protective function against apoptosis through decreasing the ratio of BAX/BCL-2 mRNA expression in cardiac fibroblasts and myocytes. siRNA-mediated knockdown of LOX isoforms in cultured canine LA myocytes revealed that LOX and LOXL-1 impaired cardiomyocyte contractility with slight changes in $Ca^{2+}$ transients.

**Conclusions:** We conclude that LOX and LOXL proteins in cardiac fibroblasts and myocytes have novel roles through mediating matrix-dependent and matrix-independent cardiac functions. Upregulation of LOX isoforms in LA fibroblasts and myocytes of a CHF model may have further potential in elucidating their mechanisms in cardiac remodeling.

**Keywords** Heart failure (HF) • Lysyl oxidase (LOX) • LOX-like (LOXL) • Collagen cross-linking • Fibroblasts • Cardiomyocytes • $Ca^{2+}$ transient.

## 1. Introduction

Heart failure (HF) is a common disorder that is associated with a high mortality rate [1]. HF commonly occurs secondary to chronic hypertension or myocardial infarction (MI), which clinically presents with cardiac fibrosis [2]. Excessive production of extracellular matrix (ECM) proteins increases myocardial stiffness and changes the heart mechanics, which contribute to the pathophysiology of HF [3, 4]. Fibroblasts are critical for the maintenance of cardiac structural integrity, contributing to normal cardiac properties and playing a major role in remodeling during pathological conditions [5]. In early studies, fibroblasts were classified as the most predominant cell population in the heart, corresponding to 50 % and 27 % of the total cell number in the ventricles of rats and mice, respectively [6-8]. Recently, Pinto *et al.* [9] reported that fibroblasts are a less plentiful cell population in the mouse heart, corresponding to 10 % of the total cell number. Cardiac fibroblasts present as sheets and strands between the cardiomyocytes [10]. Myocardial stiffness has

several beneficial roles at early stages of collagen deposition, such as wound healing and prevention of myocardial infarct expansion before the development of cardiac fibrosis [11]. Cross-linking is initiated by enzymatic (lysyl oxidase; LOX) and non-enzymatic (glycated lysine) pathways [12]. The LOX family proteins, including LOX and LOX-like proteins (LOXL), are copper-dependent amine oxidases that have a vital function in the genesis of connective tissue matrices by catalyzing lysine-derived cross-links in elastin and collagen [12-15]. To date, five isoenzymes have been recognized, including LOX, LOXL-1, LOXL-2, LOXL-3 and LOXL-4 [16, 17]. It has been reported that increased LOX levels cause an excessive deposition and stiffness of collagen fibrils, leading to cardiac fibrosis [12]. Several studies reported that angiotensin II (Ang II) has a significant role in cardiac fibrosis [18]. Ang II stimulates TGF-β1 production, which mediates proliferation of fibroblasts and differentiation into myofibroblasts and collagen secretion [19]. Adam *et al.* [20] revealed that LOX expression and collagen abundance were increased in cardiac fibroblasts treated with Ang II. Roles of Ang II in the synthesis and secretion of LOXL proteins from cardiac fibroblasts and myocytes were not studied previously. LOX isoforms have been implicated in several biological processes, including control of epithelial-mesenchymal transition, cell migration, adhesion, transformation and gene regulation [21]. It is important to study further the intracellular roles of LOX isoforms in cardiac fibroblasts and myocytes. Narayan *et al.* [22] reported that HF patients showed $Ca^{2+}$ handling abnormalities along with a decline in cardiomyocyte contractility compared with controls. This study was to evaluate the physiological roles of LOX and LOXL proteins in cardiac cells (isolated fibroblasts and myocytes), both matrix-dependent (collagen cross-linking) and matrix-independent (apoptosis, proliferation, $Ca^{2+}$ signaling and cell contractility).

## 2. Methods

### 2.1 Animal Model

The Ethics Committee of the Animals Research at the Montreal Heart Institute approved the animal care and handling procedures according to the Animal Care guidelines of the Canadian Council (NIH Publication 65-23, revised 1996). Adult male mongrel dogs (20-30 kg) were divided into three groups: control, non-paced control and congestive heart failure (CHF) induced by two weeks of ventricular tachypacing (VTP, 240 bpm). Following sedation with 0.25 mg/kg of diazepam, 5.0 mg/kg of ketamine and 1.0-2.0 % halothane, pacemakers were implanted, and the hearts were paced at 240 bpm for two weeks to induce heart failure as previously described by Tadevosyan *et al.* [23]. At the end of the study, the dogs were anesthetized with α-chloralose (120 mg/kg intravenously) and morphine (2 mg/kg subcutaneously) under mechanical ventilation. After an intra-atrial heparin injection of 10,000 U, the hearts were removed and immersed in ice-cold Tyrode's solution (0.33 mmol/L $NaH_2PO_4.H_2O$, 5 mmol/L HEPES, 5.4 mmol/L KCl, 136 mmol/L NaCl, 10 mmol/L glucose and 1 mmol/L $MgCl_2.6H_2O$; pH 7.4) containing $Ca^{2+}$ (2 mmol/L $CaCl_2$) for left atrial (LA) myocyte and fibroblast isolation. Neonatal Wistar rats (2 to 3 days old) were obtained from Charles River (Wilmington, MA). Pups were decapitated, followed by heart removal. The hearts were washed with free Hank's balanced salt solution ($Ca^{2+}$ and $Mg^{2+}$ support) for myocyte and fibroblast isolation.

### 2.2 Cardiac fibroblast and myocyte isolation

Fibroblasts and myocytes were isolated from canine LA according to the method described by Tadevosyan *et al.* [23]. Canine atria were perfused with $Ca^{2+}$-free Tyrode's solution in aerated

oxygen (100 %; 37°C) via the left circumflex coronary artery for 10 min. The atria were digested by perfusion of $Ca^{2+}$-free Tyrode's solution containing bovine serum albumin (0.1 % BSA, Sigma) and 100 U/ml of collagenase type II (CLSII, Worthington) for 1 hr to isolate myocytes and fibroblasts. Digested LA tissues were minced into pieces with scissors in Kraftbruhe solution (20 mM taurine, 10 mM $KH_2PO_4$, 0.1 % albumin, 10 mM EGTA, 20 mM KCl, 40 mM mannitol, 70 mM L-glutamic acid, 10 mM glucose and 10 mM β-hydroxybutyric acid; pH 7.5), followed by filtration with 500 μm nylon mesh. The cells were centrifuged at 500 rpm for 5 min to pellet the myocytes. The supernatants were centrifuged in sequential order two times at 850 rpm for 5 min and 1750 rpm for 6 min to pellet the fibroblasts. Freshly isolated myocytes and fibroblasts were immersed in liquid nitrogen and immediately stored in a deep freezer at -80°C for mRNA and protein quantification. For contractility and $Ca^{2+}$ analysis, isolated myocytes were cultured immediately in PCELL-100 1X medium (Wisent, Inc., QC, Canada).

The ventricular myocytes and fibroblasts from neonatal rats were isolated according to the method described by Duong *et al.* [24]. Ventricles were isolated and minced after removal of the atria. The isolated ventricles were partially digested with trypsin (50 μg/ml) at 4°C for 16 hr, followed by the addition of soybean trypsin inhibitor (2 mg/ml). The partially digested ventricles were further digested with collagenase (1500 U in 5 ml of Leibovitz L-15 medium) at 37°C for 30 min with continuous agitation, followed by centrifugation for 5 min at 60 x g. Myocyte pellets were suspended in growth medium 199 (supplemented with 1 % penicillin/streptomycin (P/S), 10 % fetal bovine serum (FBS), 0.2 % insulin/transferrin/selenium (I/T/S)). The supernatants were further centrifuged for 5 min at 60 x g, followed by 300 x g for 5 min to pellet the fibroblasts. Myocytes were further purified from non-myocytes by using low (40 %) and high density (60 %) Percoll gradient (GE Healthcare, Life Science, Broendby, Denmark) according to the procedure

described by Golden *et al.* [25]. Isolated fibroblasts and myocytes were cultured for further studies. All chemicals and enzymes used for neonatal rat isolation were purchased from Worthington Biochemical (Lakewood, NJ, US).

### 2.3 Cell culture and treatments

Canine LA myocytes were cultured on laminin-coated 6-well plates in PCELL-100 1X (Wisent, Inc., QC, Canada; supplied with 1 % P/S, 5 % FBS and 1 % I/T/S) and then incubated at 37°C for 24 hr in a humidified atmosphere (5 % $CO_2$). Neonatal rat ventricular myocytes and fibroblasts were cultured in 6-well plates (Corning Inc., Corning, NY, US) with medium 199 (supplemented with 1 % P/S, 10 % FBS, 0.2 % I/T/S) and then incubated in a humidified atmosphere (5 % $CO_2$) at 37°C.

Cultured neonatal rat ventricular myocytes and fibroblasts were maintained in culture for 3 days and then rendered quiescent in medium without serum for 24 hr. Cells were treated with different concentrations of Ang II (0.1, 1.0 and 10.0 μM; Sigma-Aldrich, St. Louis, MO, US) or β-aminopropionitrile (BAPN; 0.1, 1.0, 10.0 and 100.0 μM; Santa Cruz Biotechnology, Dallas, TX, USA) for 24 hr for quantitative real-time polymerase chain reaction (qPCR) analysis, 48 hr for Western blot analysis and 72 hr for collagen assay.

### 2.4 Cell transfection

Canine LA myocytes, neonatal rat ventricular fibroblasts, and neonatal rat ventricular myocytes were transfected 2, 24, and 24 hr after plating, respectively. Cultured cells were transfected with 100 nM small interfering RNA (siRNA; Invitrogen, Carlsbad, CA, USA) or scrambled control (ScRNA; Invitrogen, Carlsbad, CA, USA) using lipofectamine RNAiMAX

(LifeTechnologies, Carlsbad, CA, US) in Opti-MEM medium (LifeTechnologies, Carlsbad, CA, US). Supernatants and cells from cultured neonatal rat ventricular fibroblasts and myocytes were collected at 24 and 48 hr after transfection for RNA and protein isolation, respectively. Cultured canine LA myocytes were collected 24 hr after transfection for measurement of cell shortening and $Ca^{2+}$ transients. Recombinant adenoviral vectors for LOX (Aden-LOX) and negative control green fluorescent protein (Aden-GFP) were prepared using the AdEasy system as described by He *et al.* [26] and Luo *et al.* [27]. Canine LA myocytes were infected with Aden-LOX or Aden-GFP at the indicated multiplicity of infection for 24 hr. Supplementary Table S1 demonstrates the sequences of siRNA for LOX, LOXL-1, LOXL-2, LOXL-3 and LOXL-4 used in this study.

**2.5 Colorimetric cell proliferation assay**

Cell proliferation was measured using a colorimetric Cell Counting Kit-8 (water soluble tetrazolium salt (WST-8), Dojindo, Japan) according to the method previously described by Li *et al.* [28]. Dehydrogenases in viable cells reduced WST-8 and produced formazan dye (orange color). Neonatal rat ventricular fibroblasts were plated in 96-well plates at a density of 2000 cells/100 µl in each well with complete medium (M199 with 10 % FBS). After 24 hr, the media was replaced with serum-free media (M199 with 0 % FBS). Twenty-four hours later, the cells were transfected with scrambled control, siLOX, siLOXL-1, siLOXL-2, siLOXL-3 and siLOXL-4. Ten microliters of WST-8 solutions added to each well of the 96-well plate after 24 hr, followed by incubation for an additional 2 hr at 37°C. The number of viable cells was determined by monitoring the absorbance at 450 nm using a microplate reader. The absorbance represented the amount of liberated formazan dye, which is proportional to the number of viable cells.

### 2.6 Protein quantification by immunoblotting

Protein quantification was carried out by Western blot analysis according to the protocol described by Surinkaew *et al.* [29]. Cultured cardiac fibroblasts and myocytes were collected in a cold lysis buffer (5 M NaCl, 1 M Tris HCl (pH 7.5), 20 % sodium dodecyl sulfate (SDS), 10 % Triton, 100 % glycerol, 0.5 M phenylmethanesulfonyl fluoride (PMSF), protease and phosphatase inhibitor cocktail). Lysed samples and media of cultured fibroblasts and myocytes were mixed with loading buffer (0.5 M Tris HCl (pH 6.8), 20 % SDS, 100 % glycerol, dithiothreitol (DTT) and 0.3 % bromophenol blue) and then incubated at 95°C for 5 min. Protein samples were separated by SDS-polyacrylamide gel electrophoresis (SDS-PAGE; gradient gel 4-20 %) and then transferred onto polyvinylidene difluoride membranes (PVDF; EMD Millipore, Billerica, MA, US) for 80 min at 90 volts. The membranes were immersed in blocking solution (0.1 ml of Tween 20 and 5.0 g of non-fat dry milk (NFDM) in 100 ml of Tris-buffered saline (TBS)) for 1.5 hr and then incubated with primary antibodies with continuous mixing at 4°C for 16 hr. The membranes were washed with 0.1 % Tween 20 in TBS (v/v; 3 X 15 min) and then incubated with secondary antibodies with continuous mixing at 24°C for 1 hr. Immunoreactive protein bands were visualized with Western Lightning Plus ECL reagent (PerkinElmer, Waltham, MA, US) and Kodak film. Protein expression was calculated using ImageJ software and normalized to glyceraldehyde 3-phosphate dehydrogenase (GAPDH) density from the same samples and membranes. The blots were probed with antibodies of anti-LOX (1:5000, ab174316, Abcam), anti-LOXL-1 (1:2000, PA5-44213, Thermo Fisher), anti-LOXL-2 (1:2000, ab96233; Abcam), anti-LOXL-3 (1:2000, PA5-45074, Thermo Fisher), anti-LOXL-4 (1:1000, ab88186, Abcam) and anti-GAPDH (1:10,000, 10R-G109A, Fitzgerald). Horseradish peroxidase (HRP)-conjugated secondary antibodies were used in 1:10,000 dilution

(goat anti-rabbit, donkey anti-rabbit and donkey anti-mouse; Jackson ImmunoResearch Laboratories, West Grove, PA, US).

### 2.7 Determination of mRNA by qPCR

Determination of mRNA was carried out according to the method described by Duong *et al.* [24]. Cultured cardiac fibroblasts and myocytes were suspended in Trizol reagent (Invitrogen, Carlsbad, CA, US). RNA was extracted with the miRNeasy Mini Kit (Qiagen, MD, Germany). RNA quantification and qualification were estimated using a Nanodrop spectrophotometer. cDNA was synthesized from 250 ng of total RNA with the High Capacity cDNA Reverse Transcription Kit (SuperArray, Applied Biosystems, Foster City, CA, US). qPCR was performed with SuperArray SYBR Green PCR kits (Applied Biosystems, Foster City, CA, US), TaqMan Universal Master Mix (Applied Biosystems, Foster City, CA, US), custom-made SYBR Green primers (glucose 6-phosphate dehydrogenase (G6PD), α-smooth muscle actin (α-SMA), B-cell lymphoma 2 (BCL-2), BCL-2-associated X protein (BAX), cyclin D1 (CCND 1), cyclin E2 (CCNE 2), matrix metalloproteinase 2 (MMP-2), MMP-9, periostin, transforming growth factor β (TGF-β1), connective tissue growth factor (CTGF), LOX, LOXL-1, LOXL-2, LOXL-3 and LOXL-4; Applied Biosystems, Foster City, CA, US; Supplementary Table S2), TaqMan probes (LOX (Assay ID: Rn01491829_m1), GAPDH (Assay ID: Rn01775763_g1), collagen 1A1 (Col 1A1; Assay ID: Rn01463848_m1), collagen 3A1 (Col 3A1; Assay ID: Rn01437681_m1) and fibronectin 1 (FN 1; Assay ID: Rn00569575_m1); Applied Biosystems, Foster City, CA) and SYBR primer (LOXL-4 (Assay ID: qRnoCID0018064; Bio-Rad, California, US). The relative quantifications for all samples were calculated with the

comparative threshold cycle ($2^{-\Delta\Delta Ct}$) method [30]. GAPDH and G6PD were used as internal standards for rats and dogs, respectively.

### 2.8 Soluble and insoluble collagen analysis

Cultured fibroblasts treated with BAPN or Ang II were subjected to soluble and insoluble collagen determination according to the colorimetric method that was described by Chang *et al.* [31] using a total collagen assay kit (QuickZyme BioSciences, Leiden, Netherlands). The hydroxyproline contents in supernatants and cells were used to measure soluble and insoluble collagen, respectively. The supernatants and cells were hydrolyzed in 6.0 M HCl by heating at 95°C/21 hr. The hydroxyproline content in the hydrolyzed supernatants and cells was measured using the QuickZyme assay kit. Thirty-five microliters from each hydrolyzed sample was mixed with QuickZyme reagents in 96-well plates according to the manufacturer protocol. The absorbance of each sample was measured at 570 nm using a microplate reader. The soluble and insoluble collagen content of each sample was expressed as μg/well (6-well plate, cell density 500,000 cells/well for Ang II treatments and 300,000 cells/well for BAPN treatments) according to the standard curve of hydroxyproline content in collagen stock solution (QuickZyme assay kit). The degree of collagen cross-linking was calculated as the ratio of insoluble to total collagen.

### 2.9 Measurement of $Ca^{2+}$ fluorescence and cell shortening

Canine LA myocytes were cultured with PCELL-100 1X (Wisent, Inc., QC, Canada) on borosilicate glass coverslips and then incubated with 5 μM Indo-1 AM (Invitrogen, Carlsbad, CA, USA) for 15 min, followed by intracellular de-esterification while superfused with medium 199

(without phenol red) at 37°C along with stimulation (1 Hz, 40 V) for 15 min. Ultraviolet light (340 nm) was used to excite the Indo-1, and the ratio of fluorescence emissions ($R_{400/500}$) was calculated after subtraction of background as an indicator of intracellular $Ca^{2+}$ concentration. Cell shortening was monitored from field-stimulated cardiomyocytes with a video edge detector attached to a charge-coupled device camera as previously described by Yeh *et al.* [32]. Cell shortening was measured from an average of 10 consecutive contractions.

### 2.10 Statistical analysis

The results are presented as the means ± standard error mean (SEM). Statistical analysis was performed using GraphPad Prism 7 for Windows (GraphPad Software, La Jolla, CA). Unpaired Student's *t*-tests were performed to compare two groups. One-way analysis of variance (ANOVA) followed by the Bonferroni's multiple comparisons test was performed between more than two groups; $*P < 0.05$; $**P < 0.01$; $***P < 0.001$.

## 3. Results

### 3.1 Increased LOX and LOXL protein expression in LA fibroblasts and myocytes of CHF dogs

Numerous changes occur in CHF, including upregulation of atrial interstitial fibrosis and development of progressive AF [33]. We analyzed the mRNA and protein levels of LOX isoforms (LOX, LOXL-1, 2, 3 and 4) in LA fibroblasts and myocytes of control and CHF dogs. The mRNA and protein levels of LOX isoforms increased to different degrees in LA myocytes and fibroblasts

of CHF dogs compared with controls. The protein and mRNA expression levels of LOX and LOXL-1, 3 and 4 were significantly upregulated in the LA myocytes of CHF dogs ($P < 0.001$ and $P < 0.001$, $P = 0.02$ and $P < 0.001$, $P = 0.02$ and $P < 0.001$, and $P = 0.007$ and $P = 0.002$, respectively) compared with controls (Figure 1F-G, I-J and L and Figure 2F-G and I-J). However, the protein and mRNA expression levels of LOX and LOXL-2 were significantly increased in the LA fibroblasts of CHF dogs ($P = 0.03$ and $P = 0.01$, $P = 0.03$ and $P < 0.001$, respectively) compared with controls (Figure 1A, C and K and Figure 2A and C). The mRNA of LOXL-2 in LA myocytes and LOXL-4 in LA fibroblasts was significantly increased in CHF dogs compared with controls ($P < 0.001$ and $P = 0.02$, respectively; Figure 2H and E), whereas their immunoreactivity was unaffected. The upregulation of all LOX isoforms in LA myocytes and LOX, LOXL-2 and LOXL-4 in LA fibroblasts of the CHF model suggested that these isoforms may have significant roles in cardiac myocyte and fibroblast function during CHF progression.

### 3.2 Ang II increased LOX and LOXL-2 secretion from neonatal rat ventricular fibroblasts and myocytes

The effect of treatment with different concentrations of Ang II (0.1, 1.0 and 10.0 μM) in cultured cardiac fibroblasts and myocytes on the intra- and extra-cellular protein and mRNA expression of LOX isoforms was determined by Western blot and qPCR. Conditioned culture media was reserved to assess extracellular LOX isoform immunoreactivity. Ang II failed to produce any significant changes in the abundance of LOX isoform mRNA in either fibroblasts or myocytes (Supplementary Figures S1A-E and 2A-E). Regarding the intracellular protein levels in cultured cardiac fibroblasts and myocytes, LOX, LOXL-2, LOXL-3 and LOXL-4 did not change significantly upon treatment with Ang II (Supplementary Figure S1F and H-K and Supplementary

Figure S2F and H-K). However, intracellular LOXL-1 immunoreactivity was significantly increased upon treatment of cardiomyocytes with 1.0 or 10.0 μM Ang II (1.21±0.03 and 1.24±0.04-fold change, respectively) compared with controls (0.0 μM Ang II; 1.0±0.05-fold change; Supplementary Figure S2G and K). Furthermore, LOX and LOXL-2 proteins were secreted from cultured cardiac fibroblasts and myocytes, while LOXL1, LOXL-3 and LOXL-4, were not detected in the conditioned media from either fibroblasts or myocytes. Extracellular LOX immunoreactivity was increased in cultured fibroblasts (1.47±0.16-fold change; Figure 3A and C) whereas that of LOXL-2 increased in media from cardiomyocytes (1.42±0.11-fold change; Figure 3F and H) upon treatment with 10.0 μM Ang II compared with controls (0.0 μM Ang II; 1.00±0.06 and 1.00±0.06-fold change, respectively).

### 3.3 Ang II stimulated collagen cross-linking and BAPN attenuated collagen cross-linking in neonatal rat ventricular fibroblasts

There were non-significant changes in soluble and insoluble collagen upon treatment of cultured fibroblasts with Ang II (Figure 4A-B). The collagen cross-linking ratio was significantly increased upon treatment of cultured fibroblasts with 10.0 μM Ang II (0.30±0.04; Figure 4C) compared with controls (0.0 μM Ang II; 0.19.0±0.02). Our data revealed that Ang II increased the collagen cross-linking ratio in cultured cardiac fibroblasts by increasing the amount of insoluble collagen and decreasing the soluble collagen content. Treatment of cultured fibroblasts with 100.0 μM BAPN increased the amount of soluble collagen (45.28±7.69 μg/well) and decreased the cross-linking ratio (0.12±0.03) compared the controls (0.0 μM BAPN; 21.82±1.92 μg/well and 0.32±0.03, respectively; Figure 4D and F). However, the content of insoluble collagen was not significantly decreased upon treatment of fibroblasts with BAPN (Figure 4E). Furthermore, there

were no significant changes in the mRNA abundance for any of the LOX isoforms upon treatment with BAPN in cultured cardiac fibroblasts (Supplementary Figure S3A-E). These results showed that BAPN decreased the collagen cross-linking ratio in cultured cardiac fibroblasts by increasing soluble collagen and decreasing insoluble collagen.

### 3.4 LOX and LOXL immunoreactivity was reduced by specific siRNA approaches in neonatal rat ventricular fibroblasts and myocytes

The expression of individual LOX isoforms in cultured cardiac fibroblasts and myocytes were efficiently suppressed using siRNA (Figure 5 and Supplementary Figure S4). Multiple specific siRNAs were used in combination to achieve a suitable knockdown efficiency. The knockdown of LOXL-1 resulted in the decrease both LOX and LOXL-1 mRNAs in cardiac fibroblasts (Figure 5A-B) and myocytes (Supplementary Figure S4A-B). In response to the knockdown of LOXL-2, the mRNA of both LOXL-2 and LOXL-3 was reduced in cardiac fibroblasts (Figure 5C-D) and myocytes (Supplementary Figure S4C-D), while knockdown of LOXL-3 yielded a significant reduction in the mRNA of LOXL-2, LOXL-3 and LOXL-4 in cardiac fibroblasts (Figure 5C-E) and myocytes (Supplementary Figure S4C-E). The secretion of LOX or LOXL-2 immunoreactivity by fibroblasts and myocytes decreased after knockdown of LOX or LOXL-2, respectively (Figure 5F and Supplementary Figure S4F). The siRNA pools of LOX and LOXL-4 were specific in cultured cardiac fibroblasts and myocytes. However, siRNA pools for LOXL-1, LOXL-2 and LOXL-3 were not specific in cultured cardiac fibroblasts and myocytes.

### 3.5 Knockdown of individual LOX isoforms altered the expression of profibrotic markers in neonatal rat ventricular fibroblasts

Knockdown of LOXL-3 in cultured fibroblasts significantly decreased COL 1A1 mRNA (0.58±0.05-fold change; Figure 6A) compared with ScRNA (1.00±0.10-fold change; Figure 6A), while the COL 1A1 mRNA did not significantly change upon knockdown of other isoforms (Figure 6A). CTGF mRNA was significantly decreased upon knockdown of LOX (0.44±0.10-fold change; Figure 6E) or LOXL-4 (0.26±0.05-fold change; Figure 6E) in cultured cardiac fibroblasts compared with ScRNA (1.00±0.16-fold change; Figure 6E). α-SMA mRNA increased upon knockdown of LOXL-2 (1.45±0.14-fold change; Figure 6G) in cultured cardiac fibroblasts compared with ScRNA (1.00±0.04-fold change; Figure 6G). The abundance of COL 3A1, FN 1, TGF-β1, periostin, MMP-2 and MMP-9 transcripts was not significantly altered upon knockdown of any of the LOX isoforms in cultured cardiac fibroblasts (Figure 6B-D, F and H-I). These results revealed that knockdown of LOXL-3 decreased the collagen synthesis, whereas knockdown of LOX or LOXL-4 reduced the abundance of CTGF mRNA. However, knockdown of LOXL-2 increased α-SMA mRNA.

### 3.6 Knockdown of individual LOX isoforms altered proliferation and the expression of proliferation and apoptotic markers in neonatal rat ventricular cells

Fibroblast proliferation was significantly decreased upon knockdown of LOXL-2, LOXL-3 or LOXL-4 (0.69±0.04, 0.73±0.06 or 0.59±0.05-fold change, respectively; Figure 7A) compared with ScRNA (1.00±0.08-fold change; Figure 7A). The abundance of CCNE 2 mRNA was decreased upon knockdown of LOXL-2 (0.35±0.06-fold change; Figure 7B) or LOXL-3 (0.55±0.07-fold change; Figure 7B) in cultured neonatal rat fibroblasts compared with ScRNA

(1.00±0.19-fold change; Figure 7B). CCND 1 mRNA was not significantly different upon knockdown of individual LOX isoforms in cultured cardiac fibroblasts (Figure 7C). Our data revealed that LOXL-2, LOXL-3 and LOXL-4 have a role in regulating fibroblast proliferation. BAX mRNA was less abundant upon knockdown of LOXL-3 (0.50±0.02-fold change; Figure 7D) in cultured cardiac fibroblasts compared with ScRNA (1.00±0.07-fold change Figure 7D), while BCL-2 mRNA was significantly decreased upon knockdown of LOXL-1 (0.62±0.09-fold change; Figure 7E) or LOXL-4 (0.40±0.06-fold change; Figure 7E) compared with ScRNA (1.00±0.07-fold change; Figure 7E). BAX mRNA was not affected by knockdown of individual LOX isoforms in cultured cardiac myocytes (Figure 8A). However, the BCL-2 mRNA was decreased upon knockdown of LOXL-4 (0.58±0.09-fold change; Figure 8B) in cultured cardiac myocytes compared with ScRNA (1.00±0.10-fold change; Figure 8B). The BAX/BCL-2 mRNA ratio was significantly increased upon knockdown of LOXL-4 in both fibroblasts and myocytes (2.26±0.21 and 2.60±0.48-fold change, respectively; Figure 7F and Figure 8C) compared with ScRNA (1.00±0.07 and 1.00±0.16-fold change, respectively; Figure 7F and Figure 8C).

### 3.7 Knockdown or overexpression of individual LOX isoforms altered cell shortening with little change in $Ca^{2+}$ transients in canine LA myocytes

The knockdown of individual LOX isoforms and overexpression of LOX in canine LA myocytes were specific and efficient (Supplementary Figure S5 and Figure S6). Cell shortening was significantly increased upon knockdown of LOXL-1 (siRNA: 6.2±0.9 %, ScRNA: 3.8±0.4 %, $P = 0.02$, Figure 9A), while cell shortening was not significantly increased upon knockdown of LOX ($P = 0.06$; 5.8±0.5 %; Figure 9A). However, knockdown of LOXL-2, LOXL-3 or LOXL-4 had no effect on cardiomyocyte shortening. Analysis of $Ca^{2+}$ transients revealed non-significant

increases in the diastolic baseline, amplitude and decay time constant upon knockdown of LOX or LOXL-1 (Figure 9B-D). Our results indicated that LOX and LOXL-1 had a role in the modulation of cardiomyocyte contractility with little effect on $Ca^{2+}$ transients. Cell shortening was significantly decreased upon overexpression of LOX by adenovirus ($P$ = 0.007; 4.0±0.7 %; Supplementary Figure S7A) in cultured canine LA myocytes compared with Aden-GFP (7.1±0.8 %; Supplementary Figure S7A). Whereas diastolic $Ca^{2+}$ level, $Ca^{2+}$ amplitude, and decay time constant were unaffected (Supplementary Figure S7B-D).

## 4. Discussion

Many studies showed that the LOX secreted from fibroblast has a vital role in cardiac fibrosis through collagen cross-linking and excessive deposition of collagen. However, no information is currently available on the roles of other LOX isoforms (LOXL-1, LOXL-2, LOXL-3 and LOXL-4) in cardiac cell function. In the current study, the main findings were the following: (a) upregulation of LOX, LOXL-1, LOXL-3 and LOXL-4 in LA myocytes and LOX and LOXL-2 in LA fibroblasts isolated from a canine model of CHF, (b) secretion of LOX and LOXL-2 proteins from cardiac myocytes and fibroblasts, (c) Ang II induced a dose-dependent increase in LOX and LOXL-2 secretion from cardiac myocytes and fibroblasts, (d) Ang II increased collagen cross-linking ratio in cultured cardiac fibroblasts by increasing insoluble collagen and decreasing soluble collagen, (e) LOXL-2, LOXL-3 and LOXL-4 had distinct effects on fibroblast proliferation and collagen synthesis relative to the other LOX isoforms, (f) LOXL-4 might have an anti-apoptotic effect through decreasing the ratio of BAX/BCL-2 mRNA in cardiac fibroblasts and myocytes and (g) LOX and LOXL-1 impaired cardiac myocyte contractility with little change in $Ca^{2+}$ transients.

At the protein level, LOX, LOXL-1, LOXL-3 and LOXL-4 were significantly upregulated in LA myocytes of CHF dogs, whereas LOX and LOXL-2 were significantly upregulated in LA fibroblasts isolated from CHF dogs. There is currently no literature on the regulation of LOX isoforms in atrial myocytes and fibroblasts isolated from models of HF. The results of this study provide new insight into the role of LOX isoforms in LA myocytes and fibroblasts in the atrial fibrotic pathway during CHF progression. LOX isoforms have numerous intra- (matrix-independent) and extra-cellular (matrix-dependent) functions, including elastin and collagen cross-linking [21, 34]. Cardiac fibroblasts have a critical function in the genesis and remodeling of the ECM [34-36]. Collagens, type I and III, are the major cardiac structural ECM proteins [37]. LOX is secreted from cardiac fibroblasts [38] and has a role in cross-linking collagen, which is essential for increasing the stability and strength of collagen fibers [34]. Upregulation of LOX leads to excessive accumulation of cross-linked collagen, which increases myocardial stiffness and fibrosis [12]. Communication between cardiac fibroblasts and myocytes under normal conditions is important for maintaining heart function [39]. Takeda and Manabe [40] reported that cardiomyocytes affect fibroblast function, such as differentiation, proliferation and secretion of ECM proteins, leading to interstitial fibrosis through secretion of TGF-β, Ang II and other profibrotic molecules [40, 41]. Adam *et al.* [42] found that Ang II increases LOX immunoreactivity in cardiac fibroblasts. Our study showed that LOX isoforms were upregulated in LA myocytes and fibroblasts from CHF dogs. This is the first study to report the synthesis of LOX isoforms and the secretion of active LOX and LOXL-2 from cardiomyocytes and LOXL-2 from cardiac fibroblasts. Our results suggest LOX and LOXL-2 secreted from cardiomyocytes may act synergistically with LOX and LOXL-2 from fibroblasts in cardiac fibrosis. However, LOXL-1, LOXL-3 and LOXL-4 were not detected in conditioned media from cardiac fibroblasts and myocytes. The results indicated that Ang II

stimulated the secretion of LOX and LOXL-2 from cardiac fibroblasts and myocytes with little change in their intracellular levels. LOX and LOXL-2 in cardiac myocytes and fibroblasts may be downstream targets of Ang II in mediating cardiac fibrosis. We noted that the intracellular protein expression of LOXL-1 was increased in cultured cardiomyocytes upon stimulation with Ang II. Our results are consistent with the finding of Ohmura *et al.* [43], who reported the upregulation of LOXL-1 expression in cultured cardiomyocytes treated with hypertrophic agonists, such as Ang II. This result indicated that LOXL-1 may have an intracellular function in cardiac myocytes.

To date, no studies have addressed the intracellular (matrix-independent) roles of individual LOX isoforms in cardiac fibroblasts and myocytes. We used individual siRNA for LOX isoforms to investigate the involvement of each LOX isoform in apoptosis and proliferation of fibroblasts as well as the synthesis of profibrotic markers. Our results revealed that knockdown of LOX or LOXL-4 in cardiac fibroblasts and myocytes was specific, whereas the knockdown of LOXL-1, LOXL-2 or LOXL-3 was not. Mizikova *et al.* [44] reported that knockdown of individual LOX, LOXL-1 or LOXL-2 in cultured mouse lung fibroblasts had an impact on the expression of each other through compensatory or direct effects. However, Aumiller *et al.* [45] found that knockdown of individual LOX isoforms in cultured human lung fibroblasts was efficient and selective.

Upregulation of LOX family members is associated with an imbalance in degradation and synthesis of ECM proteins, leading to cardiac fibrosis [46, 47]. Upon knockdown of LOXL-3, the abundance of LOXL-2, LOXL-3 and LOXL-4 mRNA was decreased. Knocking down LOXL-3 in cardiac fibroblasts also reduced the abundance of COL 1A1 and COL 3A1 transcripts. These findings suggested a synergistic effect of LOXL-2, LOXL-3 and LOXL-4 in promoting collagen synthesis from cardiac fibroblasts. Our results demonstrated that knockdown of LOX or LOXL-4

decreased CTGF mRNA in cardiac fibroblasts. CTGF is an important mediator of ECM protein synthesis during the progression of fibrosis, including collagen type I [48, 49]. Adam *et al.* [42] showed that treatment of cultured cardiac fibroblasts with CTGF increased LOX protein expression and the knockdown of CTGF attenuated the Ang II-induced increase in LOX immunoreactivity. Upregulation of α-SMA expression is a hallmark of the differentiation of fibroblasts into myofibroblasts [36]. In the current study, we found that the abundance of LOXL-2 and LOXL-3 mRNA was decreased upon knockdown of LOXL-2 in cardiac fibroblasts along with an increase in α-SMA mRNA. These results suggested that a harmonic effect of LOXL-2 and LOXL-3 suppression may increase the differentiation of fibroblasts into myofibroblasts.

There is currently no literature available on the intracellular roles of LOX isoforms in regulating normal cardiac cell function. Apart from the extracellular role of LOX isoforms in the cross-linking of ECM proteins, several studies have reported the intracellular roles of LOX isoforms in other organs, such as apoptosis, proliferation as well as the regulation of the transcription of ECM proteins [28, 50-53]. Cyclin-dependent kinases, such as CCNE 2 and CCND 1, are essential for controlling the cell cycle and proliferation [54]. Our findings demonstrated that intracellular LOXL-2, LOXL-3 and LOXL-4 have a unique role in promoting cardiac fibroblast proliferation. This finding is important due to the greater structural similarity between LOXL-2, LOXL-3 and LOXL-4 compared with LOX and LOXL-1. LOX and LOXL-1 are more similar in chemical structure, and they have distinctive pro-peptide areas, while LOXL-2, LOXL-3 and LOXL-4 are more similar in chemical structure and contain four conserved scavenger receptor cysteine rich (SRCR) domains in their N-terminal [55]. The present study suggests that LOXL-4 may have a protective effect against apoptosis in cardiac fibroblasts and myocytes. LOX has a role in promoting apoptosis via compromising the AKT signaling pathway in breast and lung cancer cells

[56-58]. A recent study noted that knockdown of LOX or inhibition of LOX by BAPN leads to decreased BAX expression, thus protecting against apoptosis in diabetic retinopathy [52]. Raisova *et al.* [59] stated that an increase in the BAX/BCL-2 expression ratio is an indicator of cellular susceptibility to apoptosis.

This study demonstrated an increase in LOX isoform expression in LA myocytes in a canine model of CHF. Previous studies revealed a progressive decrease in cardiac function along with intracellular $Ca^{2+}$ abnormalities in CHF models [32, 60]. Our data revealed that knockdown of LOX and LOXL-1 in canine LA myocytes improved contractility, while overexpression of LOX decreased cardiomyocyte contractility. While having little effect on $Ca^{2+}$ transients. The decline in cardiomyocyte contractility in CHF can be due to several mechanisms, including alterations in myofilament function, the cytoskeleton and $Ca^{2+}$ handling [61]. de Tombe [61] reported that the contractile dysfunction during CHF is due to the decline in force generation by the contractile proteins at any level of intracellular $Ca^{2+}$. Our findings provide the first evidence that LOX and LOXL-1 may participate in cardiomyocyte contractile dysfunction.

## 5. Conclusions

Our study demonstrated that the expression of LOX isoforms in LA myocytes and fibroblasts were increased in a CHF dog model. LOX and LOXL-2 were secreted from cultured neonatal rat ventricular myocytes and fibroblasts. Ang II stimulated the secretion of LOX and LOXL-2 from cultured neonatal rat ventricular fibroblasts and myocytes along with an increase in collagen cross-linking in cultured neonatal rat ventricular fibroblasts. Furthermore, LOXL-4 might have an anti-apoptotic effect by decreasing the ratio of BAX/BCL-2 mRNA in cardiac fibroblasts and myocytes. LOXL-2, LOXL-3 and LOXL-4 appear to be involved in cardiac fibroblast proliferation

and collagen synthesis, whereas LOX and LOXL-1 altered cardiac myocyte contractility. Hence, in cardiac fibroblasts and myocytes, intracellular LOXL-2, LOXL-3 and LOXL-4 and extracellular LOX and LOXL-2 may have roles in the fibrotic response.

## References


1. Bui AL, Horwich TB, Fonarow GC. Epidemiology and risk profile of heart failure. *Nat Rev Cardiol* 2011;**8**:30-41.

2. Roche PL, Czubryt MP. Current and future strategies for the diagnosis and treatment of cardiac fibrosis. In: Dixon IMC, Wigle JT, eds. Cardiac fibrosis and heart failure: Cause or effect? Cham: Springer International Publishing, 2015:181-217.

3. Edgley AJ, Krum H, Kelly DJ. Targeting fibrosis for the treatment of heart failure: a role for transforming growth factor-beta. *Cardiovasc Ther* 2012;**30**:e30-40.

4. Creemers EE, Pinto YM. Molecular mechanisms that control interstitial fibrosis in the pressure-overloaded heart. *Cardiovasc Res* 2011;**89**:265-272.

5. Baudino TA, Carver W, Giles W, Borg TK. Cardiac fibroblasts: Friend or foe? *Am J Physiol Heart Circ Physiol* 2006;**291**:H1015-1026.

6. Zak R. Development and proliferative capacity of cardiac muscle cells. *Circ Res* 1974;**35**:suppl II:17-26.

7. Nag AC. Study of non-muscle cells of the adult mammalian heart: A fine structural analysis and distribution. *Cytobios* 1980;**28**:41-61.

8. Banerjee I, Fuseler JW, Price RL, Borg TK, Baudino TA. Determination of cell types and numbers during cardiac development in the neonatal and adult rat and mouse. *Am J Physiol Heart Circ Physiol* 2007;**293**:H1883-1891.

9. Pinto AR, Ilinykh A, Ivey MJ, Kuwabara JT, D'Antoni ML, Debuque R, Chandran A, Wang L, Arora K, Rosenthal NA, Tallquist MD. Revisiting Cardiac cellular composition. *Circ Res* 2016;**118**:400-409.

10. Talman V, Ruskoaho H. Cardiac fibrosis in myocardial infarction-from repair and remodeling to regeneration. *Cell Tissue Res* 2016;**365**:563-581.

11. Murtha LA, Schuliga MJ, Mabotuwana NS, Hardy SA, Waters DW, Burgess JK, Knight DA, Boyle AJ. The processes and mechanisms of cardiac and pulmonary fibrosis. *Front Physiol* 2017;**8**:777.

12. Lopez B, Gonzalez A, Hermida N, Valencia F, de Teresa E, Diez J. Role of lysyl oxidase in myocardial fibrosis: From basic science to clinical aspects. *Am J Physiol Heart Circ Physiol* 2010;**299**:H1-9.

13. Smith-Mungo LI, Kagan HM. Lysyl oxidase: Properties, regulation and multiple functions in biology. *Matrix Biol* 1998;**16**:387-398.

14. El Hajj EC, El Hajj MC, Ninh VK, Gardner JD. Cardioprotective effects of lysyl oxidase inhibition against volume overload-induced extracellular matrix remodeling. *Exp Biol Med* 2016;**241**:539-549.

15. El Hajj EC, El Hajj MC, Ninh VK, Bradley JM, Claudino MA, Gardner JD. Detrimental role of lysyl oxidase in cardiac remodeling. *J Mol Cell Cardiol* 2017;**109**:17-26.

16. Grau-Bove X, Ruiz-Trillo I, Rodriguez-Pascual F. Origin and evolution of lysyl oxidases. *Sci Rep* 2015;**5**:10568.

17. Miana M, Galan M, Martinez-Martinez E, Varona S, Jurado-Lopez R, Bausa-Miranda B, Antequera A, Luaces M, Martinez-Gonzalez J, Rodriguez C, Cachofeiro V. The lysyl oxidase inhibitor beta-aminopropionitrile reduces body weight gain and improves the metabolic profile in diet-induced obesity in rats. *Dis Model Mech* 2015;**8**:543-551.

18. Watanabe T, Barker TA, Berk BC. Angiotensin II and the endothelium: Diverse signals and effects. *Hypertension* 2005;**45**:163-169.

19. Rosenkranz S. TGF-beta1 and angiotensin networking in cardiac remodeling. *Cardiovasc Res* 2004;**63**:423-432.

20. Adam O, Zimmer C, Hanke N, Hartmann RW, Klemmer B, Bohm M, Laufs U. Inhibition of aldosterone synthase (CYP11B2) by torasemide prevents atrial fibrosis and atrial fibrillation in mice. *J Mol Cell Cardiol* 2015;**85**:140-150.

21. Payne SL, Hendrix MJ, Kirschmann DA. Paradoxical roles for lysyl oxidases in cancer--a prospect. *J Cell Biochem* 2007;**101**:1338-1354.

22. Narayan SM, Franz MR, Clopton P, Pruvot EJ, Krummen DE. Repolarization alternans reveals vulnerability to human atrial fibrillation. *Circulation* 2011;**123**:2922-2930.

23. Tadevosyan A, Xiao J, Surinkaew S, Naud P, Merlen C, Harada M, Qi X, Chatenet D, Fournier A, Allen BG, Nattel S. Intracellular angiotensin-II interacts with nuclear angiotensin receptors in cardiac fibroblasts and regulates rna synthesis, cell proliferation, and collagen secretion. *J Am Heart Assoc* 2017;**6**:e004965.

24. Duong E, Xiao J, Qi XY, Nattel S. MicroRNA-135a regulates sodium-calcium exchanger gene expression and cardiac electrical activity. *Heart Rhythm* 2017;**14**:739-748.

25. Golden HB, Gollapudi D, Gerilechaogetu F, Li J, Cristales RJ, Peng X, Dostal DE. Isolation of cardiac myocytes and fibroblasts from neonatal rat pups. In: Peng X, Antonyak M, eds. Cardiovascular development: Methods and protocols. Totowa, NJ: Humana Press, 2012:205-214.

26. He TC, Zhou S, da Costa LT, Yu J, Kinzler KW, Vogelstein B. A simplified system for generating recombinant adenoviruses. *Proc Natl Acad Sci U S A* 1998;**95**:2509-2514.

27. Luo J, Deng ZL, Luo X, Tang N, Song WX, Chen J, Sharff KA, Luu HH, Haydon RC, Kinzler KW, Vogelstein B, He TC. A protocol for rapid generation of recombinant adenoviruses using the AdEasy system. *Nat Protoc* 2007;**2**:1236-1247.

28. Li R-K, Zhao W-Y, Fang F, Zhuang C, Zhang X-X, Yang X-M, Jiang S-H, Kong F-Z, Tu L, Zhang W-M, Yang S-L, Cao H, Zhang Z-G. Lysyl oxidase-like 4 (LOXL4) promotes proliferation and metastasis of gastric cancer via FAK/Src pathway. *J Cancer Res and Clin Oncol* 2015;**141**:269-281.

29. Surinkaew S, Aflaki M, Takawale A, Chen Y, Qi XY, Gillis MA, Shi YF, Tardif JC, Chattipakorn N, Nattel S. Exchange-protein activated by cyclic-AMP (EPAC) regulates atrial fibroblast function and controls cardiac remodeling. *Cardiovasc Res* 2019;**115**:94-106.

30. Livak KJ, Schmittgen TD. Analysis of relative gene expression data using real-time quantitative PCR and the 2(-Delta Delta C(T)) Method. *Methods* 2001;**25**:402-408.

31. Chang K, Uitto J, Rowold EA, Grant GA, Kilo C, Williamson JR. Increased collagen cross-linkages in experimental diabetes: Reversal by beta-aminopropionitrile and D-penicillamine. *Diabetes* 1980;**29**:778-781.

32. Yeh YH, Wakili R, Qi XY, Chartier D, Boknik P, Kaab S, Ravens U, Coutu P, Dobrev D, Nattel S. Calcium-handling abnormalities underlying atrial arrhythmogenesis and contractile dysfunction in dogs with congestive heart failure. *Circ Arrhythm Electrophysiol* 2008;**1**:93-102.

33. Nattel S, Burstein B, Dobrev D. Atrial remodeling and atrial fibrillation: Mechanisms and implications. *Circ Arrhythm Electrophysiol* 2008;**1**:62-73.

34. Eyre DR, Weis MA, Wu JJ. Advances in collagen cross-link analysis. *Methods* 2008;**45**:65-74.

35. Souders CA, Bowers SL, Baudino TA. Cardiac fibroblast: The renaissance cell. *Circ Res* 2009;**105**:1164-1176.

36. Kendall RT, Feghali-Bostwick CA. Fibroblasts in fibrosis: Novel roles and mediators. *Front Pharmacol* 2014;**5**:123.

37. Valiente-Alandi I, Schafer AE, Blaxall BC. Extracellular matrix-mediated cellular communication in the heart. *J Mol Cell Cardiol* 2016;**91**:228-237.

38. Gonzalez-Santamaria J, Villalba M, Busnadiego O, Lopez-Olaneta MM, Sandoval P, Snabel J, Lopez-Cabrera M, Erler JT, Hanemaaijer R, Lara-Pezzi E, Rodriguez-Pascual F. Matrix cross-linking lysyl oxidases are induced in response to myocardial infarction and promote cardiac dysfunction. *Cardiovasc Res* 2016;**109**:67-78.

39. Dostal D, Glaser S, Baudino TA. Cardiac fibroblast physiology and pathology. *Compr Physiol* 2015;**5**:887-909.

34. Takeda N, Manabe I. Cellular interplay between cardiomyocytes and nonmyocytes in cardiac remodeling. *Int J Inflam* 2011;**2011**:535241.

41. Kong P, Christia P, Frangogiannis NG. The pathogenesis of cardiac fibrosis. *Cell Mol Life Sci* 2014;**71**:549-574.

42. Adam O, Theobald K, Lavall D, Grube M, Kroemer HK, Ameling S, Schafers HJ, Bohm M, Laufs U. Increased lysyl oxidase expression and collagen cross-linking during atrial fibrillation. *J Mol Cell Cardiol* 2011;**50**:678-685.

43. Ohmura H, Yasukawa H, Minami T, Sugi Y, Oba T, Nagata T, Kyogoku S, Ohshima H, Aoki H, Imaizumi T. Cardiomyocyte-specific transgenic expression of lysyl oxidase-like protein-1 induces cardiac hypertrophy in mice. *Hypertens Res* 2012;**35**:1063-1068.

44. Mizikova I, Palumbo F, Tabi T, Herold S, Vadasz I, Mayer K, Seeger W, Morty RE. Perturbations to lysyl oxidase expression broadly influence the transcriptome of lung fibroblasts. *Physiol Genomics* 2017;**49**:416-429.

45. Aumiller V, Strobel B, Romeike M, Schuler M, Stierstorfer BE, Kreuz S. Comparative analysis of lysyl oxidase (like) family members in pulmonary fibrosis. *Sci Rep* 2017;**7**:149.

46. Csiszar K. Lysyl oxidases: A novel multifunctional amine oxidase family. *Prog Nucleic Acid Res Mol Biol* 2001;**70**:1-32.

47. Kagan HM, Li W. Lysyl oxidase: Properties, specificity, and biological roles inside and outside of the cell. *J Cell Biochem* 2003;**88**:660-672.

48. Frangogiannis NG. Regulation of the inflammatory response in cardiac repair. *Circ Res* 2012;**110**:159-173.

49. Lin CH, Yu MC, Tung WH, Chen TT, Yu CC, Weng CM, Tsai YJ, Bai KJ, Hong CY, Chien MH, Chen BC. Connective tissue growth factor induces collagen I expression in human lung

fibroblasts through the Rac1/MLK3/JNK/AP-1 pathway. *Biochim Biophys Acta* 2013;**1833**:2823-2833.

50. Hurtado PA, Vora S, Sume SS, Yang D, St Hilaire C, Guo Y, Palamakumbura AH, Schreiber BM, Ravid K, Trackman PC. Lysyl oxidase propeptide inhibits smooth muscle cell signaling and proliferation. *Biochem Biophys Res Commun* 2008;**366**:156-161.

51. Kim HR, Park SM, Seo SU, Jung I, Yoon HI, Gabrilovich DI, Cho BC, Seong SY, Ha SJ, Youn JI. The ratio of peripheral regulatory T cells to LOX-1(+) PMN-MDSC predicts the early response to anti-PD-1 therapy in non-small cell lung cancer patients. *Am J Respir Crit Care Med* 2018. https://doi.org/10.1164/rccm.201808-1502LE**.**

52. Kim D, Mecham RP, Trackman PC, Roy S. Downregulation of lysyl oxidase protects retinal endothelial cells from high glucose–induced apoptosis. *Invest Ophthalmol Vis Sci* 2017;**58**:2725-2731.

53. Shih YH, Chang KW, Chen MY, Yu CC, Lin DJ, Hsia SM, Huang HL, Shieh TM. Lysyl oxidase and enhancement of cell proliferation and angiogenesis in oral squamous cell carcinoma. *Head Neck* 2013;**35**:250-256.

54. Hunter T. 1001 Protein Kinases Redux—Towards 2000. *Semin Cell Biol* 1994;**5**:367-376.

55. Trackman PC. Diverse biological functions of extracellular collagen processing enzymes. *J Cell Biochem* 2005;**96**:927-937.

56. Yu Z, Sato S, Trackman PC, Kirsch KH, Sonenshein GE. Blimp1 activation by AP-1 in human lung cancer cells promotes a migratory phenotype and is inhibited by the lysyl oxidase propeptide. *PloS One* 2012;**7**:e33287.

57. Palamakumbura AH, Jeay S, Guo Y, Pischon N, Sommer P, Sonenshein GE, Trackman PC. The propeptide domain of lysyl oxidase induces phenotypic reversion of ras-transformed cells. *J Biol Chem* 2004;**279**:40593-40600.

58. Bais MV, Nugent MA, Stephens DN, Sume SS, Kirsch KH, Sonenshein GE, Trackman PC. Recombinant lysyl oxidase propeptide protein inhibits growth and promotes apoptosis of pre-existing murine breast cancer xenografts. *PloS One* 2012;**7**:e31188.

59. Raisova M, Hossini AM, Eberle J, Riebeling C, Orfanos CE, Geilen CC, Wieder T, Sturm I, Daniel PT. The Bax/Bcl-2 ratio determines the susceptibility of human melanoma cells to CD95/Fas-Mediated Apoptosis. *J Inves Dermatol* 2001;**117**:333-340.

60. Francis GS, Cohn JN. Heart failure: Mechanisms of cardiac and vascular dysfunction and the rationale for pharmacologic intervention. *FASEB J* 1990;**4**:3068-3075.

61. de Tombe PP. Altered contractile function in heart failure. *Cardiovasc Res* 1998;**37**:367-380.

**Figure Legends**

**Figure 1. Lysyl oxidase (LOX) and LOX-like (LOXL) immunoreactivity was increased in the left atrial (LA) fibroblasts and myocytes from congestive heart failure (CHF) dogs.** Basal immunoreactivity of LOX isoforms in cardiac fibroblasts (Fbs; n = 7; A-E); (A) LOX, (B) LOXL-1, (C) LOXL-2, (D) LOXL-3 and (E) LOXL-4 and myocytes (CM; n = 7; F-J); (F) LOX, (G) LOXL-1, (H) LOXL-2, (I) LOXL-3 and (J) LOXL-4. (K) Representative Western blots of LOX isoforms from Fbs. (L) Representative Western blots of LOX isoforms from CM. Band intensities were normalized to that of glyceraldehyde 3-phosphate dehydrogenase (GAPDH). The results are the means ± SEM; unpaired Student's *t*-tests were performed. **P* < 0.05; ***P* < 0.01; ****P* < 0.001.

**Figure 2. The abundance of lysyl oxidase (LOX) isoform mRNA expressions were increased in the left atrial (LA) fibroblasts and myocytes from congestive heart failure (CHF) dogs.** Basal abundance of LOX isoform transcripts in cardiac fibroblasts (Fbs; n = 8; A-E); (A) LOX, (B) LOX-like protein 1 (LOXL-1), (C) LOXL-2, (D) LOXL-3 and (E) LOXL-4 and myocytes (CM; n = 9; F-J); (F) LOX, (G) LOXL-1, (H) LOXL-2, (I) LOXL-3 and (J) LOXL-4. The abundance of LOX isoform mRNA was normalized to that of glucose 6-phosphate dehydrogenase (G6PD). The results are the means ± SEM; unpaired Student's *t*-tests were performed. **P* < 0.05; ***P* < 0.01; ****P* < 0.001.

**Figure 3. Angiotensin II (Ang II) increased lysyl oxidase (LOX) and LOX-like protein 2 (LOXL-2) secretion from neonatal rat ventricular fibroblasts and myocytes.** Effect of treatment with different concentrations of Ang II (0.1, 1.0 and 10.0 μM) on the abundance of LOX and LOXL-2 immunoreactivity in conditioned media from cardiac fibroblast cultures (Fbs; n = 4; (A) LOX, (B) LOXL-2, (C) representative Western blots of LOX and (D) representative Western blots of LOXL-2) and myocytes (CM; n = 4; (E) LOX, (F) LOXL-2, (G) representative Western blots of LOX and (H) representative Western blots of LOXL-2). Band intensities were normalized to cell number. The results are the means ± SEM; one-way ANOVA followed by the Bonferroni's multiple comparisons test was performed. **P* < 0.05 vs. control; ***P* < 0.01 vs. control; ****P* < 0.001 vs. control.

**Figure 4. Angiotensin II (Ang II) stimulated collagen cross-linking and β-aminopropionitrile (BAPN) attenuated collagen cross-linking in neonatal rat ventricular fibroblasts.** Effect of treatment with different concentrations of Ang II (0.1, 1.0 and 10.0 μM; A-C) and BAPN (0.1, 1.0, 10.0 and 100.0 μM; D-F) in fibroblasts on the collagen content, including (A) Ang II doses vs. soluble collagen, (B) Ang II doses vs. insoluble collagen, (C) Ang II doses vs. collagen cross-linking ratio, (D) BAPN doses vs. soluble collagen, (E) BAPN doses vs. insoluble collagen and (F) BAPN doses vs. collagen cross-linking ratio. The results are the means ± SEM; one-way ANOVA followed by the Bonferroni's multiple comparisons test was performed, n = 6, $*P < 0.05$ vs. control; $**P < 0.01$ vs. control; $***P < 0.001$ vs. control.

**Figure 5. Lysyl oxidase (LOX) isoform expression was efficiently suppressed in neonatal rat ventricular fibroblasts using siRNA.** The efficiency and specificity of LOX isoform knockdown was estimated by qPCR (A-E) and validated by Western blot (F). Effect of knocking down individual LOX isoforms in fibroblasts (n = 5) using siRNA on the mRNA of (A) LOX, (B) LOX-like protein 1 (LOXL-1), (C) LOXL-2, (D) LOXL-3, (E) LOXL-4 and (F) representative Western blots of LOX isoforms. The abundance of LOX isoform mRNA was normalized to that of glyceraldehyde 3-phosphate dehydrogenase (GAPDH). The results are the means ± SEM; one-way ANOVA followed by the Bonferroni's multiple comparisons test was performed. $*P < 0.05$ vs. scrambled control (ScRNA); $**P < 0.01$ vs. ScRNA; $***P < 0.001$ vs. ScRNA.

**Figure 6. Knockdown of individual lysyl oxidase (LOX) isoforms altered the expression of profibrotic markers in neonatal rat ventricular fibroblasts.** Effect of siRNA-mediated knockdown of individual LOX isoforms in fibroblasts (n = 5) on the abundance of (A) collagen 1A1 (COL 1A1), (B) COL 3A1, (C) fibronectin 1 (FN 1), (D) transforming growth factor β 1 (TGF-β1), (E) connective tissue growth factor (CTGF), (F) periostin, (G) α-smooth muscle actin (α-SMA), (H) matrix metalloproteinase-2 (MMP-2) and (I) MMP-9 mRNA. mRNA abundance was normalized to that of glyceraldehyde 3-phosphate dehydrogenase (GAPDH). The results are the means ± SEM; one-way ANOVA followed by the Bonferroni's multiple comparisons test was performed. $*P < 0.05$ vs. scrambled control (ScRNA); $**P < 0.01$ vs. ScRNA; $***P < 0.001$ vs. ScRNA.

**Figure 7. Knockdown of individual lysyl oxidase (LOX) isoforms in neonatal rat ventricular fibroblasts altered proliferation and the expression of proliferation and apoptotic markers.** Effect of siRNA-mediated knockdown of individual LOX isoforms in fibroblasts (n = 5) on (A) cell proliferation and (B) cyclin E2 (CCNE 2), (C) cyclin D1 (CCND 1), (D) B-cell lymphoma 2 (BCL-2)-associate X protein (BAX), and (E) BCL-2 mRNA and (F) the ratio of BAX/BCL-2 mRNA. mRNA abundance was normalized to that of glyceraldehyde 3-phosphate dehydrogenase (GAPDH). The results are the means ± SEM; one-way ANOVA followed by the Bonferroni's multiple comparisons test was performed. **P* < 0.05 vs. scrambled control (ScRNA); ***P* < 0.01 vs. ScRNA; ****P* < 0.001 vs. ScRNA.

**Figure 8. Knockdown of individual lysyl oxidase (LOX) isoforms in neonatal rat ventricular myocytes altered the expression of apoptosis markers**. Effect of siRNA-mediated knockdown of individual LOX isoforms in cardiomyocytes (n = 4) on the abundance of (A) B-cell lymphoma 2 (BCL-2)-associate X protein (BAX), and (B) BCL-2 mRNA and (C) the ratio of BAX/BCL-2 mRNA. mRNA abundance was normalized to that of glyceraldehyde 3-phosphate dehydrogenase (GAPDH). The results are the means ± SEM; one-way ANOVA followed by the Bonferroni's multiple comparisons test was performed. **P* < 0.05 vs. scrambled control (ScRNA); ***P* < 0.01 vs. ScRNA; ****P* < 0.001 vs. ScRNA.

**Figure 9. Knocking down lysyl oxidase-like protein 1 (LOXL-1) in canine left atrial (LA) myocytes increased cell shortening without altering $Ca^{2+}$ transients.** Effect of siRNA-mediated knockdown of individual LOX isoforms in cardiomyocytes (n = 5-15 cells) on (A) cell shortening, (B) diastolic $Ca^{2+}$ level, (C) $Ca^{2+}$ amplitude and (D) decay time constant. The results are the means ± SEM; one-way ANOVA followed by the Bonferroni's multiple comparisons test was performed. **P* < 0.05 vs. Scrambled control (ScRNA); ***P* < 0.01 vs. ScRNA, ****P* < 0.001 vs. ScRNA.

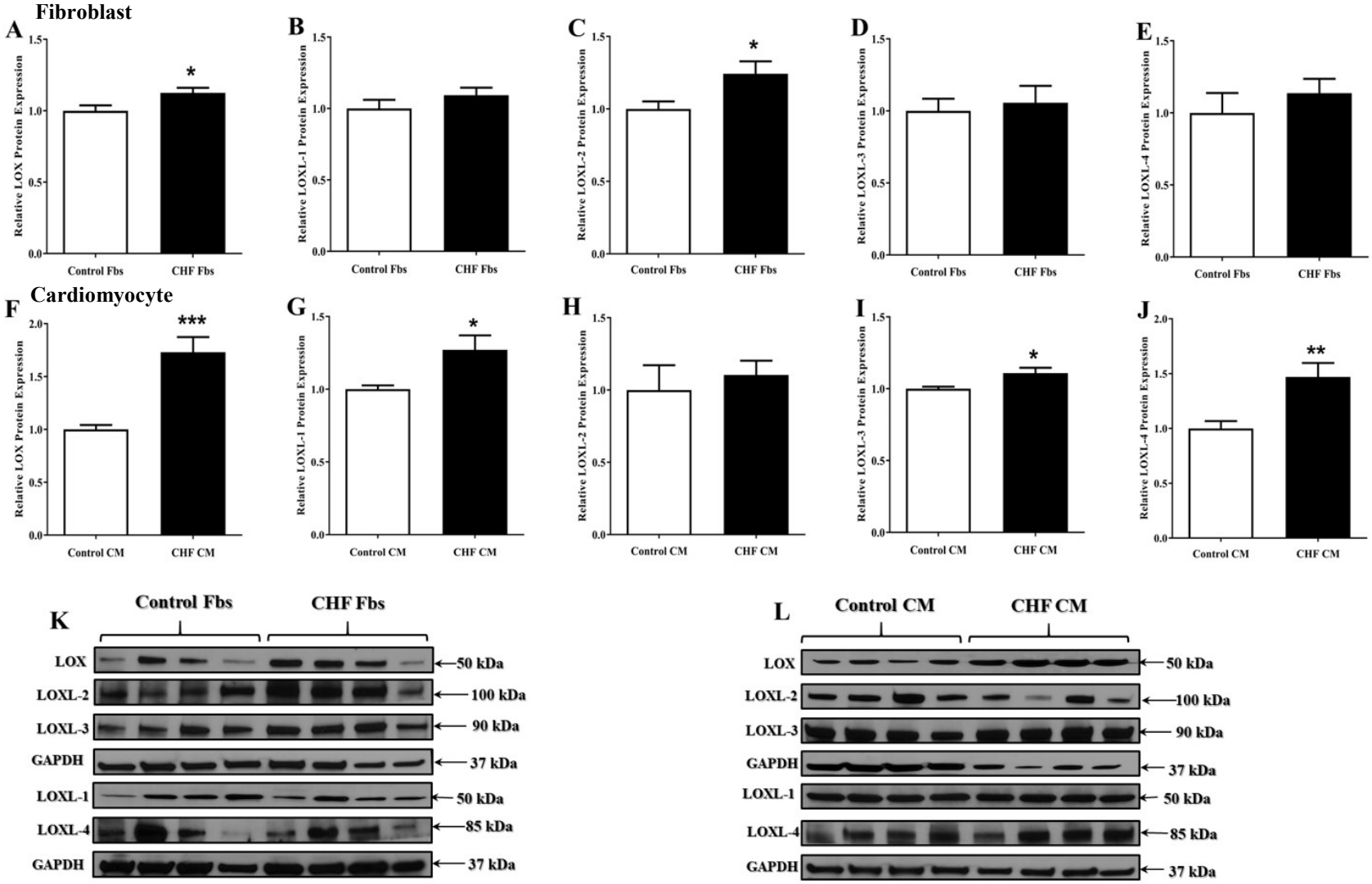
Fibroblast
A
Relative LOX Protein Expression
Control Fbs
CHF Fbs
B
Relative LOXL-1 Protein Expression
C
Relative LOXL-2 Protein Expression
D
Relative LOXL-3 Protein Expression
E
Relative LOXL-4 Protein Expression
Cardiomyocyte
F
Control CM
CHF CM
G
H
I
J
K
L
LOX
LOXL-2
LOXL-3
GAPDH
LOXL-1
LOXL-4
50 kDa
100 kDa
90 kDa
37 kDa
85 kDa

**Figure 1.**

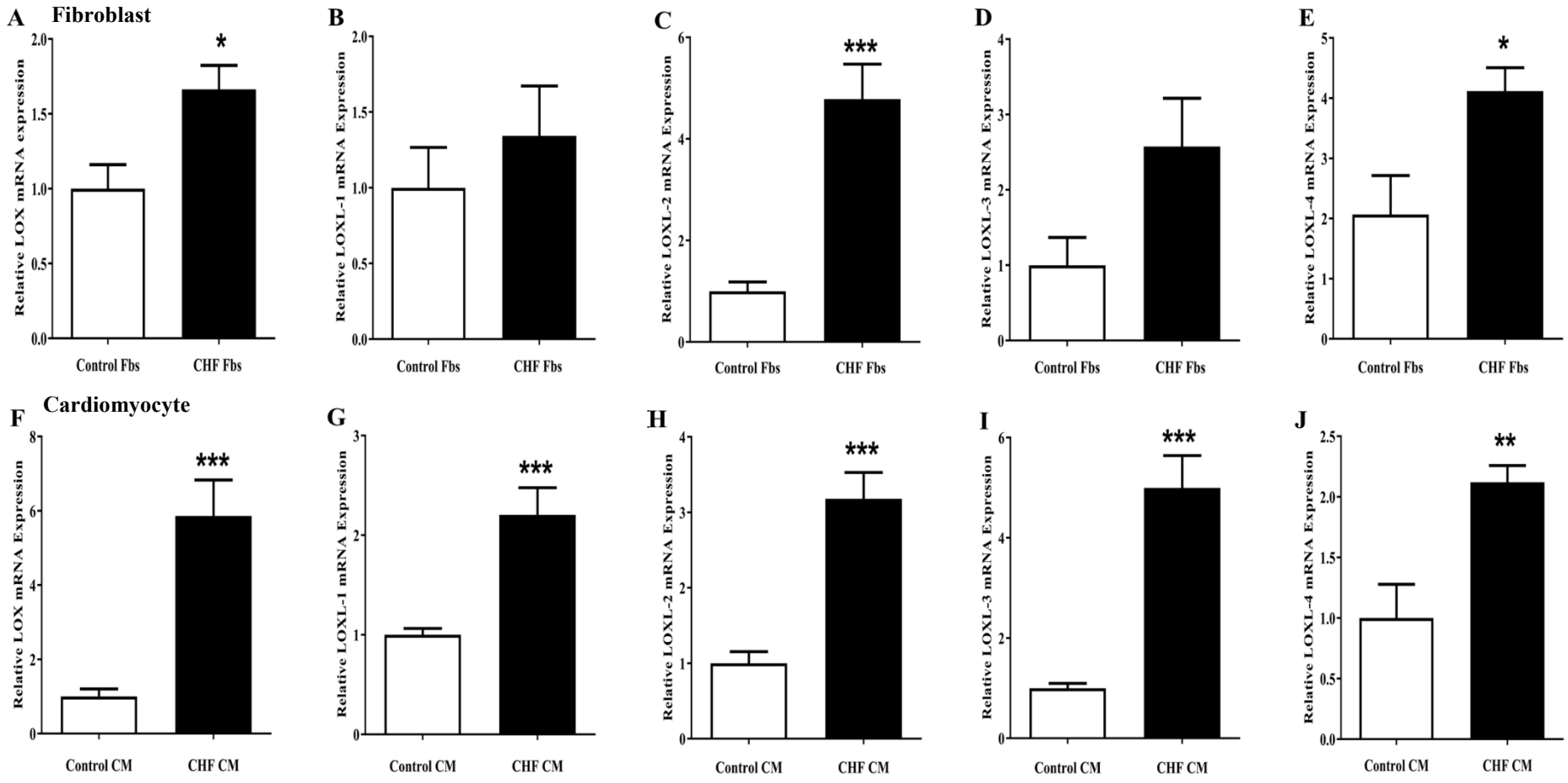
A
Fibroblast
Relative LOX mRNA expression
2.0
1.5
1.0
0.5
0.0
*
Control Fbs
CHF Fbs
B
Relative LOXL-1 mRNA Expression
2.0
1.5
1.0
0.5
0.0
Control Fbs
CHF Fbs
C
Relative LOXL-2 mRNA Expression
6
4
2
0
***
Control Fbs
CHF Fbs
D
Relative LOXL-3 mRNA Expression
4
3
2
1
0
Control Fbs
CHF Fbs
E
Relative LOXL-4 mRNA Expression
5
4
3
2
1
0
*
Control Fbs
CHF Fbs
F
Cardiomyocyte
Relative LOX mRNA Expression
8
6
4
2
0
***
Control CM
CHF CM
G
Relative LOXL-1 mRNA Expression
3
2
1
0
***
Control CM
CHF CM
H
Relative LOXL-2 mRNA Expression
4
3
2
1
0
***
Control CM
CHF CM
I
Relative LOXL-3 mRNA Expression
6
4
2
0
***
Control CM
CHF CM
J
Relative LOXL-4 mRNA Expression
2.5
2.0
1.5
1.0
0.5
0.0
**
Control CM
CHF CM

**Figure 2.**

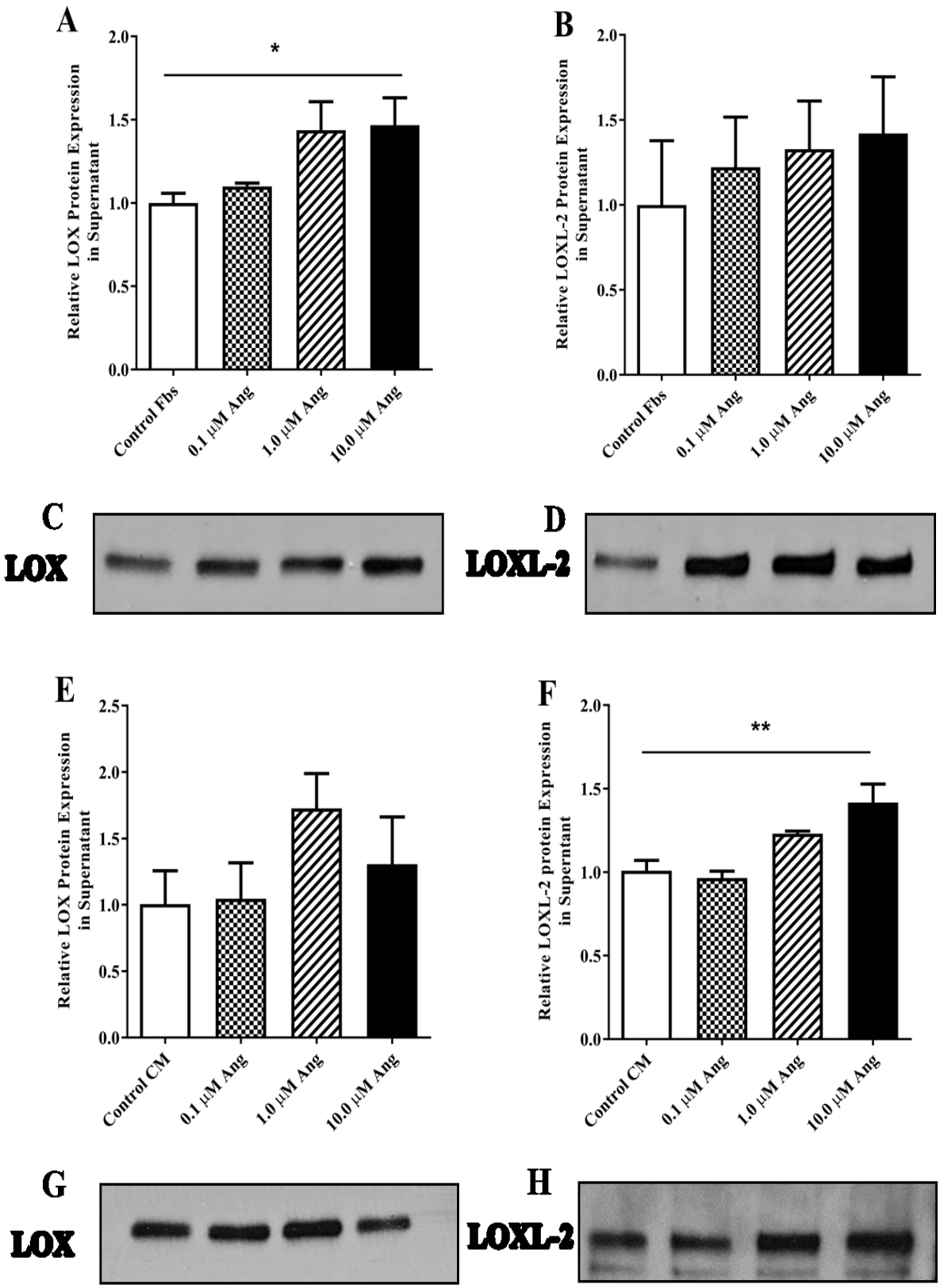
A
Relative LOX Protein Expression in Supernatant
2.0
1.5
1.0
0.5
0.0
*
Control Fbs
0.1 μM Ang
1.0 μM Ang
10.0 μM Ang
B
Relative LOXL-2 Protein Expression in Supernatant
2.0
1.5
1.0
0.5
0.0
Control Fbs
0.1 μM Ang
1.0 μM Ang
10.0 μM Ang
C
LOX
D
LOXL-2
E
Relative LOX Protein Expression in Supernatant
2.5
2.0
1.5
1.0
0.5
0.0
Control CM
0.1 μM Ang
1.0 μM Ang
10.0 μM Ang
F
Relative LOXL-2 protein Expression in Supernatant
2.0
1.5
1.0
0.5
0.0
**
Control CM
0.1 μM Ang
1.0 μM Ang
10.0 μM Ang
G
LOX
H
LOXL-2

**Figure 3.**

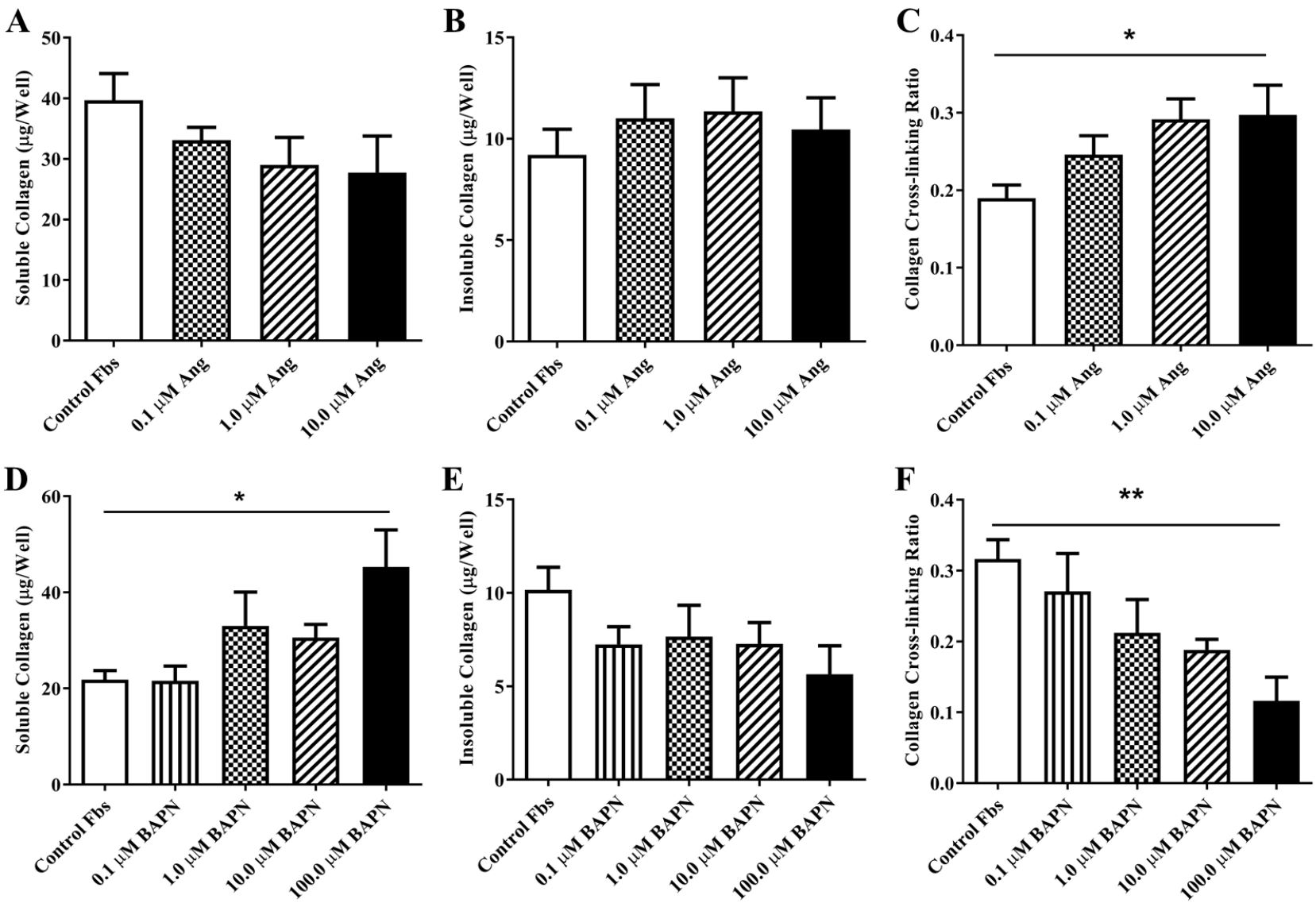
A
Soluble Collagen (µg/Well)
50
40
30
20
10
0
Control Fbs
0.1 µM Ang
1.0 µM Ang
10.0 µM Ang
B
Insoluble Collagen (µg/Well)
15
10
5
0
Control Fbs
0.1 µM Ang
1.0 µM Ang
10.0 µM Ang
C
Collagen Cross-linking Ratio
0.4
0.3
0.2
0.1
0.0
*
Control Fbs
0.1 µM Ang
1.0 µM Ang
10.0 µM Ang
D
Soluble Collagen (µg/Well)
60
40
20
0
*
Control Fbs
0.1 µM BAPN
1.0 µM BAPN
10.0 µM BAPN
100.0 µM BAPN
E
Insoluble Collagen (µg/Well)
15
10
5
0
Control Fbs
0.1 µM BAPN
1.0 µM BAPN
10.0 µM BAPN
100.0 µM BAPN
F
Collagen Cross-linking Ratio
0.4
0.3
0.2
0.1
0.0
**
Control Fbs
0.1 µM BAPN
1.0 µM BAPN
10.0 µM BAPN
100.0 µM BAPN

**Figure 4.**

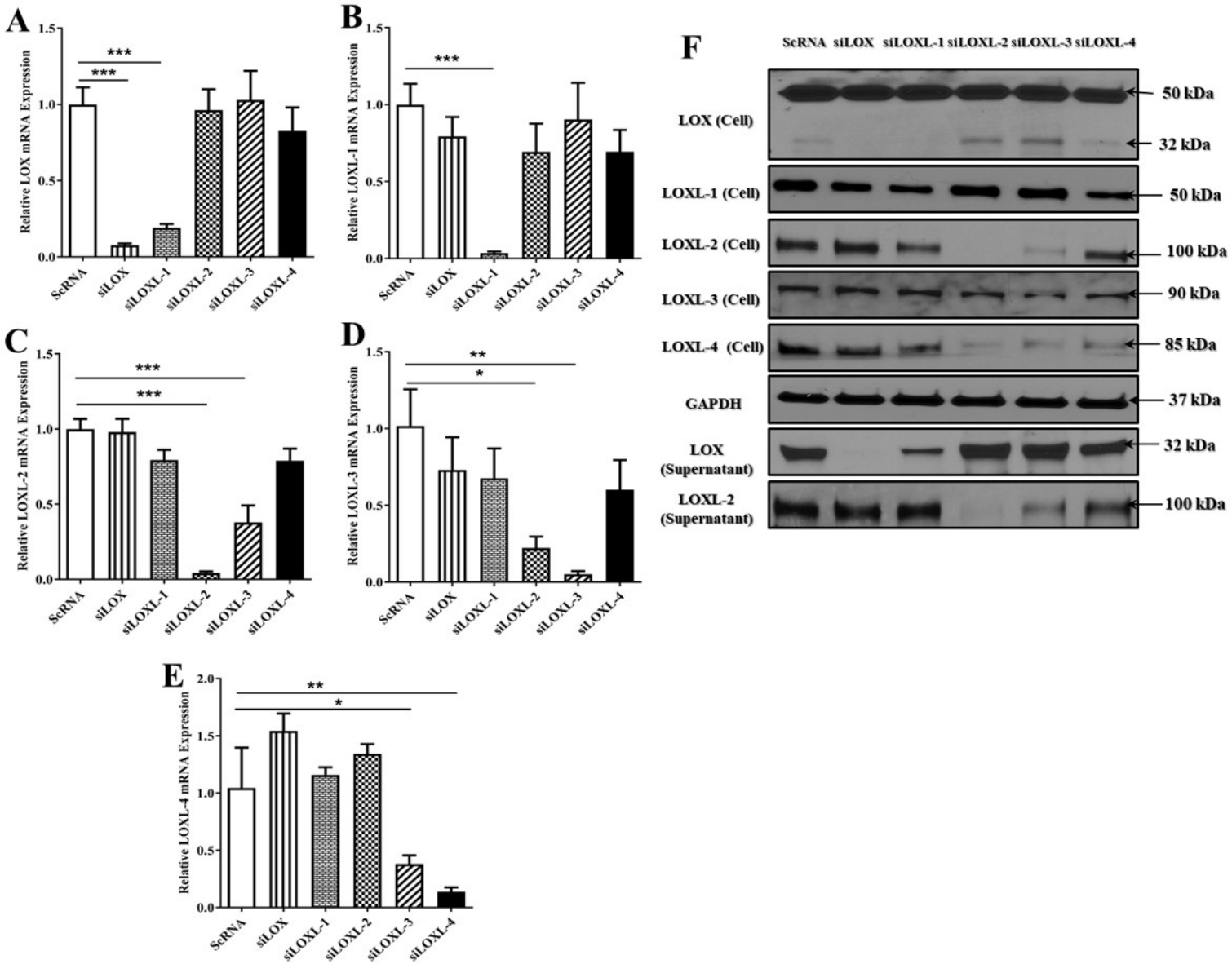
A
Relative LOX mRNA Expression
B
Relative LOXL-1 mRNA Expression
C
Relative LOXL-2 mRNA Expression
D
Relative LOXL-3 mRNA Expression
E
Relative LOXL-4 mRNA Expression
ScRNA
siLOX
siLOXL-1
siLOXL-2
siLOXL-3
siLOXL-4
F
ScRNA siLOX siLOXL-1 siLOXL-2 siLOXL-3 siLOXL-4
LOX (Cell)
LOXL-1 (Cell)
LOXL-2 (Cell)
LOXL-3 (Cell)
LOXL-4 (Cell)
GAPDH
LOX (Supernatant)
LOXL-2 (Supernatant)
50 kDa
32 kDa
50 kDa
100 kDa
90 kDa
85 kDa
37 kDa
32 kDa
100 kDa

**Figure 5.**

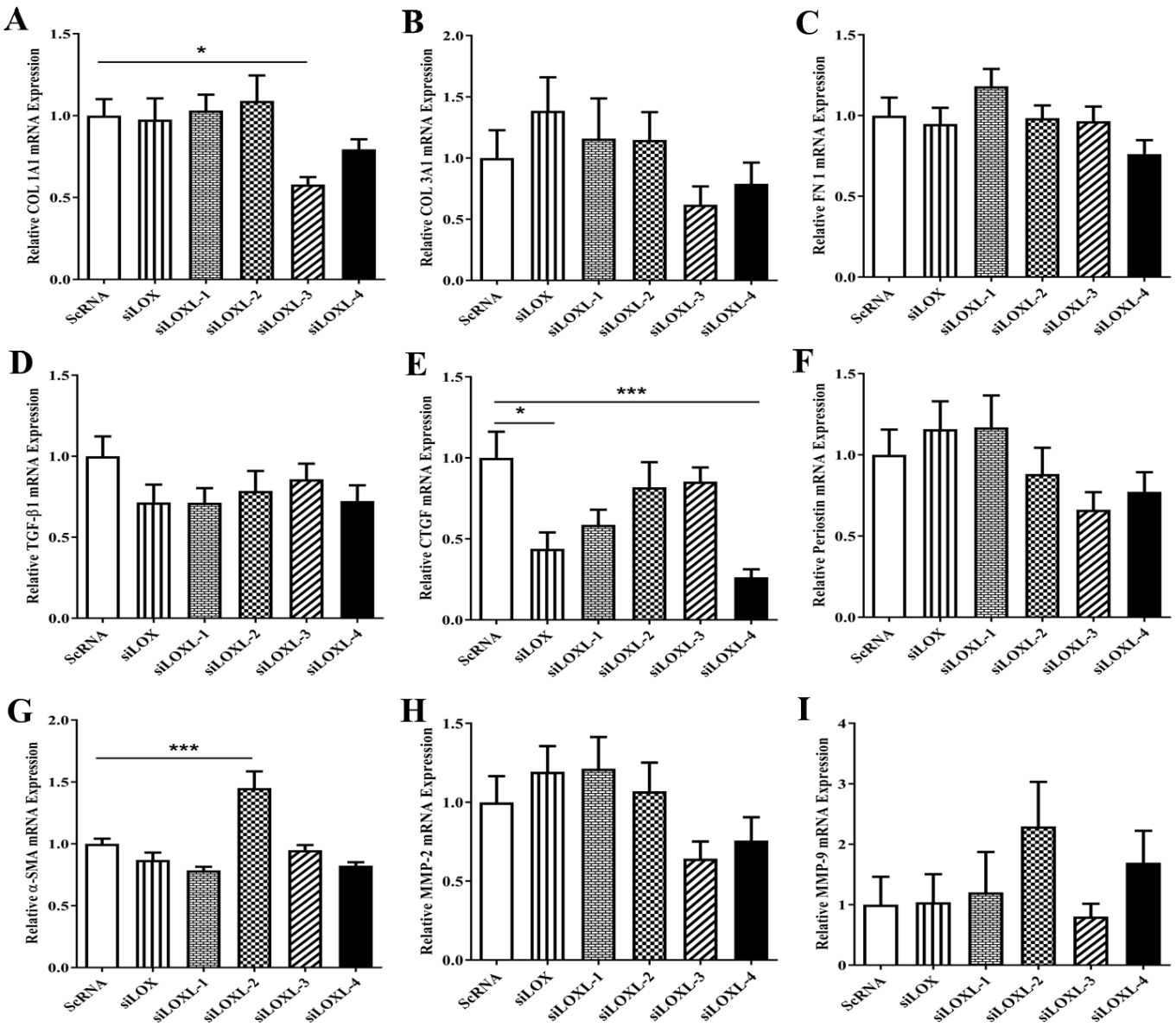
A
Relative COL 1A1 mRNA Expression
B
Relative COL 3A1 mRNA Expression
C
Relative FN 1 mRNA Expression
D
Relative TGF-β1 mRNA Expression
E
Relative CTGF mRNA Expression
F
Relative Periostin mRNA Expression
G
Relative α-SMA mRNA Expression
H
Relative MMP-2 mRNA Expression
I
Relative MMP-9 mRNA Expression
ScRNA
siLOX
siLOXL-1
siLOXL-2
siLOXL-3
siLOXL-4

**Figure 6.**

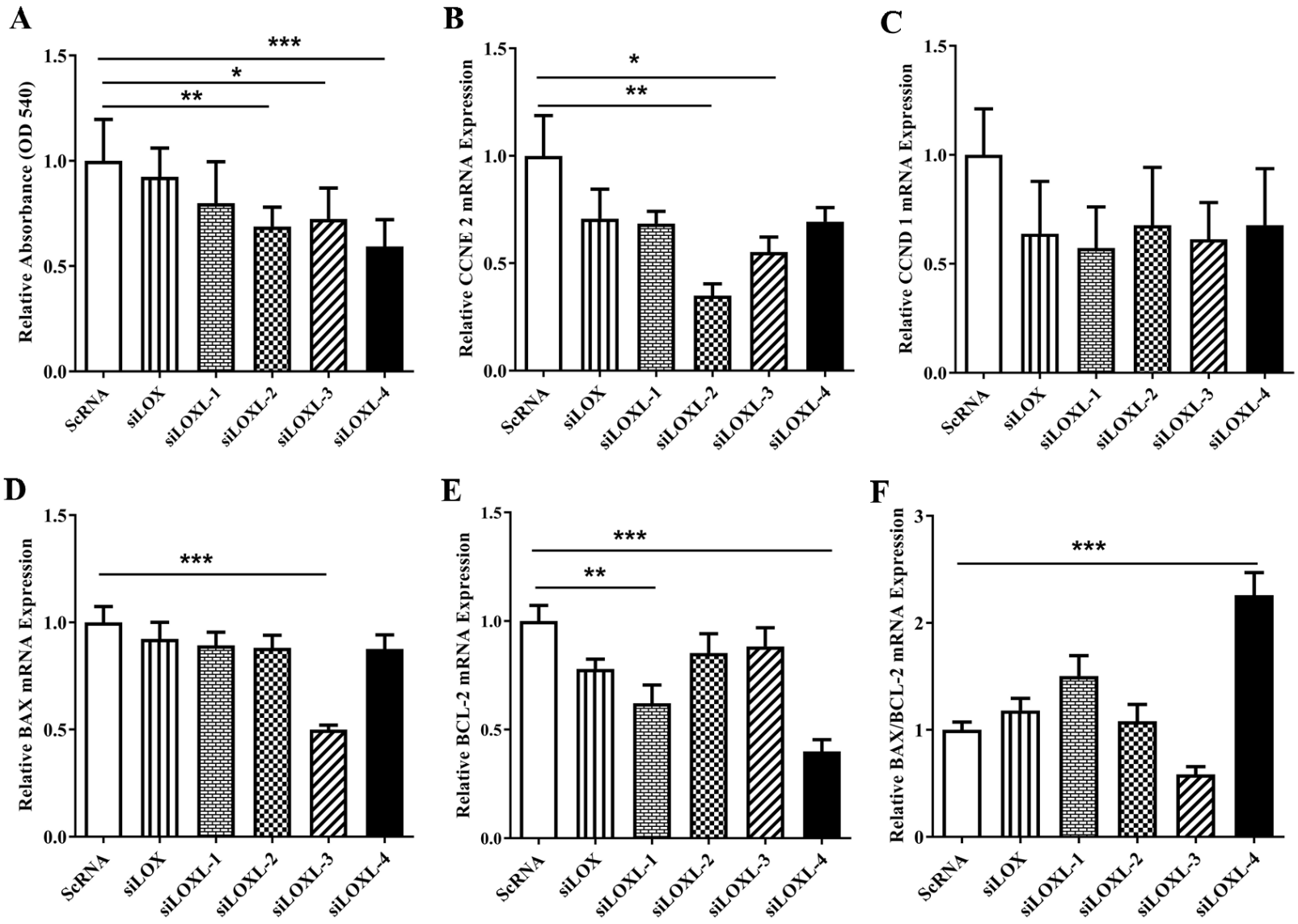
A
Relative Absorbance (OD 540)
1.5
1.0
0.5
0.0
***
*
**
ScRNA
siLOX
siLOXL-1
siLOXL-2
siLOXL-3
siLOXL-4
B
Relative CCNE 2 mRNA Expression
*
**
C
Relative CCND 1 mRNA Expression
D
Relative BAX mRNA Expression
E
Relative BCL-2 mRNA Expression
F
Relative BAX/BCL-2 mRNA Expression
3
2
1
0

**Figure 7.**

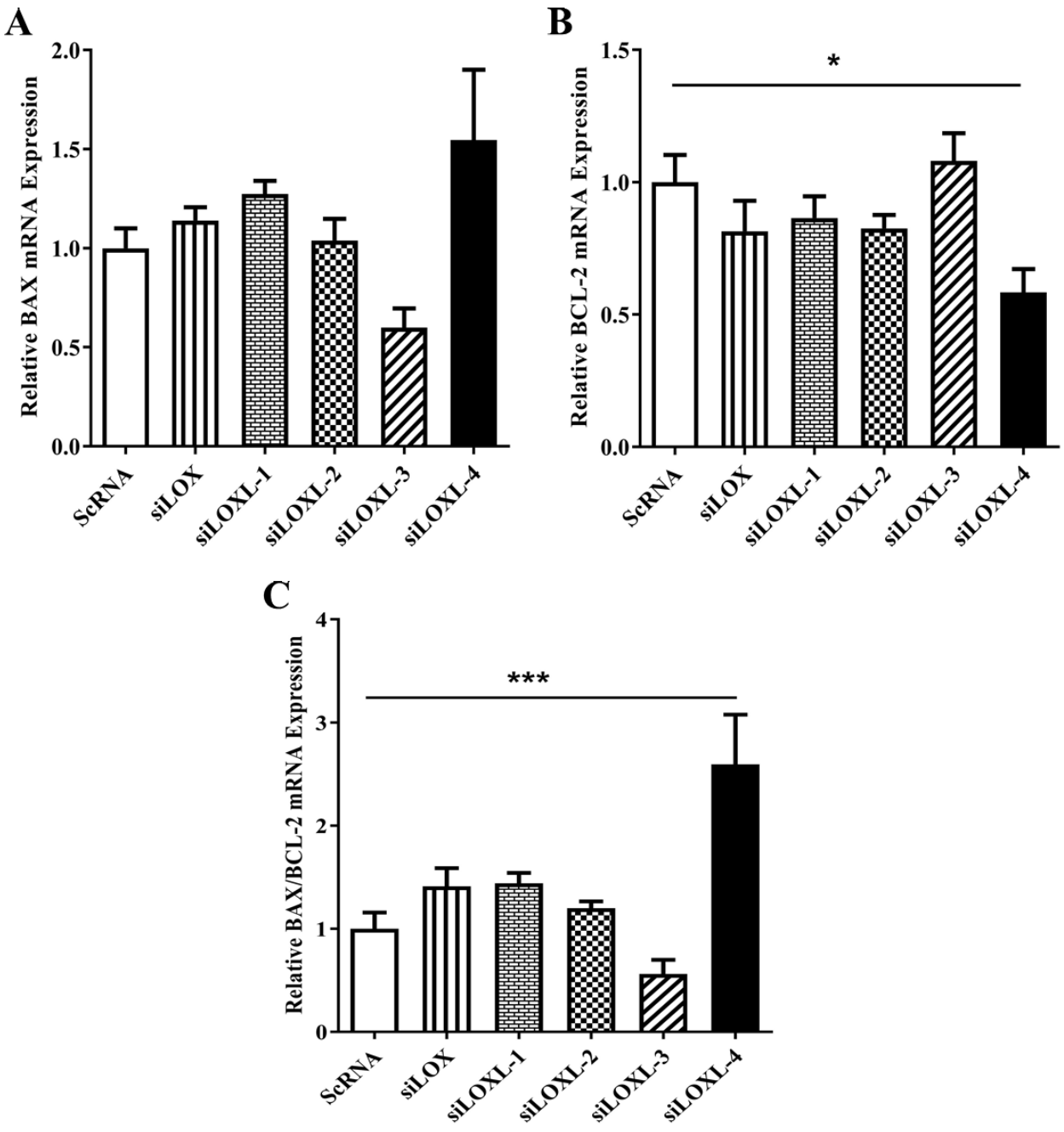
A
Relative BAX mRNA Expression
2.0
1.5
1.0
0.5
0.0
ScRNA
siLOX
siLOXL-1
siLOXL-2
siLOXL-3
siLOXL-4
B
Relative BCL-2 mRNA Expression
1.5
1.0
0.5
0.0
*
ScRNA
siLOX
siLOXL-1
siLOXL-2
siLOXL-3
siLOXL-4
C
Relative BAX/BCL-2 mRNA Expression
4
3
2
1
0
***
ScRNA
siLOX
siLOXL-1
siLOXL-2
siLOXL-3
siLOXL-4

**Figure 8.**

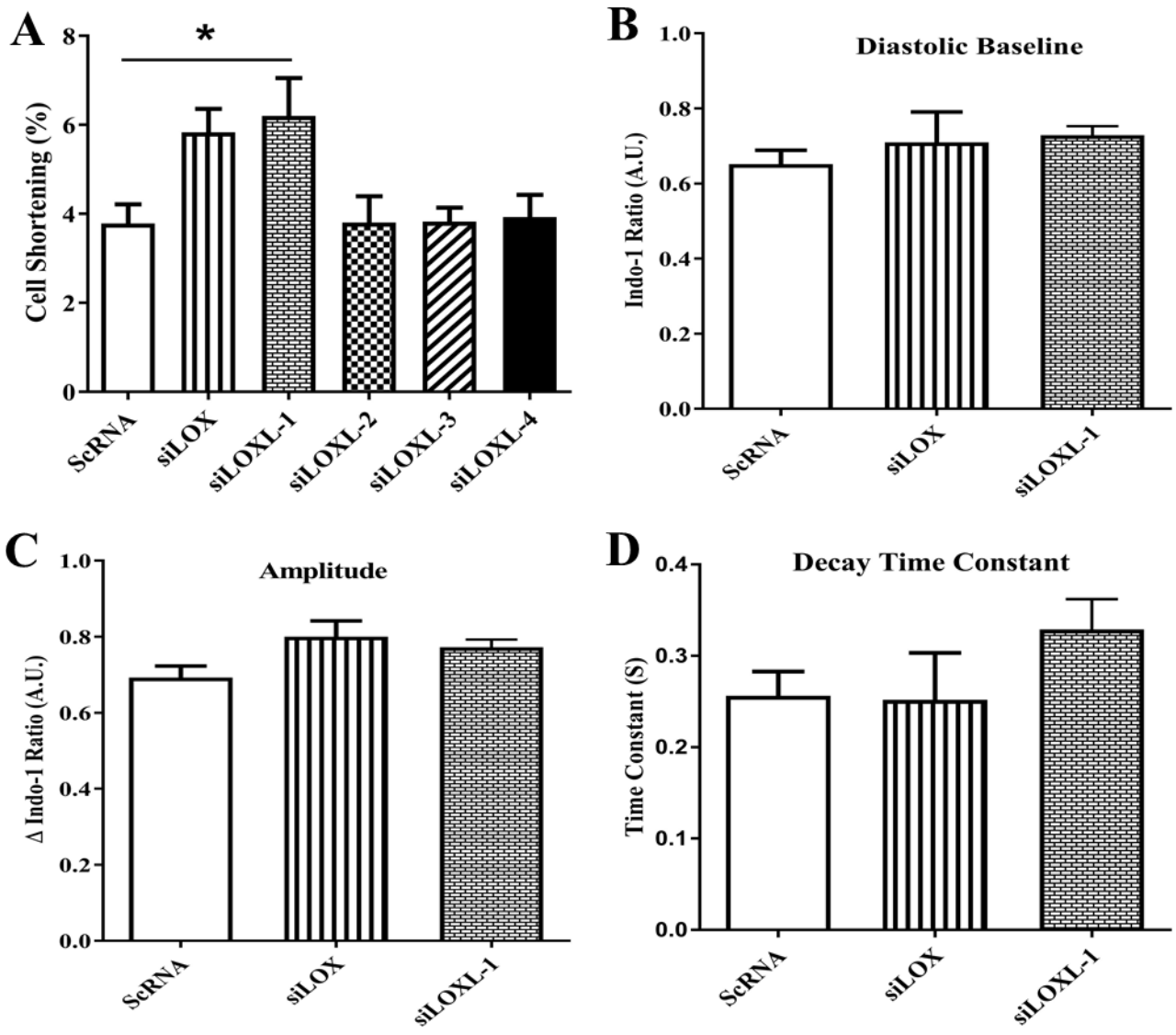
A
*
Cell Shortening (%)
8
6
4
2
0
ScRNA
siLOX
siLOXL-1
siLOXL-2
siLOXL-3
siLOXL-4
B
Diastolic Baseline
Indo-1 Ratio (A.U.)
1.0
0.8
0.6
0.4
0.2
0.0
ScRNA
siLOX
siLOXL-1
C
Amplitude
Δ Indo-1 Ratio (A.U.)
1.0
0.8
0.6
0.4
0.2
0.0
ScRNA
siLOX
siLOXL-1
D
Decay Time Constant
Time Constant (S)
0.4
0.3
0.2
0.1
0.0
ScRNA
siLOX
siLOXL-1

**Figure 9.**

## Supplementary Figure Legends

**Figure S1. Angiotensin II (Ang II) failed to change the abundance of lysyl oxidase (LOX) isoform mRNA or immunoreactivity in neonatal rat ventricular fibroblasts (Fbs).** Effect of treatment with different concentrations of Ang II (0.1, 1.0 and 10.0 μM) in Fbs on the relative quantity of (A) LOX, (B) LOX-like protein 1 (LOXL-1), (C) LOXL-2, (D) LOXL-3 and (E) LOX-4 mRNA and the intracellular (cell lysate) of (F) LOX, (G) LOXL-1, (H) LOXL-2, (I) LOXL-3 and (J) LOXL-4 immunoreactivity. (K) Representative Western blots of LOX family proteins. mRNA and immunoreactive bands were normalized to that of glyceraldehyde 3-phosphate dehydrogenase (GAPDH). Bands at a molecular weight of 32 and 50 kDa represent active and inactive LOX, respectively. The results are the means ± SEM; one-way ANOVA followed by the Bonferroni's multiple comparisons test was performed. n = 4. *$P < 0.05$ vs. control; **$P < 0.01$ vs. control; ***$P < 0.001$ vs. control.

**Figure S2. Angiotensin II (Ang II) increased lysyl oxidase like protein-1 (LOXL-1) immunoreactivity in neonatal rat ventricular myocytes (CM).** Effect of treatment with different concentrations of Ang II (0.1, 1.0 and 10.0 μM) in CM on (A) LOX, (B) LOXL-1, (C) LOXL-2, (D) LOXL-3 and (E) LOXL-4 mRNA and the intracellular (cell lysate) of (F) LOX, (G) LOXL-1, (H) LOXL-2, (I) LOXL-3 and (J) LOXL-4 immunoreactivity. (K) Representative Western blots of LOX family proteins. mRNA and immunoreactive bands were normalized to that of glyceraldehyde 3-phosphate dehydrogenase (GAPDH). Bands at a molecular weight of 32 and 50 kDa represent active and inactive LOX, respectively. The results are the means ± SEM; one-way ANOVA followed by the Bonferroni's multiple comparisons test was performed. n= 3. *$P < 0.05$ vs. control; **$P < 0.01$ vs. control; ***$P < 0.001$ vs. control.

**Figure S3. β-aminopropionitrile (BAPN) doesn't change the abundance of lysyl oxidase (LOX) isoform mRNA in neonatal rat ventricular fibroblasts (Fbs).** Effect of treatment with different concentrations of BAPN (0.1, 1.0, 10.0 and 100.0 μM) in Fbs on the abundance of (A) LOX, (B) LOX-like protein 1 (LOXL-1), (C) LOXL-2, (D) LOXL-3 and (E) LOXL-4 mRNA. mRNA was normalized to that of glyceraldehyde 3-phosphate dehydrogenase (GAPDH). The results are the means ± SEM; one-way ANOVA followed by the Bonferroni's multiple

comparisons test was performed. n = 3. *$P < 0.05$ vs. control; **$P < 0.01$ vs. control; ***$P < 0.001$ vs control.

**Figure S4. Lysyl oxidase (LOX) isoform expression was efficiently suppressed using siRNA in neonatal rat ventricular myocytes.** The efficiency and specificity of siRNA-mediated knockdown of individual LOX isoforms were estimated by qPCR (A-E) and validated by Western blot (F). Effect of siRNA knockdown of LOX isoforms in cardiomyocytes on the abundance of (A) LOX, (B) LOX-like protein 1 (LOXL-1), (C) LOXL-2, (D) LOXL-3 and (E) LOXL-4 mRNA. (F) Representative Western blots of LOX isoforms. mRNA was normalized to that of glyceraldehyde 3-phosphate dehydrogenase (GAPDH). The results are the means ± SEM; one-way ANOVA followed by the Bonferroni's multiple comparisons test was performed. n = 4. *$P < 0.05$ vs. scrambled control (ScRNA); **$P < 0.01$ vs. ScRNA; ***$P < 0.001$ vs. ScRNA.

**Figure S5. The expression of lysyl oxidase (LOX) isoforms was efficiently suppressed by specific siRNAs in canine left atrial (LA) myocytes.** The knockdown efficiency and specificity of LOX isoforms were estimated by qPCR. The effect of siRNA-mediated knockdown of individual LOX isoforms in cardiomyocytes (n = 4) on the abundance of (A) LOX, (B) LOX-like protein 1 (LOXL-1), (C) LOXL-2, (D) LOXL-3 and (E) LOXL-4 mRNA. mRNA was normalized to that of glucose 6-phosphate dehydrogenase (G6PD). The results are the means ± SEM; one-way ANOVA followed by the Bonferroni's multiple comparisons test was performed. *$P < 0.05$ vs. scrambled control (ScRNA); **$P < 0.01$ vs. ScRNA; ***$P < 0.001$ vs. ScRNA.

**Figure S6. Adenovirally-mediated lysyl oxidase (LOX) overexpression increased LOX mRNA in canine left atrial (LA) myocytes.** Effect of overexpression of LOX in cardiomyocytes (n = 4) using adenovirus (Aden-LOX) on the abundance of (A) LOX, (B) LOX-like protein 1 (LOXL-1), (C) LOXL-2, (D) LOXL-3 and (E) LOXL-4 mRNA. mRNA was normalized to that of glucose 6-phosphate dehydrogenase (G6PD). The results are the means ± SEM; unpaired Student's *t*-tests were performed. *$P < 0.05$ vs. adenovirus encoding green fluorescent protein (Aden-GFP); **$P < 0.01$ vs. Aden-GFP, ***$P < 0.001$ vs. Aden-GFP.

**Figure S7. Overexpression of lysyl oxidase (LOX) in canine left atrial (LA) myocytes reduced cell shortening without altering $Ca^{2+}$ transients.** Effect of LOX overexpression (n = 5-15 cells)

using adenovirus (Aden-LOX) in cardiomyocytes on (A) cell shortening, (B) diastolic $Ca^{2+}$ level, (C) $Ca^{2+}$ amplitude and (D) decay time constant. The results are the means ± SEM; unpaired Student's *t*-tests were performed. **P* < 0.05 vs. adenovirus encoding green fluorescent protein (Aden-GFP); ***P* < 0.01 vs. Aden-GFP, ****P* < 0.001 vs. Aden-GFP.

**Table S1:** Sequences of siRNA for LOX isoforms used in this study.

| siRNA | Species | Abbreviation | | Sequence (5´ to 3´) |
|---|---|---|---|---|
| Lysyl oxidase | Rat | LOX | **F:** | CAAGGGACGUCUGACUUCUUACCAA |
| | | | **R:** | UUGGUAAGAAGUCAGACGUCCCUUG |
| Lysyl oxidase like-1 | Rat | LOXL-1 | **F:** | AGUGGCAUAGCUGUCACCAACAUUA |
| | | | **R:** | UAAUGUUGGUGACAGCUAUGCCACU |
| Lysyl oxidase like-2 | Rat | LOXL-2 | **F:** | UCGAACACUUCAGUGGACUCCUAAA |
| | | | **R:** | UUUAGGAGUCCACUGAAGUGUUCGA |
| Lysyl oxidase like-3 | Rat | LOXL-3 | **F:** | CCACUUGAGUGAAGUUCGGUGCUCU |
| | | | **R:** | AGAGCACCGAACUUCACUCAAGUGG |
| Lysyl oxidase like-4 | Rat | LOXL-4 | **F:** | CCCAGAAUGGUUGUCAACAUGCAAA |
| | | | **R** | UUUGCAUGUUGACAACCAUUCUGGG |
| Lysyl oxidase | Dog | LOX | **F:** | CGCCUUGCACGUUUCCAAUCGCAUU |
| | | | **R:** | AAUGCGAUUGGAAACGUGCAAGGCG |
| Lysyl oxidase like-1 | Dog | LOXL-1 | **F:** | CACAGAAGUGCUCGUGGGCAGGUCU |
| | | | **R:** | AGACCUGCCCACGAGCACUUCUGUG |
| Lysyl oxidase like-2 | Dog | LOXL-2 | **F:** | AAGGACCCAUCUGGUUGGACAAUAU |
| | | | **R:** | AUAUUGUCCAACCAGAUGGGUCCUU |
| Lysyl oxidase like-3 | Dog | LOXL-3 | **F:** | CCACUUAAGUGAAGUUCAAUGCUCU |
| | | | **R:** | AGAGCAUUGAACUUCACUUAAGUGG |
| Lysyl oxidase like-4 | Dog | LOXL-4 | **F:** | GCGUGGCUAUCUUUCUGAGAGGGUU |
| | | | **R:** | AACCCUCUCAGAAAGAUAGCCACGC |

**F: Forward, R: Reverse.**

**Table S2:** Sequences of custom-made SYBR Green primers used in this study.

| Gene Name | Species | Abbreviation | | Primer sequence (5′ to 3′) |
|---|---|---|---|---|
| Lysyl oxidase like-1 | Rat | LOXL-1 | **F:** | AGGGCCGTCTCAGCGTGGGTAGT |
| | | | **R:** | ATGCCTGCACGTAGTTGGGATCTGG |
| Lysyl oxidase like-2 | Rat | LOXL-2 | **F:** | GGCCAGCTTCTGCTTGGAGGACAC |
| | | | **R:** | GCCTTGTTCTCCGAAGTTGGCACAC |
| Lysyl oxidase like-3 | Rat | LOXL-3 | **F:** | ACCCACAGTGCCAAATACGG |
| | | | **R:** | TTGCAGATGACCCCAGCATC |
| Transforming growth factor-β1 | Rat | TGF-β1 | **F:** | CCATGACATGAACCGACCCT |
| | | | **R:** | TGCCGTACACAGCAGTTCTT |
| Matrix metalloproteinase-2 | Rat | MMP-2 | **F:** | AAGAGGCCTGGTTACCCTGT |
| | | | **R:** | AAGTAGCACCTGGGAGGGAT |
| Matrix metalloproteinase-9 | Rat | MMP-9 | **F:** | TCCAGTAGACAATCCTTGCAATGTG |
| | | | **R:** | CTCCGTGATTCGAGAACTTCCAATA |
| Periostin | Rat | Periostin | **F:** | CTGCCCCGGCTATATGAGAA |
| | | | **R:** | TGTTGAGTGGTCGTGGCTC |
| Connective tissue growth factor | Rat | CTGF | **F:** | CAAGGGTCTCTTCTGCGACT |
| | | | **R:** | GTACACGGACCCACCGAAG |
| α-smooth muscle actin | Rat | α-SMA | **F:** | AGCCAGTCGCCATCAGGAAC |
| | | | **R:** | CCGGAGCCATTGTCACACAC |
| B-cell lymphoma 2 | Rat | BCL-2 | **F:** | GGATCCAGGATAACGGAGGC |
| | | | **R:** | ATGCACCCAGAGTGATGCAG |
| BCL-2- associated X protein | Rat | BAX | **F:** | CTCCCCGTGAGGTCTTCTTC |
| | | | **R:** | TCCAGTGTCCAGCCCATGAT |
| Cyclin D1 | Rat | CCND 1 | **F:** | AGGGAGATTGTGCCATCCAT |
| | | | **R:** | AAGACCTCCTCTTCGCACTTC |
| Cyclin E2 | Rat | CCNE 2 | **F:** | TCTGCATTCTGACCTGGAACC |
| | | | **R:** | GGTAATCCCAATGAGTTGAAGCA |
| Lysyl oxidase | Dog | LOX | **F:** | CGTACTACATCCAGGCGTCC |
| | | | **R:** | GGGAATCTTAGCAGCACCCT |
| Lysyl oxidase like-1 | Dog | LOXL-1 | **F:** | AGCCCGGGAACTACATCCT |
| | | | **R:** | GTAGTGGATGTTGCAACGCA |
| Lysyl oxidase like-2 | Dog | LOXL-2 | **F:** | GGAGAAGACGTACAACGCCA |
| | | | **R:** | GAGATATGAGCCTCCGTGCC |
| Lysyl oxidase like-3 | Dog | LOXL-3 | **F:** | CAGGATGCTGGAGTCCGATG |
| | | | **R:** | CCCCAGTCATCCCCACAAAT |
| Lysyl oxidase like-4 | Dog | LOXL-4 | **F:** | AGAGAACTGCCTCTCCCAGT |
| | | | **R:** | GAAGACCTCGATGCTGTGGT |
| Glucose 6-phosphate dehydrogenase | Dog | G6PD | **F:** | GGCGGTCACCAAGAACATCC |
| | | | **R:** | GCTTCTCCACGATGACACGG |

**F: Forward, R: Reverse.**

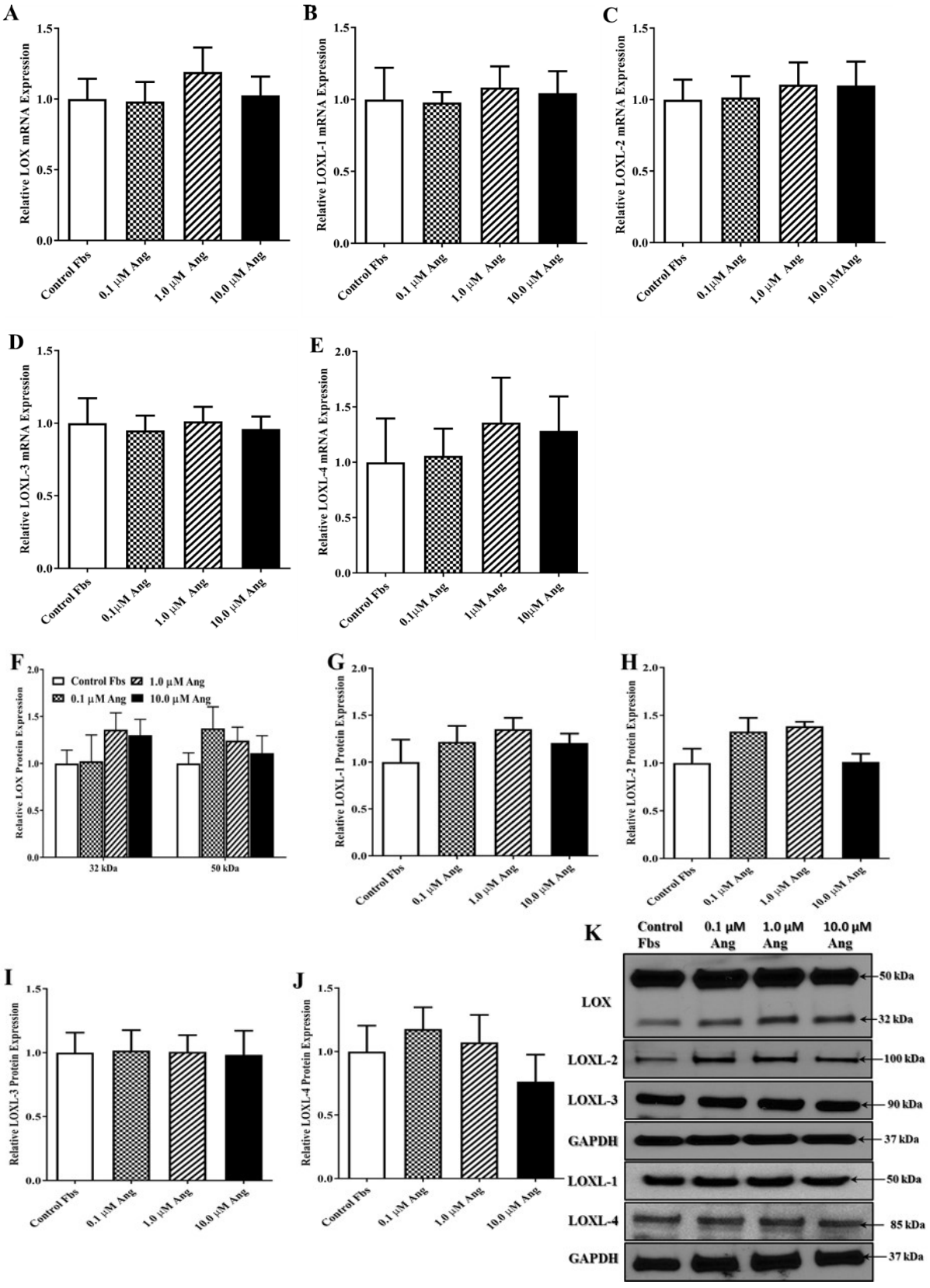
A
Relative LOX mRNA Expression
B
Relative LOXL-1 mRNA Expression
C
Relative LOXL-2 mRNA Expression
D
Relative LOXL-3 mRNA Expression
E
Relative LOXL-4 mRNA Expression
F
Control Fbs
1.0 µM Ang
0.1 µM Ang
10.0 µM Ang
Relative LOX Protein Expression
32 kDa
50 kDa
G
Relative LOXL-1 Protein Expression
H
Relative LOXL-2 Protein Expression
I
Relative LOXL-3 Protein Expression
J
Relative LOXL-4 Protein Expression
K
Control Fbs
0.1 µM Ang
1.0 µM Ang
10.0 µM Ang
LOX
50 kDa
32 kDa
LOXL-2
100 kDa
LOXL-3
90 kDa
GAPDH
37 kDa
LOXL-1
50 kDa
LOXL-4
85 kDa
GAPDH
37 kDa

**Figure S1.**

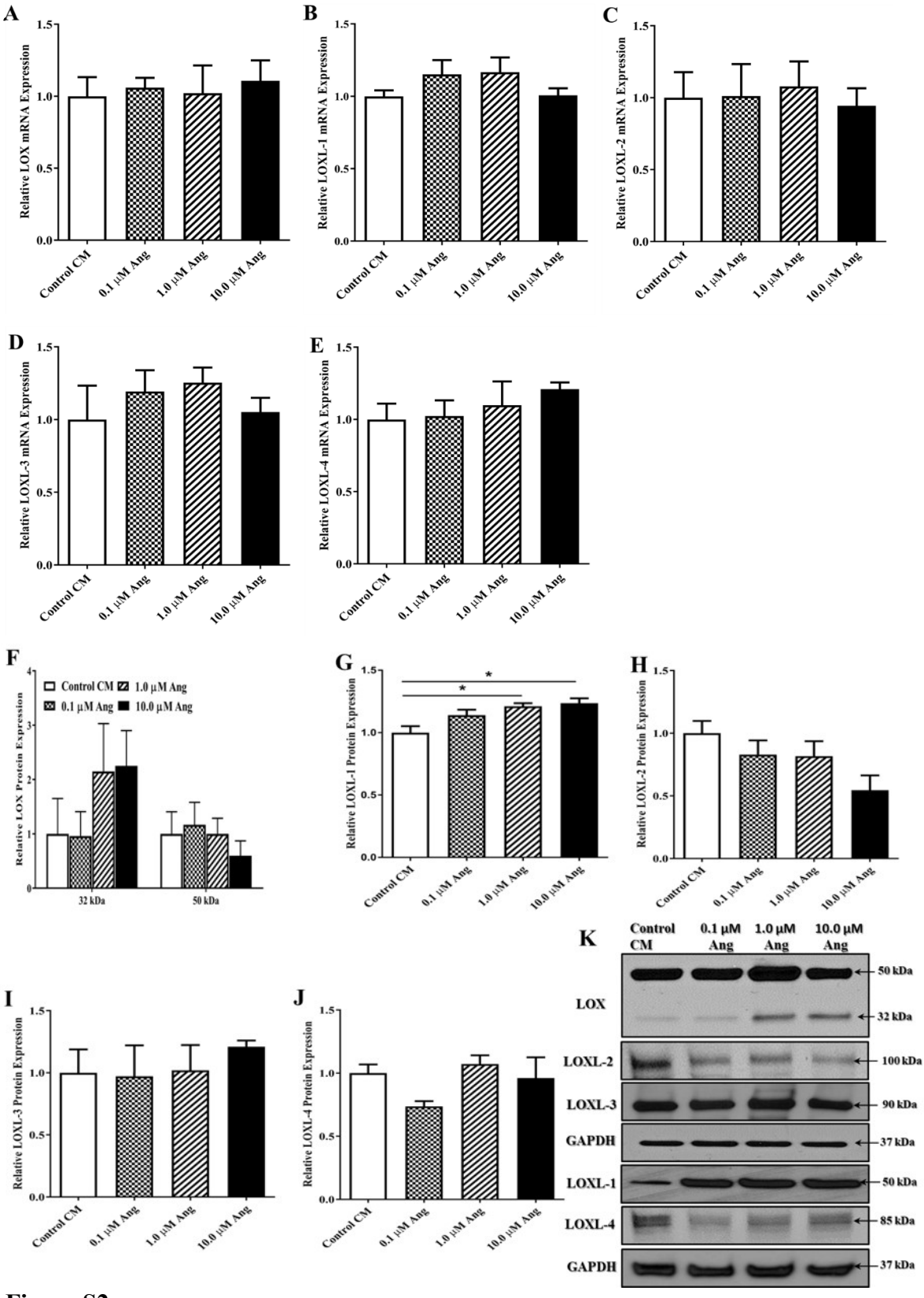
A
Relative LOX mRNA Expression
B
Relative LOXL-1 mRNA Expression
C
Relative LOXL-2 mRNA Expression
D
Relative LOXL-3 mRNA Expression
E
Relative LOXL-4 mRNA Expression
F
Control CM
0.1 μM Ang
1.0 μM Ang
10.0 μM Ang
Relative LOX Protein Expression
32 kDa
50 kDa
G
Relative LOXL-1 Protein Expression
H
Relative LOXL-2 Protein Expression
I
Relative LOXL-3 Protein Expression
J
Relative LOXL-4 Protein Expression
K
Control CM
0.1 μM Ang
1.0 μM Ang
10.0 μM Ang
LOX
LOXL-2
LOXL-3
GAPDH
LOXL-1
LOXL-4
GAPDH
50 kDa
32 kDa
100 kDa
90 kDa
37 kDa
50 kDa
85 kDa
37 kDa

**Figure S2.**

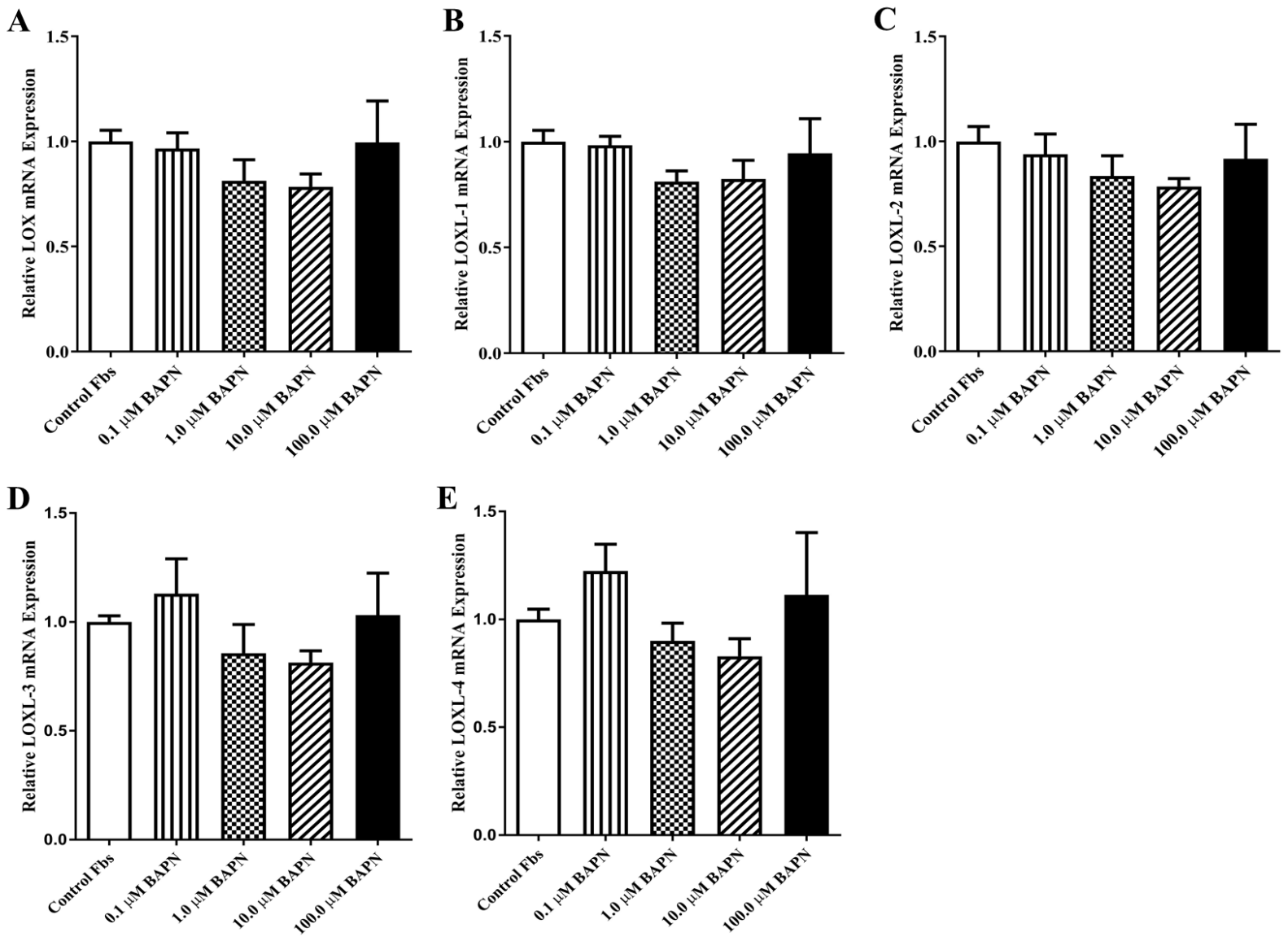
A
Relative LOX mRNA Expression
1.5
1.0
0.5
0.0
Control Fbs
0.1 μM BAPN
1.0 μM BAPN
10.0 μM BAPN
100.0 μM BAPN
B
Relative LOXL-1 mRNA Expression
C
Relative LOXL-2 mRNA Expression
D
Relative LOXL-3 mRNA Expression
E
Relative LOXL-4 mRNA Expression

**Figure S3.**

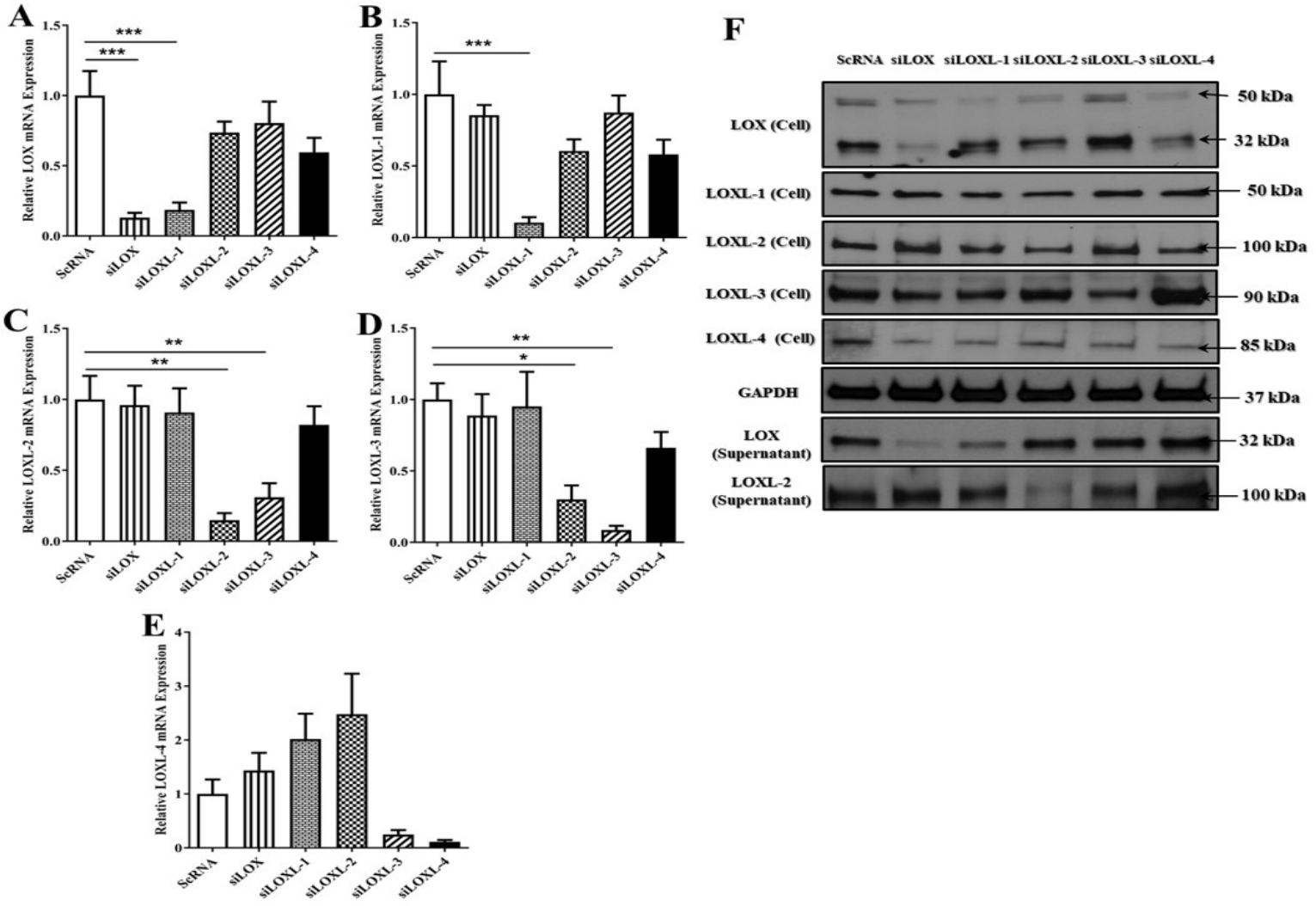
A
Relative LOX mRNA Expression
***
***
B
Relative LOXL-1 mRNA Expression
***
C
Relative LOXL-2 mRNA Expression
**
**
D
Relative LOXL-3 mRNA Expression
**
*
E
Relative LOXL-4 mRNA Expression
ScRNA
siLOX
siLOXL-1
siLOXL-2
siLOXL-3
siLOXL-4
F
ScRNA siLOX siLOXL-1 siLOXL-2 siLOXL-3 siLOXL-4
LOX (Cell)
LOXL-1 (Cell)
LOXL-2 (Cell)
LOXL-3 (Cell)
LOXL-4 (Cell)
GAPDH
LOX (Supernatant)
LOXL-2 (Supernatant)
50 kDa
32 kDa
50 kDa
100 kDa
90 kDa
85 kDa
37 kDa
32 kDa
100 kDa

**Figure S4.**

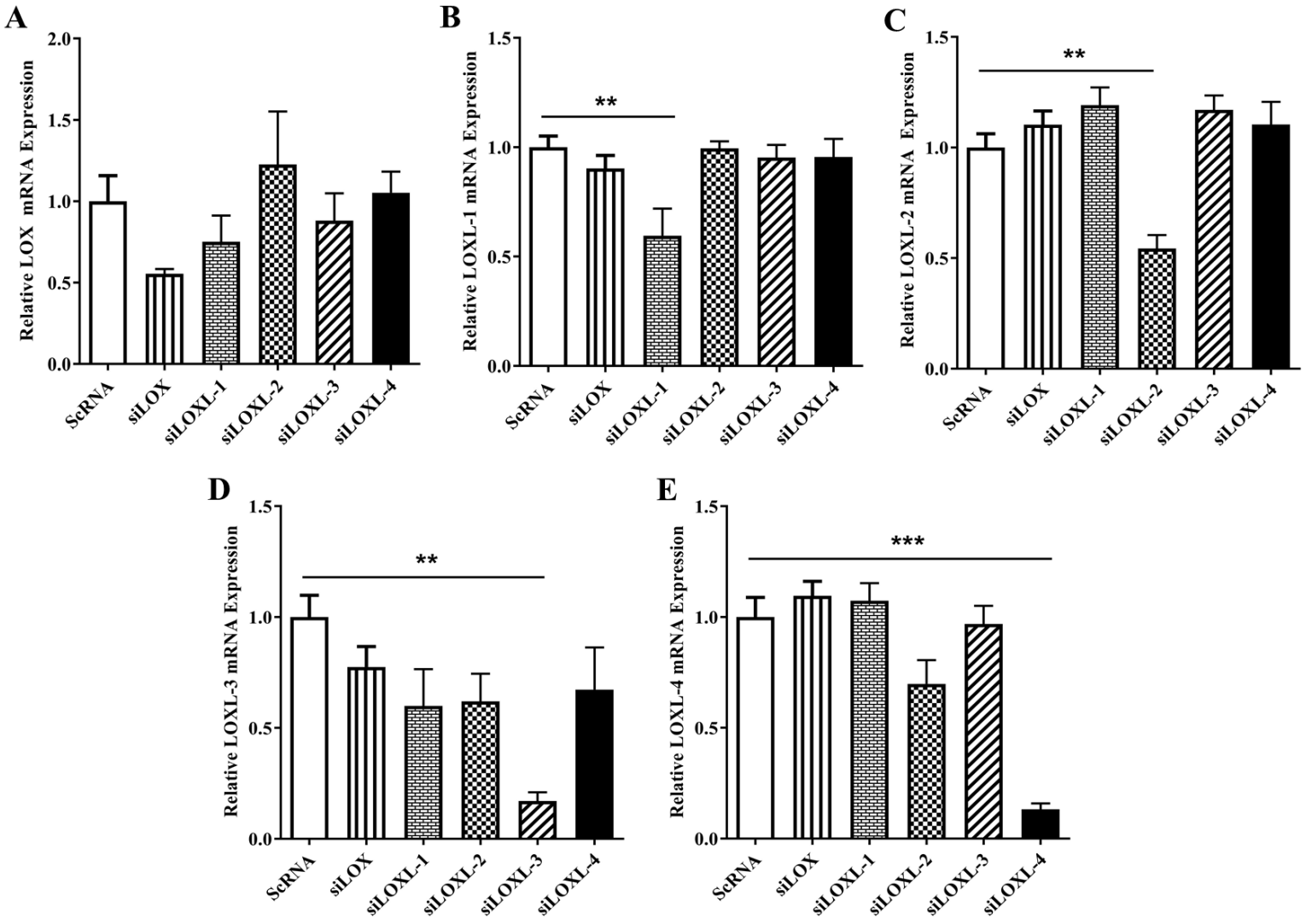
A
Relative LOX mRNA Expression
2.0
1.5
1.0
0.5
0.0
ScRNA
siLOX
siLOXL-1
siLOXL-2
siLOXL-3
siLOXL-4
B
Relative LOXL-1 mRNA Expression
1.5
1.0
0.5
0.0
**
ScRNA
siLOX
siLOXL-1
siLOXL-2
siLOXL-3
siLOXL-4
C
Relative LOXL-2 mRNA Expression
1.5
1.0
0.5
0.0
**
ScRNA
siLOX
siLOXL-1
siLOXL-2
siLOXL-3
siLOXL-4
D
Relative LOXL-3 mRNA Expression
1.5
1.0
0.5
0.0
**
ScRNA
siLOX
siLOXL-1
siLOXL-2
siLOXL-3
siLOXL-4
E
Relative LOXL-4 mRNA Expression
1.5
1.0
0.5
0.0
***
ScRNA
siLOX
siLOXL-1
siLOXL-2
siLOXL-3
siLOXL-4

**Figure S5.**

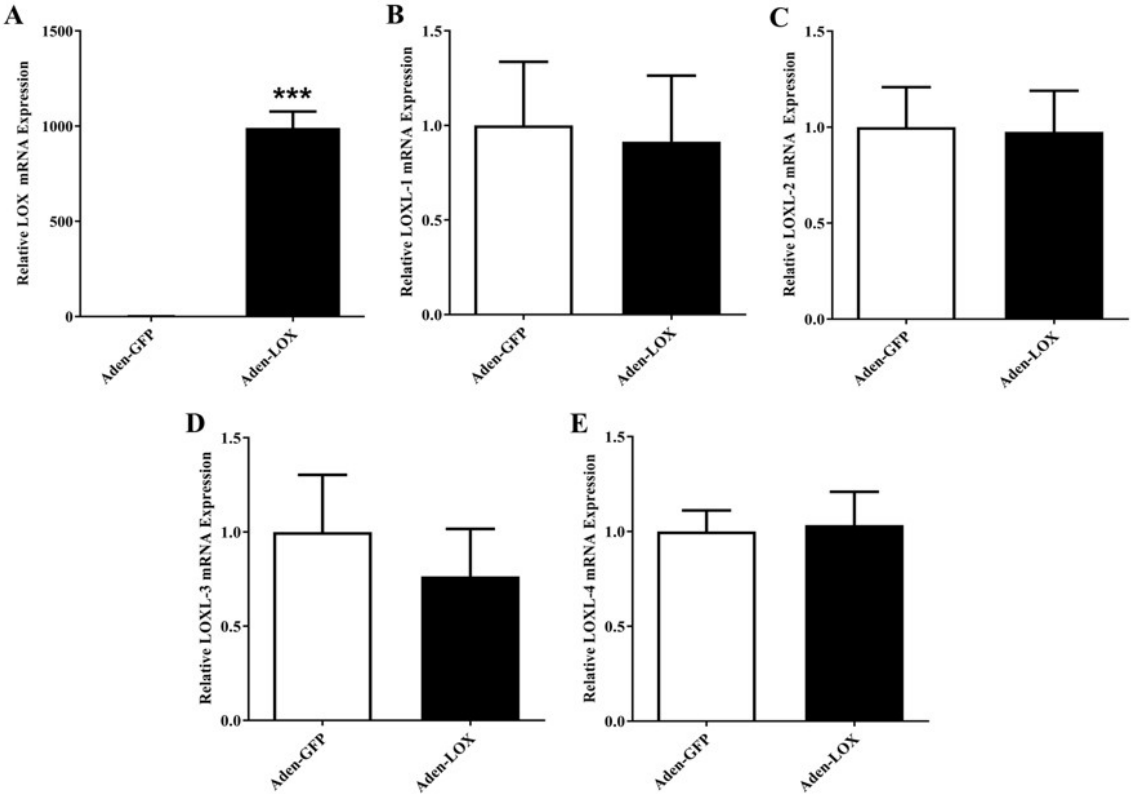
A
Relative LOX mRNA Expression
1500
1000
500
0
***
Aden-GFP
Aden-LOX
B
Relative LOXL-1 mRNA Expression
1.5
1.0
0.5
0.0
Aden-GFP
Aden-LOX
C
Relative LOXL-2 mRNA Expression
1.5
1.0
0.5
0.0
Aden-GFP
Aden-LOX
D
Relative LOXL-3 mRNA Expression
1.5
1.0
0.5
0.0
Aden-GFP
Aden-LOX
E
Relative LOXL-4 mRNA Expression
1.5
1.0
0.5
0.0
Aden-GFP
Aden-LOX

**Figure S6.**

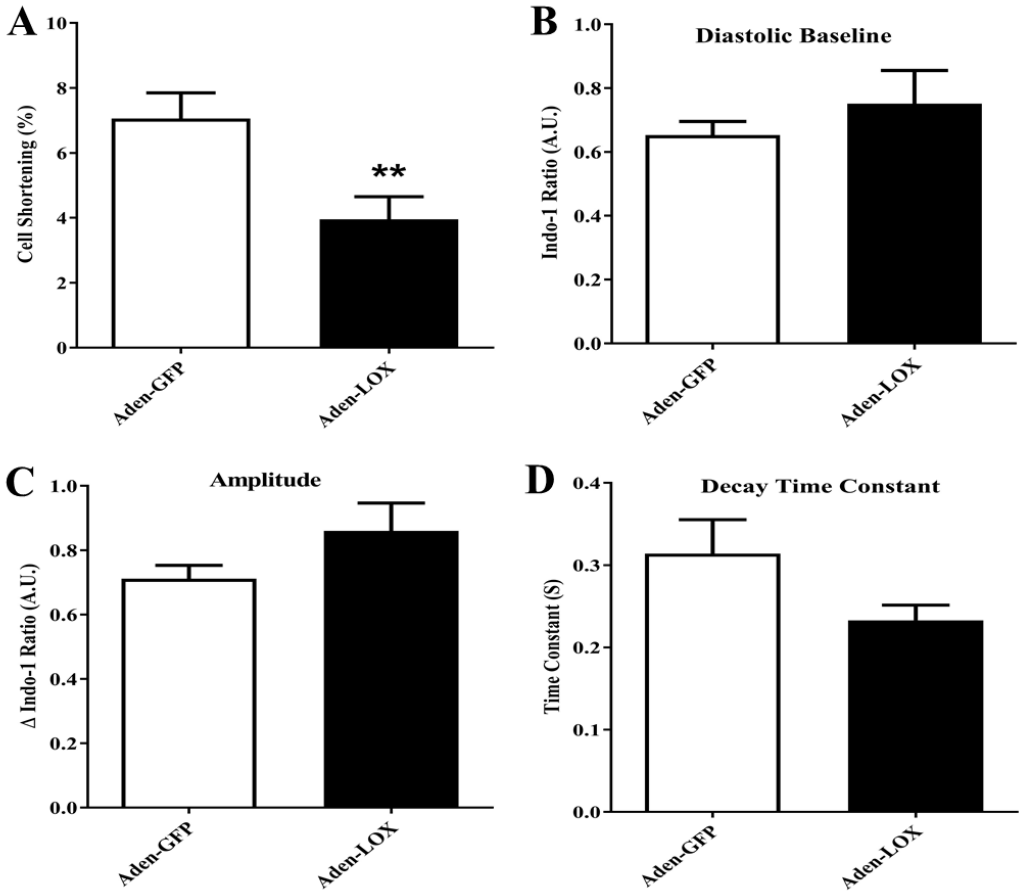
A
Cell Shortening (%)
10
8
6
4
2
0
**
Aden-GFP
Aden-LOX
B
Diastolic Baseline
Indo-1 Ratio (A.U.)
1.0
0.8
0.6
0.4
0.2
0.0
Aden-GFP
Aden-LOX
C
Amplitude
Δ Indo-1 Ratio (A.U.)
1.0
0.8
0.6
0.4
0.2
0.0
Aden-GFP
Aden-LOX
D
Decay Time Constant
Time Constant (S)
0.4
0.3
0.2
0.1
0.0
Aden-GFP
Aden-LOX

**Figure S7.**

# Chapter 4: General discussion and conclusions

## 1. Major findings and original contribution to the literature

Our *in vivo* and *in vitro* studies revealed a composite representation of lysyl oxidase (LOX) and LOX-like (LOXL) protein roles in the AF pathophysiology, including the following: (a) an upregulation of LOX and LOXL-1 in tissues, LOX and LOXL-2 in fibroblasts and LOX, LOXL-1, LOXL-3 and LOXL-4 in myocytes from the left atrium (LA) of congestive heart failure (CHF) dogs, (b) a significant improvement of LA electrical remodeling and reduction of atrial fibrillation (AF) inducibility upon β-aminopropionitrile (BAPN) administration following myocardial infarction (MI), (c) a substantial reduction in LA fibrosis and amelioration of LA structural remodeling without any significant alterations in LV fibrosis and remodeling upon BAPN administration following MI, (d) a significant reduction in transcript levels of LOXL-1, LOXL-2 and LOXL-3 along with some profibrotic markers in LA tissues without variations of those in LV tissues upon administration of BAPN post-MI, (e) secretion of LOX and LOXL-2 from cardiac fibroblasts and myocytes, (f) a significant increase in the extracellular LOX immunoreactivity in cardiac fibroblasts and LOXL-2 immunoreactivity in cardiac myocytes upon Ang II stimulation, (g) a possible role of LOXL-2, LOXL-3 and LOXL-4 in collagen synthesis and fibroblast proliferation, (h) evidence for a possible protective function of LOXL-4 against apoptosis in cardiac fibroblasts and myocytes through decreasing the ratio of BAX/BCL-2 mRNA and (i) evidence for a role of LOX or LOXL-1 in cardiac myocyte contractile dysfunction. These findings have not been previously reported in the literature; thus, our major findings are considered as original contributions to the literature.

## 2. Discussion and relationship to prior work area

We used an *in vivo* MI rat model to study the functions of LOX isoforms in LA fibrosis and AF, followed by an *in vitro* study to characterize the roles of each LOX isoform in cardiac fibroblast and myocyte functions. LOX isoforms are involved in many functions apart from elastin and collagen cross-linking, such as control of cell migration, ras oncogene inhibition, epithelial-mesenchymal transition, cell adhesion, chemotaxis, gene regulation, transformation, collagen promotor activation and cell growth [343-347]. In cardiac tissues, LOX and LOXL-2 have an extracellular function through collagen cross-linking [337, 348]. However, the intracellular functions of LOX isoforms in the heart have not been addressed. To date, limited information has been reported on the synthesis and upregulation of LOX and LOXL proteins in cardiomyocytes during cardiac diseases. Atrial interstitial fibrosis and AF susceptibility were increased in a CHF dog model [349]. Nevertheless, the underlying mechanism is not clearly understood. We found a significant upregulation of LOX and LOXL-1 in tissues, LOX and LOXL-2 in fibroblasts and LOX, LOXL-1, LOXL-3 and LOXL-4 in myocytes from the LA of CHF dogs. These results, for the first time, revealed that LOX isoforms in cardiac myocytes and fibroblasts may contribute to LA structural remodeling during CHF progression. This observation revealed a new important regulatory mechanism in controlling ECM deposition, LA fibrosis and AF during CHF development. In our *in vitro* study, LOX and LOXL-2 proteins were secreted from neonatal rat ventricular fibroblasts and myocytes. LOX is secreted from cardiac fibroblast [342] and is crucial for stability and strength of collagen by catalyzing the cross-linking process [350]. Under normal conditions, cardiac fibroblasts communicate with myocytes to maintain cardiac functions [63]. Cardiomyocytes secrete TGF-β, Ang II and other profibrotic

molecules, which induce ECM protein synthesis, differentiation and proliferation of fibroblasts, resulting in interstitial fibrosis [67, 85]. Ang II induces cardiac fibrosis in a wide range of heart diseases, such as MI, CHF, cardiomyopathy and hypertension [13]. Upregulation of LOX mediates myocardial stiffness and fibrosis through increasing the cross-linking and deposition of collagen [6]. Adam *et al.* [280] reported that the intracellular protein expression of LOX in cardiac fibroblasts was increased upon treatment with Ang II. We found that secretion of LOX and LOXL-2 was increased in the cultured neonatal rat ventricular fibroblasts and myocytes along with an increase in the collagen cross-linking ratio in cultured cardiac fibroblasts upon treatment with Ang II. These results suggested that the secreted LOX and LOXL-2 from cardiac myocytes and fibroblasts may contribute to ECM remodeling.

Recently, LOX isoforms have been shown to play a prominent role in left ventricular (LV) fibrosis in a variety of animal models [335-337, 339, 342, 351]. BAPN improved cardiac function and decreased LV fibrosis without changing the expression of LOX isoforms [342]. Adam *et al.* [280] reported that LA fibrosis and LOX expression were increased in AF patients. LOXL-2 may contribute to atrial fibrosis, which is the main substrate for AF maintenance [352]. However, none of the studies to date have examined the direct roles of LOX isoforms in atrial fibrosis and AF. MI is commonly associated with LA fibrosis, AF and high mortality rate [353-355]. In the current study, a rat MI model was used to study the roles of LOX isoforms in LA fibrosis and AF. We selected an inhibitor of LOX isoforms (BAPN) to target the signaling pathway of LA fibrosis and AF. Progressive cardiac remodeling occurs following MI, including replacement of dead cells in the infarcted area of the LV by a collagen scar, thickening of non-infarcted areas of the LA and LV and

thinning of the infarcted LV wall [310, 355-358]. MI mice showed an increase in LV reparative fibrosis along with an increase in LOX isoform expression [342].

During stressful conditions such as MI or chronic pressure overload, cardiac fibroblasts and myofibroblasts are the major cells that are responsible for promoting cardiac fibrosis [40, 359]. Activated fibroblasts and myofibroblasts secrete numerous profibrogenic molecules, such as COL1, COL3, TGF-β, LOX isoforms, MMP, CTGF, FN, α-SMA and periostin [8, 13, 40, 98, 360]. The LOX family catalyze intra- and inter-molecular collagen cross-linking within the cardiac ECM [6, 361]. In our study, the upregulation of LOX isoform mRNA was accompanied by an increase in COL 1A1, FN 1, TGF-β1, CTGF, periostin, α-SMA and MMP-2 mRNA expression and a decrease in Cx 43 mRNA in the infarcted area of the LV. Furthermore, we noted an increase in LOXL-1, LOXL-3, COL 1A1, TGF-β1 and periostin mRNA in LA tissues post-MI. Moreover, BAPN administration post-MI reduced the mRNA of LOX isoforms along with a decrease in the mRNA of some profibrotic markers in LA tissues. However, BAPN administration post-MI had no significant effects on the mRNA of LOX isoforms and profibrotic markers in the infarcted and non-infarcted areas of the LV. Our result was consistent with the result of Gonzalez-Santamaria *et al.* [342], who reported no changes in the mRNA expression of LOX isoforms, MMP-2 and MMP-9 in the infarcted area of the LV upon BAPN administration.

Recent studies showed that atrial fibroblasts had a higher response to proliferation than ventricular fibroblasts during pathological conditions [362]. The fibrotic susceptibility was higher in the atria than the ventricles [277, 363]. We found that BAPN had a greater ability to decrease LA fibrosis than LV interstitial fibrosis post-MI. These results may indicate

that LA fibroblasts are more sensitive to BAPN than LV fibroblasts. Furthermore, LV replacement fibrosis was greater than LA and LV interstitial fibrosis post-MI. Administration of BAPN post-MI decreased LA fibrosis and the collagen cross-linking ratio without significantly changing those in the LV tissues. These results suggested that LV replacement fibrosis started earlier than LA and LV interstitial fibrosis. Therefore, the effect of BAPN was greater in LA fibrosis than LV fibrosis. Cleutjens *et al.* [364] found that myofibroblast number and collagen synthesis were higher in the infarcted area of the LV compared with the non-infarcted area of the LV post-MI. BAPN decreased collagen deposition via inhibition of LOX-induced cross-linking [341]. Our findings were not in agreement with the results of Gonzalez-Santamaria *et al.* [342], who reported that fibrosis and collagen cross-linking in the infarcted area of the LV were decreased upon administration of BAPN in mice post-MI. The discrepancy in the results may be related to the differences in the administration method and dose of BAPN as well as animal species. To date, this is the first study to explore the effect of LOX and LOXL protein inhibition on LA fibrosis and AF.

The LV remodeling induced LA remodeling as a result of blood movement from the LA to the LV [365]. Hereafter, MI impaired the structure and function of the LA and the LV, and the administration of BAPN post-MI attenuated the adverse LA remodeling without significantly changing those in the LV. The relationships of WMSI with LA dimensions, areas and FAC were reduced along with little effect on the correlations of WMSI with LV structural and functional parameters upon administration of BAPN post-MI. Moreover, LA interstitial and LV replacement fibrosis, hallmarks for structural remodeling, interrupted the propagation and conduction of cardiac impulses, resulting in AF [366]. Our *in vivo* data

demonstrated that MI increased AF inducibility and prolonged P-wave and AF durations, whereas the values of those parameters were significantly decreased upon administration of BAPN post-MI. Prolongation of the P-P interval and P-wave duration post-MI reflected a delay in the atrial conduction due to the development of LA fibrosis.

We used the siRNA approach to investigate the intracellular role of individual LOX isoforms in cardiac fibroblast and myocyte functions. Knockdown of individual LOX, LOXL-1 or LOXL-2 in cultured mouse lung fibroblasts had an impact on the expression of each other through compensatory or direct effects [367]. The cell cycle and proliferation were regulated by cyclin-dependent kinases, such as CCNE 2 and CCND 1 [368]. Knockdown of LOXL-3 in fibroblasts decreased LOXL-2, LOXL-3 and LOXL-4 mRNA expressions along with a decrease in proliferation and mRNA expression of COL 1A1, COL 3A1 and CCNE 2. The results suggested that LOXL-2, LOXL-3 and LOXL-4 play a role in fibroblast proliferation and collagen synthesis. CTGF enhances ECM protein synthesis during fibrosis progression [98, 369]. We found that knockdown of LOX or LOXL-4 decreased the amount of CTGF mRNA. Our result is consistent with the finding of Adam *et al.* [280], who reported that CTGF induces an increase in LOX protein in cultured cardiac fibroblasts. Cardiac fibrosis is associated with an upregulation of LOX isoforms that causes an imbalance between ECM synthesis and degradation [370, 371]. Kendall and Feghali-Bostwick [47] reported that the upregulation of α-SMA expression is a marker of differentiation of fibroblasts into myofibroblasts. Knocking down of LOXL-2 in cardiac fibroblasts decreased the abundance of LOXL-2 and LOXl-3 mRNA along with an increase in α-SMA mRNA. These results indicated a synergistic effect of LOXL-2 and LOXL-3 in preventing the differentiation of fibroblasts into myofibroblasts. An increase in the BAX/BCL-2

expression ratio is a sign of cellular susceptibility to apoptosis [372]. Upon knockdown of LOXL-4, the mRNA expression of the BAX/BCL-2 ratio was significantly increased in cardiac myocytes and fibroblasts. These results suggested that LOXL-4 may protect against apoptosis of cardiac fibroblasts and myocytes.

HF is characterized by impaired excitation-contraction coupling along with abnormalities in $Ca^{2+}$ handling [132, 373]. We noted that contractility of canine LA myocytes was improved upon knockdown of LOX or LOXL-1 and impaired upon overexpression of LOX, while there was no significant change in the $Ca^{2+}$ transient. The contractile dysfunction of CHF myocytes occurs due to alterations in myofilament function or $Ca^{2+}$ handling [374]. Our data provided the first evidence that LOX or LOXL-1 may have a significant role in myocyte contractility via alterations in contractile protein function.

## 3. Potential limitations

There were limitations to the current study that should be addressed. First, we used a LOX inhibitor (BAPN) that had non-specific effects on LOX isoforms. In this study, the cardioprotective effects of BAPN post-MI in the LA tissues resulted from the inhibition of all LOX isoforms. Second, the present study revealed significant changes in the transcript levels of LOX isoforms without significant changes at the protein level for LOX isoforms in the LA tissues. It is possible that the significant changes observed at the mRNA level may result in the small changes at the protein level of each LOX isoform. The sum of these small changes in protein levels of all LOX isoforms may result in a significant effect on cardiac fibrosis. Third, we used non-specific siRNA for LOXL-1, LOXL-2 and LOXL-3 in neonatal rat ventricular fibroblasts and myocytes. Finally, there is a need for further

investigations to understand the role of individual LOX isoforms in signal transduction pathways of LA fibrosis and AF.

## 4. Future research directions

A limited number of synthesized molecules have been used as inhibitors targeting LOX isoforms in the treatment of fibrous diseases due to their specificity, efficiency and safety issues. In our study, BAPN had beneficial effects in attenuating atrial fibrosis and decreasing AF inducibility in rats post-MI. Furthermore, we did not observe any toxic effect of BAPN administration for three consecutive weeks in either the sham or MI rats. Patients treated with large doses of BAPN for long periods showed toxic and undesirable effects that had not been observed in animals [375]. Long-term treatment of scleroderma patients with BAPN is extremely dangerous [376, 377]. Keiser and Sjoerdsma [376] reported that BAPN administration up to 3.5 g per single dose or 2.0 g per day for five consecutive days had no toxic effect in scleroderma patients. Peacock and Madden [378] stated that BAPN treatment up to 5, 4, 3, 2 and 2 g for 12, 15, 20, 21 and 14 days, respectively, yielded unexpected signs and symptoms (e.g., fever, elevated serum glutamic oxaloacetic transaminase, gastrointestinal irritability, dermatitis and eosinophilia) in patients with lacerated flexor tendons, whereas BAPN treatment up to 67 days caused lathyrism in scleroderma patients. Moreover, Peacock and Madden [375] revealed that treatment of posterior urethral strictures with 1 g/day of BAPN for 21 days had no toxic effects or unwanted symptoms in humans. Thus, the future use of BAPN as a drug for AF patients should be limited to clinical circumstances in which short-term therapy would be recommended. Further studies will be required to define the pharmacological properties of

BAPN to control lathyrism and unwanted symptoms in AF patients. Overall, there is still a need for future clinical studies to assess the therapeutic implications, safety and feasibility of BAPN in AF patients.

In addition to the potential therapeutic role of the LOX family in AF, serum levels of LOXL-2 were significantly increased and correlated with the atrial fibrous tissue content in AF patients [379]. Yang *et al.* [348] reported that serum levels of LOXL-2 were elevated and correlated with HF biomarkers in HF patients. Furthermore, LOX expression and collagen cross-linking were increased in the atrial tissues of AF patients compared with those in sinus rhythm patients [280]. Currently, the optimal AF biomarker is still unknown. Therefore, there is a growing need for the identification of new serum or tissue biomarkers for AF that are capable of categorizing patients at substantial risk for AF and estimating the prognosis and severity of AF. Further clinical investigation is required to correlate the levels of individual LOX isoforms in the blood with prognosis and severity of AF. It is expected that additional investigation of LOX family isoforms as potential biomarkers may substantially contribute to the development of early diagnosis and treatment for AF and pathological cardiac remodeling.

Further *in vivo* investigations are needed to confirm our *in vitro* results through genetic inhibition of individual LOX isoforms in cardiac myocytes or fibroblasts to understand the exact underlying mechanisms of each LOX or LOXL protein in AF pathophysiology. We could use LOX or LOXL protein knockout mice that are crossed with cell-specific promoters, including transcription factor 21 for fibroblasts and alpha-myosin heavy chain for cardiomyocytes. Deletion of each LOX isoform in cardiac fibroblasts or

myocytes may help to interpret the roles of each LOX isoform in the signaling pathways of atrial fibrosis and AF.

In our study, we found that the administration of BAPN post-MI significantly decreased the mRNA expression of TGF-β in LA tissues. It is necessary to further study the effect of BAPN on TGF-β signaling, including canonical and non-canonical pathways, that are important in atrial fibrosis and AF development. In our *in vitro* study, we used siRNA-mediated knockdown of LOX isoforms to assess the precise intracellular role of LOX isoforms in regulating cardiac myocyte and fibroblast functions. There is a need to confirm the protective function of LOXL-4 against apoptosis in cardiac fibroblasts and myocytes using other techniques, such as annexin v staining. It would be interesting to conduct microarray analyses for several genes that are involved in AF, such as $Ca^{2+}$ handling genes, ion channels, contractile proteins and profibrotic factors, following knockdown of each LOX isoform or use of catalytically incompetent LOX variants in cardiac myocytes and fibroblasts. Furthermore, the effect of LOX or LOXL-1 on contractility of cardiomyocytes without any concomitant change in $Ca^{2+}$ transients needs further investigation to clarify whether LOX or LOXL-1 can have a direct impact on the contractile proteins or an indirect effect through other signaling pathways.

## 5. Conclusions

In conclusion, BAPN reversed structural remodeling and decreased AF inducibility along with suppression of LOX isoform and profibrotic marker expression, collagen cross-linking and fibrosis in the LA post-MI. Our findings provide a new strategy targeting the LOX family signaling pathway in atrial fibrosis-induced AF. The results from the present

study provide novel evidence regarding the beneficial effects of BAPN administration on the electrical and structural remodeling of LA post-MI. The expressions of LOX and LOXL-1 in tissues, LOX and LOXL-2 in fibroblasts and LOX, LOXL-1, LOXL-3 and LOXL-4 in myocytes from the LA of CHF model were increased compared with those in the control. Moreover, LOX and LOXL-2 were secreted from cultured neonatal rat ventricular myocytes and fibroblasts. The secreted LOX and LOXL-2 from cultured neonatal rat ventricular fibroblasts and myocytes were increased along with an increase in collagen cross-linking in cultured fibroblasts upon treatment with Ang II. LOXL-2, LOXL-3 and LOXL-4 may have a role in fibroblast proliferation and collagen synthesis. LOXL-4 may exhibit a protective function against apoptosis by decreasing the ratio of mRNA BAX/BCL-2 in fibroblasts and myocytes. LOX and LOXL-1 reduced the contractility of cardiomyocytes along with slight changes in $Ca^{2+}$ transients. We conclude that the intracellular LOXL-2, LOXL-3 and LOXL-4 as well as extracellular LOX and LOXL-2 in cardiac fibroblasts and myocytes may have roles in regulating the cardiac fibrotic response. *In vivo* and *in vitro* findings illustrated new innovative and important regulatory functions of each LOX isoform at the intra- and extra-cellular levels in structural remodeling, ECM protein deposition, myocardial fibrosis and AF. The role of each LOX isoform in the signal transduction pathways of LA fibrosis and AF requires further investigation.

## References


1. Krenning G, Zeisberg EM, Kalluri R. The origin of fibroblasts and mechanism of cardiac fibrosis. *Journal of Cellular Physiology* 2010;**225**:631-637.

2. Nicoletti A, Michel JB. Cardiac fibrosis and inflammation: Interaction with hemodynamic and hormonal factors. *Cardiovascular Research* 1999;**41**:532-543.

3. Murtha LA, Schuliga MJ, Mabotuwana NS, Hardy SA, Waters DW, Burgess JK, Knight DA, Boyle AJ. The processes and mechanisms of cardiac and pulmonary fibrosis. *Frontiers in Physiology* 2017;**8**:777.

4. Erler JT, Bennewith KL, Nicolau M, Dornhofer N, Kong C, Le QT, Chi JT, Jeffrey SS, Giaccia AJ. Lysyl oxidase is essential for hypoxia-induced metastasis. *Nature* 2006;**440**:1222-1226.

5. Lucero HA, Kagan HM. Lysyl oxidase: An oxidative enzyme and effector of cell function. *Cellular and Molecular Life Sciences* 2006;**63**:2304-2316.

6. Lopez B, Gonzalez A, Hermida N, Valencia F, de Teresa E, Diez J. Role of lysyl oxidase in myocardial fibrosis: From basic science to clinical aspects. *American Journal of Physiology Heart and Circulatory Physiology* 2010;**299**:H1-9.

7. Organization WH. Global status report on noncommunicable diseases. *Geneva: World Health Organization* 2014.

8. Murtha LA, Schuliga MJ, Mabotuwana NS, Hardy SA, Waters DW, Burgess JK, Knight DA, Boyle AJ. The processes and mechanisms of cardiac and pulmonary fibrosis. *Frontiers in Physiology* 2017;**8**:777.

9. Cieslik KA, Trial J, Crawford JR, Taffet GE, Entman ML. Adverse fibrosis in the aging heart depends on signaling between myeloid and mesenchymal cells; role of inflammatory fibroblasts. *Journal of Molecular and Cellular Cardiology* 2014;**70**:56-63.

10. Chen W, Frangogiannis NG. The role of inflammatory and fibrogenic pathways in heart failure associated with aging. *Heart Failure Reviews* 2010;**15**:415-422.

11. Burashnikov A, Di Diego JM, Sicouri S, Doss MX, Sachinidis A, Barajas-Martinez H, Hu D, Minoura Y, Sydney Moise N, Kornreich BG, Chi L, Belardinelli L, Antzelevitch C. A temporal window of vulnerability for development of atrial fibrillation with advancing heart failure. *European Journal of Heart Failure* 2014;**16**:271-280.

12. Camm AJ, Kirchhof P, Lip GYH, Schotten U, Savelieva I, Ernst S, Van Gelder IC, Al-Attar N, Hindricks G, Prendergast B, Heidbuchel H, Alfieri O, Angelini A, Atar D, Colonna P, De Caterina R, De Sutter J, Goette A, Gorenek B, Heldal M, Hohloser SH, Kolh P, Le Heuzey J-Y, Ponikowski P, Rutten FH, Guidelines ESCCfP, Vahanian A, Auricchio A, Bax J, Ceconi C, Dean V, Filippatos G, Funck-Brentano C, Hobbs R, Kearney P, McDonagh T, Popescu BA, Reiner Z, Sechtem U, Sirnes PA, Tendera M, Vardas PE, Widimsky P, Document R, Vardas PE, Agladze V, Aliot E, Balabanski T, Blomstrom-Lundqvist C, Capucci A, Crijns H, Dahlöf B, Folliguet T, Glikson M, Goethals M, Gulba DC, Ho SY, Klautz RJM, Kose S, McMurray J, Perrone Filardi P, Raatikainen P, Salvador MJ, Schalij MJ, Shpektor A, Sousa J, Stepinska J, Uuetoa H, Zamorano JL, Zupan I. Guidelines for the management of atrial fibrillation: The task force for the management of atrial fibrillation of the European Society of Cardiology (ESC). *Europace* 2010;**31**:2369-2429.

13. Nattel S, Burstein B, Dobrev D. Atrial remodeling and atrial fibrillation: Mechanisms and implications. *Circulation Arrhythmia and Electrophysiology* 2008;**1**:62-73.

14. Allessie MA, Boyden PA, Camm AJ, Kleber AG, Lab MJ, Legato MJ, Rosen MR, Schwartz PJ, Spooner PM, Van Wagoner DR, Waldo AL. Pathophysiology and prevention of atrial fibrillation. *Circulation* 2001;**103**:769-777.

15. Rose-Jones LJ, Bode WD, Gehi AK. Current approaches to antiarrhythmic therapy in heart failure. *Heart Failure Clinics* 2014;**10**:635-652.

16. Miyazaki S, Shah AJ, Scherr D, Haïssaguerre M. Atrial fibrillation: Pathophysiology and current therapy. *Annals of Medicine* 2011;**43**:425-436.

17. Barrett KE, Barman SM, Boitano S, Brooks HL. Notice. Ganong's Review of Medical Physiology, 25e. New York, NY: McGraw-Hill Education, 2016.

18. Whitaker RH. Anatomy of the heart. *Medicine* 2010;**38**:333-335.

19. Mahadevan V. Anatomy of the heart. *Surgery (Oxford)* 2018;**36**:43-47.

20. Weinhaus AJ, Roberts KP. Anatomy of the human heart. In: Iaizzo PA, ed. Handbook of Cardiac Anatomy, Physiology, and Devices. Totowa, NJ: Humana Press, 2005:51-79.

21. Guyton AC. The relationship of cardiac output and arterial pressure control. *Circulation* 1981;**64**:1079-1088.

22. Hall JE. Guyton and Hall: Textbook of Medical Physiology. *Surgical Neurology International* 2017;**8**:275.

23. Antzelevitch C, Burashnikov A. Overview of basic mechanisms of cardiac arrhythmia. *Cardiac Electrophysiology Clinics* 2011;**3**:23-45.

24. Harikumar R, Shivappriya SN. Analysis of QRS detection algorithm for cardiac abnormalities. *International Journal of Soft Computing and Engineering* 2011;**1**:80-88.

25. Pinto AR, Ilinykh A, Ivey MJ, Kuwabara JT, D'Antoni ML, Debuque R, Chandran A, Wang L, Arora K, Rosenthal NA, Tallquist MD. Revisiting cardiac cellular composition. *Circulation Research* 2016;**118**:400-409.

26. Chen Y. Molecular regulation of atrial-selective fibrotic remodeling and its role in atrial fibrillation *PhD Thesis at McGill University* 2015:1-246.

27. Gersch C, Dewald O, Zoerlein M, Michael LH, Entman ML, Frangogiannis NG. Mast cells and macrophages in normal C57/BL/6 mice. *Histochemistry and Cell Biology* 2002;**118**:41-49.

28. Ieda M, Tsuchihashi T, Ivey KN, Ross RS, Hong TT, Shaw RM, Srivastava D. Cardiac fibroblasts regulate myocardial proliferation through beta1 integrin signaling. *Developmental Cell* 2009;**16**:233-244.

29. Banerjee I, Fuseler JW, Price RL, Borg TK, Baudino TA. Determination of cell types and numbers during cardiac development in the neonatal and adult rat and mouse. *American Journal of Physiology Heart and Circulatory Physiology* 2007;**293**:H1883-1891.

30. Vliegen HW, van der Laarse A, Cornelisse CJ, Eulderink F. Myocardial changes in pressure overload-induced left ventricular hypertrophy. A study on tissue composition, polyploidization and multinucleation. *European Heart Journal* 1991;**12**:488-494.

31. Ahuja P, Sdek P, MacLellan WR. Cardiac myocyte cell cycle control in development, disease, and regeneration. *Physiological Reviews* 2007;**87**:521-544.

32. Severs NJ. The cardiac muscle cell. *Bioessays* 2000;**22**:188-199.

33. Vasquez C, Benamer N, Morley GE. The cardiac fibroblast: Functional and electrophysiological considerations in healthy and diseased hearts. *Journal of Cardiovascular Pharmacology* 2011;**57**:380-388.

34. Porter KE, Turner NA. Cardiac fibroblasts: At the heart of myocardial remodeling. *Pharmacology and Therapeutics* 2009;**123**:255-278.

35. Zeisberg EM, Tarnavski O, Zeisberg M, Dorfman AL, McMullen JR, Gustafsson E, Chandraker A, Yuan X, Pu WT, Roberts AB, Neilson EG, Sayegh MH, Izumo

S, Kalluri R. Endothelial-to-mesenchymal transition contributes to cardiac fibrosis. *Nature Medicine* 2007;**13**:952-961.

36. van Tuyn J, Atsma DE, Winter EM, van der Velde-van Dijke I, Pijnappels DA, Bax NA, Knaan-Shanzer S, Gittenberger-de Groot AC, Poelmann RE, van der Laarse A, van der Wall EE, Schalij MJ, de Vries AA. Epicardial cells of human adults can undergo an epithelial-to-mesenchymal transition and obtain characteristics of smooth muscle cells *in vitro*. *Stem Cells* 2007;**25**:271-278.

37. Zhou B, von Gise A, Ma Q, Hu YW, Pu WT. Genetic fate mapping demonstrates contribution of epicardium-derived cells to the annulus fibrosis of the mammalian heart. *Developmental Biology* 2010;**338**:251-261.

38. van Amerongen MJ, Bou-Gharios G, Popa E, van Ark J, Petersen AH, van Dam GM, van Luyn MJ, Harmsen MC. Bone marrow-derived myofibroblasts contribute functionally to scar formation after myocardial infarction. *The Journal of Pathology* 2008;**214**:377-386.

39. Souders CA, Bowers SL, Baudino TA. Cardiac fibroblast: The renaissance cell. *Circulation Research* 2009;**105**:1164-1176.

40. Talman V, Ruskoaho H. Cardiac fibrosis in myocardial infarction from repair and remodeling to regeneration. *Cell and Tissue Research* 2016;**365**:563-581.

41. Lajiness JD, Conway SJ. The dynamic role of cardiac fibroblasts in development and disease. *Journal of Cardiovascular Translational Research* 2012;**5**:739-748.

42. Kuhn B, del Monte F, Hajjar RJ, Chang YS, Lebeche D, Arab S, Keating MT. Periostin induces proliferation of differentiated cardiomyocytes and promotes cardiac repair. *Nature Medicine* 2007;**13**:962-969.

43. Ongstad E, Kohl P. Fibroblast-myocyte coupling in the heart: Potential relevance for therapeutic interventions. *Journal of Molecular and Cellular Cardiology* 2016;**91**:238-246.

44. Li GR, Sun HY, Chen JB, Zhou Y, Tse HF, Lau CP. Characterization of multiple ion channels in cultured human cardiac fibroblasts. *Plos One* 2009;**4**:e7307.

45. Isenberg G, Kazanski V, Kondratev D, Gallitelli MF, Kiseleva I, Kamkin A. Differential effects of stretch and compression on membrane currents and $[Na^+]_c$ in ventricular myocytes. *Progress in Biophysics and Molecular Biology* 2003;**82**:43-56.

46. Kamkin A, Kiseleva I, Isenberg G, Wagner KD, Gunther J, Theres H, Scholz H. Cardiac fibroblasts and the mechano-electric feedback mechanism in healthy and diseased hearts. *Progress in Biophysics and Molecular Biology* 2003;**82**:111-120.

47. Kendall RT, Feghali-Bostwick CA. Fibroblasts in fibrosis: Novel roles and mediators. *Frontiers in Pharmacology* 2014;**5**:123.

48. Chistiakov DA, Orekhov AN, Bobryshev YV. The role of cardiac fibroblasts in post-myocardial heart tissue repair. *Experimental and Molecular Pathology* 2016;**101**:231-240.

49. van Nieuwenhoven FA, Turner NA. The role of cardiac fibroblasts in the transition from inflammation to fibrosis following myocardial infarction. *Vascular Pharmacology* 2013;**58**:182-188.

50. Frangogiannis NG. Pathophysiology of myocardial infarction. *Comprehensive Physiology* 2015;**5**:1841-1875.

51. Zhao L, Eghbali-Webb M. Release of pro- and anti-angiogenic factors by human cardiac fibroblasts: Effects on DNA synthesis and protection under hypoxia in human endothelial cells. *Biochimica et Biophysica Acta* 2001;**1538**:273-282.

52. Catalucci D, Latronico MV, Ellingsen O, Condorelli G. Physiological myocardial hypertrophy: How and why? *Frontiers in Bioscience* 2008;**13**:312-324.

53. Holmes JW, Borg TK, Covell JW. Structure and mechanics of healing myocardial infarcts. *Annual Review of Biomedical Engineering* 2005;**7**:223-253.

54. Dostal DE, Booz GW, Baker KM. Angiotensin II signalling pathways in cardiac fibroblasts: Conventional versus novel mechanisms in mediating cardiac growth and function. *Molecular and Cellular Biochemistry* 1996;**157**:15-21.

55. Virag JA, Rolle ML, Reece J, Hardouin S, Feigl EO, Murry CE. Fibroblast growth factor-2 regulates myocardial infarct repair: Effects on cell proliferation, scar contraction, and ventricular function. *The American Journal of Pathology* 2007;**171**:1431-1440.

56. Dzeshka MS, Lip GY, Snezhitskiy V, Shantsila E. Cardiac fibrosis in patients with atrial fibrillation: Mechanisms and clinical implications. *Journal of the American College of Cardiology* 2015;**66**:943-959.

57. Wang YF, Hsu YJ, Wu HF, Lee GL, Yang YS, Wu JY, Yet SF, Wu KK, Kuo CC. Endothelium-derived 5-methoxytryptophan is a circulating anti-inflammatory molecule that blocks systemic inflammation. *Circulation Research* 2016;**119**:222-236.

58. Murakami M, Simons M. Fibroblast growth factor regulation of neovascularization. *Current Opinion in Hematology* 2008;**15**:215-220.

59. Travers JG, Kamal FA, Robbins J, Yutzey KE, Blaxall BC. Cardiac fibrosis: The fibroblast awakens. *Circulation Research* 2016;**118**:1021-1040.

60. Epelman S, Liu PP, Mann DL. Role of innate and adaptive immune mechanisms in cardiac injury and repair. *Nature Reviews Immunology* 2015;**15**:117-129.

61. Wong SP, Rowley JE, Redpath AN, Tilman JD, Fellous TG, Johnson JR. Pericytes, mesenchymal stem cells and their contributions to tissue repair. *Pharmacology and Therapeutics* 2015;**151**:107-120.

62. Dulauroy S, Di Carlo SE, Langa F, Eberl G, Peduto L. Lineage tracing and genetic ablation of ADAM12(+) perivascular cells identify a major source of profibrotic cells during acute tissue injury. *Nature Medicine* 2012;**18**:1262-1270.

63. Dostal D, Glaser S, Baudino TA. Cardiac fibroblast physiology and pathology. *Comprehensive Physiology* 2015;**5**:887-909.

64. Zeisberg EM, Kalluri R. Origins of cardiac fibroblasts. *Circulation Research* 2010;**107**:1304-1312.

65. Kamo T, Akazawa H, Komuro I. Cardiac nonmyocytes in the hub of cardiac hypertrophy. *Circulation Research* 2015;**117**:89-98.

66. Cartledge JE, Kane C, Dias P, Tesfom M, Clarke L, McKee B, Al Ayoubi S, Chester A, Yacoub MH, Camelliti P, Terracciano CM. Functional crosstalk between cardiac fibroblasts and adult cardiomyocytes by soluble mediators. *Cardiovascular Research* 2015;**105**:260-270.

67. Takeda N, Manabe I. Cellular interplay between cardiomyocytes and nonmyocytes in cardiac remodeling. *International Journal of Inflammation* 2011;**2011**:535241.

68. Valiente-Alandi I, Schafer AE, Blaxall BC. Extracellular matrix-mediated cellular communication in the heart. *Journal of Molecular and Cellular Cardiology* 2016;**91**:228-237.

69. Talman V, Ruskoaho H. Cardiac fibrosis in myocardial infarction-from repair and remodeling to regeneration. *Cell and Tissue Research* 2016;**365**:563-581.

70. Dobaczewski M, de Haan JJ, Frangogiannis NG. The extracellular matrix modulates fibroblast phenotype and function in the infarcted myocardium. *Journal of Cardiovascular Translational Research* 2012;**5**:837-847.

71. Chang CW, Dalgliesh AJ, Lopez JE, Griffiths LG. Cardiac extracellular matrix proteomics: Challenges, techniques, and clinical implications. *Proteomics Clinical Applications* 2016;**10**:39-50.

72. Baudino TA, Carver W, Giles W, Borg TK. Cardiac fibroblasts: Friend or foe? *American journal of physiology Heart and Circulatory Physiology* 2006;**291**:H1015-1026.

73. Shoulders MD, Raines RT. Collagen structure and stability. *Annual Review of Biochemistry* 2009;**78**:929-958.

74. Weber KT. Cardiac interstitium in health and disease: The fibrillar collagen network. *Journal of the American College of Cardiology* 1989;**13**:1637-1652.

75. Jugdutt BI. Ventricular remodeling after infarction and the extracellular collagen matrix: When is enough enough? *Circulation* 2003;**108**:1395-1403.

76. Kadler KE, Holmes DF, Trotter JA, Chapman JA. Collagen fibril formation. *The Biochemical Journal* 1996;**316 ( Pt 1)**:1-11.

77. Woodiwiss AJ, Tsotetsi OJ, Sprott S, Lancaster EJ, Mela T, Chung ES, Meyer TE, Norton GR. Reduction in myocardial collagen cross-linking parallels left ventricular dilatation in rat models of systolic chamber dysfunction. *Circulation* 2001;**103**:155-160.

78. Heymans S, Gonzalez A, Pizard A, Papageorgiou AP, Lopez-Andres N, Jaisser F, Thum T, Zannad F, Diez J. Searching for new mechanisms of myocardial fibrosis with diagnostic and/or therapeutic potential. *European Journal of Heart Failure* 2015;**17**:764-771.

79. Cox TR, Bird D, Baker AM, Barker HE, Ho MW, Lang G, Erler JT. LOX-mediated collagen crosslinking is responsible for fibrosis-enhanced metastasis. *Cancer Research* 2013;**73**:1721-1732.

80. Gelse K, Poschl E, Aigner T. Collagens--structure, function, and biosynthesis. *Advanced Drug Delivery Reviews* 2003;**55**:1531-1546.

81. Heymans S, González A, Pizard A, Papageorgiou AP, López-Andrés N, Jaisser F, Thum T, Zannad F, Díez J. Searching for new mechanisms of myocardial fibrosis with diagnostic and/or therapeutic potential. *European Journal of Heart Failure* 2015;**17**:764-771.

82. Gonzalez A, Lopez B, Querejeta R, Diez J. Regulation of myocardial fibrillar collagen by angiotensin II. A role in hypertensive heart disease? *Journal of Molecular and Cellular Cardiology* 2002;**34**:1585-1593.

83. McAnulty RJ, Laurent GJ. Collagen synthesis and degradation *in vivo*. Evidence for rapid rates of collagen turnover with extensive degradation of newly synthesized collagen in tissues of the adult rat. *Collagen and Related Research* 1987;**7**:93-104.

84. Spinale FG. Myocardial matrix remodeling and the matrix metalloproteinases: Influence on cardiac form and function. *Physiological Reviews* 2007;**87**:1285-1342.

85. Kong P, Christia P, Frangogiannis NG. The pathogenesis of cardiac fibrosis. *Cellular and Molecular Life Sciences* 2014;**71**:549-574.

86. Lindsey ML, Iyer RP, Jung M, DeLeon-Pennell KY, Ma Y. Matrix metalloproteinases as input and output signals for post-myocardial infarction remodeling. *Journal of Molecular and Cellular Cardiology* 2016;**91**:134-140.

87. Shirwany A, Weber KT. Extracellular matrix remodeling in hypertensive heart disease. *Journal of the American College of Cardiology* 2006;**48**:97-98.

88. Bosman FT, Stamenkovic I. Functional structure and composition of the extracellular matrix. *The Journal of Pathology* 2003;**200**:423-428.

89. Jane-Lise S, Corda S, Chassagne C, Rappaport L. The extracellular matrix and the cytoskeleton in heart hypertrophy and failure. *Heart Failure Reviews* 2000;**5**:239-250.

90. Corda S, Samuel JL, Rappaport L. Extracellular matrix and growth factors during heart growth. *Heart Failure Reviews* 2000;**5**:119-130.

91. Klingberg F, Hinz B, White ES. The myofibroblast matrix: Implications for tissue repair and fibrosis. *The Journal of Pathology* 2013;**229**:298-309.

92. Bowers SL, Banerjee I, Baudino TA. The extracellular matrix: At the center of it all. *Journal of Molecular and Cellular Cardiology* 2010;**48**:474-482.

93. Ma Y, de Castro Bras LE, Toba H, Iyer RP, Hall ME, Winniford MD, Lange RA, Tyagi SC, Lindsey ML. Myofibroblasts and the extracellular matrix network in post-myocardial infarction cardiac remodeling. *Pflugers Archiv: European Journal of Physiology* 2014;**466**:1113-1127.

94. Jourdan-Lesaux C, Zhang J, Lindsey ML. Extracellular matrix roles during cardiac repair. *Life Sciences* 2010;**87**:391-400.

95. Sottile J, Hocking DC. Fibronectin polymerization regulates the composition and stability of extracellular matrix fibrils and cell-matrix adhesions. *Molecular Biology of the Cell* 2002;**13**:3546-3559.

96. Halper J, Kjaer M. Basic components of connective tissues and extracellular matrix: Elastin, fibrillin, fibulins, fibrinogen, fibronectin, laminin, tenascins and thrombospondins. *Advances in Experimental Medicine and Biology* 2014;**802**:31-47.

97. Arslan F, Smeets MB, Riem Vis PW, Karper JC, Quax PH, Bongartz LG, Peters JH, Hoefer IE, Doevendans PA, Pasterkamp G, de Kleijn DP. Lack of fibronectin-EDA promotes survival and prevents adverse remodeling and heart function deterioration after myocardial infarction. *Circulation Research* 2011;**108**:582-592.

98. Frangogiannis NG. Regulation of the inflammatory response in cardiac repair. *Circulation Research* 2012;**110**:159-173.

99. Bornstein P. Matricellular proteins: An overview. *Journal of Cell Communication and Signaling* 2009;**3**:163-165.

100. Imanaka-Yoshida K, Hiroe M, Nishikawa T, Ishiyama S, Shimojo T, Ohta Y, Sakakura T, Yoshida T. Tenascin-C modulates adhesion of cardiomyocytes to extracellular matrix during tissue remodeling after myocardial infarction. *Laboratory investigation; A Journal of Technical Methods and Pathology* 2001;**81**:1015-1024.

101. Cohn JN, Ferrari R, Sharpe N. Cardiac remodeling--concepts and clinical implications: A consensus paper from an international forum on cardiac remodeling. Behalf of an International Forum on Cardiac Remodeling. *Journal of the American College of Cardiology* 2000;**35**:569-582.

102. Dorn GW, 2nd, Robbins J, Sugden PH. Phenotyping hypertrophy: Eschew obfuscation. *Circulation Research* 2003;**92**:1171-1175.

103. Weeks KL, McMullen JR. The athlete's heart vs. the failing heart: Can signaling explain the two distinct outcomes? *Physiology* 2011;**26**:97-105.

104. Olivetti G, Abbi R, Quaini F, Kajstura J, Cheng W, Nitahara JA, Quaini E, Di Loreto C, Beltrami CA, Krajewski S, Reed JC, Anversa P. Apoptosis in the failing human heart. *The New England Journal of Medicine* 1997;**336**:1131-1141.

105. Sharov VG, Sabbah HN, Shimoyama H, Goussev AV, Lesch M, Goldstein S. Evidence of cardiocyte apoptosis in myocardium of dogs with chronic heart failure. *The American Journal of Pathology* 1996;**148**:141-149.

106. Teiger E, Than VD, Richard L, Wisnewsky C, Tea BS, Gaboury L, Tremblay J, Schwartz K, Hamet P. Apoptosis in pressure overload-induced heart hypertrophy in the rat. *The Journal of Clinical Investigation* 1996;**97**:2891-2897.

107. Bujak M, Frangogiannis NG. The role of TGF-beta signaling in myocardial infarction and cardiac remodeling. *Cardiovascular Research* 2007;**74**:184-195.

108. Allessie M, Ausma J, Schotten U. Electrical, contractile and structural remodeling during atrial fibrillation. *Cardiovascular Research* 2002;**54**:230-246.

109. Stewart S, Hart CL, Hole DJ, McMurray JJ. Population prevalence, incidence, and predictors of atrial fibrillation in the Renfrew/Paisley study. *Heart* 2001;**86**:516-521.

110. Leong DP, Dokainish H. Left atrial volume and function in patients with atrial fibrillation. *Current Opinion in Cardiology* 2014;**29**:437-444.

111. Heeringa J, van der Kuip DA, Hofman A, Kors JA, van Herpen G, Stricker BH, Stijnen T, Lip GY, Witteman JC. Prevalence, incidence and lifetime risk of atrial fibrillation: The Rotterdam study. *European Heart Journal* 2006;**27**:949-953.

112. Neilan TG, Coelho-Filho OR, Shah RV, Abbasi SA, Heydari B, Watanabe E, Chen Y, Mandry D, Pierre-Mongeon F, Blankstein R, Kwong RY, Jerosch-Herold M. Myocardial extracellular volume fraction from T1 measurements in healthy volunteers and mice: Relationship to aging and cardiac dimensions. *JACC Cardiovascular Imaging* 2013;**6**:672-683.

113. Stewart S, Hart CL, Hole DJ, McMurray JJ. A population-based study of the long-term risks associated with atrial fibrillation: 20-year follow-up of the Renfrew/Paisley study. *The American Journal of Medicine* 2002;**113**:359-364.

114. Bui AL, Horwich TB, Fonarow GC. Epidemiology and risk profile of heart failure. *Nature Reviews Cardiology* 2011;**8**:30-41.

115. Maisel WH, Stevenson LW. Atrial fibrillation in heart failure: Epidemiology, pathophysiology, and rationale for therapy. *The American Journal of Cardiology* 2003;**91**:2d-8d.

116. Hunt SA, Abraham WT, Chin MH, Feldman AM, Francis GS, Ganiats TG, Jessup M, Konstam MA, Mancini DM, Michl K, Oates JA, Rahko PS, Silver MA, Stevenson LW, Yancy CW. 2009 focused update incorporated into the ACC/AHA 2005 guidelines for the diagnosis and management of heart failure in adults: A report of the american college of cardiology foundation/american heart association task force on practice guidelines: Developed in collaboration with the international society for heart and lung transplantation. *Circulation* 2009;**119**:e391-479.

117. Staerk L, Sherer JA, Ko D, Benjamin EJ, Helm RH. Atrial fibrillation: Epidemiology, pathophysiology, and clinical outcomes. *Circulation Research* 2017;**120**:1501-1517.

118. Schoonderwoerd BA, Smit MD, Pen L, Van Gelder IC. New risk factors for atrial fibrillation: Causes of 'not-so-lone atrial fibrillation'. *Europace* 2008;**10**:668-673.

119. Hu YF, Chen YJ, Lin YJ, Chen SA. Inflammation and the pathogenesis of atrial fibrillation. *Nature Reviews Cardiology* 2015;**12**:230-243.

120. Frustaci A, Chimenti C, Bellocci F, Morgante E, Russo MA, Maseri A. Histological substrate of atrial biopsies in patients with lone atrial fibrillation. *Circulation* 1997;**96**:1180-1184.

121. Pan M, Zhu JH, Jiang WP, Liu ZH, Li HM, Yu XH, Yang XJ. Inflammation: A possible pathogenic link to atrial fibrillation. *Med Hypotheses* 2006;**67**:1305-1307.

122. Jalife J. Mechanisms of persistent atrial fibrillation. *Current Opinion in Cardiology* 2014;**29**:20-27.

123. Dudley SC, Jr., Hoch NE, McCann LA, Honeycutt C, Diamandopoulos L, Fukai T, Harrison DG, Dikalov SI, Langberg J. Atrial fibrillation increases production of superoxide by the left atrium and left atrial appendage: Role of the NADPH and xanthine oxidases. *Circulation* 2005;**112**:1266-1273.

124. Pathak RK, Mahajan R, Lau DH, Sanders P. The implications of obesity for cardiac arrhythmia mechanisms and management. *The Canadian Journal of Cardiology* 2015;**31**:203-210.

125. Abed HS, Samuel CS, Lau DH, Kelly DJ, Royce SG, Alasady M, Mahajan R, Kuklik P, Zhang Y, Brooks AG, Nelson AJ, Worthley SG, Abhayaratna WP, Kalman JM, Wittert GA, Sanders P. Obesity results in progressive atrial structural and electrical remodeling: Implications for atrial fibrillation. *Heart Rhythm* 2013;**10**:90-100.

126. Matassini MV, Brambatti M, Guerra F, Scappini L, Capucci A. Sleep-disordered breathing and atrial fibrillation: Review of the evidence. *Cardiology in Review* 2015;**23**:79-86.

127. Nattel S, Dobrev D. Electrophysiological and molecular mechanisms of paroxysmal atrial fibrillation. *Nature Reviews Cardiology* 2016;**13**:575-590.

128. Nattel S, Harada M. Atrial remodeling and atrial fibrillation. *Recent Advances and Translational Perspectives* 2014;**63**:2335-2345.

129. Nattel S. New ideas about atrial fibrillation 50 years on. *Nature* 2002;**415**:219-226.

130. Seiler J, Stevenson WG. Atrial fibrillation in congestive heart failure. *Cardiology in Review* 2010;**18**:38-50.

131. El-Armouche A, Boknik P, Eschenhagen T, Carrier L, Knaut M, Ravens U, Dobrev D. Molecular determinants of altered $Ca^{2+}$ handling in human chronic atrial fibrillation. *Circulation* 2006;**114**:670-680.

132. Yeh YH, Wakili R, Qi XY, Chartier D, Boknik P, Kaab S, Ravens U, Coutu P, Dobrev D, Nattel S. Calcium-handling abnormalities underlying atrial

arrhythmogenesis and contractile dysfunction in dogs with congestive heart failure. *Circulation Arrhythmia and Electrophysiology* 2008;**1**:93-102.

133. Narayan SM, Franz MR, Clopton P, Pruvot EJ, Krummen DE. Repolarization alternans reveals vulnerability to human atrial fibrillation. *Circulation* 2011;**123**:2922-2930.

134. Yue L, Feng J, Gaspo R, Li GR, Wang Z, Nattel S. Ionic remodeling underlying action potential changes in a canine model of atrial fibrillation. *Circulation Research* 1997;**81**:512-525.

135. Burashnikov A, Antzelevitch C. Is extensive atrial fibrosis in the setting of heart failure associated with a reduced atrial fibrillation burden? *Pacing and Clinical Electrophysiology* 2018;**41**:1289-1297.

136. Cha TJ, Ehrlich JR, Chartier D, Qi XY, Xiao L, Nattel S. Kir3-based inward rectifier potassium current: Potential role in atrial tachycardia remodeling effects on atrial repolarization and arrhythmias. *Circulation* 2006;**113**:1730-1737.

137. Dobrev D, Graf E, Wettwer E, Himmel HM, Hala O, Doerfel C, Christ T, Schuler S, Ravens U. Molecular basis of downregulation of G-protein-coupled inward rectifying $K^{(+)}$ current $I_{(K,ACh)}$ in chronic human atrial fibrillation: Decrease in GIRK4 mRNA correlates with reduced $I_{(K,ACh)}$ and muscarinic receptor-mediated shortening of action potentials. *Circulation* 2001;**104**:2551-2557.

138. Dobrev D, Friedrich A, Voigt N, Jost N, Wettwer E, Christ T, Knaut M, Ravens U. The G protein-gated potassium current $I_{(K,ACh)}$ is constitutively active in patients with chronic atrial fibrillation. *Circulation* 2005;**112**:3697-3706.

139. Li D, Melnyk P, Feng J, Wang Z, Petrecca K, Shrier A, Nattel S. Effects of experimental heart failure on atrial cellular and ionic electrophysiology. *Circulation* 2000;**101**:2631-2638.

140. Carnes CA, Janssen PM, Ruehr ML, Nakayama H, Nakayama T, Haase H, Bauer JA, Chung MK, Fearon IM, Gillinov AM, Hamlin RL, Van Wagoner DR. Atrial glutathione content, calcium current, and contractility. *The Journal of Biological Chemistry* 2007;**282**:28063-28073.

141. Etzion Y, Ganiel A, Beharier O, Shalev A, Novack V, Volvich L, Abrahamov D, Matsa M, Sahar G, Moran A, Katz A. Correlation between atrial ZnT-1 expression and atrial fibrillation in humans: A pilot study. *Journal of Cardiovascular Electrophysiology* 2008;**19**:157-164.

142. Greiser M, Halaszovich CR, Frechen D, Boknik P, Ravens U, Dobrev D, Luckhoff A, Schotten U. Pharmacological evidence for altered src kinase regulation of $I_{(Ca,L)}$

in patients with chronic atrial fibrillation. *Naunyn Schmiedebergs Arch Pharmacol* 2007;**375**:383-392.

143. van der Velden HM, Ausma J, Rook MB, Hellemons AJ, van Veen TA, Allessie MA, Jongsma HJ. Gap junctional remodeling in relation to stabilization of atrial fibrillation in the goat. *Cardiovascular Research* 2000;**46**:476-486.

144. Coetzee WA, Amarillo Y, Chiu J, Chow A, Lau D, McCormack T, Moreno H, Nadal MS, Ozaita A, Pountney D, Saganich M, Vega-Saenz de Miera E, Rudy B. Molecular diversity of $K^+$ channels. *Annals of the New York Academy of Sciences* 1999;**868**:233-285.

145. Gaborit N, Steenman M, Lamirault G, Le Meur N, Le Bouter S, Lande G, Leger J, Charpentier F, Christ T, Dobrev D, Escande D, Nattel S, Demolombe S. Human atrial ion channel and transporter subunit gene-expression remodeling associated with valvular heart disease and atrial fibrillation. *Circulation* 2005;**112**:471-481.

146. Voigt N, Friedrich A, Bock M, Wettwer E, Christ T, Knaut M, Strasser RH, Ravens U, Dobrev D. Differential phosphorylation-dependent regulation of constitutively active and muscarinic receptor-activated $I_{K,ACh}$ channels in patients with chronic atrial fibrillation. *Cardiovascular Research* 2007;**74**:426-437.

147. Yue L, Melnyk P, Gaspo R, Wang Z, Nattel S. Molecular mechanisms underlying ionic remodeling in a dog model of atrial fibrillation. *Circulation Research* 1999;**84**:776-784.

148. Shen MJ, Zipes DP. Role of the autonomic nervous system in modulating cardiac arrhythmias. *Circulation Research* 2014;**114**:1004-1021.

149. Chen PS, Chen LS, Fishbein MC, Lin SF, Nattel S. Role of the autonomic nervous system in atrial fibrillation: Pathophysiology and therapy. *Circulation Research* 2014;**114**:1500-1515.

150. Miyauchi Y, Zhou S, Okuyama Y, Miyauchi M, Hayashi H, Hamabe A, Fishbein MC, Mandel WJ, Chen LS, Chen PS, Karagueuzian HS. Altered atrial electrical restitution and heterogeneous sympathetic hyperinnervation in hearts with chronic left ventricular myocardial infarction: Implications for atrial fibrillation. *Circulation* 2003;**108**:360-366.

151. Chou CC, Chen PS. New concepts in atrial fibrillation: Neural mechanisms and calcium dynamics. *Cardiology Clinics* 2009;**27**:35-43.

152. Kumar S, Teh AW, Medi C, Kistler PM, Morton JB, Kalman JM. Atrial remodeling in varying clinical substrates within beating human hearts: Relevance to atrial fibrillation. *Progress in Biophysics and Molecular Biology* 2012;**110**:278-294.

153. Nishida K, Qi XY, Wakili R, Comtois P, Chartier D, Harada M, Iwasaki YK, Romeo P, Maguy A, Dobrev D, Michael G, Talajic M, Nattel S. Mechanisms of atrial tachyarrhythmias associated with coronary artery occlusion in a chronic canine model. *Circulation* 2011;**123**:137-146.

154. Goette A, Kalman JM, Aguinaga L, Akar J, Cabrera JA, Chen SA, Chugh SS, Corradi D, D'Avila A, Dobrev D, Fenelon G, Gonzalez M, Hatem SN, Helm R, Hindricks G, Ho SY, Hoit B, Jalife J, Kim YH, Lip GY, Ma CS, Marcus GM, Murray K, Nogami A, Sanders P, Uribe W, Van Wagoner DR, Nattel S. EHRA/HRS/APHRS/SOLAECE expert consensus on atrial cardiomyopathies: Definition, characterization, and clinical implication. *Heart Rhythm* 2017;**14**:e3-e40.

155. Xu J, Cui G, Esmailian F, Plunkett M, Marelli D, Ardehali A, Odim J, Laks H, Sen L. Atrial extracellular matrix remodeling and the maintenance of atrial fibrillation. *Circulation* 2004;**109**:363-368.

156. Burstein B, Nattel S. Atrial fibrosis: Mechanisms and clinical relevance in atrial fibrillation. *Journal of the American College of Cardiology* 2008;**51**:802-809.

157. Melenovsky V, Hwang SJ, Redfield MM, Zakeri R, Lin G, Borlaug BA. Left atrial remodeling and function in advanced heart failure with preserved or reduced ejection fraction. *Circulation Heart Failure* 2015;**8**:295-303.

158. Watson T, Shantsila E, Lip GY. Mechanisms of thrombogenesis in atrial fibrillation: Virchow's triad revisited. *Lancet (London, England)* 2009;**373**:155-166.

159. Manabe I, Shindo T, Nagai R. Gene expression in fibroblasts and fibrosis: Involvement in cardiac hypertrophy. *Circulation Research* 2002;**91**:1103-1113.

160. Biernacka A, Frangogiannis NG. Aging and cardiac fibrosis. *Aging and Disease* 2011;**2**:158-173.

161. Kurose H, Mangmool S. Myofibroblasts and inflammatory cells as players of cardiac fibrosis. *Archives of Pharmacal Research* 2016;**39**:1100-1113.

162. Tarone G, Balligand JL, Bauersachs J, Clerk A, De Windt L, Heymans S, Hilfiker-Kleiner D, Hirsch E, Iaccarino G, Knoll R, Leite-Moreira AF, Lourenco AP, Mayr M, Thum T, Tocchetti CG. Targeting myocardial remodelling to develop novel therapies for heart failure: A position paper from the working group on myocardial function of the European Society of Cardiology. *European Journal of Heart Failure* 2014;**16**:494-508.

163. Borer JS, Truter S, Herrold EM, Falcone DJ, Pena M, Carter JN, Dumlao TF, Lee JA, Supino PG. Myocardial fibrosis in chronic aortic regurgitation: Molecular and cellular responses to volume overload. *Circulation* 2002;**105**:1837-1842.

164. Berk BC, Fujiwara K, Lehoux S. ECM remodeling in hypertensive heart disease. *The Journal of Clinical Investigation* 2007;**117**:568-575.

165. Asbun J, Villarreal FJ. The pathogenesis of myocardial fibrosis in the setting of diabetic cardiomyopathy. *Journal of the American College of Cardiology* 2006;**47**:693-700.

166. Baum J, Duffy HS. Fibroblasts and myofibroblasts: What are we talking about? *Journal of Cardiovascular Pharmacology* 2011;**57**:376-379.

167. Meng XM, Nikolic-Paterson DJ, Lan HY. TGF-beta: The master regulator of fibrosis. *Nature Reviews Nephrology* 2016;**12**:325-338.

168. Bujak M, Ren G, Kweon HJ, Dobaczewski M, Reddy A, Taffet G, Wang XF, Frangogiannis NG. Essential role of Smad3 in infarct healing and in the pathogenesis of cardiac remodeling. *Circulation* 2007;**116**:2127-2138.

169. Small EM, Thatcher JE, Sutherland LB, Kinoshita H, Gerard RD, Richardson JA, Dimaio JM, Sadek H, Kuwahara K, Olson EN. Myocardin-related transcription factor-a controls myofibroblast activation and fibrosis in response to myocardial infarction. *Circulation Research* 2010;**107**:294-304.

170. Hashimoto S, Gon Y, Takeshita I, Matsumoto K, Maruoka S, Horie T. Transforming growth factor-beta1 induces phenotypic modulation of human lung fibroblasts to myofibroblast through a c-Jun-NH2-terminal kinase-dependent pathway. *American Journal of Respiratory and Critical Care Medicine* 2001;**163**:152-157.

171. Sousa AM, Liu T, Guevara O, Stevens J, Fanburg BL, Gaestel M, Toksoz D, Kayyali US. Smooth muscle alpha-actin expression and myofibroblast differentiation by TGFbeta are dependent upon MK2. *Journal of Cellular Biochemistry* 2007;**100**:1581-1592.

172. Naugle JE, Olson ER, Zhang X, Mase SE, Pilati CF, Maron MB, Folkesson HG, Horne WI, Doane KJ, Meszaros JG. Type VI collagen induces cardiac myofibroblast differentiation: Implications for postinfarction remodeling. *American Journal of Physiology Heart and Circulatory Physiology* 2006;**290**:H323-330.

173. Kong P, Christia P, Saxena A, Su Y, Frangogiannis NG. Lack of specificity of fibroblast-specific protein 1 in cardiac remodeling and fibrosis. *American Journal of Physiology Heart and Circulatory Physiology* 2013;**305**:H1363-1372.

174. Sun KH, Chang Y, Reed NI, Sheppard D. alpha-smooth muscle actin is an inconsistent marker of fibroblasts responsible for force-dependent TGFbeta activation or collagen production across multiple models of organ fibrosis. *American Journal of Physiology Lung Cellular and Molecular Physiology* 2016;**310**:L824-836.

175. Bochmann L, Sarathchandra P, Mori F, Lara-Pezzi E, Lazzaro D, Rosenthal N. Revealing new mouse epicardial cell markers through transcriptomics. *PloS One* 2010;**5**:e11429.

176. Goldsmith EC, Hoffman A, Morales MO, Potts JD, Price RL, McFadden A, Rice M, Borg TK. Organization of fibroblasts in the heart. *Developmental Dynamics* 2004;**230**:787-794.

177. Morales MO, Price RL, Goldsmith EC. Expression of discoidin domain receptor 2 (DDR2) in the developing heart. *Microscopy and Microanalysis* 2005;**11**:260-267.

178. Oka T, Xu J, Kaiser RA, Melendez J, Hambleton M, Sargent MA, Lorts A, Brunskill EW, Dorn GW, 2nd, Conway SJ, Aronow BJ, Robbins J, Molkentin JD. Genetic manipulation of periostin expression reveals a role in cardiac hypertrophy and ventricular remodeling. *Circulation Research* 2007;**101**:313-321.

179. Smith CL, Baek ST, Sung CY, Tallquist MD. Epicardial-derived cell epithelial-to-mesenchymal transition and fate specification require PDGF receptor signaling. *Circulation Research* 2011;**108**:e15-26.

180. Piras BA, Tian Y, Xu Y, Thomas NA, O'Connor DM, French BA. Systemic injection of AAV9 carrying a periostin promoter targets gene expression to a myofibroblast-like lineage in mouse hearts after reperfused myocardial infarction. *Gene Therapy* 2016;**23**:469-478.

181. Acharya A, Baek ST, Huang G, Eskiocak B, Goetsch S, Sung CY, Banfi S, Sauer MF, Olsen GS, Duffield JS, Olson EN, Tallquist MD. The bHLH transcription factor Tcf21 is required for lineage-specific EMT of cardiac fibroblast progenitors. *Development* 2012;**139**:2139-2149.

182. Pei Y, Sherry DM, McDermott AM. Thy-1 distinguishes human corneal fibroblasts and myofibroblasts from keratocytes. *Experimental Eye Research* 2004;**79**:705-712.

183. Hudon-David F, Bouzeghrane F, Couture P, Thibault G. Thy-1 expression by cardiac fibroblasts: Lack of association with myofibroblast contractile markers. *Journal of Molecular and Cellular Cardiology* 2007;**42**:991-1000.

184. Duprey P, Paulin D. What can be learned from intermediate filament gene regulation in the mouse embryo. *The International Journal of Developmental Biology* 1995;**39**:443-457.

185. Chen C, Li R, Ross RS, Manso AM. Integrins and integrin-related proteins in cardiac fibrosis. *Journal of Molecular and Cellular Cardiology* 2016;**93**:162-174.

186. Leask A. Getting to the heart of the matter: New insights into cardiac fibrosis. *Circulation Research* 2015;**116**:1269-1276.

187. Nathan CF. Secretory products of macrophages. *The Journal of Clinical Investigation* 1987;**79**:319-326.

188. Leask A. Potential therapeutic targets for cardiac fibrosis: TGFbeta, angiotensin, endothelin, CCN2, and PDGF, partners in fibroblast activation. *Circulation Research* 2010;**106**:1675-1680.

189. Dobaczewski M, Chen W, Frangogiannis NG. Transforming growth factor (TGF)-beta signaling in cardiac remodeling. *Journal of Molecular and Cellular Cardiology* 2011;**51**:600-606.

190. Schiller M, Javelaud D, Mauviel A. TGF-beta-induced SMAD signaling and gene regulation: Consequences for extracellular matrix remodeling and wound healing. *Journal of Dermatological Science* 2004;**35**:83-92.

191. Annes JP, Munger JS, Rifkin DB. Making sense of latent TGFbeta activation. *Journal of Cell Science* 2003;**116**:217-224.

192. Greene RM, Nugent P, Mukhopadhyay P, Warner DR, Pisano MM. Intracellular dynamics of Smad-mediated TGFbeta signaling. *Journal of Cellular Physiology* 2003;**197**:261-271.

193. Cieslik KA, Trial J, Crawford JR, Taffet GE, Entman ML. Adverse fibrosis in the aging heart depends on signaling between myeloid and mesenchymal cells; role of inflammatory fibroblasts. *Journal of Molecular and Cellular Cardiology* 2014;**0**:56-63.

194. Derynck R, Zhang YE. Smad-dependent and Smad-independent pathways in TGF-beta family signalling. *Nature* 2003;**425**:577-584.

195. Dobaczewski M, Bujak M, Li N, Gonzalez-Quesada C, Mendoza LH, Wang X-F, Frangogiannis NG. Smad3 signaling critically regulates fibroblast phenotype and function in healing myocardial infarction. *Circulation Research* 2010;**107**:418-428.

196. Conway SJ, Molkentin JD. Periostin as a heterofunctional regulator of cardiac development and disease. *Current Genomics* 2008;**9**:548-555.

197. Li L, Chen Y, Doan J, Murray J, Molkentin JD, Liu Q. Transforming growth factor beta-activated kinase 1 signaling pathway critically regulates myocardial survival and remodeling. *Circulation* 2014;**130**:2162-2172.

198. Lyons RM, Keski-Oja J, Moses HL. Proteolytic activation of latent transforming growth factor-beta from fibroblast-conditioned medium. *The Journal of Cell Biology* 1988;**106**:1659-1665.

199. Barcellos-Hoff MH, Derynck R, Tsang ML, Weatherbee JA. Transforming growth factor-beta activation in irradiated murine mammary gland. *The Journal of Clinical Investigation* 1994;**93**:892-899.

200. Campbell SE, Katwa LC. Angiotensin II stimulated expression of transforming growth factor-beta1 in cardiac fibroblasts and myofibroblasts. *Journal of Molecular and Cellular Cardiology* 1997;**29**:1947-1958.

201. Weber KT, Sun Y, Bhattacharya SK, Ahokas RA, Gerling IC. Myofibroblast-mediated mechanisms of pathological remodelling of the heart. *Nature Reviews Cardiology* 2013;**10**:15-26.

202. Ehrlich JR, Hohnloser SH, Nattel S. Role of angiotensin system and effects of its inhibition in atrial fibrillation: Clinical and experimental evidence. *European Heart Journal* 2006;**27**:512-518.

203. Schneider MP, Hua TA, Bohm M, Wachtell K, Kjeldsen SE, Schmieder RE. Prevention of atrial fibrillation by renin-angiotensin system inhibition a meta-analysis. *Journal of the American College of Cardiology* 2010;**55**:2299-2307.

204. Hunyady L, Catt KJ. Pleiotropic AT1 receptor signaling pathways mediating physiological and pathogenic actions of angiotensin II. *Molecular Endocrinology* 2006;**20**:953-970.

205. Attisano L, Wrana JL. Signal transduction by the TGF-beta superfamily. *Science* 2002;**296**:1646-1647.

206. Goette A, Staack T, Rocken C, Arndt M, Geller JC, Huth C, Ansorge S, Klein HU, Lendeckel U. Increased expression of extracellular signal-regulated kinase and angiotensin-converting enzyme in human atria during atrial fibrillation. *Journal of the American College of Cardiology* 2000;**35**:1669-1677.

207. Sciarretta S, Paneni F, Palano F, Chin D, Tocci G, Rubattu S, Volpe M. Role of the renin-angiotensin-aldosterone system and inflammatory processes in the development and progression of diastolic dysfunction. *Clinical Science* 2009;**116**:467-477.

208. Teder P, Noble PW. A cytokine reborn? Endothelin-1 in pulmonary inflammation and fibrosis. *American Journal of Respiratory Cell and Molecular Biology* 2000;**23**:7-10.

209. Rodriguez-Pascual F, Busnadiego O, Gonzalez-Santamaria J. The profibrotic role of endothelin-1: Is the door still open for the treatment of fibrotic diseases? *Life Sciences* 2014;**118**:156-164.

210. Oie E, Yndestad A, Robins SP, Bornerheim R, Asberg A, Attramadal H. Early intervention with a potent endothelin-A/endothelin-B receptor antagonist aggravates left ventricular remodeling after myocardial infarction in rats. *Basic Research in Cardiology* 2002;**97**:239-247.

211. Mueller EE, Momen A, Masse S, Zhou YQ, Liu J, Backx PH, Henkelman RM, Nanthakumar K, Stewart DJ, Husain M. Electrical remodelling precedes heart failure in an endothelin-1-induced model of cardiomyopathy. *Cardiovascular Research* 2011;**89**:623-633.

212. Yamamoto K, Masuyama T, Sakata Y, Mano T, Nishikawa N, Kondo H, Akehi N, Kuzuya T, Miwa T, Hori M. Roles of renin-angiotensin and endothelin systems in development of diastolic heart failure in hypertensive hearts. *Cardiovascular Research* 2000;**47**:274-283.

213. Magnusson PU, Looman C, Ahgren A, Wu Y, Claesson-Welsh L, Heuchel RL. Platelet-derived growth factor receptor-beta constitutive activity promotes angiogenesis *in vivo* and *in vitro*. *Arteriosclerosis, Thrombosis, and Vascular Biology* 2007;**27**:2142-2149.

214. Simm A, Nestler M, Hoppe V. Mitogenic effect of PDGF-AA on cardiac fibroblasts. *Basic Research in Cardiology* 1998;**93 Suppl 3**:40-43.

215. Betsholtz C. Biology of platelet-derived growth factors in development. *Birth Defects Research Part C, Embryo Today: Reviews* 2003;**69**:272-285.

216. Ponten A, Li X, Thoren P, Aase K, Sjoblom T, Ostman A, Eriksson U. Transgenic overexpression of platelet-derived growth factor-C in the mouse heart induces cardiac fibrosis, hypertrophy, and dilated cardiomyopathy. *The American Journal of Pathology* 2003;**163**:673-682.

217. Ponten A, Folestad EB, Pietras K, Eriksson U. Platelet-derived growth factor D induces cardiac fibrosis and proliferation of vascular smooth muscle cells in heart-specific transgenic mice. *Circulation Research* 2005;**97**:1036-1045.

218. Orenes-Pinero E, Montoro-Garcia S, Patel JV, Valdes M, Marin F, Lip GY. Role of microRNAs in cardiac remodelling: New insights and future perspectives. *International Journal of Cardiology* 2013;**167**:1651-1659.

219. Thum T. Noncoding RNAs and myocardial fibrosis. *Nature Reviews Cardiology* 2014;**11**:655-663.

220. Piccoli MT, Bar C, Thum T. Non-coding RNAs as modulators of the cardiac fibroblast phenotype. *Journal of Molecular and Cellular Cardiology* 2016;**92**:75-81.

221. Matkovich SJ, Wang W, Tu Y, Eschenbacher WH, Dorn LE, Condorelli G, Diwan A, Nerbonne JM, Dorn GW, 2nd. MicroRNA-133a protects against myocardial fibrosis and modulates electrical repolarization without affecting hypertrophy in pressure-overloaded adult hearts. *Circulation Research* 2010;**106**:166-175.

222. Karakikes I, Chaanine AH, Kang S, Mukete BN, Jeong D, Zhang S, Hajjar RJ, Lebeche D. Therapeutic cardiac-targeted delivery of miR-1 reverses pressure overload-induced cardiac hypertrophy and attenuates pathological remodeling. *Journal of the American Heart Association* 2013;**2**:e000078.

223. Liu N, Bezprozvannaya S, Williams AH, Qi X, Richardson JA, Bassel-Duby R, Olson EN. microRNA-133a regulates cardiomyocyte proliferation and suppresses smooth muscle gene expression in the heart. *Genes and Development* 2008;**22**:3242-3254.

224. van Rooij E, Sutherland LB, Thatcher JE, DiMaio JM, Naseem RH, Marshall WS, Hill JA, Olson EN. Dysregulation of microRNAs after myocardial infarction reveals a role of miR-29 in cardiac fibrosis. *Proceedings of the National Academy of Sciences of the United States of America* 2008;**105**:13027-13032.

225. Thum T, Gross C, Fiedler J, Fischer T, Kissler S, Bussen M, Galuppo P, Just S, Rottbauer W, Frantz S, Castoldi M, Soutschek J, Koteliansky V, Rosenwald A, Basson MA, Licht JD, Pena JT, Rouhanifard SH, Muckenthaler MU, Tuschl T, Martin GR, Bauersachs J, Engelhardt S. MicroRNA-21 contributes to myocardial disease by stimulating MAP kinase signalling in fibroblasts. *Nature* 2008;**456**:980-984.

226. Cheng Y, Liu X, Zhang S, Lin Y, Yang J, Zhang C. MicroRNA-21 protects against the H(2)O(2)-induced injury on cardiac myocytes via its target gene PDCD4. *Journal of Molecular and Cellular Cardiology* 2009;**47**:5-14.

227. Shi-Wen X, Leask A, Abraham D. Regulation and function of connective tissue growth factor/CCN2 in tissue repair, scarring and fibrosis. *Cytokine and Growth Factor Reviews* 2008;**19**:133-144.

228. Chen MM, Lam A, Abraham JA, Schreiner GF, Joly AH. CTGF expression is induced by TGF- beta in cardiac fibroblasts and cardiac myocytes: A potential role in heart fibrosis. *Journal of Molecular and Cellular Cardiology* 2000;**32**:1805-1819.

229. Grotendorst GR. Connective tissue growth factor: A mediator of TGF-beta action on fibroblasts. *Cytokine and Growth Factor Reviews* 1997;**8**:171-179.

230. Leask A, Abraham DJ. The role of connective tissue growth factor, a multifunctional matricellular protein, in fibroblast biology. *Biochemistry and Cell Biology* 2003;**81**:355-363.

231. Szabo Z, Magga J, Alakoski T, Ulvila J, Piuhola J, Vainio L, Kivirikko KI, Vuolteenaho O, Ruskoaho H, Lipson KE, Signore P, Kerkela R. Connective tissue growth factor inhibition attenuates left ventricular remodeling and dysfunction in pressure overload-induced heart failure. *Hypertension* 2014;**63**:1235-1240.

232. Fields GB. Interstitial collagen catabolism. *The Journal of Biological Chemistry* 2013;**288**:8785-8793.

233. Chakraborti S, Mandal M, Das S, Mandal A, Chakraborti T. Regulation of matrix metalloproteinases: An overview. *Molecular and Cellular Biochemistry* 2003;**253**:269-285.

234. Nagase H, Woessner JF, Jr. Matrix metalloproteinases. *The Journal of Biological Chemistry* 1999;**274**:21491-21494.

235. Phatharajaree W, Phrommintikul A, Chattipakorn N. Matrix metalloproteinases and myocardial infarction. *The Canadian Journal of Cardiology* 2007;**23**:727-733.

236. Fan D, Takawale A, Lee J, Kassiri Z. Cardiac fibroblasts, fibrosis and extracellular matrix remodeling in heart disease. *Fibrogenesis and Tissue Repair* 2012;**5**:15.

237. Nagase H, Visse R, Murphy G. Structure and function of matrix metalloproteinases and TIMPs. *Cardiovascular Research* 2006;**69**:562-573.

238. Kakkar R, Lee RT. Intramyocardial fibroblast myocyte communication. *Circulation Research* 2010;**106**:47-57.

239. Kim HE, Dalal SS, Young E, Legato MJ, Weisfeldt ML, D'Armiento J. Disruption of the myocardial extracellular matrix leads to cardiac dysfunction. *The Journal of Clinical Investigation* 2000;**106**:857-866.

240. Tsuchida K, Zhu Y, Siva S, Dunn SR, Sharma K. Role of Smad4 on TGF-beta-induced extracellular matrix stimulation in mesangial cells. *Kidney International* 2003;**63**:2000-2009.

241. Deschamps AM, Spinale FG. Pathways of matrix metalloproteinase induction in heart failure: Bioactive molecules and transcriptional regulation. *Cardiovascular Research* 2006;**69**:666-676.

242. Creemers EE, Cleutjens JP, Smits JF, Daemen MJ. Matrix metalloproteinase inhibition after myocardial infarction: A new approach to prevent heart failure? *Circulation Research* 2001;**89**:201-210.

243. Li YY, McTiernan CF, Feldman AM. Interplay of matrix metalloproteinases, tissue inhibitors of metalloproteinases and their regulators in cardiac matrix remodeling. *Cardiovascular Research* 2000;**46**:214-224.

244. Etoh T, Joffs C, Deschamps AM, Davis J, Dowdy K, Hendrick J, Baicu S, Mukherjee R, Manhaini M, Spinale FG. Myocardial and interstitial matrix metalloproteinase activity after acute myocardial infarction in pigs. *American Journal of Physiology Heart and Circulatory Physiology* 2001;**281**:H987-994.

245. Siwik DA, Chang DL, Colucci WS. Interleukin-1beta and tumor necrosis factor-alpha decrease collagen synthesis and increase matrix metalloproteinase activity in cardiac fibroblasts *in vitro*. *Circulation Research* 2000;**86**:1259-1265.

246. Sarkar S, Vellaichamy E, Young D, Sen S. Influence of cytokines and growth factors in ang II-mediated collagen upregulation by fibroblasts in rats: Role of myocytes. *American Journal of Physiology Heart and Circulatory Physiology* 2004;**287**:H107-117.

247. Murdoch CE, Zhang M, Cave AC, Shah AM. NADPH oxidase-dependent redox signalling in cardiac hypertrophy, remodelling and failure. *Cardiovascular Research* 2006;**71**:208-215.

248. Mewton N, Liu CY, Croisille P, Bluemke D, Lima JA. Assessment of myocardial fibrosis with cardiovascular magnetic resonance. *Journal of the American College of Cardiology* 2011;**57**:891-903.

249. Shinde AV, Frangogiannis NG. Fibroblasts in myocardial infarction: A role in inflammation and repair. *Journal of Molecular and Cellular Cardiology* 2014;**70**:74-82.

250. Poss KD, Wilson LG, Keating MT. Heart regeneration in zebrafish. *Science* 2002;**298**:2188-2190.

251. Porrello ER, Mahmoud AI, Simpson E, Hill JA, Richardson JA, Olson EN, Sadek HA. Transient regenerative potential of the neonatal mouse heart. *Science* 2011;**331**:1078-1080.

252. van den Borne SW, Diez J, Blankesteijn WM, Verjans J, Hofstra L, Narula J. Myocardial remodeling after infarction: The role of myofibroblasts. *Nature Reviews Cardiology* 2010;**7**:30-37.

253. Squires CE, Escobar GP, Payne JF, Leonardi RA, Goshorn DK, Sheats NJ, Mains IM, Mingoia JT, Flack EC, Lindsey ML. Altered fibroblast function following myocardial infarction. *Journal of Molecular and Cellular Cardiology* 2005;**39**:699-707.

254. Frangogiannis NG. Targeting the transforming growth factor (TGF)-beta cascade in the remodeling heart: Benefits and perils. *Journal of Molecular and Cellular Cardiology* 2014;**76**:169-171.

255. Nong Z, O'Neil C, Lei M, Gros R, Watson A, Rizkalla A, Mequanint K, Li S, Frontini MJ, Feng Q, Pickering JG. Type I collagen cleavage is essential for effective fibrotic repair after myocardial infarction. *The American Journal of Pathology* 2011;**179**:2189-2198.

256. Dai Z, Aoki T, Fukumoto Y, Shimokawa H. Coronary perivascular fibrosis is associated with impairment of coronary blood flow in patients with non-ischemic heart failure. *Journal of Cardiology* 2012;**60**:416-421.

257. Swynghedauw B. Molecular mechanisms of myocardial remodeling. *Physiological Reviews* 1999;**79**:215-262.

258. Heineke J, Molkentin JD. Regulation of cardiac hypertrophy by intracellular signalling pathways. *Nature Reviews Molecular Cell Biology* 2006;**7**:589-600.

259. Sun Y, Zhang JQ, Zhang J, Ramires FJA. Angiotensin II, transforming growth factor-β1and repair in the infarcted heart. *Journal of Molecular and Cellular Cardiology* 1998;**30**:1559-1569.

260. Xu X, Wan W, Powers AS, Li J, Ji LL, Lao S, Wilson B, Erikson JM, Zhang JQ. Effects of exercise training on cardiac function and myocardial remodeling in post myocardial infarction rats. *Journal of Molecular and Cellular Cardiology* 2008;**44**:114-122.

261. Sanders P, Morton JB, Davidson NC, Spence SJ, Vohra JK, Sparks PB, Kalman JM. Electrical remodeling of the atria in congestive heart failure: Electrophysiological and electroanatomic mapping in humans. *Circulation* 2003;**108**:1461-1468.

262. Everett TH, Wilson EE, Verheule S, Guerra JM, Foreman S, Olgin JE. Structural atrial remodeling alters the substrate and spatiotemporal organization of atrial fibrillation: A comparison in canine models of structural and electrical atrial remodeling. *American Journal of Physiology Heart and Circulatory Physiology* 2006;**291**:H2911-H2923.

263. Ohtani K, Yutani C, Nagata S, Koretsune Y, Hori M, Kamada T. High prevalence of atrial fibrosis in patients with dilated cardiomyopathy. *Journal of the American College of Cardiology* 1995;**25**:1162-1169.

264. Anyukhovsky EP, Sosunov EA, Plotnikov A, Gainullin RZ, Jhang JS, Marboe CC, Rosen MR. Cellular electrophysiologic properties of old canine atria provide a substrate for arrhythmogenesis. *Cardiovascular Research* 2002;**54**:462-469.

265. Cardin S, Pelletier P, Libby E, Le Bouter S, Xiao L, Kaab S, Demolombe S, Glass L, Nattel S. Marked differences between atrial and ventricular gene-expression remodeling in dogs with experimental heart failure. *Journal of Molecular and Cellular Cardiology* 2008;**45**:821-831.

266. Mukherjee R, Herron AR, Lowry AS, Stroud RE, Stroud MR, Wharton JM, Ikonomidis JS, Crumbley AJ, 3rd, Spinale FG, Gold MR. Selective induction of matrix metalloproteinases and tissue inhibitor of metalloproteinases in atrial and ventricular myocardium in patients with atrial fibrillation. *The American Journal of Cardiology* 2006;**97**:532-537.

267. Lee KW, Everett THt, Rahmutula D, Guerra JM, Wilson E, Ding C, Olgin JE. Pirfenidone prevents the development of a vulnerable substrate for atrial fibrillation in a canine model of heart failure. *Circulation* 2006;**114**:1703-1712.

268. De Jong AM, Van Gelder IC, Vreeswijk-Baudoin I, Cannon MV, Van Gilst WH, Maass AH. Atrial remodeling is directly related to end-diastolic left ventricular pressure in a mouse model of ventricular pressure overload. *PloS One* 2013;**8**:e72651.

269. Hanna N, Cardin S, Leung TK, Nattel S. Differences in atrial versus ventricular remodeling in dogs with ventricular tachypacing-induced congestive heart failure. *Cardiovascular Research* 2004;**63**:236-244.

270. Ling LH, Kistler PM, Ellims AH, Iles LM, Lee G, Hughes GL, Kalman JM, Kaye DM, Taylor AJ. Diffuse ventricular fibrosis in atrial fibrillation: Noninvasive evaluation and relationships with aging and systolic dysfunction. *Journal of the American College of Cardiology* 2012;**60**:2402-2408.

271. Rahmutula D, Marcus GM, Wilson EE, Ding CH, Xiao Y, Paquet AC, Barbeau R, Barczak AJ, Erle DJ, Olgin JE. Molecular basis of selective atrial fibrosis due to overexpression of transforming growth factor-beta1. *Cardiovascular Research* 2013;**99**:769-779.

272. Li H, Li S, Yu B, Liu S. Expression of miR-133 and miR-30 in chronic atrial fibrillation in canines. *Molecular Medicine Reports* 2012;**5**:1457-1460.

273. Verheule S, Sato T, Everett Tt, Engle SK, Otten D, Rubart-von der Lohe M, Nakajima HO, Nakajima H, Field LJ, Olgin JE. Increased vulnerability to atrial fibrillation in transgenic mice with selective atrial fibrosis caused by overexpression of TGF-beta1. *Circulation Research* 2004;**94**:1458-1465.

274. Musa H, Kaur K, O'Connell R, Klos M, Guerrero-Serna G, Avula UM, Herron TJ, Kalifa J, Anumonwo JM, Jalife J. Inhibition of platelet-derived growth factor-AB signaling prevents electromechanical remodeling of adult atrial myocytes that contact myofibroblasts. *Heart Rhythm* 2013;**10**:1044-1051.

275. Liao C-h, Akazawa H, Tamagawa M, Ito K, Yasuda N, Kudo Y, Yamamoto R, Ozasa Y, Fujimoto M, Wang P, Nakauchi H, Nakaya H, Komuro I. Cardiac mast cells cause atrial fibrillation through PDGF-A-mediated fibrosis in pressure-overloaded mouse hearts. *The Journal of Clinical Investigation* 2010;**120**:242-253.

276. Healey JS, Israel CW, Connolly SJ, Hohnloser SH, Nair GM, Divakaramenon S, Capucci A, Van Gelder IC, Lau CP, Gold MR, Carlson M, Themeles E, Morillo CA. Relevance of electrical remodeling in human atrial fibrillation: Results of the asymptomatic atrial fibrillation and stroke evaluation in pacemaker patients and the atrial fibrillation reduction atrial pacing trial mechanisms of atrial fibrillation study. *Circulation Arrhythmia and Electrophysiology* 2012;**5**:626-631.

277. Xiao HD, Fuchs S, Campbell DJ, Lewis W, Dudley SC, Jr., Kasi VS, Hoit BD, Keshelava G, Zhao H, Capecchi MR, Bernstein KE. Mice with cardiac-restricted angiotensin-converting enzyme (ACE) have atrial enlargement, cardiac arrhythmia, and sudden death. *The American Journal of Pathology* 2004;**165**:1019-1032.

278. Cardin S, Li D, Thorin-Trescases N, Leung T-K, Thorin E, Nattel S. Evolution of the atrial fibrillation substrate in experimental congestive heart failure: Angiotensin-dependent and -independent pathways. *Cardiovascular Research* 2003;**60**:315-325.

279. Adam O, Lavall D, Theobald K, Hohl M, Grube M, Ameling S, Sussman MA, Rosenkranz S, Kroemer HK, Schafers HJ, Bohm M, Laufs U. Rac1-induced connective tissue growth factor regulates connexin 43 and N-cadherin expression in atrial fibrillation. *Journal of the American College of Cardiology* 2010;**55**:469-480.

280. Adam O, Theobald K, Lavall D, Grube M, Kroemer HK, Ameling S, Schafers HJ, Bohm M, Laufs U. Increased lysyl oxidase expression and collagen cross-linking during atrial fibrillation. *Journal of Molecular and Cellular Cardiology* 2011;**50**:678-685.

281. Li Y, Jian Z, Yang ZY, Chen L, Wang XF, Ma RY, Xiao YB. Increased expression of connective tissue growth factor and transforming growth factor-beta-1 in atrial

myocardium of patients with chronic atrial fibrillation. *Cardiology* 2013;**124**:233-240.

282. Song ZP, Liu X, Zhang DD. Connective tissue growth factor: A predictor of recurrence after catheter ablation in patients with nonparoxysmal atrial fibrillation. *Pacing and Clinical Electrophysiology* 2014;**37**:630-637.

283. Hoit BD, Takeishi Y, Cox MJ, Gabel M, Kirkpatrick D, Walsh RA, Tyagi SC. Remodeling of the left atrium in pacing-induced atrial cardiomyopathy. *Molecular and Cellular Biochemistry* 2002;**238**:145-150.

284. Zhang W, Zhong M, Yang GR, Li JP, Guo C, Wang Z, Zhang Y. Matrix metalloproteinase-9/tissue inhibitors of metalloproteinase-1 expression and atrial structural remodeling in a dog model of atrial fibrillation: Inhibition with angiotensin-converting enzyme. *Cardiovascular Pathology* 2008;**17**:399-409.

285. Nakano Y, Niida S, Dote K, Takenaka S, Hirao H, Miura F, Ishida M, Shingu T, Sueda T, Yoshizumi M, Chayama K. Matrix metalloproteinase-9 contributes to human atrial remodeling during atrial fibrillation. *Journal of the American College of Cardiology* 2004;**43**:818-825.

286. Sheet-Populations SF. International cardiovascular disease statistics. *American Heart Association* 2004.

287. Cheitlin MD, McAllister HA, de Castro CM. Myocardial infarction without atherosclerosis. *Jama* 1975;**231**:951-959.

288. Frangogiannis NG. The immune system and cardiac repair. *Pharmacological Research* 2008;**58**:88-111.

289. Kubler W, Spieckermann PG. Regulation of glycolysis in the ischemic and the anoxic myocardium. *Journal of Molecular and Cellular Cardiology* 1970;**1**:351-377.

290. Willems IE, Havenith MG, De Mey JG, Daemen MJ. The alpha-smooth muscle actin-positive cells in healing human myocardial scars. *The American Journal of Pathology* 1994;**145**:868-875.

291. Freed DH, Moon MC, Borowiec AM, Jones SC, Zahradka P, Dixon IM. Cardiotrophin-1: Expression in experimental myocardial infarction and potential role in post-MI wound healing. *Molecular and Cellular Biochemistry* 2003;**254**:247-256.

292. Freed DH, Cunnington RH, Dangerfield AL, Sutton JS, Dixon IM. Emerging evidence for the role of cardiotrophin-1 in cardiac repair in the infarcted heart. *Cardiovascular Research* 2005;**65**:782-792.

293. Deb A. Cell-cell interaction in the heart via Wnt/beta-catenin pathway after cardiac injury. *Cardiovascular Research* 2014;**102**:214-223.

294. Yu CM, Zhang Q, Yip GW, Lee PW, Kum LC, Lam YY, Fung JW. Diastolic and systolic asynchrony in patients with diastolic heart failure: A common but ignored condition. *Journal of the American College of Cardiology* 2007;**49**:97-105.

295. Serhan CN. Pro-resolving lipid mediators are leads for resolution physiology. *Nature* 2014;**510**:92-101.

296. van Amerongen MJ, Harmsen MC, van Rooijen N, Petersen AH, van Luyn MJ. Macrophage depletion impairs wound healing and increases left ventricular remodeling after myocardial injury in mice. *The American Journal of Pathology* 2007;**170**:818-829.

297. Chen W, Frangogiannis NG. Fibroblasts in post-infarction inflammation and cardiac repair. *Biochimica et Biophysica Acta* 2013;**1833**:945-953.

298. Takemura G, Ohno M, Hayakawa Y, Misao J, Kanoh M, Ohno A, Uno Y, Minatoguchi S, Fujiwara T, Fujiwara H. Role of apoptosis in the disappearance of infiltrated and proliferated interstitial cells after myocardial infarction. *Circulation Research* 1998;**82**:1130-1138.

299. Zhang Y, Li J, Partovian C, Sellke FW, Simons M. Syndecan-4 modulates basic fibroblast growth factor 2 signaling *in vivo*. *American Journal of Physiology Heart and Circulatory Physiology* 2003;**284**:H2078-2082.

300. Lopez B, Gonzalez A, Lindner D, Westermann D, Ravassa S, Beaumont J, Gallego I, Zudaire A, Brugnolaro C, Querejeta R, Larman M, Tschope C, Diez J. Osteopontin-mediated myocardial fibrosis in heart failure: A role for lysyl oxidase? *Cardiovascular Research* 2013;**99**:111-120.

301. Konstam MA, Kramer DG, Patel AR, Maron MS, Udelson JE. Left ventricular remodeling in heart failure: Current concepts in clinical significance and assessment. *JACC Cardiovascular Imaging* 2011;**4**:98-108.

302. Yang Y, Ma Y, Han W, Li J, Xiang Y, Liu F, Ma X, Zhang J, Fu Z, Su YD, Du XJ, Gao XM. Age-related differences in postinfarct left ventricular rupture and remodeling. *American Journal of Physiology Heart and Circulatory Physiology* 2008;**294**:H1815-1822.

303. Picard MH, Wilkins GT, Gillam LD, Thomas JD, Weyman AE. Immediate regional endocardial surface expansion following coronary occlusion in the canine left ventricle: Disproportionate effects of anterior versus inferior ischemia. *American Heart Journal* 1991;**121**:753-762.

304. Pierard LA, Albert A, Gilis F, Sprynger M, Carlier J, Kulbertus HE. Hemodynamic profile of patients with acute myocardial infarction at risk of infarct expansion. *The American Journal of Cardiology* 1987;**60**:5-9.

305. Dorfman TA, Aqel R. Regional pericarditis: A review of the pericardial manifestations of acute myocardial infarction. *Clinical Cardiology* 2009;**32**:115-120.

306. Widimsky P, Gregor P. Pericardial involvement during the course of myocardial infarction. A long-term clinical and echocardiographic study. *Chest* 1995;**108**:89-93.

307. Gao XM, White DA, Dart AM, Du XJ. Post-infarct cardiac rupture: Recent insights on pathogenesis and therapeutic interventions. *Pharmacology and Therapeutics* 2012;**134**:156-179.

308. Vanhoutte D, Schellings M, Pinto Y, Heymans S. Relevance of matrix metalloproteinases and their inhibitors after myocardial infarction: A temporal and spatial window. *Cardiovascular Research* 2006;**69**:604-613.

309. Hayashidani S, Tsutsui H, Ikeuchi M, Shiomi T, Matsusaka H, Kubota T, Imanaka-Yoshida K, Itoh T, Takeshita A. Targeted deletion of MMP-2 attenuates early LV rupture and late remodeling after experimental myocardial infarction. *American Journal of Physiology Heart and Circulatory Physiology* 2003;**285**:H1229-1235.

310. Pfeffer MA, Braunwald E. Ventricular remodeling after myocardial infarction. Experimental observations and clinical implications. *Circulation* 1990;**81**:1161-1172.

311. Wang Y, Ait-Oufella H, Herbin O, Bonnin P, Ramkhelawon B, Taleb S, Huang J, Offenstadt G, Combadiere C, Renia L, Johnson JL, Tharaux PL, Tedgui A, Mallat Z. TGF-beta activity protects against inflammatory aortic aneurysm progression and complications in angiotensin II-infused mice. *The Journal of Clinical Investigation* 2010;**120**:422-432.

312. Savelieva I, Kakouros N, Kourliouros A, Camm AJ. Upstream therapies for management of atrial fibrillation: Review of clinical evidence and implications for European Society of Cardiology guidelines. Part II: Secondary prevention. *Europace* 2011;**13**:610-625.

313. Connolly SJ, Ezekowitz MD, Yusuf S, Eikelboom J, Oldgren J, Parekh A, Pogue J, Reilly PA, Themeles E, Varrone J, Wang S, Alings M, Xavier D, Zhu J, Diaz R, Lewis BS, Darius H, Diener HC, Joyner CD, Wallentin L. Dabigatran versus warfarin in patients with atrial fibrillation. *The New England Journal of Medicine* 2009;**361**:1139-1151.

314. Nattel S, Opie LH. Controversies in atrial fibrillation. *Lancet* 2006;**367**:262-272.

315. Goldstein RN, Stambler BS. New antiarrhythmic drugs for prevention of atrial fibrillation. *Progress in Cardiovascular Diseases* 2005;**48**:193-208.

316. McMurray JJ, Adamopoulos S, Anker SD, Auricchio A, Bohm M, Dickstein K, Falk V, Filippatos G, Fonseca C, Gomez-Sanchez MA, Jaarsma T, Kober L, Lip GY, Maggioni AP, Parkhomenko A, Pieske BM, Popescu BA, Ronnevik PK, Rutten FH, Schwitter J, Seferovic P, Stepinska J, Trindade PT, Voors AA, Zannad F, Zeiher A. ESC Guidelines for the diagnosis and treatment of acute and chronic heart failure 2012: the task force for the diagnosis and treatment of acute and chronic heart failure 2012 of the European Society of Cardiology. Developed in collaboration with the Heart Failure Association (HFA) of the ESC. *European Heart Journal* 2012;**33**:1787-1847.

317. Savelieva I, Kakouros N, Kourliouros A, Camm AJ. Upstream therapies for management of atrial fibrillation: Review of clinical evidence and implications for European Society of Cardiology guidelines. Part I: Primary prevention. *Europace* 2011;**13**:308-328.

318. Madrid AH, Peng J, Zamora J, Marin I, Bernal E, Escobar C, Munos-Tinoco C, Rebollo JM, Moro C. The role of angiotensin receptor blockers and/or angiotensin converting enzyme inhibitors in the prevention of atrial fibrillation in patients with cardiovascular diseases: Meta-analysis of randomized controlled clinical trials. *Pacing and Clinical Electrophysiology* 2004;**27**:1405-1410.

319. Yared JP, Starr NJ, Torres FK, Bashour CA, Bourdakos G, Piedmonte M, Michener JA, Davis JA, Rosenberger TE. Effects of single dose, postinduction dexamethasone on recovery after cardiac surgery. *The Annals Thoracic Surgery* 2000;**69**:1420-1424.

320. Shiroshita-Takeshita A, Brundel BJ, Burstein B, Leung TK, Mitamura H, Ogawa S, Nattel S. Effects of simvastatin on the development of the atrial fibrillation substrate in dogs with congestive heart failure. *Cardiovascular Research* 2007;**74**:75-84.

321. Pedersen OD, Bagger H, Kober L, Torp-Pedersen C. Trandolapril reduces the incidence of atrial fibrillation after acute myocardial infarction in patients with left ventricular dysfunction. *Circulation* 1999;**100**:376-380.

322. Maggioni AP, Latini R, Carson PE, Singh SN, Barlera S, Glazer R, Masson S, Cere E, Tognoni G, Cohn JN. Valsartan reduces the incidence of atrial fibrillation in patients with heart failure: Results from the valsartan heart failure trial (Val-HeFT). *American Heart Journal* 2005;**149**:548-557.

323. Shimada YJ, Passeri JJ, Baggish AL, O'Callaghan C, Lowry PA, Yannekis G, Abbara S, Ghoshhajra BB, Rothman RD, Ho CY, Januzzi JL, Seidman CE, Fifer MA. Effects of losartan on left ventricular hypertrophy and fibrosis in patients with nonobstructive hypertrophic cardiomyopathy. *JACC Heart Failure* 2013;**1**:480-487.

324. Camm AJ, Kirchhof P, Lip GY, Schotten U, Savelieva I, Ernst S, Van Gelder IC, Al-Attar N, Hindricks G, Prendergast B, Heidbuchel H, Alfieri O, Angelini A, Atar D, Colonna P, De Caterina R, De Sutter J, Goette A, Gorenek B, Heldal M, Hohloser SH, Kolh P, Le Heuzey JY, Ponikowski P, Rutten FH. Guidelines for the management of atrial fibrillation: The task force for the management of atrial fibrillation of the European Society of Cardiology (ESC). *Europace* 2010;**12**:1360-1420.

325. Sakabe M, Shiroshita-Takeshita A, Maguy A, Dumesnil C, Nigam A, Leung TK, Nattel S. Omega-3 polyunsaturated fatty acids prevent atrial fibrillation associated with heart failure but not atrial tachycardia remodeling. *Circulation* 2007;**116**:2101-2109.

326. Sarrazin JF, Comeau G, Daleau P, Kingma J, Plante I, Fournier D, Molin F. Reduced incidence of vagally induced atrial fibrillation and expression levels of connexins by n-3 polyunsaturated fatty acids in dogs. *Journal of the American College of Cardiology* 2007;**50**:1505-1512.

327. Mayyas F, Sakurai S, Ram R, Rennison JH, Hwang ES, Castel L, Lovano B, Brennan ML, Bibus D, Lands B, Barnard J, Chung MK, Van Wagoner DR. Dietary omega 3 fatty acids modulate the substrate for post-operative atrial fibrillation in a canine cardiac surgery model. *Cardiovascular Research* 2011;**89**:852-861.

328. Marik PE, Fromm R. The efficacy and dosage effect of corticosteroids for the prevention of atrial fibrillation after cardiac surgery: A systematic review. *Journal of Critical Care* 2009;**24**:458-463.

329. Baker WL, White CM, Kluger J, Denowitz A, Konecny CP, Coleman CI. Effect of perioperative corticosteroid use on the incidence of postcardiothoracic surgery atrial fibrillation and length of stay. *Heart Rhythm* 2007;**4**:461-468.

330. Chiappini B, El Khoury G. Risk of atrial fibrillation with high-dose corticosteroids. *Expert Opinion on Drug Safety* 2006;**5**:811-814.

331. Ramos-Mondragón R, Galindo CA, Avila G. Role of TGF-beta on cardiac structural and electrical remodeling. *Vascular Health and Risk Management* 2008;**4**:1289-1300.

332. Engebretsen KV, Skardal K, Bjornstad S, Marstein HS, Skrbic B, Sjaastad I, Christensen G, Bjornstad JL, Tonnessen T. Attenuated development of cardiac

fibrosis in left ventricular pressure overload by SM16, an orally active inhibitor of ALK5. *Journal of Molecular and Cellular Cardiology* 2014;**76**:148-157.

333. Liu C, Zhao W, Meng W, Zhao T, Chen Y, Ahokas RA, Liu H, Sun Y. Platelet-derived growth factor blockade on cardiac remodeling following infarction. *Molecular and Cellular Biochemistry* 2014;**397**:295-304.

334. Payne SL, Hendrix MJ, Kirschmann DA. Paradoxical roles for lysyl oxidases in cancer--a prospect. *Journal of Cellular Biochemistry* 2007;**101**:1338-1354.

335. Galan M, Varona S, Guadall A, Orriols M, Navas M, Aguilo S, de Diego A, Navarro MA, Garcia-Dorado D, Rodriguez-Sinovas A, Martinez-Gonzalez J, Rodriguez C. Lysyl oxidase overexpression accelerates cardiac remodeling and aggravates angiotensin II-induced hypertrophy. *The Federation of American Societies for Experimental Biology Journal* 2017;**31**:3787-3799.

336. Miguel-Carrasco JL, Beaumont J, San Jose G, Moreno MU, Lopez B, Gonzalez A, Zalba G, Diez J, Fortuno A, Ravassa S. Mechanisms underlying the cardiac antifibrotic effects of losartan metabolites. *Scientific Reports* 2017;**7**:41865.

337. El Hajj EC, El Hajj MC, Ninh VK, Bradley JM, Claudino MA, Gardner JD. Detrimental role of lysyl oxidase in cardiac remodeling. *Journal of Molecular and Cellular Cardiology* 2017;**109**:17-26.

338. Xiao Y, Nie X, Han P, Fu H, James Kang Y. Decreased copper concentrations but increased lysyl oxidase activity in ischemic hearts of rhesus monkeys. *Metallomics: Integrated Biometal Science* 2016;**8**:973-980.

339. Gonzalez GE, Rhaleb NE, Nakagawa P, Liao TD, Liu Y, Leung P, Dai X, Yang XP, Carretero OA. N-acetyl-seryl-aspartyl-lysyl-proline reduces cardiac collagen cross-linking and inflammation in angiotensin II-induced hypertensive rats. *Clinical Science* 2014;**126**:85-94.

340. El Hajj EC, El Hajj MC, Ninh VK, Gardner JD. Cardioprotective effects of lysyl oxidase inhibition against volume overload-induced extracellular matrix remodeling. *Experimental Biology and Medicine* 2016;**241**:539-549.

341. El Hajj EC, El Hajj MC, Ninh VK, Gardner JD. Inhibitor of lysyl oxidase improves cardiac function and the collagen/MMP profile in response to volume overload. *American Journal of Physiology Heart and Circulatory Physiology* 2018;**315**:H463-h473.

342. Gonzalez-Santamaria J, Villalba M, Busnadiego O, Lopez-Olaneta MM, Sandoval P, Snabel J, Lopez-Cabrera M, Erler JT, Hanemaaijer R, Lara-Pezzi E, Rodriguez-Pascual F. Matrix cross-linking lysyl oxidases are induced in response to

myocardial infarction and promote cardiac dysfunction. *Cardiovascular Research* 2016;**109**:67-78.

343. Higgins DF, Kimura K, Bernhardt WM, Shrimanker N, Akai Y, Hohenstein B, Saito Y, Johnson RS, Kretzler M, Cohen CD, Eckardt KU, Iwano M, Haase VH. Hypoxia promotes fibrogenesis *in vivo* via HIF-1 stimulation of epithelial-to-mesenchymal transition. *The Journal of Clinical Investigation* 2007;**117**:3810-3820.

344. Lazarus HM, Cruikshank WW, Narasimhan N, Kagan HM, Center DM. Induction of human monocyte motility by lysyl oxidase. *Matrix Biology* 1995;**14**:727-731.

345. Giampuzzi M, Botti G, Di Duca M, Arata L, Ghiggeri G, Gusmano R, Ravazzolo R, Di Donato A. Lysyl oxidase activates the transcription activity of human collagene III promoter. Possible involvement of Ku antigen. *The Journal of Biological Chemistry* 2000;**275**:36341-36349.

346. Nellaiappan K, Risitano A, Liu G, Nicklas G, Kagan HM. Fully processed lysyl oxidase catalyst translocates from the extracellular space into nuclei of aortic smooth-muscle cells. *Journal of Cellular Biochemistry* 2000;**79**:576-582.

347. Kobayashi H, Ishii M, Chanoki M, Yashiro N, Fushida H, Fukai K, Kono T, Hamada T, Wakasaki H, Ooshima A. Immunohistochemical localization of lysyl oxidase in normal human skin. *The British Journal of Dermatology* 1994;**131**:325-330.

348. Yang J, Savvatis K, Kang JS, Fan P, Zhong H, Schwartz K, Barry V, Mikels-Vigdal A, Karpinski S, Kornyeyev D, Adamkewicz J, Feng X, Zhou Q, Shang C, Kumar P, Phan D, Kasner M, Lopez B, Diez J, Wright KC, Kovacs RL, Chen PS, Quertermous T, Smith V, Yao L, Tschope C, Chang CP. Targeting LOXL2 for cardiac interstitial fibrosis and heart failure treatment. *Nature Communications* 2016;**7**:13710.

349. Chen Y. Molecular regulation of atrial-selective fibrotic remodeling and its role in atrial fibrillation. *PhD Thesis at McGill University* 2015:1-246.

350. Eyre DR, Weis MA, Wu JJ. Advances in collagen cross-link analysis. *Methods* 2008;**45**:65-74.

351. Xia SJ, Du X, Li C, Wu JH, Tang RB, Chang SS, Guo XY, Yu RH, Long DY, Bai R, Liu N, Sang CH, Li SN, Liu XH, Pan JH, Dong JZ, Lip GY, Ma CS. Uptake of evidence-based statin therapy among atrial fibrillation patients in China: A report from the CAFR (chinese atrial fibrillation registry) study. *International Journal of Cardiology* 2016;**220**:284-289.

352. Zhong H, Liang X-H, Neef S, Popov A, Maier LS, Yao L, Belardinelli L. Expression of lysyl oxidase-like 2 (LOXL2) correlates with left atrial size and fibrotic gene expression in human atrial fibrillation. *Journal of the American College of Cardiology* 2014;**63**:A285.

353. Jabre P, Jouven X, Adnet F, Thabut G, Bielinski SJ, Weston SA, Roger VL. Atrial fibrillation and death after myocardial infarction: A community study. *Circulation* 2011;**123**:2094-2100.

354. Mehta RH, Dabbous OH, Granger CB, Kuznetsova P, Kline-Rogers EM, Anderson FA, Jr., Fox KA, Gore JM, Goldberg RJ, Eagle KA. Comparison of outcomes of patients with acute coronary syndromes with and without atrial fibrillation. *The American Journal of Cardiology* 2003;**92**:1031-1036.

355. Cardin S, Guasch E, Luo X, Naud P, Le Quang K, Shi Y, Tardif JC, Comtois P, Nattel S. Role for MicroRNA-21 in atrial profibrillatory fibrotic remodeling associated with experimental postinfarction heart failure. *Circulation Arrhythmia and Electrophysiology* 2012;**5**:1027-1035.

356. Yamani M, Massie BM. Congestive heart failure: Insights from epidemiology, implications for treatment. *Mayo Clinic Proceedings* 1993;**68**:1214-1218.

357. Ho KK, Anderson KM, Kannel WB, Grossman W, Levy D. Survival after the onset of congestive heart failure in Framingham Heart Study subjects. *Circulation* 1993;**88**:107-115.

358. Surinkaew S, Aflaki M, Takawale A, Chen Y, Qi XY, Gillis MA, Shi YF, Tardif JC, Chattipakorn N, Nattel S. Exchange-protein activated by cyclic-AMP (EPAC) regulates atrial fibroblast function and controls cardiac remodeling. *Cardiovascular Research* 2019.;**115**:94-106.

359. Moore-Morris T, Cattaneo P, Puceat M, Evans SM. Origins of cardiac fibroblasts. *Journal of Molecular and Cellular Cardiology* 2016;**91**:1-5.

360. Stefanon I, Valero-Munoz M, Fernandes AA, Ribeiro RF, Jr., Rodriguez C, Miana M, Martinez-Gonzalez J, Spalenza JS, Lahera V, Vassallo PF, Cachofeiro V. Left and right ventricle late remodeling following myocardial infarction in rats. *PloS One* 2013;**8**:e64986.

361. Rodriguez C, Martinez-Gonzalez J, Raposo B, Alcudia JF, Guadall A, Badimon L. Regulation of lysyl oxidase in vascular cells: Lysyl oxidase as a new player in cardiovascular diseases. *Cardiovascular Research* 2008;**79**:7-13.

362. Yue L, Xie J, Nattel S. Molecular determinants of cardiac fibroblast electrical function and therapeutic implications for atrial fibrillation. *Cardiovascular Research* 2011;**89**:744-753.

363. Nakajima H, Nakajima HO, Salcher O, Dittie AS, Dembowsky K, Jing S, Field LJ. Atrial but not ventricular fibrosis in mice expressing a mutant transforming growth factor-beta (1) transgene in the heart. *Circulation Research* 2000;**86**:571-579.

364. Cleutjens JP, Verluyten MJ, Smiths JF, Daemen MJ. Collagen remodeling after myocardial infarction in the rat heart. *The American Journal of Pathology* 1995;**147**:325-338.

365. Yamada S, Fong MC, Hsiao YW, Chang SL, Tsai YN, Lo LW, Chao TF, Lin YJ, Hu YF, Chung FP, Liao JN, Chang YT, Li HY, Higa S, Chen SA. Impact of renal denervation on atrial arrhythmogenic substrate in ischemic model of heart failure. *Journal of the American Heart Association* 2018;**7**:e007312.

366. Tse G, Yeo JM. Conduction abnormalities and ventricular arrhythmogenesis: The roles of sodium channels and gap junctions. *International Journal of Cardiology Heart and Vasculature* 2015;**9**:75-82.

367. Mizikova I, Palumbo F, Tabi T, Herold S, Vadasz I, Mayer K, Seeger W, Morty RE. Perturbations to lysyl oxidase expression broadly influence the transcriptome of lung fibroblasts. *Physiological Genomics* 2017;**49**:416-429.

368. Hunter T. 1001 Protein kinases redux-towards 2000. *Seminars in Cell Biology* 1994;**5**:367-376.

369. Lin CH, Yu MC, Tung WH, Chen TT, Yu CC, Weng CM, Tsai YJ, Bai KJ, Hong CY, Chien MH, Chen BC. Connective tissue growth factor induces collagen I expression in human lung fibroblasts through the Rac1/MLK3/JNK/AP-1 pathway. *Biochimica et Biophysica Acta* 2013;**1833**:2823-2833.

370. Csiszar K. Lysyl oxidases: A novel multifunctional amine oxidase family. *Progress in Nucleic Acid Research and Molecular Biology* 2001;**70**:1-32.

371. Kagan HM, Li W. Lysyl oxidase: Properties, specificity, and biological roles inside and outside of the cell. *Journal of Cellular Biochemistry* 2003;**88**:660-672.

372. Raisova M, Hossini AM, Eberle J, Riebeling C, Orfanos CE, Geilen CC, Wieder T, Sturm I, Daniel PT. The Bax/Bcl-2 ratio determines the susceptibility of human melanoma cells to CD95/Fas-mediated apoptosis. *Journal of Investigative Dermatology* 2001;**117**:333-340.

373. Francis GS, Cohn JN. Heart failure: Mechanisms of cardiac and vascular dysfunction and the rationale for pharmacologic intervention. *The Federation of American Societies for Experimental Biology Journal* 1990;**4**:3068-3075.

374. de Tombe PP. Altered contractile function in heart failure. *Cardiovascular Research* 1998;**37**:367-380.

375. Peacock EE, Madden JW. Administration of beta-aminopropionitrile to human beings with urethral strictures: A preliminary report. *The American Journal of Surgery* 1978;**136**:600-605.

376. Keiser HR, Sjoerdsma A. Studies on beta-aminopropionitrile in patients with scleroderma. *Clinical Pharmacology and Therapeutics* 1967;**8**:593-602.

377. Barrow MV, Simpson CF. Caution against the use of lathyrogens. *Surgery* 1972;**71**:309-310.

378. Peacock EE, Jr., Madden JW. Some studies on the effects of beta-aminopropionitrile in patients with injured flexor tendons. *Surgery* 1969;**66**:215-223.

379. Zhao Y, Tang K, Tianbao X, Wang J, Yang J, Li D. Increased serum lysyl oxidase-like 2 levels correlate with the degree of left atrial fibrosis in patients with atrial fibrillation. *Bioscience Reports* 2017;**37**:BSR20171332.